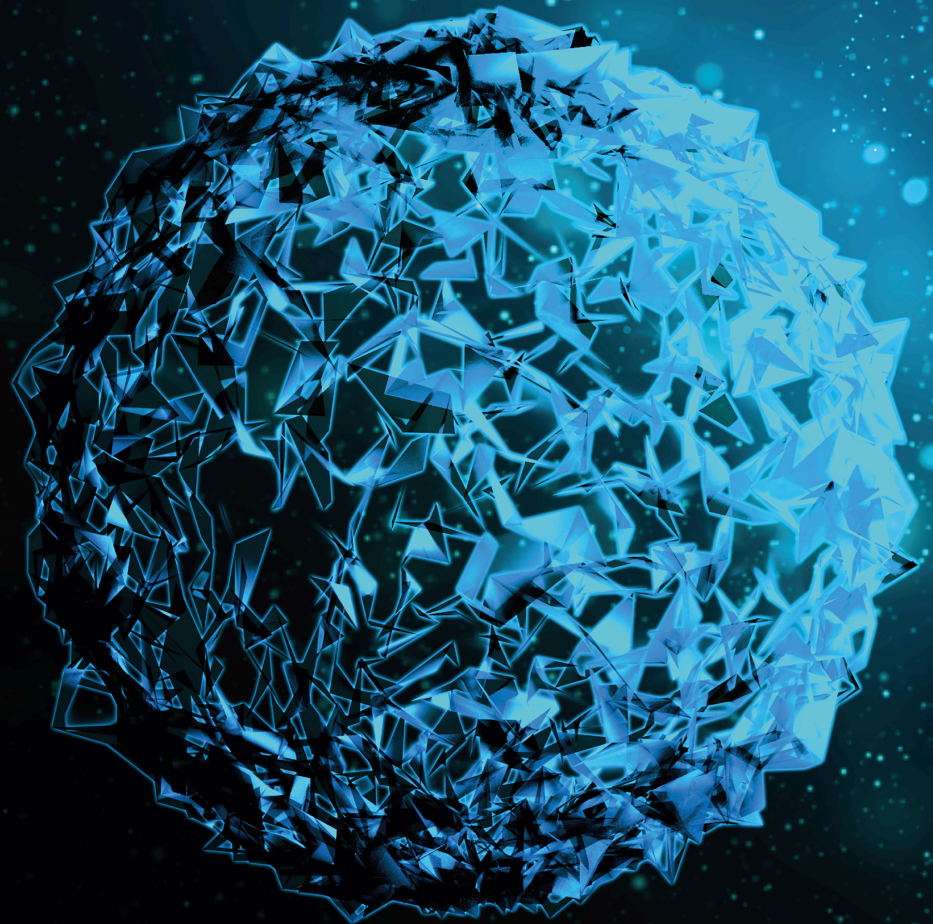


# Non-coding RNA in Cardiovascular Disease

Lead Guest Editor: Lei Chen

Guest Editors: Dafeng Yang, Shenglan Tan, Dabin Kuang, Zhousheng Yang, and Xian Zhang





---

# **Non-coding RNA in Cardiovascular Disease**



BioMed Research International

---

## **Non-coding RNA in Cardiovascular Disease**

Lead Guest Editor: Lei Chen

Guest Editors: Dafeng Yang, Shenglan Tan, Dabin  
Kuang, Zhousheng Yang, and Xian Zhang



---

Copyright © 2024 Hindawi Limited. All rights reserved.

This is a special issue published in "BioMed Research International." All articles are open access articles distributed under the Creative Commons Attribution License, which permits unrestricted use, distribution, and reproduction in any medium, provided the original work is properly cited.

## Section Editors

Penny A. Asbell, USA  
David Bernardo , Spain  
Gerald Brandacher, USA  
Kim Bridle , Australia  
Laura Chronopoulou , Italy  
Gerald A. Colvin , USA  
Aaron S. Dumont, USA  
Pierfrancesco Franco , Italy  
Raj P. Kandpal , USA  
Fabrizio Montecucco , Italy  
Mangesh S. Pednekar , India  
Letterio S. Politi , USA  
Jinsong Ren , China  
William B. Rodgers, USA  
Harry W. Schroeder , USA  
Andrea Scribante , Italy  
Germán Vicente-Rodríguez , Spain  
Momiao Xiong , USA  
Hui Zhang , China

## Academic Editors

### Biomedical Genetics & Genomics

# Contents

**Retracted: Atomic Scale Interactions between RNA and DNA Aptamers with the TNF- $\alpha$  Protein**

BioMed Research International

Retraction (1 page), Article ID 9870151, Volume 2024 (2024)

**Retracted: A Systematic Review and Meta-Analysis of Therapeutic Efficacy and Safety of Alirocumab and Evolocumab on Familial Hypercholesterolemia**

BioMed Research International

Retraction (1 page), Article ID 9865038, Volume 2024 (2024)

**Retracted: SOCS3 Gene Polymorphism and Hypertension Susceptibility in Chinese Population: A Two-Center Case-Control Study**

BioMed Research International

Retraction (1 page), Article ID 9843281, Volume 2024 (2024)

**Retracted: Antiangiogenic Effect of Platelet P2Y<sub>12</sub> Inhibitor in Ischemia-Induced Angiogenesis in Mice Hindlimb**

BioMed Research International








Retraction (1 page), Article ID 9765981, Volume 2024 (2024)

**Association of lncRNA PVT1 Gene Polymorphisms with the Risk of Essential Hypertension in Chinese Population**

Rong Li, Xia Yu, Yang Chen, Mulun Xiao, Meiling Zuo, Yuanlin Xie, Zhousheng Yang , and Dabin Kuang 

Research Article (9 pages), Article ID 9976909, Volume 2022 (2022)

**Analyses of Long Noncoding RNA and mRNA Profiles in Subjects with the Phlegm-Dampness Constitution**

Lidan Dong , Yanfei Zheng , Dan Liu , Fuhong He , Kaiki Lee , Lingru Li , and Qi Wang 


Research Article (14 pages), Article ID 4896282, Volume 2021 (2021)

**[Retracted] SOCS3 Gene Polymorphism and Hypertension Susceptibility in Chinese Population: A Two-Center Case-Control Study**

Dabin Kuang, Lichen Dong, Lingyun Liu, Meiling Zuo, Yuanlin Xie, Taoming Li, and Zhousheng Yang 



Research Article (8 pages), Article ID 8445461, Volume 2021 (2021)

**[Retracted] A Systematic Review and Meta-Analysis of Therapeutic Efficacy and Safety of Alirocumab and Evolocumab on Familial Hypercholesterolemia**

Xiaoyue Ge, Tiantian Zhu, Hao Zeng, Xin Yu, Juan Li, Shanshan Xie, Jinjin Wan, Huiyao Yang, Keke Huang, and Weifang Zhang 

Review Article (16 pages), Article ID 8032978, Volume 2021 (2021)



**An Overview of miRNAs Involved in PSMC Phenotypic Switching in Pulmonary Hypertension**

Weifang Zhang , Zeying Tao, Fei Xu, Qian Diao, Juan Li, Lu Zhou, Yaxin Miao, Shanshan Xie, Jinjin Wan, and Ruilai Xu 

Review Article (18 pages), Article ID 5765029, Volume 2021 (2021)




**MicroRNA-137 Inhibited Hypoxia-Induced Proliferation of Pulmonary Artery Smooth Muscle Cells by Targeting Calpain-2**

Xiao-Yue Ge, Tian-Tian Zhu, Mao-Zhong Yao, Hong Liu, Qian Wu, Jie Qiao, Wei-Fang Zhang , and Chang-Ping Hu 


Research Article (15 pages), Article ID 2202888, Volume 2021 (2021)

**miR-129 Attenuates Myocardial Ischemia Reperfusion Injury by Regulating the Expression of PTEN in Rats**

Zhao-Hui Dai, Zhi-Ming Jiang, Hua Tu, Li Mao, Gui-Lin Song, Zhong-Bao Yang , Fang Liu, and Md Sayed Ali Sheikh


Research Article (10 pages), Article ID 5535788, Volume 2021 (2021)

**Roles of MicroRNAs in Peripheral Artery In-Stent Restenosis after Endovascular Treatment**

Mo Wang, Weichang Zhang, Lei Zhang, Lunchang Wang, Jiehua Li, Chang Shu, and Xin Li 



Review Article (11 pages), Article ID 9935671, Volume 2021 (2021)

**[Retracted] Atomic Scale Interactions between RNA and DNA Aptamers with the TNF- $\alpha$  Protein**

Homayoun Asadzadeh, Ali Moosavi , Georgios Alexandrakis, and Mohammad R. K. Mofrad


Research Article (11 pages), Article ID 9926128, Volume 2021 (2021)

**Inhibition of miR-214-3p Protects Endothelial Cells from ox-LDL-Induced Damage by Targeting GPX4**

Min Xie, Panhao Huang, Tian Wu, Li Chen , and Ren Guo 

Research Article (9 pages), Article ID 9919729, Volume 2021 (2021)

**[Retracted] Antiangiogenic Effect of Platelet P2Y<sub>12</sub> Inhibitor in Ischemia-Induced Angiogenesis in Mice Hindlimb**

Xiaoli Wang, Huan Zhao, Naiquan Yang , Yue Jin, and Jianguo Chen 

Research Article (6 pages), Article ID 5529431, Volume 2021 (2021)

## Retraction

# Retracted: Atomic Scale Interactions between RNA and DNA Aptamers with the TNF- $\alpha$ Protein

### BioMed Research International

Received 12 March 2024; Accepted 12 March 2024; Published 20 March 2024

Copyright © 2024 BioMed Research International. This is an open access article distributed under the Creative Commons Attribution License, which permits unrestricted use, distribution, and reproduction in any medium, provided the original work is properly cited.

This article has been retracted by Hindawi following an investigation undertaken by the publisher [1]. This investigation has uncovered evidence of one or more of the following indicators of systematic manipulation of the publication process:

- (1) Discrepancies in scope
- (2) Discrepancies in the description of the research reported
- (3) Discrepancies between the availability of data and the research described
- (4) Inappropriate citations
- (5) Incoherent, meaningless and/or irrelevant content included in the article
- (6) Manipulated or compromised peer review

The presence of these indicators undermines our confidence in the integrity of the article's content and we cannot, therefore, vouch for its reliability. Please note that this notice is intended solely to alert readers that the content of this article is unreliable. We have not investigated whether authors were aware of or involved in the systematic manipulation of the publication process.

Wiley and Hindawi regrets that the usual quality checks did not identify these issues before publication and have since put additional measures in place to safeguard research integrity.

We wish to credit our own Research Integrity and Research Publishing teams and anonymous and named external researchers and research integrity experts for contributing to this investigation.

The corresponding author, as the representative of all authors, has been given the opportunity to register their agreement or disagreement to this retraction. We have kept a record of any response received.

### References

- [1] H. Asadzadeh, A. Moosavi, G. Alexandrakis, and M. R. K. Mofrad, "Atomic Scale Interactions between RNA and DNA Aptamers with the TNF- $\alpha$  Protein," *BioMed Research International*, vol. 2021, Article ID 9926128, 11 pages, 2021.

## Retraction

# Retracted: A Systematic Review and Meta-Analysis of Therapeutic Efficacy and Safety of Alirocumab and Evolocumab on Familial Hypercholesterolemia

### BioMed Research International

Received 12 March 2024; Accepted 12 March 2024; Published 20 March 2024

Copyright © 2024 BioMed Research International. This is an open access article distributed under the Creative Commons Attribution License, which permits unrestricted use, distribution, and reproduction in any medium, provided the original work is properly cited.

This article has been retracted by Hindawi following an investigation undertaken by the publisher [1]. This investigation has uncovered evidence of one or more of the following indicators of systematic manipulation of the publication process:

- (1) Discrepancies in scope
- (2) Discrepancies in the description of the research reported
- (3) Discrepancies between the availability of data and the research described
- (4) Inappropriate citations
- (5) Incoherent, meaningless and/or irrelevant content included in the article
- (6) Manipulated or compromised peer review

The presence of these indicators undermines our confidence in the integrity of the article's content and we cannot, therefore, vouch for its reliability. Please note that this notice is intended solely to alert readers that the content of this article is unreliable. We have not investigated whether authors were aware of or involved in the systematic manipulation of the publication process.

Wiley and Hindawi regrets that the usual quality checks did not identify these issues before publication and have since put additional measures in place to safeguard research integrity.

We wish to credit our own Research Integrity and Research Publishing teams and anonymous and named external researchers and research integrity experts for contributing to this investigation.

The corresponding author, as the representative of all authors, has been given the opportunity to register their agreement or disagreement to this retraction. We have kept a record of any response received.

### References

- [1] X. Ge, T. Zhu, H. Zeng et al., "A Systematic Review and Meta-Analysis of Therapeutic Efficacy and Safety of Alirocumab and Evolocumab on Familial Hypercholesterolemia," *BioMed Research International*, vol. 2021, Article ID 8032978, 16 pages, 2021.

## Retraction

# Retracted: SOCS3 Gene Polymorphism and Hypertension Susceptibility in Chinese Population: A Two-Center Case-Control Study

### BioMed Research International

Received 12 March 2024; Accepted 12 March 2024; Published 20 March 2024

Copyright © 2024 BioMed Research International. This is an open access article distributed under the Creative Commons Attribution License, which permits unrestricted use, distribution, and reproduction in any medium, provided the original work is properly cited.

This article has been retracted by Hindawi following an investigation undertaken by the publisher [1]. This investigation has uncovered evidence of one or more of the following indicators of systematic manipulation of the publication process:

- (1) Discrepancies in scope
- (2) Discrepancies in the description of the research reported
- (3) Discrepancies between the availability of data and the research described
- (4) Inappropriate citations
- (5) Incoherent, meaningless and/or irrelevant content included in the article
- (6) Manipulated or compromised peer review

The presence of these indicators undermines our confidence in the integrity of the article's content and we cannot, therefore, vouch for its reliability. Please note that this notice is intended solely to alert readers that the content of this article is unreliable. We have not investigated whether authors were aware of or involved in the systematic manipulation of the publication process.

Wiley and Hindawi regrets that the usual quality checks did not identify these issues before publication and have since put additional measures in place to safeguard research integrity.

We wish to credit our own Research Integrity and Research Publishing teams and anonymous and named external researchers and research integrity experts for contributing to this investigation.

The corresponding author, as the representative of all authors, has been given the opportunity to register their agreement or disagreement to this retraction. We have kept a record of any response received.

### References

- [1] D. Kuang, L. Dong, L. Liu et al., "SOCS3 Gene Polymorphism and Hypertension Susceptibility in Chinese Population: A Two-Center Case-Control Study," *BioMed Research International*, vol. 2021, Article ID 8445461, 8 pages, 2021.



## Retraction

# Retracted: Antiangiogenic Effect of Platelet P2Y<sub>12</sub> Inhibitor in Ischemia-Induced Angiogenesis in Mice Hindlimb

### BioMed Research International

Received 12 March 2024; Accepted 12 March 2024; Published 20 March 2024

Copyright © 2024 BioMed Research International. This is an open access article distributed under the Creative Commons Attribution License, which permits unrestricted use, distribution, and reproduction in any medium, provided the original work is properly cited.

This article has been retracted by Hindawi following an investigation undertaken by the publisher [1]. This investigation has uncovered evidence of one or more of the following indicators of systematic manipulation of the publication process:

- (1) Discrepancies in scope
- (2) Discrepancies in the description of the research reported
- (3) Discrepancies between the availability of data and the research described
- (4) Inappropriate citations
- (5) Incoherent, meaningless and/or irrelevant content included in the article
- (6) Manipulated or compromised peer review

The presence of these indicators undermines our confidence in the integrity of the article's content and we cannot, therefore, vouch for its reliability. Please note that this notice is intended solely to alert readers that the content of this article is unreliable. We have not investigated whether authors were aware of or involved in the systematic manipulation of the publication process.

Wiley and Hindawi regrets that the usual quality checks did not identify these issues before publication and have since put additional measures in place to safeguard research integrity.

We wish to credit our own Research Integrity and Research Publishing teams and anonymous and named external researchers and research integrity experts for contributing to this investigation.

The corresponding author, as the representative of all authors, has been given the opportunity to register their agreement or disagreement to this retraction. We have kept a record of any response received.

### References

- [1] X. Wang, H. Zhao, N. Yang, Y. Jin, and J. Chen, "Antiangiogenic Effect of Platelet P2Y<sub>12</sub> Inhibitor in Ischemia-Induced Angiogenesis in Mice Hindlimb," *BioMed Research International*, vol. 2021, Article ID 5529431, 6 pages, 2021.

## Research Article

# Association of lncRNA PVT1 Gene Polymorphisms with the Risk of Essential Hypertension in Chinese Population

Rong Li,<sup>1</sup> Xia Yu,<sup>1</sup> Yang Chen,<sup>1</sup> Mulun Xiao,<sup>2</sup> Meiling Zuo,<sup>3</sup> Yuanlin Xie,<sup>3</sup> Zhousheng Yang ,<sup>4</sup> and Dabin Kuang <sup>3</sup>

<sup>1</sup>Institute of Pharmacy & Pharmacology and the Second Affiliated Hospital, University of South China, Hengyang 421001, China

<sup>2</sup>Department of Urology, The First Affiliated Hospital of Zhengzhou University, Zhengzhou 450000, China

<sup>3</sup>The Affiliated Changsha Hospital of Hunan Normal University, Changsha, Hunan 410006, China

<sup>4</sup>Department of Pharmacy, The People's Hospital of Guangxi Zhuang Autonomous Region, Nanning, China

Correspondence should be addressed to Dabin Kuang; [kdb@hunnu.edu.cn](mailto:kdb@hunnu.edu.cn)

Received 15 March 2021; Accepted 18 December 2021; Published 6 January 2022

Academic Editor: Jing He

Copyright © 2022 Rong Li et al. This is an open access article distributed under the Creative Commons Attribution License, which permits unrestricted use, distribution, and reproduction in any medium, provided the original work is properly cited.

Vascular dysfunction and hyperlipidemia are essential risk factors contributing to essential hypertension (EH). The plasmacytoma variant translocation 1 (PVT1) is involved in modulating angiogenesis in tumor tissues and plays an important role in fat differentiation in the progress of obesity. Therefore, we selected two tagSNPs of PVT1 (rs10956390 and rs80177647) to investigate whether they are contributing to the risk of hypertension in Chinese patients. In total, 524 adult patients with EH and 439 matched healthy controls were enrolled for two central of China. *Results.* PVT1 rs10956390 and rs80177647 polymorphisms were genotyped by using TaqMan assay. PVT1 rs10956390 TT genotype was associated with a decreased risk of EH (OR = 0.561, 95% CI = 0.372-0.846,  $P = 0.006$ ), while rs80177647 TA genotype was associated with an increased risk (OR = 2.236, 95% CI = 1.515-3.301,  $P < 0.001$ ). Rs10956390 T allele was associated with lower triglyceride levels in the plasma both from healthy and EH donors. What is more, there is an association between rs10956390 polymorphism and HDL-C level, as well as LDL-C. *Conclusion.* PVT1 rs10956390 and rs80177647 polymorphisms may contribute to the risk of EH in Chinese population by regulating blood lipid levels.

## 1. Introduction

Essential hypertension (EH), a noninfectious multifactorial disease, is a crucial risk factor for the morbidity and mortality of cardiovascular disease worldwide [1]. For the low treatment rate, control rate, and poor prognosis in EH patients, there is an urgent need to reveal the complex mechanism of EH. Over decades, accumulating evidence has confirmed that the factors causing hypertension include gene-gene and gene-environment interactions as well as biological systems [2].

Long noncoding RNAs (lncRNAs) are a class of noncoding RNAs longer than 200 nt. After long-time defined as “gene desert” for a long time, it has been recognized that lncRNAs play a pivotal role in diseases including cardiovascular diseases in a delicate and sophisticated network modulation manner

[3–6]. The plasmacytoma variant translocation 1 (PVT1) is located at cancer risk region 8q24.21 [7], which has been identified to aberrantly expressed in various cancers including pancreatic [8], prostate [9, 10], bladder [11] cancers, and hepatocellular carcinoma [12]. Zhao et al. found that PVT1 activates STAT3/VEGFA signaling axis to boost angiogenesis in gastric cancer [13]. Similarly, Zheng et al. revealed that PVT1 orchestrates the angiogenesis of vascular endothelial cells by evoking connective tissue growth factor (CTGF) and angiopoietin 2 (ANGPT2) expression in a miR-26b dependent manner [14]. Sun et al. found that PVT1 reduces the expression of miR-190a-5p in vascular endothelial cells (ECs), resulting in proliferation [15]. Guo et al. unraveled that PVT1 knockdown ameliorates ox-LDL-induced vascular endothelial cell injury and atherosclerosis through the miR-153-3p/GRB2 axis [16]. Furthermore, recent studies have shown that PVT1

was found to be a potential biomarker for obesity treatment [17]. The potential mechanism in the interaction between obesity, atherosclerosis, and hypertension is elaborated and sophisticated, which contains activation of the sympathetic nervous system, epithelial dysfunction and oxidative stress, leptin, and adiponectin [18]. In the light of all the above, we assume that PVT1 may regulate biological processes of angiogenesis abnormality-associated diseases including diabetes, obesity, and hypertension. However, it is not clear whether PVT1 can regulate hypertension by affecting the blood lipid levels in the human plasma.

Accumulating evidence has shown that genetic polymorphism may be a novel treatment strategy to improve the control and management of diseases. Notably, in a recent study, Yan et al. revealed that PVT1 rs4410871 was a protective factor for coronary heart disease (CHD) susceptibility in Chinese population and influenced the complications (hypertension or diabetes) [19]. Considering the key role of PVT1 in affecting angiogenesis and regulating obesity, PVT1 may be a potential candidate gene related to EH risk. However, there is no report on the correlation between PVT1 polymorphism and EH risk. To clarify the clinical relevance of PVT1 polymorphisms, we conducted a case-control study in this article to investigate the association between PVT1 polymorphisms and the risk of EH in Chinese population. Meanwhile, we are trying to provide a promising biomarker in the subsequent occurrence mechanism of EH and improve the prognosis for patients.

## 2. Materials and Methods

**2.1. Subjects.** 261 EH patients and 294 healthy controls were consecutively recruited between January 2021 and March 2021 from the second affiliated hospital of south China. 263 EH patients and 145 control individuals were enrolled between January 2018 and December 2019 from the First People's Hospital of Jining City, Shandong Province, in the north of China. The information of all participants including gender, age, BMI, smoking history, blood pressure, triglyceride (TG), total cholesterol (TC), high-density lipoprotein (HDL), low-density lipoprotein (LDL), and blood glucose was obtained. The presence of hypertension was clinically defined as having a systolic blood pressure (SBP) of at least 140 mmHg and a diastolic blood pressure (DBP) of at least 90 mmHg (without any antihypertensive medication), 30 years  $\leq$  age  $\leq$  70 years, and the course of hypertension between 1 year and 15 years. The exclusion criteria were as follows: severe organic lesions, with other malignancies, secondary hypertension, and recent history of glucocorticoid use. The healthy subjects undergoing routine healthy examinations were enrolled in the same period. This study protocol was approved by the Medical Ethics Committee of hospital involved in the study, and the written informed consent was gained from all participants or their first-degree relatives.

**2.2. Genomic DNA Extraction and Genotyping.** EDTA anticoagulation tubes were used to collect the peripheral blood samples of the subjects and stored at  $-20^{\circ}\text{C}$  until analysis. Use the E.Z.N.A.TM Blood DNA Midi kit (D3494, Omega)

to extract and purify the genomic DNA following the standard protocol of the kit.

Genetic polymorphisms were screened by the 1000 Genomes Project (<http://www.internationalgenome.org/>). Haploview 4.2 was used to select according to CHB and CHS, and the minimum allele frequency (Minor Allele Frequency (MAF)) was greater than 5%. At last, we selected two PVT1 tagSNPs (rs10956390 and rs80177647).

Genomic DNA was diluted to working concentrations of 20 ng/L for genotyping. The assay was performed utilizing TaqMan™ Genotyping Master Mix (4371355, Thermo) as recommended by the manufacturer. Assay ID for rs10956390 is C\_\_317048\_10 (Thermo), and assay ID for rs80177647 is C\_\_101092625\_10 (Thermo). SNP genotyping was performed by TaqMan real-time PCR system as reported elsewhere. And the reaction was conducted under the following conditions:  $95^{\circ}\text{C}$  for 10 min, followed by 45 two-step cycles of  $95^{\circ}\text{C}$  for 15 s and  $60^{\circ}\text{C}$  for 1 min.

**2.3. Statistical Assay.** Statistical analysis was performed using SPSS 19.0 (version 19.0 for Windows; Chicago, IL, USA). Continuous variables were presented as mean  $\pm$  standard deviation (SD) or the mean  $\pm$  standard error of the mean (SEM). Student *t*-tests were conducted to analyze the differences between two groups, while the significance of differences among multiple groups was evaluated using ANOVA. Hardy-Weinberg Equilibrium (HWE) was done by using  $\chi^2$  test to validate the genotype frequency. Logistic regression was used to determine the association between PVT1 polymorphism and the risk of EH adjusting for multiple EH risk factors, such as the smoking history and blood glucose. In genetic association analysis, we used additive, dominant, and recessive genetic models. A two-tailed *P* value  $< 0.05$  was considered as statistically significant.

## 3. Results

**3.1. The Baseline Characteristics of the Subjects.** The demographic and clinical characteristics of EH and control subjects were shown in Table 1. A total of 963 subjects (535 males, 428 females), with a mean age of  $53 \pm 8$  years old, were selected including 524 EH patients and 439 control subjects. In cases, there are 261 and 263 EH patients from the south and north of China, respectively. The distribution of smoking history and the mean of body mass index (BMI,  $P < 0.001$ ), fasting blood glucose (FBG,  $P < 0.001$ ), serum low-density lipoprotein cholesterol (LDL-C,  $P < 0.001$ ), systolic blood pressure (SBP,  $P < 0.001$ ), diastolic blood pressure (DBP,  $P < 0.001$ ), and total cholesterol (TC,  $P < 0.001$ ) were also significantly different between cases and controls. However, triglyceride (TG,  $P = 0.412$ ) is no significant association between cases and controls in the north of China, and high-density lipoprotein cholesterol (HDL-C,  $P = 0.714$ ) is no significant association between cases and controls in the south of China.

Genotype distribution of the PVT1 rs10956390 and rs80177647 polymorphisms in both controls and EH patients were in agreement with the Hardy-Weinberg Equilibrium (Table 2).

TABLE 1: General characteristics of the EH case and control population.

Characteristics	The south of China			The north of China			Total		
	Control	EH	P	Control	EH	P	Control	EH	P
Gender	294	261		145	263		439	524	
Male (%)	173 (46.6%)	157 (60.2%)		75 (51.7%)	130 (49.4%)		248 (56.5%)	287 (54.8%)	
Female (%)	121 (53.4%)	104 (39.8%)	0.754	70 (48.3%)	133 (50.6%)	0.658	191 (43.5%)	237 (45.2%)	0.593
Age (years)	52 ± 8	54 ± 8.0	0.098	53 ± 9	53 ± 8	0.844	53 ± 8	53 ± 8	0.223
BMI (kg/m <sup>2</sup> )	22.20 ± 1.63	24.76 ± 2.71	< 0.001	22.64 ± 1.84	24.94 ± 3.34	< 0.001	22.35 ± 1.71	24.85 ± 3.04	< 0.001
SBP (mmHg)	120 ± 12	136 ± 20	< 0.001	122 ± 10	138 ± 19	< 0.001	120 ± 11	137 ± 19	< 0.001
DBP (mmHg)	76 ± 8	85 ± 13	< 0.001	75 ± 9	80 ± 13	< 0.001	76 ± 8	83 ± 13	< 0.001
Smoking history (%)	38 (12.9%)	63 (24.1%)	0.001	20 (13.8%)	80 (30.4%)	< 0.001	58 (13.2%)	143 (27.3%)	< 0.001
FBG, mmol/L	4.54 ± 0.48	5.4 ± 1.17	< 0.001	4.75 ± 1.49	5.5 ± 0.87	< 0.001	4.61 ± 0.95	5.45 ± 1.03	< 0.001
TG, mmol/L	1.30 ± 0.46	1.86 ± 1.99	< 0.001	1.36 ± 0.43	1.41 ± 0.72	0.412	1.32 ± 0.45	1.64 ± 0.89	< 0.001
TC, mmol/L	4.42 ± 0.62	4.83 ± 0.92	< 0.001	4.22 ± 0.63	4.57 ± 0.97	< 0.001	4.36 ± 0.63	4.70 ± 0.95	< 0.001
HDL-C, mmol/L	1.27 ± 0.35	1.28 ± 0.41	0.741	1.26 ± 0.33	1.36 ± 0.52	0.013	1.26 ± 0.34	1.32 ± 0.47	0.032
LDL-C, mmol/L	2.52 ± 0.62	2.74 ± 0.81	< 0.001	2.19 ± 0.52	2.41 ± 0.75	< 0.001	2.41 ± 0.61	2.58 ± 0.80	< 0.001

EH: essential hypertension; BMI: body mass index; SBP: systolic blood pressure; DBP: diastolic blood pressure; FBG: fasting blood glucose; TC: total cholesterol; TG: triglyceride; HDL-C: high-density lipoprotein cholesterol; LDL-C: low-density lipoprotein cholesterol.

3.2. Association of PVT1 rs10956390 C>T and rs80177647 T>A Polymorphisms and Risk for EH in the South of China. Table 3 shows the association between PVT1 polymorphisms and EH risk in the south of China. Logistic regression analysis showed that rs10956390 CT and TT genotypes were associated with decreased risk of EH (additive model: CT: odds ratio (OR) = 0.657, 95% confidence interval (CI) = 0.445-0.968, P = 0.034; TT: OR = 0.571, 95% CI = 0.355-0.918, P = 0.021; dominant model: OR = 0.629, 95% CI = 0.437-0.906, P = 0.013). However, no significant association was observed after adjustment for age, gender, BMI, smoking history, FBG, and dyslipidemia.

In addition, we also found that rs80177647 A allele was associated with increased risk of EH (additive model: TA: OR = 1.855, 95% CI = 1.181-2.914, P = 0.007; recessive model: OR = 1.842, 95% CI = 1.188-2.855, P = 0.006). Moreover, the adjusted result was also significant (additive model: TA: OR = 1.950, 95% CI = 1.023-3.781, P = 0.042; dominant model: OR = 1.956, 95% CI = 1.041-3.676, P = 0.037).

3.3. Association of PVT1 rs10956390 C>T and rs80177647 T>A Polymorphisms and Risk for EH in the North of China. Logistic regression analyses revealed that EH risk was decreased significantly in carriers of T allele of rs10956390 polymorphism than CC genotype (additive model: CT: OR = 0.525, 95% CI = 0.321-0.860, P = 0.010; TT: OR = 0.402, 95% CI = 0.228-0.712, P = 0.002; dominant model: OR = 0.480, 95% CI = 0.303-0.762, P = 0.002; recessive model: OR = 0.595, 95% CI = 0.370-0.957, P = 0.032) as shown in Table 4. And after adjustment, the association was still significant (additive model: CT: OR = 0.409, 95% CI = 0.221-0.757, P = 0.004; TT: OR = 0.341, 95% CI = 0.168-0.693, P = 0.003; dominant model: OR = 0.384, 95% CI = 0.216-0.684, P = 0.001).

While compared with TT genotype of rs80177647, A allele carriers have increased EH risk (additive model: TA:

TABLE 2: Test results of Hardy-Weinberg Equilibrium among all PVT1 gene sites.

Site	South of China				North of China			
	Control		EH		Control		EH	
	$\chi^2$	P	$\chi^2$	P	$\chi^2$	P	$\chi^2$	P
rs10956390	0.06	0.81	0.78	0.38	0.05	0.83	3.09	0.08
rs80177647	1.30	0.25	0.001	0.96	1.53	0.22	0.11	0.74

OR = 2.119, 95% CI = 1.210-3.711, P = 0.009; dominant model: OR = 2.100, 95% CI = 1.226-3.596, P = 0.007). However, no significant association was observed after adjustment.

3.4. Association of PVT1 Polymorphisms and Risk for EH in China. Then, we aggregated and analyzed all the data from the two centers in southern and northern China. We found that the polymorphisms of the two SNPs of PVT1 were associated with the risk of EH. Logistic regression analysis showed that rs10956390 CT and TT genotypes were associated with decreased risk of EH (additive model: CT: OR = 0.596, 95% CI = 0.442-0.804, P = 0.001; TT: OR = 0.502, 95% CI = 0.350-0.718, P < 0.001; dominant model: OR = 0.564, 95% CI = 0.426-0.747, P < 0.001; recessive model: OR = 0.688, 95% CI = 0.506-0.936, P = 0.017, Table 5). And after adjustment, the association was still significant (additive model: CT: OR = 0.488, 95% CI = 0.326-0.729, P < 0.001; TT: OR = 0.460, 95% CI = 0.286-0.740, P = 0.001; dominant model: OR = 0.478, 95% CI = 0.328-0.698, P < 0.001).

Rs80177647 has similar results. The TA genotype and the dominant model showed stronger relations with higher EH risk (P < 0.001, OR = 1.993, 95% CI = 1.410-2.816; P < 0.001, OR = 1.986, 95% CI = 1.422-2.774, respectively). When adjusted for EH risk factors, including age, gender, BMI, smoking history, FBG, and dyslipidemia, the significant association between PVT1 rs80177647 was also



TABLE 3: Association between lncRNA PVT1 polymorphisms and EH risk in the south of China.

Models	Genotypes	Control, <i>n</i> = 294 (%)	EH, <i>n</i> = 261 (%)	Unadjusted OR (95% CI)	<i>P</i> value	*Adjusted OR (95% CI)	*Adjusted <i>P</i> value
rs10956390							
Additive	CC	75 (25.5)	92 (35.2)	1.00 (reference)		1.00 (reference)	
	CT	149 (50.7)	120 (46.0)	0.657 (0.445-0.968)	0.034	0.610 (0.340-1.094)	0.097
	TT	70 (23.8)	49 (18.8)	0.571 (0.355-0.918)	0.021	0.657 (0.319-1.354)	0.254
Dominant	CC	75 (25.5)	92 (35.2)	1.00 (reference)		1.00 (reference)	
	CT/TT	119 (74.5)	169 (64.8)	0.629 (0.437-0.906)	0.013	0.623 (0.357-1.085)	0.094
Recessive	CC/CT	224 (76.2)	212 (81.2)	1.00 (reference)		1.00 (reference)	
	TT	70 (23.8)	49 (18.8)	0.740 (0.491-1.115)	0.150	0.911 (0.494-1.680)	0.766
rs80177647							
Additive	TT	253 (86.1)	201 (77.0)	1.00 (reference)		1.00 (reference)	
	TA	38 (12.9)	56 (21.5)	1.855 (1.181-2.914)	0.007	1.950 (1.023-3.718)	0.042
	AA	3 (1.0)	4 (1.5)	1.678 (0.371-7.585)	0.501	2.063 (0.183-23.305)	0.558
Dominant	TT	253 (86.1)	201 (77.0)	1.00 (reference)		1.00 (reference)	
	TA/AA	41 (13.9)	60 (23.0)	1.842 (1.188-2.855)	0.006	1.956 (1.041-3.676)	0.037
Recessive	TT/TA	291 (99.0)	257 (98.5)	1.00 (reference)		1.00 (reference)	
	AA	3 (1.0)	4 (1.5)	1.510 (0.335-6.809)	0.592	1.843 (0.163-20.785)	0.621

OR: odd ratio; CI: confidence interval; EH: essential hypertension. \*Adjusted for age, gender, BMI, smoking history, FBG, and dyslipidemia.

TABLE 4: Association between lncRNA PVT1 polymorphisms and EH risk in the north of China.

Models	Genotypes	Control, <i>n</i> = 145 (%)	EH, <i>n</i> = 263 (%)	Unadjusted OR (95% CI)	<i>P</i> value	*Adjusted OR (95% CI)	*Adjusted <i>P</i> value
rs10956390							
Additive	CC	33 (22.8)	100 (38.0)	1.00 (reference)		1.00 (reference)	
	CT	71 (48.3)	113 (43.0)	0.525 (0.321-0.860)	0.010	0.409 (0.221-0.757)	0.004
	TT	41 (28.3)	50 (19.0)	0.402 (0.228-0.712)	0.002	0.341 (0.168-0.693)	0.003
Dominant	CC	33 (22.8)	100 (38.0)	1.00 (reference)		1.00 (reference)	
	CT/TT	112 (77.2)	163 (62.0)	0.480 (0.303-0.762)	0.002	0.384 (0.216-0.684)	0.001
Recessive	CC/CT	104 (71.7)	223 (81.0)	1.00 (reference)		1.00 (reference)	
	TT	41 (28.3)	50 (19.0)	0.595 (0.370-0.957)	0.032	0.598 (0.333-1.072)	0.084
rs80177647							
Additive	TT	124 (85.5)	194 (73.8)	1.00 (reference)		1.00 (reference)	
	TA	19 (13.1)	63 (24.0)	2.119 (1.210-3.711)	0.009	1.535 (0.802-2.938)	0.196
	AA	2 (1.4)	6 (2.3)	1.918 (0.381-9.652)	0.430	0.734 (0.109-4.944)	0.751
Dominant	TT	124 (85.5)	194 (73.8)	1.00 (reference)		1.00 (reference)	
	TA/AA	21 (14.5)	69 (26.3)	2.100 (1.226-3.596)	0.007	1.449 (0.775-2.710)	0.246
Recessive	TT/TA	143 (98.6)	257 (97.7)	1.00 (reference)		1.00 (reference)	
	AA	2 (1.4)	6 (2.3)	1.669 (0.333-8.379)	0.534	0.664 (0.098-4.483)	0.674

OR: odd ratio; CI: confidence interval; EH: essential hypertension. \*Adjusted for age, gender, BMI, smoking history, FBG, and dyslipidemia.

observed (additive model: TA: OR = 1.768, 95% CI = 1.144-2.731, *P* = 0.10; dominant model: OR = 1.723, 95% CI = 1.128-2.631, *P* = 0.012).

**3.5. Influence of PVT1 rs10956390 C>T and rs80177647 T>A Polymorphisms of Lipid Levels in Subjects.** Lipid levels, such as triglyceride, total cholesterol, high-density lipoprotein, and low-density lipoprotein were determined in 963 EH patients and normal controls. Moreover, the effects of rs10956390 and

rs80177647 of PVT1 genotypes on lipid levels were analyzed. In controls, TG levels in CT and TT genotypes were significantly lower than those in subjects for rs10956390 CC genotype (\**P* < 0.05, Figure 1(a)). And in EH patients, TG levels in TT genotype were lower than CT genotype (#*P* < 0.05, Figure 1(a)). More interestingly, we found that HDL-C levels in CT and TT genotypes were higher than CC genotype in control and EH patients, respectively (\**P* < 0.05, \*\**P* < 0.01, Figure 1(c)). What is more, the levels of LDL-C were lower in

TABLE 5: Association between lncRNA PVT1 polymorphisms and EH risk in China.

Models	Genotypes	Control, <i>n</i> = 439 (%)	EH, <i>n</i> = 524 (%)	Unadjusted OR (95% CI)	<i>P</i> value	*Adjusted OR (95% CI)	*Adjusted <i>P</i> value
<b>rs10956390</b>							
Additive	CC	108 (24.6)	192 (36.6)	1.00 (reference)		1.00 (reference)	
	CT	220 (50.1)	233 (44.5)	0.596 (0.442-0.804)	0.001	0.488 (0.326-0.729)	<0.001
	TT	111 (25.3)	99 (18.9)	0.502 (0.350-0.718)	<0.001	0.460 (0.286-0.740)	0.001
Dominant	CC	108 (24.6)	192 (36.6)	1.00 (reference)		1.00 (reference)	
	CT/TT	331 (75.4)	332 (63.4)	0.564 (0.426-0.747)	<0.001	0.478 (0.328-0.698)	<0.001
Recessive	CC/CT	328 (74.7)	425 (81.1)	1.00 (reference)		1.00 (reference)	
	TT	111 (25.3)	99 (18.9)	0.688 (0.506-0.936)	0.017	0.721 (0.483-1.077)	0.110
<b>rs80177647</b>							
Additive	TT	377 (85.9)	395 (75.4)	1.00 (reference)		1.00 (reference)	
	TA	57 (13.0)	119 (22.7)	1.993 (1.410-2.816)	<0.001	1.768 (1.144-2.731)	0.010
	AA	5 (1.1)	10 (1.9)	1.909 (0.646-5.636)	0.242	1.170 (0.250-5.40)	0.842
Dominant	TT	377 (85.9)	395 (75.4)	1.00 (reference)		1.00 (reference)	
	TA/AA	62 (14.1)	129 (24.6)	1.986 (1.422-2.774)	<0.001	1.723 (1.128-2.631)	0.012
Recessive	TT/TA	434 (98.9)	514 (98.1)	1.00 (reference)		1.00 (reference)	
	AA	5 (1.1)	10 (1.9)	1.689 (0.573-4.978)	0.342	1.045 (0.221-4.927)	0.956

OR: odd ratio; CI: confidence interval; EH: essential hypertension. \*Adjusted for age, gender, BMI, smoking history, FBG, and dyslipidemia.

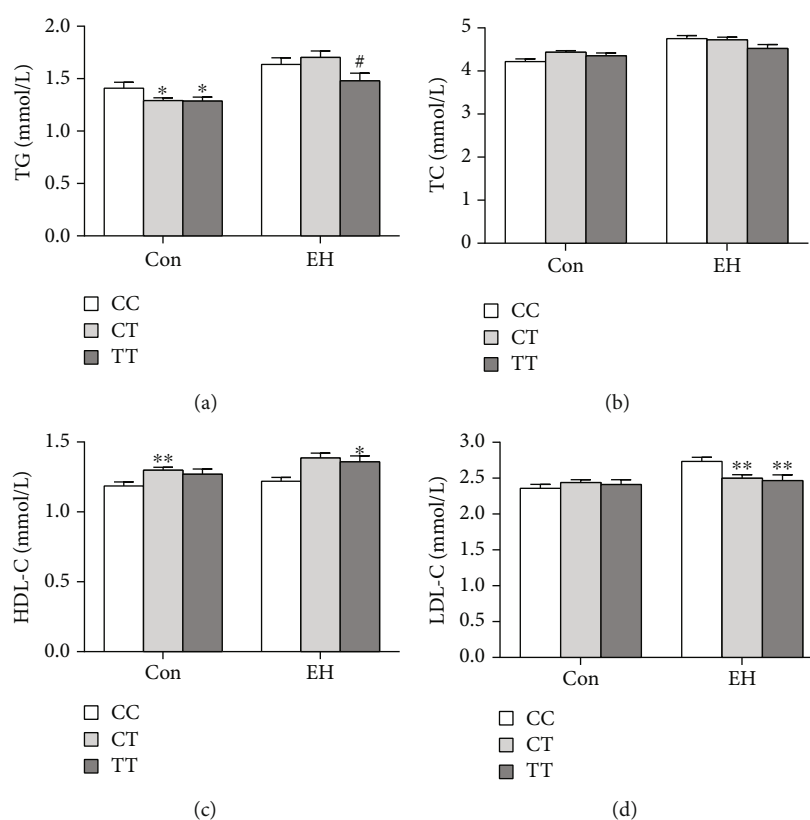


FIGURE 1: Influence of PVT1 rs10956390 polymorphism on lipid level of subjects: (a) TG; (b) TC; (c) HDL-C; (d) LDL-C. (Data are expressed as the mean  $\pm$  SEM. Control: CC, *n* = 108, CT, *n* = 220, TT, *n* = 111; EH: CC, *n* = 192, CT, *n* = 233, TT, *n* = 99. \**P* < 0.05, \*\**P* < 0.01, as compared with CC genotype in interclass; #*P* < 0.05, as compared with CT genotype in interclass).

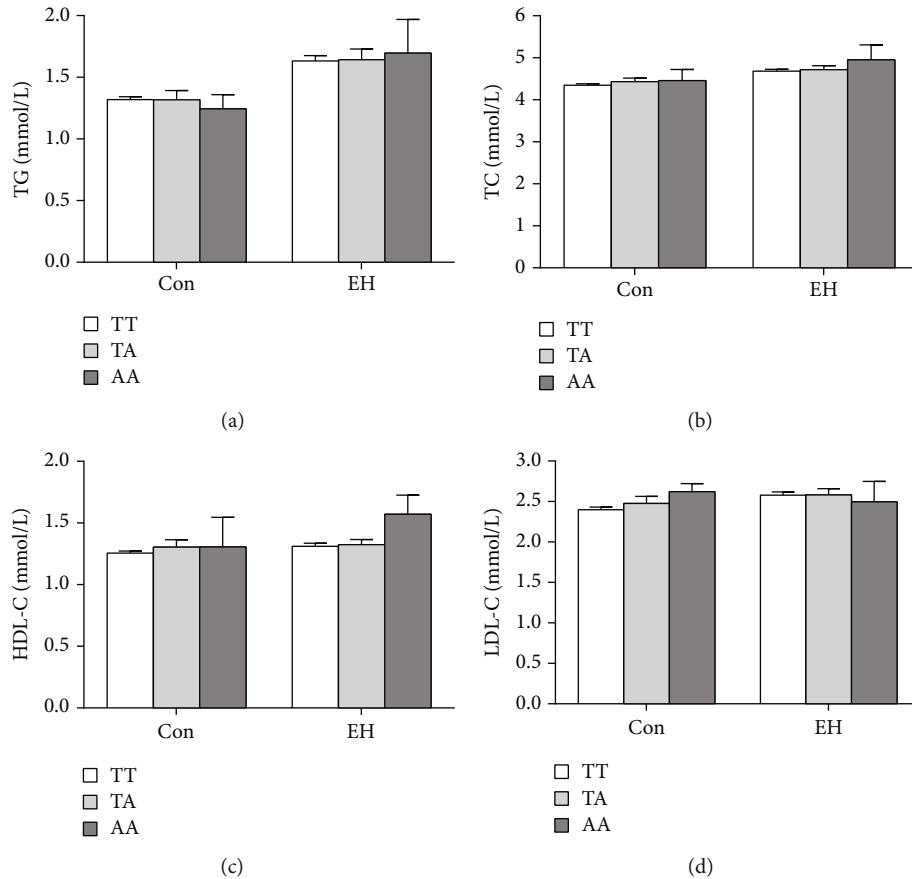


FIGURE 2: Influence of PVT1 rs80177647 polymorphism on lipid level of subjects: (a) TG; (b) TC; (c) HDL-C; (d) LDL-C. (Data are expressed as the mean  $\pm$  SEM. Control: TT,  $n = 377$ , TA,  $n = 57$ , AA,  $n = 5$ ; EH: TT,  $n = 395$ , TA,  $n = 119$ , AA,  $n = 10$ .)

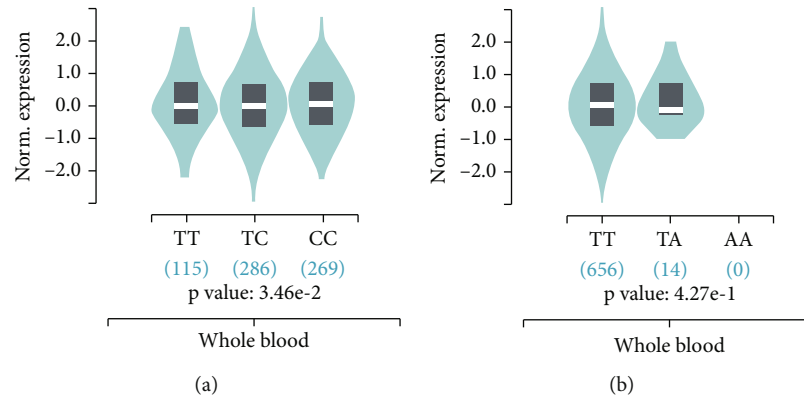


FIGURE 3: Effect of PVT1 mRNA expression in whole blood from healthy normal donors: (a) rs10956390; (b) rs80177647.

CT and TT genotypes in EH patients (\*\* $P < 0.01$ , compared with CC genotype, Figure 1(c)). However, by comparing the correlation between rs80177647 and lipid level in different subjects, we did not find significant differences between lipid levels and genotypes (Figure 2).

**3.6. Association of PVT1 rs10956390 and rs80177647 Polymorphisms with PVT1 Expression.** The Genotype-Tissue Expression (GTEx) project is one of the most widely used resources for studying the relationship between genetic varia-

tion and gene expression. This dataset contains genotype data from 838 postmortem donors and 17,382 RNA-seq samples across 54 tissue sites and 2 cell lines. We accessed the database to determine whether rs10956390 and rs80177647 polymorphisms were associated with PVT1 expression in multitissue through the GTEx eQTL Dashboard (<https://www.gtexportal.org/home/eqtlDashboardPage>). As shown in Figure 3(a), rs10956390 T allele was associated with decreased PVT1 mRNA in whole blood from 670 healthy donors (the relative expression median: TT: -0.04297, TC: -0.05181, CC: 0.02802,

$P = 0.0346$ ). But there was no significant difference between rs80177647 polymorphism and PVT1 mRNA expression (Figure 3(b),  $P = 0.427$ ).

#### 4. Discussion

This study reveals, for the first time, there is an association between rs80177647 and rs10956390 gene polymorphisms of PVT1 and the risk of essential hypertension in two populations in southern and northern China. Our results demonstrated that EH risk was significantly decreased in carriers of T allele of rs10956390 polymorphism than those with the CC genotype. In addition, we also found that EH risk was significantly increased in carriers of A allele of rs80177647 polymorphism than those with TT.

The majority of studies in the past have focused on the relationship between PVT1 and the occurrence and development of various cancers. It is reported that PVT1 is typically upregulated in many types of cancer samples [20]. Some of those have found that PVT1 was involved in the regulation of angiogenesis in tumor tissues. Ma et al. showed that PVT1 overexpression promoted the proliferation, migration, and angiogenesis of glioma vascular endothelial cells [21]. However, a few recent studies have implied that PVT1 was involved in cardiovascular diseases. For instance, PVT1 acted as a sponge for miR-128-3p to facilitate Sp1 expression, resulting in activating the TGF- $\beta$ 1/Smad signaling pathway and regulating the development of atrial fibrosis [22]. Zhang et al. also found that PVT1 expression was significantly upregulated in abdominal aortic tissues from AAA patients, and knockdown PVT1 in AngII-induced AAA murine model suppresses VSMC apoptosis, ECM disruption, and serum proinflammatory cytokine level [23]. Strikingly, Quan et al. revealed that PVT1 was proved to be an independent risk factor for coronary atherosclerosis disease [24]. Thus, all those researches indicated the role of PVT1 involved in diseases is related to angiogenesis and endothelial dysfunction.

Previous studies in the association between PVT1 polymorphisms and diseases were only reported in the field of cancer and kidney disease. Our present data found two new SNP loci, rs10956390 and rs80177647, which polymorphisms were related to the risk of EH in Chinese population. However, the underlying mechanism is still unclear. lncRNAs play crucial roles in many human diseases; their structure and subcellular localization determine their functions [25]. A large amount of evidence has been demonstrated that the causality relationship between higher grade disequilibrium in endothelial homeostasis and diabetes or hypertension. The risky factors from vascular endothelial cell including reduced plasma nitric oxide level, suppressed L-arginine/endothelial nitric oxide synthase (eNOS) pathway, generation of reactive oxygen species (ROS), and enhanced leukocyte adhesion to the vascular wall may cooperatively contribute to the pathogenesis and progress of EH [26]. In our study, there were significant differences in TG, LDL-C, and HDL-C levels among rs10956390. Similarly, Wang et al. revealed that APOE-E3 homozygote and APOE-E4 allele were related to elevated triglycerides level; in addition, APOE-E2 allele was correlated with increased serum UA level

in patients with hypertension or coronary heart disease [27]. Pan et al. found that ACE2 rs4646188 and rs879922 were associated with increased LDL-C level, while rs2106809 and rs4646188 were associated with hypertriglyceridemia [28]. The evidence we mentioned above demonstrates that different alleles in one gene may affect blood lipids differently. Most importantly, numerous studies have been revealed that there is a positive correlation between dyslipidemia and hypertension [29, 30]. A newly published study found that PVT1 was upregulated in the adipose tissue of obese mice and accelerated lipid accumulation by increasing the expression of peroxisome proliferator-activated receptor  $\gamma$ , CCAAT/enhancer-binding protein  $\alpha$ , and adipocyte protein 2. In addition, PVT1 promoted fatty acid synthesis and inhibited fatty acid oxidation [17]. Based on all those studies and our data, we speculate that PVT1 may affect the risk of EH by regulating human blood lipid levels.

Several limitations of this study should be considered. Firstly, a limited number of samples were chosen in this study. Secondly, only the association between the PVT1 polymorphisms of the two loci, the risks of EH and plasma lipid levels have been investigated. However, the precise mechanism of how PVT1 influences lipid level in vivo or in vitro has not been studied. Further mechanism studies and larger population-based prospective studies are required.

#### 5. Conclusion

In summary, our study demonstrates firstly that the PVT1 rs10956390 and rs80177647 polymorphisms are associated with the risk of EH in Chinese population. We speculate that the rs10956390 polymorphism is responsible for dyslipidemia. PVT1 is a potential biomarker and target for therapeutic strategies in EH. Further investigations in larger cohorts are needed to confirm our findings. More functional experiments are also required to illuminate the function role of rs10956390 and rs80177647 polymorphisms.

#### Data Availability

The research data used to support the findings of this study are available from the corresponding author upon request.

#### Conflicts of Interest

The authors declare that they have no competing interests.

#### Authors' Contributions

DBK and RL conceived and designed the experiments. XY, YC, and MLX performed the experiments. MLZ, ZSY, and YLX analyzed the data. RL and XY contributed reagents/materials/analysis tools. DBK wrote the paper. All authors read and approved the final manuscript.

#### Acknowledgments

This work was supported by research grants of the National Natural Science Foundation of China (No. 81803767), the Hunan Provincial Natural Science Foundation of China



(No. 2021JJ40617), the Hospital Pharmacy Research Funds of Hunan Pharmaceutical Association (2020YXH005), the Science and Technology Project of Hengyang City (202010031549), the Self-financing Scientific Research Project of Guangxi Health Commission (grant number Z20201003), and the Hospital Management Research and Reform Project of University of South China (2019YYGL02).

## References

- [1] “Global, regional, and national age-sex specific mortality for 264 causes of death, 1980–2016: a systematic analysis for the Global Burden of Disease Study 2016,” *Lancet*, vol. 390, no. 10100, pp. 1151–1210, 2017.
- [2] D. Colomba, G. Duro, S. Corrao et al., “Endothelial nitric oxide synthase gene polymorphisms and cardiovascular damage in hypertensive subjects: an Italian case-control study,” *Immunity & Ageing*, vol. 5, no. 1, p. 4, 2008.
- [3] P. J. Batista and H. Y. Chang, “Long noncoding RNAs: cellular address codes in development and disease,” *Cell*, vol. 152, no. 6, pp. 1298–1307, 2013.
- [4] M. Zeng, C. Lu, F. Zhang et al., “SDLDA: lncRNA-disease association prediction based on singular value decomposition and deep learning,” *Methods*, vol. 179, pp. 73–80, 2020.
- [5] C. Y. Liu, Y. H. Zhang, R. B. Li et al., “LncRNA CAIF inhibits autophagy and attenuates myocardial infarction by blocking p53-mediated myocardial transcription,” *Nature Communications*, vol. 9, no. 1, p. 29, 2018.
- [6] L. Shi, C. Tian, L. Sun, F. Cao, and Z. Meng, “The lncRNA TUG1/miR-145-5p/FGF10 regulates proliferation and migration in VSMCs of hypertension,” *Biochemical and Biophysical Research Communications*, vol. 501, no. 3, pp. 688–695, 2018.
- [7] M. Xiao, Y. Feng, C. Liu, and Z. Zhang, “Prognostic values of long noncoding RNA PVT1 in various carcinomas: an updated systematic review and meta-analysis,” *Cell Proliferation*, vol. 51, no. 6, article e12519, 2018.
- [8] L. You, H. Wang, G. Yang et al., “Gemcitabine exhibits a suppressive effect on pancreatic cancer cell growth by regulating processing of PVT1 to miR1207,” *Molecular Oncology*, vol. 12, no. 12, pp. 2147–2164, 2018.
- [9] Z. Chang, J. Cui, and Y. Song, “Long noncoding RNA PVT1 promotes EMT via mediating microRNA-186 targeting of Twist1 in prostate cancer,” *Gene*, vol. 654, pp. 36–42, 2018.
- [10] Y. Wang, X. Li, W. Liu et al., “MicroRNA-1205, encoded on chromosome 8q24, targets EGLN3 to induce cell growth and contributes to risk of castration-resistant prostate cancer,” *Oncogene*, vol. 38, no. 24, pp. 4820–4834, 2019.
- [11] Z. Tian, S. Cao, C. Li et al., “LncRNA PVT1 regulates growth, migration, and invasion of bladder cancer by miR-31/CDK1,” *Journal of Cellular Physiology*, vol. 234, no. 4, pp. 4799–4811, 2019.
- [12] L. Yang, X. Peng, H. Jin, and J. Liu, “Long non-coding RNA PVT1 promotes autophagy as ceRNA to target ATG3 by sponging microRNA-365 in hepatocellular carcinoma,” *Gene*, vol. 697, pp. 94–102, 2019.
- [13] J. Zhao, P. du, P. Cui et al., “LncRNA PVT1 promotes angiogenesis via activating the STAT3/VEGFA axis in gastric cancer,” *Oncogene*, vol. 37, no. 30, pp. 4094–4109, 2018.
- [14] J. Zheng, L. Hu, J. Cheng et al., “LncRNA PVT1 promotes the angiogenesis of vascular endothelial cell by targeting miR26b to activate CTGF/ANGPT2,” *International Journal of Molecular Medicine*, vol. 42, no. 1, pp. 489–496, 2018.
- [15] B. Sun, M. Meng, J. Wei, and S. Wang, “Long noncoding RNA PVT1 contributes to vascular endothelial cell proliferation via inhibition of miR-190a-5p in diagnostic biomarker evaluation of chronic heart failure,” *Experimental and Therapeutic Medicine*, vol. 19, no. 5, pp. 3348–3354, 2020.
- [16] J. Guo, J. Li, J. Zhang et al., “LncRNA PVT1 knockdown alleviated ox-LDL-induced vascular endothelial cell injury and atherosclerosis by miR-153-3p/GRB2 axis via ERK/p38 pathway,” *Nutrition, Metabolism, and Cardiovascular Diseases*, vol. 31, no. 12, pp. 3508–3521, 2021.
- [17] L. Zhang, D. Zhang, Z. Y. Qin, J. Li, and Z. Y. Shen, “The role and possible mechanism of long noncoding RNA PVT1 in modulating 3T3-L1 preadipocyte proliferation and differentiation,” *IUBMB Life*, vol. 72, no. 7, pp. 1460–1467, 2020.
- [18] G. Seravalle and G. Grassi, “Obesity and hypertension,” *Pharmacological Research*, vol. 122, pp. 1–7, 2017.
- [19] Y. Lu, W. Yuan, L. Wang et al., “Contribution of lncRNA CASC8, CASC11, and PVT1 genetic variants to the susceptibility of coronary heart disease,” *Journal of Cardiovascular Pharmacology*, vol. 77, no. 6, pp. 756–766, 2021.
- [20] D. Guo, Y. Wang, K. Ren, and X. Han, “Knockdown of lncRNA PVT1 inhibits tumorigenesis in non-small-cell lung cancer by regulating miR-497 expression,” *Experimental Cell Research*, vol. 362, no. 1, pp. 172–179, 2018.
- [21] Y. Ma, P. Wang, Y. Xue et al., “PVT1 affects growth of glioma microvascular endothelial cells by negatively regulating miR-186,” *Tumour Biology*, vol. 39, no. 3, p. 1010428317694326, 2017.
- [22] F. Cao, Z. Li, W. M. Ding, L. Yan, and Q. Y. Zhao, “LncRNA PVT1 regulates atrial fibrosis via miR-128-3p-SP1-TGF- $\beta$ 1-Smad axis in atrial fibrillation,” *Molecular Medicine*, vol. 25, no. 1, p. 7, 2019.
- [23] Z. Zhang, G. Zou, X. Chen et al., “Knockdown of lncRNA PVT1 inhibits vascular smooth muscle cell apoptosis and extracellular matrix disruption in a murine abdominal aortic aneurysm model,” *Molecules and Cells*, vol. 42, no. 3, pp. 218–227, 2019.
- [24] W. Quan, P. F. Hu, X. Zhao, C. G. Lianhua, and B. R. Batu, “Expression level of lncRNA PVT1 in serum of patients with coronary atherosclerosis disease and its clinical significance,” *European Review for Medical and Pharmacological Sciences*, vol. 24, no. 11, pp. 6333–6337, 2020.
- [25] M. Zeng, Y. Wu, C. Lu, F. Zhang, F. X. Wu, and M. Li, “DeepLncLoc: a deep learning framework for long non-coding RNA subcellular localization prediction based on subsequence embedding,” *Briefings in Bioinformatics*, 2021.
- [26] H. N. Zhang, Q. Q. Xu, A. Thakur et al., “Endothelial dysfunction in diabetes and hypertension: role of microRNAs and long non-coding RNAs,” *Life Sciences*, vol. 213, pp. 258–268, 2018.
- [27] C. Wang, W. Yan, H. Wang, J. Zhu, and H. Chen, “APOE polymorphism is associated with blood lipid and serum uric acid metabolism in hypertension or coronary heart disease in a Chinese population,” *Pharmacogenomics*, vol. 20, no. 14, pp. 1021–1031, 2019.
- [28] Y. Pan, T. Wang, Y. Li et al., “Association of ACE2 polymorphisms with susceptibility to essential hypertension and dyslipidemia in Xinjiang, China,” *Lipids in Health and Disease*, vol. 17, no. 1, p. 241, 2018.

- [29] T. Otsuka, H. Takada, Y. Nishiyama et al., “Dyslipidemia and the risk of developing hypertension in a working-age male population,” *Journal of the American Heart Association*, vol. 5, no. 3, article e003053, 2016.
- [30] C. Borghi, F. Rodriguez-Artalejo, G. de Backer et al., “The association between blood pressure and lipid levels in Europe,” *Journal of Hypertension*, vol. 34, no. 11, pp. 2155–2163, 2016.

## Research Article

# Analyses of Long Noncoding RNA and mRNA Profiles in Subjects with the Phlegm-Dampness Constitution

Lidan Dong <sup>1</sup>, Yanfei Zheng <sup>1</sup>, Dan Liu <sup>2</sup>, Fuhong He <sup>2</sup>, Kaiki Lee <sup>1</sup>, Lingru Li <sup>1</sup>, and Qi Wang <sup>1</sup>

<sup>1</sup>National Institute of Traditional Chinese Medicine Constitution and Preventive Medicine, Beijing University of Chinese Medicine, Beijing 100029, China

<sup>2</sup>Key Laboratory of Genomics and Precision Medicine, Collaborative Innovation Center of Genetics and Development, Beijing Institute of Genomics, Chinese Academy of Sciences, Beijing 100101, China

Correspondence should be addressed to Lingru Li; [lingru912@163.com](mailto:lingru912@163.com) and Qi Wang; [wangqi710@126.com](mailto:wangqi710@126.com)

Received 15 April 2021; Accepted 2 November 2021; Published 10 December 2021

Academic Editor: Lei Chen

Copyright © 2021 Lidan Dong et al. This is an open access article distributed under the Creative Commons Attribution License, which permits unrestricted use, distribution, and reproduction in any medium, provided the original work is properly cited.

**Background.** Constitution in traditional Chinese medicine (TCM) plays a key role in the genesis, development, and prognosis of diseases. Phlegm-dampness constitution (PDC) is one of the nine constitutions in TCM, susceptible to metabolic disorders, which is mainly manifested by profuse phlegm, loose abdomen, and greasy face. Epidemiologic, genomic, and epigenetic studies have been carried out in previous works, confirming that PDC represents a distinctive population with microcosmic changes related to metabolic disorders. However, whether long noncoding RNAs (lncRNAs) play a regulatory role in metabolic disease in subjects with PDC remains largely unknown. We aimed to investigate distinct lncRNA and mRNA expression signatures and lncRNA-mRNA regulatory networks in the phlegm-dampness constitution (PDC). **Methods.** The peripheral blood mononuclear cells (PBMCs) were isolated from the subjects with PDC ( $n = 13$ ) and balanced constitution (BC) ( $n = 9$ ). The profiles of lncRNAs and mRNAs in PBMCs were analyzed using microarray and further validated with RT-qPCR. Subsequently, pathway analysis was performed to investigate the function of differentially expressed mRNAs by using Ingenuity Pathway Analysis (IPA). **Results.** Results suggested that some mRNAs, which were regulated by the differentially expressed lncRNAs, were mainly enriched in lipid metabolism and immune inflammation-related pathways. This was consistent with the molecular characteristics of previous studies, indicating that the clinical characteristics of metabolic disorders in PDC might be regulated by lncRNAs. Furthermore, by making coexpression network construction as well as *cis*-regulated target gene analysis, several lncRNA-mRNA pairs with potential regulatory relationships were identified by bioinformatic analyses, including RP11-317J10.2-CA3, RP11-809C18.3-PIP4K2A, LINC0069-RFTN1, TTTY15-ARHGEF9, and AC135048.13-ORAI3. **Conclusions.** This study first revealed that the expression characteristics of lncRNAs/mRNAs may be potential biomarkers, indicating that the distinctive physical and clinical characteristics of PDC might be partially attributed to the specific expression signatures of lncRNAs/mRNAs.

## 1. Background

Constitution in traditional Chinese medicine (TCM) plays an important role in the initiation, development, and prognosis of diseases. The term “constitution” is coined to indicate the distinct TCM entity or “type.” Based on clinical presentations, healthy people can be classified into nine constitutions according to the concept of TCM, including one

balanced constitution (BC) and eight biased constitutions [1–3]. Each constitution exhibits specific physical features and psychological characteristics, and each biased constitution demonstrates a specific predisposition to certain diseases and should be treated differently. Phlegm-dampness constitution (PDC), which is one of the biased constitutions, is a group of individuals who tend to develop diseases, or those in a dysfunctional/subhealth status but do not reach

the diagnostic criteria for a specified disorder, and these subjects with PDC are usually obese and not considered healthy in modern medicine [4, 5]. Moreover, through years of clinical practice, we summarized the common characteristics of the PDC, including obesity, abundant sputum, greasy and soft lower abdomen, oily skin in the face, chest distress, sticky and sweet taste in the mouth, and slippery pulse [6]. Accumulating evidence has suggested that PDC plays an important role in the prevention stage of multiple metabolic diseases [7, 8]. Therefore, it is necessary to identify which population tends to have the potential risk of metabolic disorders and what molecular markers can be used to identify subjects with PDC.

The epidemiological investigation, single-nucleotide polymorphisms (SNPs), genomics, and methylation investigation have previously confirmed that subjects with PDC belong to a population with clinical features of microcosmic changes related to metabolic disorders [8–10]. A previous study demonstrated that certain differentially expressed genes in the peripheral blood mononuclear cells (PBMCs) of individuals with PDC were associated with the adipocytokine signaling pathway, insulin signaling pathway, and fatty acid elongation in mitochondria [11–13]. In a separate report, methylation in the SQSTM1, DLGAP2, DAB1, HOXC4, and SMPD3 genes were shown to be associated with specific constitution types (diabetes mellitus, obesity, and so on), and differentially methylated genes are abundantly enriched in multiple metabolic pathways [14, 15]. In addition, individuals with PDC, who have specific gene expression signatures (such as SOCS3, ACSL4, CLU, and ABCG1), are more susceptible to metabolic disorders [16].

These previous reports have provided insights into the molecular basis of individuals with PDC; however, the roles of long noncoding RNAs (lncRNAs) in metabolic disorders in the PDC remain poorly understood. lncRNAs are a large group of noncoding transcripts that are more than 200 nucleotides in length [17]. lncRNAs have been extensively reported to be involved in gene regulation and cellular processes through a diversity of mechanisms, such as epigenetic, transcriptional, and posttranscriptional levels [18–20]. Numerous studies have indicated that dysregulation of lncRNAs is highly associated with a wide variety of diseases, such as heart failure, myocardial infarction (MI), cardiovascular disease, and diabetes [21–23]. For example, lncRNAs Gadd7 is necessary for lipid- and general oxidative stress-mediated cell death and its depletion or suppression may be a promising approach to treat or prevent heart failure [24]. A previous study has demonstrated that a small SNP mutation (rs2301523) in MIAT can upregulate the expression of MIAT, leading to a high risk of MI [25]. Besides, Shi and coworkers have reported that lncRNA GAS5 is a target for therapeutic intervention in the management of type 2 diabetes [26]. These previous reports have confirmed that lncRNAs play a crucial role in metabolic disorders. However, the expression patterns, potential targets, and functions of lncRNAs in the development and pathogenesis of the metabolic disorders in subjects with PDC remain largely unexplored.

In the present study, we analyzed the expression profiles of lncRNAs and mRNAs in PBMCs. The key lncRNAs and target genes have the molecular characteristics of metabolic disorder tendency in the PDC, which were verified by RT-qPCR in independent samples. Besides, bioinformatic analyses were performed to reveal the regulatory role of lncRNAs in metabolic disorders of subjects with PDC. Collectively, our study first pointed out which populations with PDC were susceptible to metabolic disease from the perspective of lncRNA.

## 2. Materials and Methods

**2.1. Study Subjects.** Subjects in this study were recruited from the Physical Examination Center, Hong Yi Tang of Traditional Chinese Medicine, in March 2014. This study was performed in compliance with the Declaration of Helsinki, and the research protocol was approved by the ethics committee of the Beijing University of Traditional Chinese Medicine (2012BZHYYL0301). Written informed consent was obtained from all participants. Individuals with BC ( $n = 9$ ) and PDC ( $n = 13$ ) were chosen using a standardized questionnaire (Wang Qi's Body Constitution Classification Questionnaire-Chinese version, frequent code: ZYYXH/T 157-2009) (Table 1) issued by the Chinese Association of Traditional Chinese Medicine and confirmed by Chinese medicine clinical practitioners ( $n = 15$ ). Any differences in the opinions of these practitioners were resolved after careful discussion. The criteria for inclusion and exclusion of patients are as follows:

- (1) The inclusion criteria include the following: (1) natural population aged 18-65 in Beijing; (2) according to the "TCM Constitution Classification and Judgment Standard" approved by the Chinese Academy of Traditional Chinese Medicine, those who meet the judgment criteria of all constitutions and peaceful constitutions; (3) signed informed consent; (4) have no medical diseases, and (5) not taking medication.
- (2) The exclusion criteria include the following: (1) failure to meet diagnostic criteria or inclusion criteria; (2) people with mixed physique; (3) those who have been diagnosed with a chronic disease; and (4) pregnant women.

**2.2. RNA Extraction.** Peripheral blood (6 mL) was collected by phlebotomy and stored in sodium citrate vacuum tubes. The isolation of PBMCs was performed within 4 h after the blood collection by density-gradient centrifugation using Lymphoprep (Sigma, Life Science, USA). The isolated PBMCs were treated with TRIzol reagent (Invitrogen, Carlsbad, CA, USA) to avoid RNA degradation and then stored at  $-80^{\circ}\text{C}$ . Total RNA was extracted and purified from each sample in blood in 2014, according to the manufacturer's instructions. The RNA concentration was determined using a NanoDrop 2000 spectrophotometer (Thermo Fisher Scientific, USA), and the RNA integrity was analyzed by agarose gel electrophoresis.



TABLE 1: Diagnostic standards for the phlegm-dampness constitution (PDC) and balanced constitutions (BC).

Variables	PDC	BC
Main characteristics	Profuse phlegm	Energetic
	Fat body	Without any symptoms or characteristics of other constitutions
	Loose abdomen	Eat well
	Greasy face	Sleep well
Secondary characteristics	Chest distress	Good posture
	Sticky and sweet taste in the mouth	The tongue is pale red with thin white coating
	Slippery pulse	
	The tongue is fat and white with coating	

**2.3. Microarray Analysis.** This experiment was performed technically as a dual channel. Total RNA was hybridized to lncRNA+mRNA Human Gene Expression Microarray V4.0 (4 \* 180 K) (CapitalBio). An improved Eberwine’s linear RNA amplification approach and enzymatic reaction mentioned in a CapitalBio cRNA Amplification and Labeling Kit from CapitalBio were utilized to get greater yields of cDNA labeled with a fluorescent dye (Cy3-dCTP and Cy5-dCTP) [27]. Feature Extraction software (version10.7.1.1) from Agilent Technologies was adopted to produce raw data from array images. The quality control, normalization, and summarization of mRNA and lncRNA data were carried out by using GeneSpring software (v13.0) from Agilent. The differentially expressed lncRNAs (DELncRNAs) and mRNAs (DEmRNAs) were identified based on the fold change and the “limma” package in R software. The mRNAs and lncRNAs with a  $P < 0.05$  and  $|\text{fold change}| \geq 1.5$  were considered differentially expressed in populations with PDC and BC.

**2.4. Coexpression Network of lncRNAs with mRNAs and Associated Functional Prediction.** To explore the potential functions of lncRNAs, a coexpression network was constructed between the expression values of mRNAs and lncRNAs based on the correlation analysis. An absolute value of Pearson’s correlation coefficient ( $|\text{PCC}| > 0.7$  and a  $P < 0.05$ ) was considered statistically significant. A strong correlation ( $|\text{PCC}| > 0.7$ ) is a commonly selected threshold in research [28, 29]. Subsequently, the enriched functions of mRNAs could be used to predict the functions of lncRNAs that were coexpressed with these mRNAs. Datasets of target genes of lncRNAs were analyzed as input data to identify enriched signaling pathways and biological functions using Ingenuity Pathway Analysis (IPA) (Ingenuity System Inc., USA). The threshold of significance of pathways was defined by the  $P$  value, and the selection criterion for significant IPA pathway terms was  $P < 0.05$ . The enriched functional terms were used as the predicted functional terms of given lncRNAs. The interactions between lncRNAs and mRNAs were analyzed, and the coding-noncoding gene coexpression network (CNC) was constructed with Cytoscape (version 3.7.0) software.

**2.5. Prediction of lncRNA Target Genes.** Target genes of lncRNAs were predicted including two aspects as follows:

TABLE 2: Demographic and clinical characteristics of subjects.

Variables	PDC ( $n = 13$ )	BC ( $n = 9$ )	$P$ -value
Male, $n$ (%)	46.15	44.44	0.94
Age (years), mean (SD)	$37 \pm 6.78$	$37 \pm 7.38$	0.78
Body mass index ( $\text{kg}/\text{m}^2$ )	$23.27 \pm 1.26$	$22.86 \pm 3.05$	0.12

(a) the CNC ( $|\text{PCC}| > 0.7$ ) of DELncRNAs and DEmRNAs was constructed; (b) coding genes, 300 kb upstream and downstream of DELncRNAs, were used to predict the functions of lncRNAs. We choose 300 kb upstream and downstream of lncRNAs as criteria that are a commonly selected threshold in research (see references as follows for details [30, 31]). The intersection of the DELncRNA-DEmRNA pairs was obtained, and these DEmRNAs were the target genes of DELncRNAs. The expression levels of the DELncRNAs and coding genes were used to analyze their co-expression relationships.  $|\text{PCC}| > 0.7$  and  $P < 0.05$  were considered to be correlated expression. We applied Cytoscape (version 3.7.2) to visualize the networks. The degree was performed using the CentiScaPe in Cytoscape to illuminate the most important nodes in the network [32].

**2.6. Validation by RT-qPCR of Key lncRNAs and mRNAs in Independent Samples.** According to the inclusion and exclusion criteria, nine subjects with PDC and 12 BC were incorporated in our study in June 2019. Clinical information of these 21 subjects is presented in Table S3. All patients provided informed consent to participate in this study. Quantification was performed with a reaction process consisting of two steps, including reverse transcription (RT) and RT-qPCR, to confirm the microarray results. RT-qPCR for lncRNAs and mRNAs was performed as previously described [33]. Primers used for RT-qPCR are listed in Table S1. Moreover,  $\beta$ -actin was selected as the housekeeping gene. The relative expressions of target genes were calculated using the  $2^{-\Delta\Delta\text{Ct}}$  method [34].

**2.7. Statistical Analysis.** The numerical data were expressed as the mean  $\pm$  standard deviation (SD). Statistical comparisons between groups of normalized data were performed using the “limma” package of R software,  $t$ -test, or Mann-Whitney  $U$  test when appropriate. Statistical comparisons between paired PDC and BC were performed using a paired  $t$ -test. A  $P < 0.05$  was considered statistically significant with

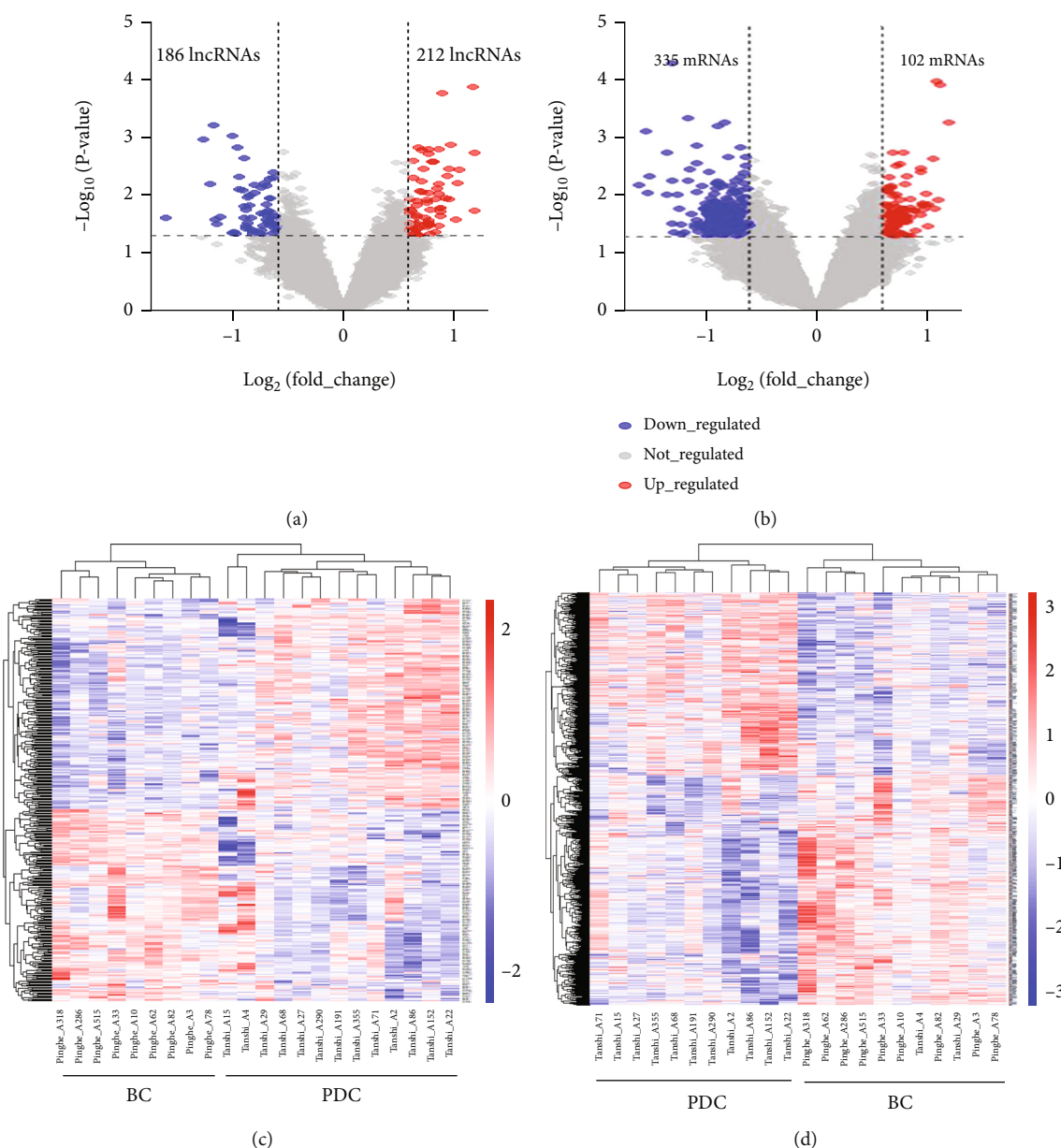


FIGURE 1: The hierarchical clustering heatmaps and volcano plots of differentially expressed lncRNAs and mRNAs. The row and column represent differentially expressed lncRNAs (a and c)/mRNAs (b and d) and samples, respectively, in the heatmaps ( $P < 0.05$ ,  $|\text{fold change}| \geq 1.5$ ) in phlegm-dampness constitution (PDC) compared with balanced constitution (BC). Red and blue indicate up- and downregulation, respectively. -3, -1, 0, 1, and 3 represent fold changes in the corresponding spectrum.

a 95% confidence level. Statistical analyses were performed using SPSS software 25.0, and mappings were performed using the R 3.3.1 software (the R Foundation of Statistical Computing).

### 3. Results

**3.1. Differentially Expressed lncRNAs and mRNAs in the PDC.** To determine the transcriptome characteristics and which lncRNAs could be used to PDC from those with BC, we surveyed the lncRNA and mRNA expression profiles of subjects with a total of 22 samples from PDC ( $n = 13$ ) and BC ( $n = 9$ ) using microarray analysis (NCBI GEO accession

number GSE158042). The purity and integrity of Total RNA were good, and these samples were used for the microarray analysis in 2014. The distributions of lncRNAs and mRNAs are shown in Fig. S1. All subjects were Chinese Han individuals, 20-53 years old, including both genders. There was no significant difference in age ( $P = 0.78$ ), sex ( $P = 0.94$ ), and body mass index (BMI) ( $P = 0.12$ ) between the two groups of subjects. Table 2 summarizes the main clinical characteristics of enrolled patients with no medical records of diagnosed diseases.

After the microarray analysis, the raw total count of lncRNA and mRNA after normalization is 22,621 and 31,860, respectively. A total of 398 differentially expressed

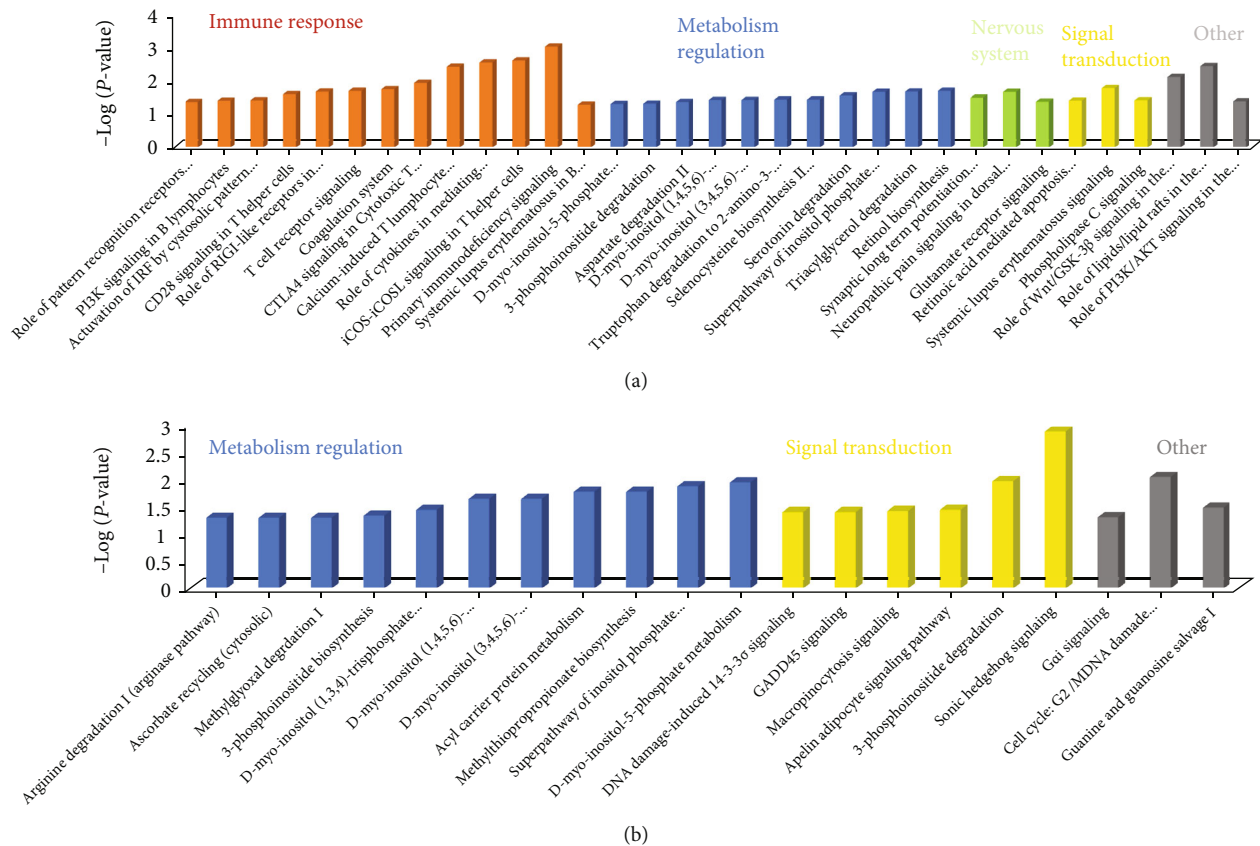


FIGURE 2: Ingenuity Pathway Analysis (IPA) annotates the canonical pathway analysis of differentially expressed mRNAs. These differentially expressed mRNAs were regulated by differentially expressed lncRNAs between PDC and BC (Pearson’s correlation coefficient  $|PCC| > 0.7$  and  $P < 0.05$ ) ((a) 115 upregulated mRNAs; (b) 321 downregulated mRNAs).

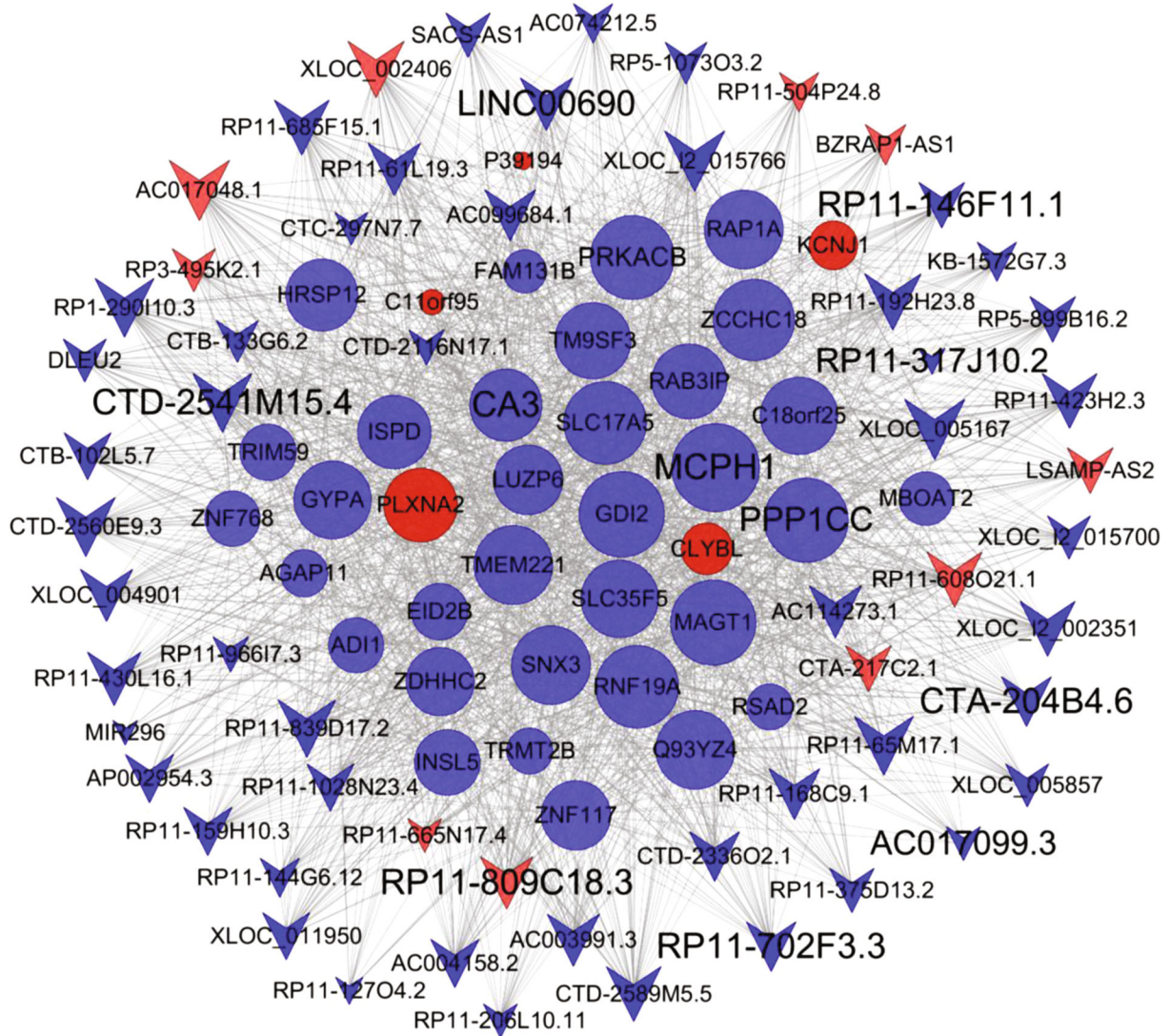
lncRNAs and 437 differentially expressed mRNAs were identified based on  $|\text{fold change}| \geq 1.5$  and  $P < 0.05$  in the PDC compared with the BC. The volcano plot, respectively, is shown in Figure 1(a) and 1(b). The sample grouping was largely consistent when using DELncRNAs (Figure 1(c)) or DEMRNAs (Figure 1(d)). Among them, it is known that TMPO is associated with the progression of type 1 diabetes [35]. ACSL3 plays a key role in lipid biosynthesis and fatty acid degradation [36]. Among the dysregulated lncRNAs, suppression of TTTY15 attenuates hypoxia-induced cardiomyocyte injury by targeting miR-455-5p [37]. The above-mentioned genes are related to metabolic disorders, which are consistent with previous studies, [10, 12, 14], and they were significantly expressed in subjects with PDC in this study.

**3.2. Functional Analysis of Differentially Expressed mRNAs in the PDC.** The differentially expressed mRNA-lncRNA formed coexpression network (CNC) ( $|PCC| > 0.7$  and  $P < 0.05$ ) consists of 421 DEMRNAs and 357 DELncRNAs (Table S2). These were 421 DEMRNAs (102 upregulated and 319 downregulated) in CNC subjected to the Ingenuity Pathway Analysis (IPA). The 102 upregulated mRNAs generated 33 significantly enriched pathways ( $P < 0.05$ ) (Figure 2(a)), which were involved in metabolic regulation and immunizing inflammatory reaction, such as the T cell

receptor signaling ( $P = 0.01$ ), retinol biosynthesis ( $P = 0.02$ ), and triacylglycerol degradation ( $P = 0.02$ ). Meanwhile, we identified 20 IPA pathways ( $P < 0.05$ ) from 319 downregulated mRNAs (Figure 2(b)), most of which were associated with the metabolism of lipids/lipoproteins (such as 3-phosphoinositide degradation, acyl carrier protein metabolism, and D-myo-inositol-5-phosphate metabolism). We subsequently classified these 20 pathways into functional groups that were the metabolism (12/20), signal transduction (5/20) pathways, and so on. These data indicated that individuals with PDC showed specific gene expression profiles and lncRNA expression features in peripheral blood. Among them, ARHGAP9 has been found to lead to endothelial dysfunction in patients with coronary spastic angina [38]. These results suggest that the majority of pathways with DELncRNAs were consistent with these pathways of DEMRNAs.

Next, we explored which key lncRNAs regulated the mRNA of the above-mentioned. According to the correlation coefficient analysis in Table S2, in order to further focus on these lncRNAs and their target genes, lncRNA-mRNA coexpression network showed that 58 lncRNAs (10 upregulated and 48 downregulated lncRNAs), which were at the central positions of the network (degree centrality  $> 60$ ), might play key roles in regulating metabolism pathways (Figure 3(a)). There are 38 DEMRNAs (5 upregulated and





(a)

FIGURE 3: Continued.

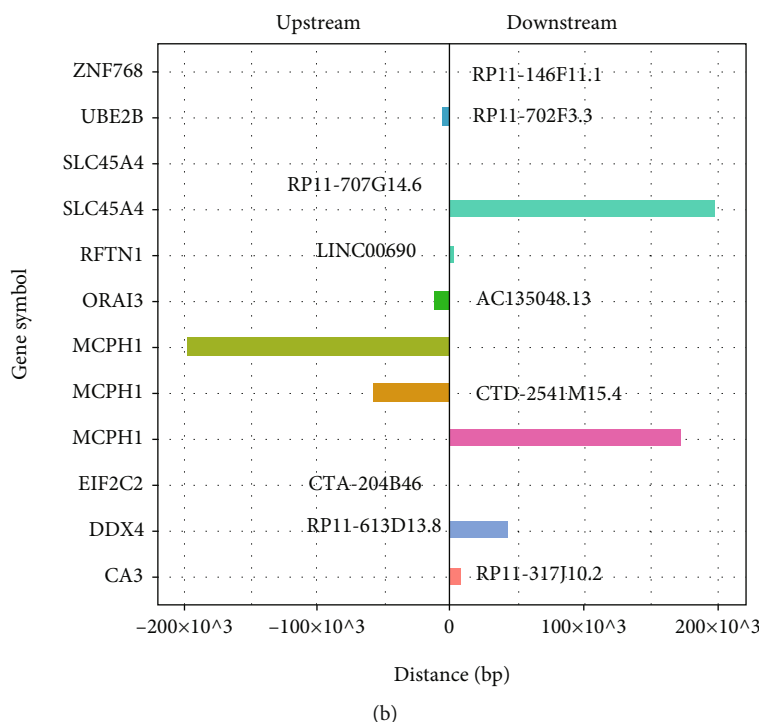


FIGURE 3: Target gene prediction of differentially expressed lncRNAs between PDC and BC. (a) The differentially expressed mRNAs and lncRNAs from Figure 2 were constructed into the coding-noncoding gene network (degree > 60). Red represents upregulated and blue represents downregulated genes. Size represents the importance of a node (degree). The edge denotes the interaction strength. Circles and inverted triangles represent genes and lncRNAs, respectively. (b) Distances between lncRNAs and their predicted target genes (<300 kb). The left vertical axis shows the gene symbol of the coding genes, on the right side of each row, that is, the corresponding gene symbol of lncRNA. The pathways of these mRNAs might mainly be related to lipid metabolism.

33 downregulated), which were regulated by these 58 lncRNAs, which were mostly related to metabolic pathways (such as lipid metabolism and fatty acid metabolism). Especially, nearly half of the pathways (12/35) were related to metabolic regulation in the downregulated genes, which was consistent with the proportion of lipid metabolic pathways in Figure 2(b) (12/20). Among them, GYPA is the high-degree gene (it is regulated by multiple lncRNAs) that affects the expression of glycoprotein A, and it is an important indicator of carotid atherosclerotic lesions [39].

If the genome position of the mRNA-encoding genes is adjacent to that of the coexpressed lncRNA-encoding gene, it suggests that the lncRNA regulates the expression of the mRNA. By combining the lncRNA-mRNA coexpression network and the targets of lncRNA in upstream or downstream 300 kb of lipid metabolism and immune inflammation-related pathways, we identified a total of 12 lncRNA transcripts and their predicted regulatory protein-coding genes (<300 kb and |PCC| > 0.7) (Figure 3(b)). Among these 12 lncRNA-mRNA pairs, these data provided valuable clues about these lncRNAs and their nearby coding genes in metabolic disorders of subjects with PDC (Figures 3(a) and 3(b)).

3.3. The Target Gene Prediction of lncRNAs in the Lipid Metabolism Pathway of PDC. Figure 3 reveals that lipid metabolism accounted for a large proportion of these pathways. To find out which lncRNAs regulated these genes in

the lipid metabolism pathway, we constructed a coexpression network for these mRNAs and corresponding lncRNAs in subjects with PDC. Next, we selected the top 30 pairs of lncRNA-mRNA with the lowest *P* to map the coexpression network, including nine mRNAs and 25 lncRNAs (Figure 4(a)). The functions of these mRNAs were mostly related to pathways of metabolism of lipids and/or lipoproteins. It indicated that these nine mRNAs (two upregulated and seven downregulated mRNAs) in the lipid metabolism pathway were mainly regulated by these DELncRNAs (25 genes). However, little is known about the functions of lncRNAs and lncRNA-mRNA interactions, which should be further studied in the future.

Then, we further analyzed how these dysregulated lncRNAs regulate mRNAs in the lipid metabolism pathway [22]. We chose 26 DEmRNAs to hunt their nearby DELncRNAs in the lipid metabolism pathway in the PDC. The coexpressed protein-coding genes were defined as target genes with one DELncRNA within 300 kb upstream and downstream on the same chromosome. The filtering results are shown in Figure 4(b) (including seven lncRNA transcripts and their predicted regulatory protein-coding genes). Each lncRNA had a different number of neighboring coding genes. For example, RP11-317J10.2 had only one nearby coding gene. In contrast, lncRNAs TTTY15 and RP11-809C18.3, respectively, had two nearby coding genes (Figure 4(b)). It indicated that these neighboring genes might be regulated by lncRNAs.

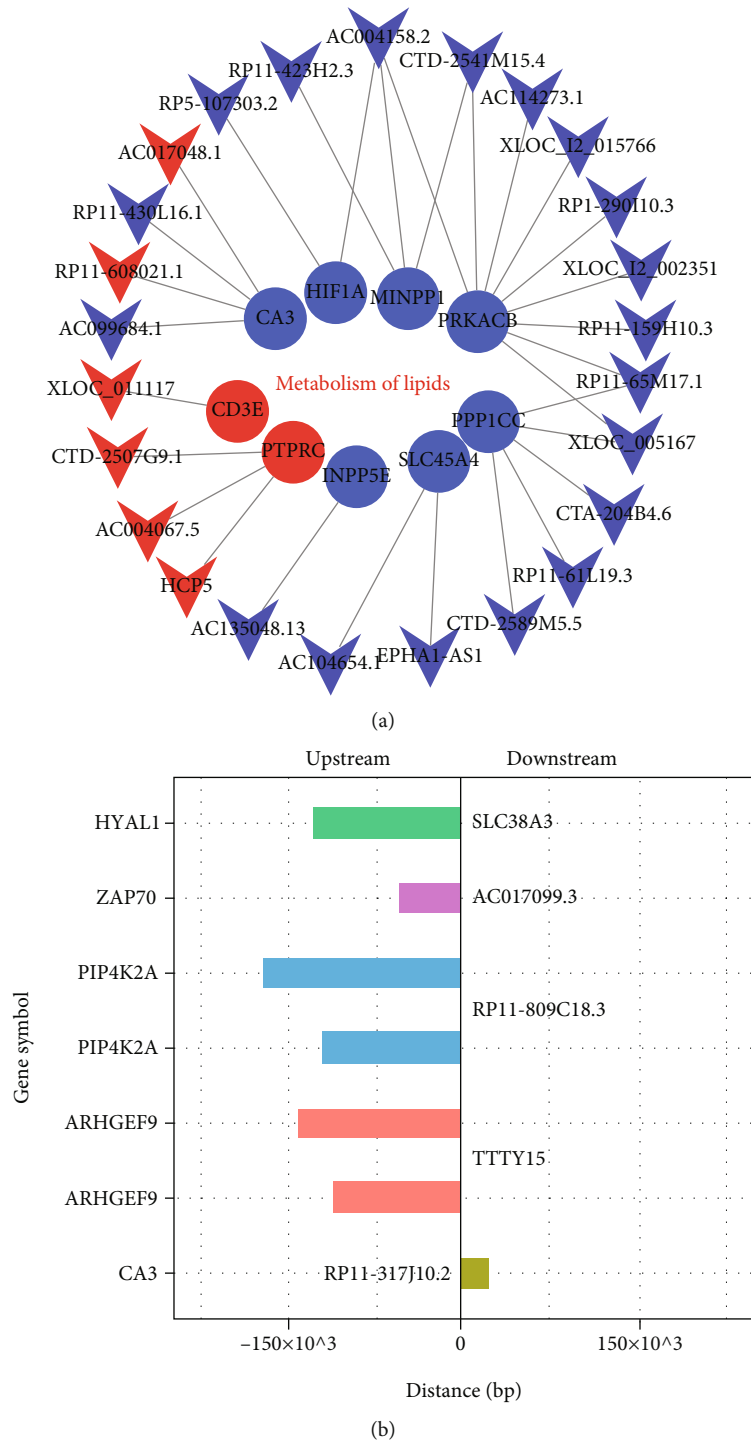


FIGURE 4: Target gene prediction of lncRNAs in the lipid metabolism pathway. (a) Coexpression network of the differentially expressed lncRNAs and genes in the lipid metabolism pathway. Red represents upregulated and blue represents downregulated genes. Circles and inverted triangles represent genes and lncRNAs, respectively. (b) Regulation of differentially expressed lncRNAs to nearby coding genes in the lipid metabolism pathway (<300 kb). The left vertical axis shows the gene symbol of the coding genes, on the right side of each row, that is, the corresponding gene symbol of lncRNA.

3.4. Validation of Deregulated lncRNAs and mRNAs by RT-qPCR in Independent 21 Subjects of PDC and BC. To verify the reliability of the microarray data, some key functional genes of metabolic disorders, including five DElncRNAs

and five DEMRNAs from Figures 3(b) and 4(b), were confirmed in 21 subjects with PDC and BC by RT-qPCR, as shown in Figure 5. The relative expressions of CA3, ORAI3, PIP4K2A, RP11-317J10.2, LINC00690, and AC135048.13

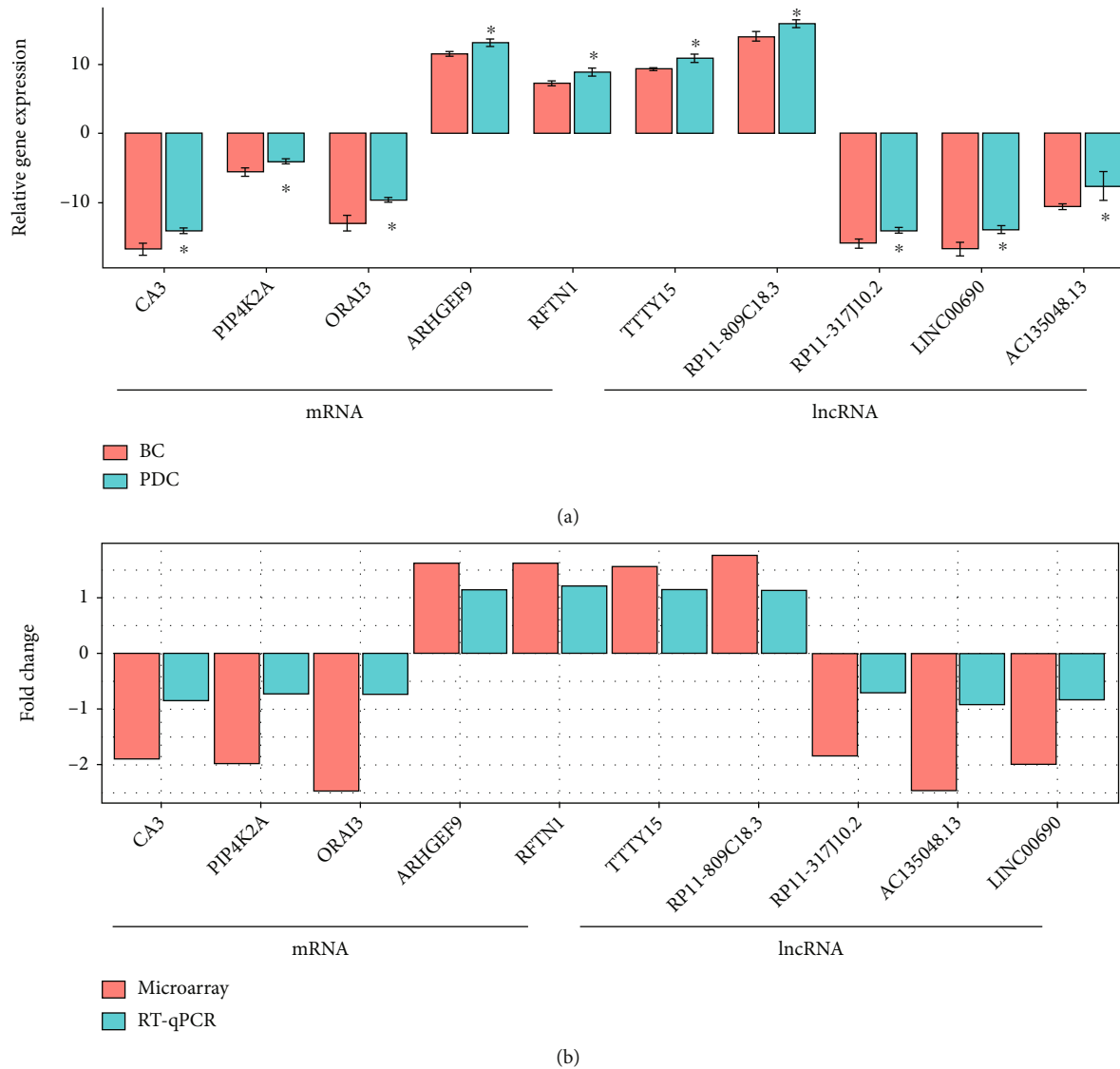


FIGURE 5: Validation for the expression of significant transcripts by quantitative RT-qPCR. (a) RT-qPCR verification of the expression profiles of differentially expressed lncRNAs/mRNAs. PDC and BC represent the phlegm-dampness constitution and balanced constitution, respectively. (b) Comparison of RT-qPCR and microarray analysis data. The x-axis and y-axis present mRNA/lncRNA name and relative expression (fold change), respectively. Fold change > 0 and < 0 represents the upregulation and downregulation, respectively. \*P < 0.05; \*\*P < 0.01.

were significantly downregulated ( $P < 0.05$ ) in the blood of the subjects with PDC, compared to those with BC. In contrast, the relative expressions of RFTN1, ARHGEF9, TTTY15, and RP11-809C18.3 were upregulated in the blood of the subjects with PDC. Therefore, the RT-qPCR data verified the veracity of microarray results (Figures 5(a) and 5(b)). The finding provided reliable evidence that these lncRNAs and mRNAs could be implicated in the pathogenesis of metabolic diseases in PDC. A biomarker means a panel that could distinct case and control with as few features as possible. These 5 lncRNA-mRNA pairs could be used as potential biomarkers that they distinct BC and PDC. The heatmap of 5 lncRNA-mRNA pairs is of the expression of significant transcripts by quantitative RT-qPCR (Figure 6).

#### 4. Discussion

In the present study, we identified several interaction pairs of lncRNA-nearby targeted mRNAs, such as RP11-317J10.2-CA3, RP11-809C18.3-PIP4K2A, LINC0069-RFTN1, TTTY15-ARHGEF9, and AC135048.13-ORAI3. Meanwhile, individuals with PDC exhibited transcriptional characteristics regarding lipid metabolism and immune inflammation-related pathways. These findings were consistent with the observations of profuse phlegm, fat body, loose abdomen, and greasy face in individuals with PDC. In short, our study first identified several differentially expressed lncRNAs and mRNAs and suggested that their interactions played a crucial role in the process of metabolic dysregulation in the PDC.

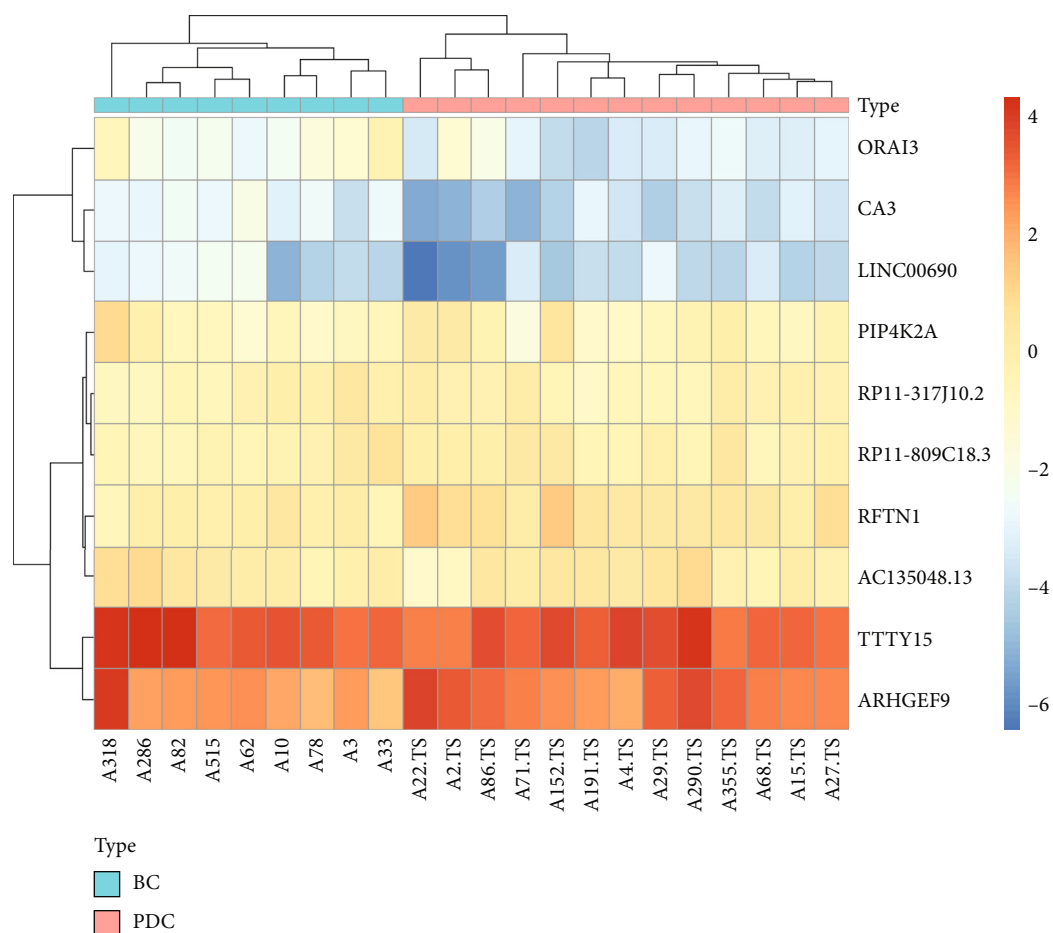


FIGURE 6: The heatmap of 5 lncRNA-mRNA pairs is of the expression of significant transcripts by quantitative RT-qPCR. Row and column represent differentially expressed lncRNAs/mRNAs and samples, respectively, in the heatmaps ( $P < 0.05$ ,  $|\text{fold change}| \geq 1.5$ ) in phlegm-dampness constitution (PDC) compared with Balanced constitution (BC). Red and blue indicate up- and downregulation, respectively. -6, -2, 0, 2, and 4 represent fold changes in the corresponding spectrum.

RP11-317J10.2 is identified in human blood as an antisense lncRNA [40]. In our study, we found that RP11-317J10.2 was the most downregulated lncRNA in the blood of the subjects with PDC. Furthermore, downregulated CA3 was the nearby targeted mRNA of RP11-317J10.2. It is well known that CA3 is one of the diagnostic markers of perioperative MI during coronary bypass surgery [41]. Our results indicated that the downregulation of CA3 and RP11-317J10.2 might be involved in lipid metabolism, which could provide a new therapeutic regimen of metabolic diseases in the PDC.

It is found that RP11-809C18.3 is an antisense lncRNA in the PDC [42]. In the present study, we first found the upregulation of RP11-809C18.3 in the blood of the subjects with PDC. Besides, upregulated PIP4K2A was the nearby targeted mRNA of RP11-809C18.3. It has been observed that the expression of PIP4K2A is significantly increased in subjects with PDC, which regulates intracellular cholesterol transport through modulating PI(4,5)P2 homeostasis [43]. Additionally, noncoding RNA RP11-809C18.3 regulates PIP4K2A, which is related to phospholipid metabolism by modulating PI(4,5)P2 homeostasis [44, 45]. It has been proposed that increased expressions of RP11-809C18.3 and

PIP4K2A may promote inositol phosphate metabolism, which contributes to the process of PDC.

Up to now, only a few articles have investigated LINC00690 in the PDC. Herein, we found that LINC00690 was downregulated in the blood of the subjects with PDC. Furthermore, upregulated RFTN1 was the nearby targeted mRNA of LINC00690. It is pointed out that RFTN1 is involved in controlling lipopolysaccharide-induced TLR4 internalization and TICAM-1 signaling in a cell type-specific manner [46]. A relevant study of RFTN1 has revealed that common body mass index-associated variants confer the risk of extreme obesity [47]. Our findings indicated that the downregulation of LINC00690 and the upregulation of RFTN1 played a key role in the metabolic disorders of PDC. However, further research is required to validate the deeper function of LINC00690 and RFTN1 in the PDC.

Among the dysregulated mRNAs, ARHGAP9 was the nearby targeted mRNA of TTTY15. It has been demonstrated that TTTY15 plays an important role in regulating hypoxia-induced vascular endothelial cell injury [48]. Knockdown of long noncoding RNA TTTY15 helps protect cardiomyocytes in case of hypoxia-induced apoptosis and



mitochondrial energy metabolism dysfunction via TTTY15/let-7i-5p and TLR3/NF- $\kappa$ B pathways [49]; and TTTY15 knockdown also protects cardiomyocytes from hypoxia-induced injury by regulating the let-7b/MAPK6 axis [50] or by regulating the miR-98-5p/CRP pathway [51]. Moreover, the polymorphism of ARHGAP9 is associated with coronary artery spasm [38]. Herein, we found the interaction between TTTY15 and ARHGAP9 in the PDC. Our result suggested that upregulated TTTY15 and ARHGAP9 may play a vital role in metabolic disease, which could be used as PDC biomarkers to assist in clinical diagnosis.

AC135048.13 is associated with the occurrence and recurrence of myocardial infarction [52]. In this study, we first found the top 10 downregulated expressions of AC135048.13 in the blood of the subjects with PDC. Besides, downregulated ORAI3 is associated with the changes in cerebrovascular contractile responses in high-salt intake-induced hypertension. The expression of ORAI3 proteins has been linked to vascular and airway pathologies, including restenosis, hypertension, and atopic asthma [53]. ORAI3 was the nearby targeted mRNA of AC135048.13. It has been demonstrated that ORAI3 plays an important role in patients with cardiac hypertrophy [54]. Herein, the interaction between AC135048.13 and ORAI3 suggested that decreased expression of AC135048.13 and ORAI3 was involved in the lipid metabolism of the PDC. These findings provided solid evidence that these lncRNAs and mRNAs could be implicated in the pathogenesis of metabolic disorders with the PDC. Furthermore, we speculated that these lncRNAs played a potential regulatory role in the metabolic regulation of phlegm-dampness-susceptible diseases.

Previous studies have found that subjects with PDC have specific mRNA expression signatures and methylation profiles [12, 14]. As indicated in Fig. S2, the reproducibility of the pathway was studied between this study and a previous study by IPA. It showed that metabolism-related pathways accounted for a large proportion of the two studies. Consistent with the clinical observation that subjects with PDC tend to develop a metabolic disorder, series-clustering analysis detected several key lipid metabolic genes (PRKAR1A, ACSL4, SMPD3, etc.) [10, 12]. This study also confirmed that subjects with PDC were a population with a dysregulation tendency of metabolic disorder-related mRNAs (Figure 2).

Nowadays, most studies have focused on the pathological study of metabolic disease, while only a few have been carried out on the prevention of metabolic diseases [55, 56]. Previously, Ma and coworkers have reported that lncRNAs may regulate diverse gene expressions, which are roughly summarized to epigenetic, transcriptional, and post-transcriptional levels in cardiovascular diseases [22]. One of the principles for “P4 medicine” is the preventive treatment of disease. The “P4 medicine” plays an important role in the diagnosis, prevention, and treatment of metabolic disease [5]. This study explains which people are more likely to have metabolic diseases, indicating that the research of the PDC is a good pointcut to explore the undiseased state of metabolic disorders. When PDC develops to metabolic diseases, it will still have the characteristics of PDC. The PDC is a suscepti-

bility factor for metabolic diseases and coexists with metabolic diseases. According to the results of epidemiological studies, the occurrence of metabolic diseases is related to the phlegm-dampness constitution (PDC) ( $P < 0.001$ ) [57], which is positively associated with the level of PDC ( $P < 0.001$ ) [9]. Compared with the balanced constitution (BC), the patients of PDC are more likely to have hypertension and hyperlipidemia. Moreover, the use of peripheral blood is a suitable method to identify surrogate markers in TCM constitutions. Liew et al. have compared the peripheral blood transcriptome with genes expressed in nine different human tissue types [58]. They have found that expression of over 80% is shared in any given tissue, and tissue-specific gene transcripts can be detected in circulating blood cells. Another advantage of peripheral blood is that it can be dynamically monitored in real time, which is very convenient. Furthermore, there are several limitations in the present study. First, we need further experiments to gain mechanistic insights. Related research should be viewed in the future. Second, a larger sample size is necessary for further in vivo and in vitro validation of identified differentially lncRNAs and mRNAs. Third, lncRNAs and mRNAs in exosomes might be a better choice in the future.

## 5. Conclusions

Our study identified five pairs of lncRNA and mRNA that could be used as potential biomarkers for the PDC, including RP11-317J10.2-CA3, RP11-809C18.3-PIP4K2A, LINC0069-RFTN1, TTTY15-ARHGAP9, and AC135048.13-ORAI3. And lipid metabolic disorders could be associated with the PDC. In conclusion, these results indicated several dysregulated lncRNAs that were potentially associated with the development and progression of metabolic diseases in the PDC. These findings provided valuable insights into novel therapeutic strategies for the prevention and treatment of metabolic disorders.

## Data Availability

The datasets used and/or analyzed during the current study would be available from the first author and corresponding author on reasonable request. The raw data of this study were uploaded to the NCBI GEO database (NCBI GEO accession number GSE158042).

## Ethical Approval

All specimens were taken after informed consent disclosing future use for research. All procedures performed in studies involving human participants were in accordance with the ethical standards of the Medical and Experimental Animal Ethics Committee of Beijing University of Chinese Medicine (Ethical approval No. 2012BZHYYL0301) and with the 1964 Helsinki Declaration and its later amendments or comparable ethical standards.

## Consent

Participants were informed of the purpose, general contents, and data use of the study, and they all signed the informed consent.

## Conflicts of Interest

The authors declare that they have no conflict interests.

## Authors' Contributions

Lidan Dong, Yanfei Zheng, and Dan Liu contributed equally to this work.

## Acknowledgments

This work was supported by the key project of National Natural Science Foundation of China (No. 81730112), China Postdoctoral Science Foundation (No. 2018M641283), the Beijing Nova Program (No. Z201100000820027), and the Innovation Team and Talents Cultivation Program of National Administration of Traditional Chinese Medicine (No. ZYYCXTD-C-202001).

## Supplementary Materials

Fig. S1: box plots summarizing the lncRNA and mRNA profiles. After normalization, the distributions of the log<sub>2</sub> ratios of fluorescence signals in phlegm-dampness constitution (PDC) samples were nearly identical among balanced constitution (BC) samples. Fig. S2: the reproducibility of the pathway was researched by IPA between this study and previous studies. The li<sub>up</sub> and li<sub>down</sub>, respectively, represent the upregulated and downregulated mRNAs of Wang's paper [1]. Table S1: lncRNA RT-qPCR primers and product sizes. Table S2: the top 100 coexpression networks (CNC) of 421 differentially expressed mRNAs and 357 lncRNAs were involved ( $P < 0.05$ ,  $|PCC| > 0.7$ ). PCC: Pearson's correlation coefficient. Table S3: demographic and clinical characteristics of 21 subjects. (*Supplementary Materials*)

## References

- [1] Q. Wang, "Classification and diagnosis basis of nine basic constitutions in Chinese medicine," *Journal-Beijing University of Traditional Chinese Medicine*, vol. 28, no. 4, pp. 1–8, 2005.
- [2] J. Wang, Y. Li, C. Ni, H. Zhang, L. Li, and Q. Wang, "Cognition research and constitutional classification in Chinese medicine," *The American Journal of Chinese Medicine*, vol. 39, no. 4, pp. 651–660, 2011.
- [3] Q. Wang, "Individualized medicine, health medicine, and constitutional theory in Chinese medicine," *Frontiers in Medicine*, vol. 6, no. 1, pp. 1–7, 2012.
- [4] J. Wang, Y. S. Li, and Q. Wang, "Identification of Chinese medicine constitution in public health services," *Chinese Journal of Integrative Medicine*, vol. 25, no. 7, pp. 550–553, 2019.
- [5] H. Vogt, B. Hofmann, and L. Getz, "The new holism: P4 systems medicine and the medicalization of health and life itself," *Medicine, Health Care, and Philosophy*, vol. 19, no. 2, pp. 307–323, 2016.
- [6] Q. Wang, J. N. Ye, Y. B. Zhu et al., "Research on diagnosis standard of phlegm-dampness constitution of TCM," *China Journal of Traditional Chinese Medicine and Pharmacy*, vol. 21, no. 2, pp. 73–75, 2006.
- [7] W. Qi, D. Jing, W. Hongdong, W. Dongpo, Y. Shilin, and R. Xiaojuan, "Study on the molecular characteristics in phlegm-dampness constitution," *Engineering Sciences*, vol. 10, no. 7, 2008.
- [8] Q. Wang and Y. B. Zhu, "Epidemiological investigation of constitutional types of Chinese medicine in general population: base on 21,948 epidemiological investigation data of nine provinces in China," *China Journal of Traditional Chinese Medicine and Pharmacy*, vol. 24, no. 1, pp. 7–12, 2009.
- [9] Y. R. Wu, Y. N. Cun, J. Dong et al., "Polymorphisms in PPARG, PPARG and APM1 associated with four types of Traditional Chinese Medicine constitutions," *Journal of Genetics and Genomics*, vol. 37, no. 6, pp. 371–379, 2010.
- [10] R. Yu, D. Liu, and Y. Yang, "Expression profiling-based clustering of healthy subjects recapitulates classifications defined by clinical observation in Chinese medicine," *Journal of Genetics and Genomics*, vol. 44, no. 4, pp. 191–197, 2017.
- [11] J. Dong, *Basic research on phlegm-dampness constitution and its correlation with metabolic syndrome*, Beijing Univ of Chinese Medicine, 2007.
- [12] L. Li, J. Feng, H. Yao et al., "Gene expression signatures for phlegm-dampness constitution of Chinese medicine," *Science China Life Sciences*, vol. 60, no. 1, pp. 105–107, 2017.
- [13] J. Zhou and H. M. Luo, "Exploration of the relationship between phlegm-dampness constitution and polymorphism of low density lipoprotein receptor genes Pvu II and Ava II," *Chinese Journal of Integrative Medicine*, vol. 13, no. 3, pp. 170–174, 2007.
- [14] H. Yao, S. Mo, J. Wang et al., "Genome-wide DNA methylation profiles of phlegm-dampness constitution," *Cellular Physiology and Biochemistry*, vol. 45, no. 5, pp. 1999–2008, 2018.
- [15] H. S. Mohamad, S. Wenli, and C. Qi, "DNA methylation as the most important content of epigenetics in traditional Chinese herbal medicine," *Journal of Medicinal Plants Research*, vol. 13, no. 16, pp. 357–369, 2019.
- [16] Q. M. Su and Q. Wang, "Detection of  $na^+ - k^+ - atpase$  activity in blood lipid, blood glucose, pancreas, islet and ellipsis cells of obese people with phlegm-dampness constitution," *Journal of Basic Chinese Medicine*, vol. 5, no. 2, pp. 39–41, 1995.
- [17] M. Li, L. Duan, Y. Li, and B. Liu, "Long noncoding RNA/circular noncoding RNA-miRNA-mRNA axes in cardiovascular diseases," *Life Sciences*, vol. 233, article 116440, 2019.
- [18] L. Hobuß, C. Bär, and T. Thum, "long non-coding RNAs: at the heart of cardiac dysfunction?," *Frontiers in Physiology*, vol. 10, pp. 10–30, 2019.
- [19] T. R. Mercer, M. E. Dinger, and J. S. Mattick, "Long non-coding RNAs: insights into functions," *Nature Reviews Genetics*, vol. 10, no. 3, pp. 155–159, 2009.
- [20] Y. Su, L. Li, S. Zhao, Y. Yue, and S. Yang, "The long noncoding RNA expression profiles of paroxysmal atrial fibrillation identified by microarray analysis," *Gene*, vol. 642, pp. 125–134, 2018.
- [21] L. W. Harries, "Long non-coding RNAs and human disease," *Biochemical Society Transactions*, vol. 40, no. 4, pp. 902–906, 2012.
- [22] Y. Ma, W. Ma, L. Huang, D. Feng, and B. Cai, "Long non-coding RNAs, a new important regulator of cardiovascular



- physiology and pathology,” *International Journal of Cardiology*, vol. 188, pp. 105–110, 2015.
- [23] N. Goyal, D. Kesharwani, and M. Datta, “Lnc-ing non-coding RNAs with metabolism and diabetes: roles of lncRNAs,” *Cellular and Molecular Life Sciences*, vol. 75, no. 10, pp. 1827–1837, 2018.
- [24] R. T. Brookheart, C. I. Michel, L. L. Listenberger, D. S. Ory, and J. E. Schaffer, “The Non-coding RNA gadd7 Is a Regulator of Lipid-induced Oxidative and Endoplasmic Reticulum Stress,” *The Journal of Biological Chemistry*, vol. 284, no. 12, pp. 7446–7454, 2009.
- [25] N. Ishii, K. Ozaki, H. Sato et al., “Identification of a novel non-coding RNA, MIAT, that confers risk of myocardial infarction,” *Journal of Human Genetics*, vol. 51, no. 12, pp. 1087–1099, 2006.
- [26] Y. Shi, S. Parag, R. Patel et al., “Stabilization of lncRNA GAS5 by a small molecule and its implications in diabetic adipocytes,” *Cell Chemical Biology*, vol. 26, no. 3, pp. 319–330.e6, 2019.
- [27] T. A. Patterson, E. K. Lobenhofer, S. B. Fulmer-Smentek et al., “Performance comparison of one-color and two-color platforms within the MicroArray Quality Control (MAQC) project,” *Nature Biotechnology*, vol. 24, no. 9, pp. 1140–1150, 2006.
- [28] Y. H. Shi, X. W. He, F. D. Liu et al., “Comprehensive analysis of differentially expressed profiles of long non-coding RNAs and messenger RNAs in kaolin-induced hydrocephalus,” *Gene*, vol. 697, pp. 184–193, 2019.
- [29] J. L. Ma, Y. H. Xiao, B. Tian et al., “Genome-wide analyses of long non-coding RNA expression profiles and functional network analysis in esophageal squamous cell carcinoma,” *Scientific Reports*, vol. 9, no. 1, p. 9162, 2019.
- [30] W. Huang, X. Zhang, A. Li, L. Xie, and X. Miao, “Genome-wide analysis of mRNAs and lncRNAs of intramuscular fat related to lipid metabolism in two pig breeds,” *Cellular Physiology and Biochemistry*, vol. 50, no. 6, pp. 2406–2422, 2018.
- [31] M. Huang, Z. Zhong, M. Lv, J. Shu, Q. Tian, and J. Chen, “Comprehensive analysis of differentially expressed profiles of lncRNAs and circRNAs with associated co-expression and ceRNA networks in bladder carcinoma,” *Oncotarget*, vol. 7, no. 30, pp. 47186–47200, 2016.
- [32] W. Zheng, Z. Zou, S. Lin et al., “Identification and functional analysis of spermatogenesis-associated gene modules in azoospermia by weighted gene coexpression network analysis,” *Journal of Cellular Biochemistry*, vol. 120, no. 3, pp. 3934–3944, 2019.
- [33] S. He, S. Yang, Y. Zhang et al., “LncRNA ODIR1 inhibits osteogenic differentiation of hUC-MSCs through the FBXO25/H2BK120ub/H3K4me3/OSX axis,” *Cell Death & Disease*, vol. 10, no. 12, article 2148, p. 947, 2019.
- [34] K. J. Livak and T. Schmittgen, “Analysis of Relative Gene Expression Data Using Real-Time Quantitative PCR and the  $2^{-\Delta\Delta C_T}$  Method,” *Methods*, vol. 25, no. 4, pp. 402–408, 2001.
- [35] D. W. Craig, M. P. Millis, and J. K. DiStefano, “Genome-wide SNP genotyping study using pooled DNA to identify candidate markers mediating susceptibility to end-stage renal disease attributed to type 1 diabetes,” *Diabetic Medicine*, vol. 26, no. 11, pp. 1090–1098, 2009.
- [36] H. Yao and J. Ye, “Long Chain Acyl-CoA Synthetase 3-mediated Phosphatidylcholine Synthesis Is Required for Assembly of Very Low Density Lipoproteins in Human Hepatoma Huh7 Cells,” *The Journal of Biological Chemistry*, vol. 283, no. 2, pp. 849–854, 2008.
- [37] S. Huang, W. Tao, Z. Guo, J. Cao, and X. Huang, “Suppression of long noncoding RNA TTTY15 attenuates hypoxia-induced cardiomyocytes injury by targeting miR-455-5p,” *Gene*, vol. 701, pp. 1–8, 2019.
- [38] M. Takefuji, H. Asano, K. Mori et al., “Mutation of ARHGAP9 in patients with coronary spastic angina,” *Journal of Human Genetics*, vol. 55, no. 1, pp. 42–49, 2010.
- [39] M. Hakimi, A. hyhlik-dürr, A. von Au et al., “The expression of glycoprotein a and osteoprotegerin is locally increased in carotid atherosclerotic lesions of symptomatic compared to asymptomatic patients,” *International Journal of Molecular Medicine*, vol. 32, no. 2, pp. 331–338, 2013.
- [40] [http://grch37.ensembl.org/Homo\\_sapiens/Gene/Summary?db=core;g=ENSG00000253549;r=8:86354080-86377144](http://grch37.ensembl.org/Homo_sapiens/Gene/Summary?db=core;g=ENSG00000253549;r=8:86354080-86377144).
- [41] P. Vuotikka, K. Ylitalo, J. Vuori et al., “Serum myoglobin/carbonic anhydrase III ratio in the diagnosis of perioperative myocardial infarction during coronary bypass surgery,” *Scandinavian Cardiovascular Journal*, vol. 37, no. 1, pp. 23–29, 2003.
- [42] [http://grch37.ensembl.org/Homo\\_sapiens/Gene/Summary?db=core;g=ENSG00000225140;r=10:674578-677195;t=ENST00000451601](http://grch37.ensembl.org/Homo_sapiens/Gene/Summary?db=core;g=ENSG00000225140;r=10:674578-677195;t=ENST00000451601).
- [43] A. Hu, X. T. Zhao, H. Tu et al., “PIP4K2A regulates intracellular cholesterol transport through modulating PI(4,5)P<sub>2</sub> homeostasis,” *Journal of Lipid Research*, vol. 59, no. 3, pp. 507–514, 2018.
- [44] L. E. Rameh, K. F. Tolia, B. C. Duckworth, and L. C. Cantley, “A new pathway for synthesis of phosphatidylinositol-4,5-bisphosphate,” *Nature*, vol. 390, no. 6656, pp. 192–196, 1997.
- [45] M. R. Lundquist, M. D. Goncalves, R. M. Loughran et al., “Phosphatidylinositol-5-phosphate 4-kinases regulate cellular lipid metabolism by facilitating autophagy,” *Molecular Cell*, vol. 70, no. 3, pp. 531–544.e9, 2018.
- [46] K. Saeki, Y. Miura, D. Aki, T. Kurosaki, and A. Yoshimura, “The B cell-specific major raft protein, Raftlin, is necessary for the integrity of lipid raft and BCR signal transduction,” *The EMBO Journal*, vol. 22, no. 12, pp. 3015–3026, 2003.
- [47] M. Tatematsu, R. Yoshida, Y. Morioka et al., “Raftlin controls lipopolysaccharide-induced TLR4 internalization and TICAM-1 signaling in a cell type-specific manner,” *Journal of Immunology*, vol. 196, no. 9, pp. 3865–3876, 2016.
- [48] J. Zheng, Y. Y. Zhuo, C. Zhang, G. Y. Tang, X. Y. Gu, and F. Wang, “LncRNA TTTY15 regulates hypoxia-induced vascular endothelial cell injury via targeting miR-186-5p in cardiovascular disease,” *European Review for Medical and Pharmacological Sciences*, vol. 24, no. 6, pp. 3293–3301, 2020.
- [49] H. Zhang, X. Zou, and F. Liu, “Silencing TTTY15 mitigates hypoxia-induced mitochondrial energy metabolism dysfunction and cardiomyocytes apoptosis via TTTY15/let-7i-5p and TLR3/NF- $\kappa$ B pathways,” *Cellular Signalling*, vol. 12, no. 76, article 109779, 2020.
- [50] X. Xie, Q. Ji, X. Han, L. Zhang, and J. Li, “Knockdown of long non-coding RNA TTTY15 protects cardiomyocytes from hypoxia-induced injury by regulating let-7b/MAPK6 axis,” *International Journal of Clinical and Experimental Pathology*, vol. 13, no. 8, pp. 1951–1961, 2020.
- [51] R. Ma, L. Gao, Y. Liu, P. du, X. Chen, and G. Li, “LncRNA TTTY15 knockdown alleviates H<sub>2</sub>O<sub>2</sub>-stimulated myocardial

- cell injury by regulating the miR-98-5p/CRP pathway,” *Molecular and Cellular Biochemistry*, vol. 476, no. 1, pp. 81–92, 2021.
- [52] G. Zhang, H. Sun, Y. Zhang et al., “Characterization of dysregulated lncRNA-mRNA network based on ceRNA hypothesis to reveal the occurrence and recurrence of myocardial infarction,” *Cell Death Discovery*, vol. 4, no. 1, p. 35, 2018.
- [53] W. Jiang, L. Ye, Y. Yang et al., “TRPP2 associates with STIM1 to regulate cerebral vasoconstriction and enhance high salt intake-induced hypertensive cerebrovascular spasm,” *Hypertension Research*, vol. 42, no. 12, pp. 1894–1904, 2019.
- [54] Y. Saliba, M. Keck, A. Marchand et al., “Emergence of Orai3 activity during cardiac hypertrophy,” *Cardiovascular Research*, vol. 105, no. 3, pp. 248–259, 2015.
- [55] C. Riley, A. Maxwell, A. Parsons, E. Andrist, and A. F. Beck, “Disease prevention & health promotion: what’s critical care got to do with it,” *Translational Pediatrics*, vol. 7, no. 4, pp. 262–266, 2018.
- [56] J. Wang, Q. Ma, Y. Li et al., “Research progress on traditional Chinese medicine syndromes of diabetes mellitus,” *Biomedicine & Pharmacotherapy*, vol. 121, p. 109565, 2020.
- [57] J. Dong, *Basic research on phlegm-dampness constitution and its correlation with metabolic syndrome*, Beijing University of Chinese Medicine, 2007.
- [58] C. C. Liew, J. Ma, H. C. Tang, R. Zheng, and A. A. Dempsey, “The peripheral blood transcriptome dynamically reflects system wide biology: a potential diagnostic tool,” *The Journal of Laboratory and Clinical Medicine*, vol. 147, no. 3, pp. 126–132, 2006.

## Retraction

# Retracted: SOCS3 Gene Polymorphism and Hypertension Susceptibility in Chinese Population: A Two-Center Case-Control Study

### BioMed Research International

Received 12 March 2024; Accepted 12 March 2024; Published 20 March 2024

Copyright © 2024 BioMed Research International. This is an open access article distributed under the Creative Commons Attribution License, which permits unrestricted use, distribution, and reproduction in any medium, provided the original work is properly cited.

This article has been retracted by Hindawi following an investigation undertaken by the publisher [1]. This investigation has uncovered evidence of one or more of the following indicators of systematic manipulation of the publication process:

- (1) Discrepancies in scope
- (2) Discrepancies in the description of the research reported
- (3) Discrepancies between the availability of data and the research described
- (4) Inappropriate citations
- (5) Incoherent, meaningless and/or irrelevant content included in the article
- (6) Manipulated or compromised peer review

The presence of these indicators undermines our confidence in the integrity of the article's content and we cannot, therefore, vouch for its reliability. Please note that this notice is intended solely to alert readers that the content of this article is unreliable. We have not investigated whether authors were aware of or involved in the systematic manipulation of the publication process.

Wiley and Hindawi regrets that the usual quality checks did not identify these issues before publication and have since put additional measures in place to safeguard research integrity.

We wish to credit our own Research Integrity and Research Publishing teams and anonymous and named external researchers and research integrity experts for contributing to this investigation.

The corresponding author, as the representative of all authors, has been given the opportunity to register their agreement or disagreement to this retraction. We have kept a record of any response received.

### References

- [1] D. Kuang, L. Dong, L. Liu et al., "SOCS3 Gene Polymorphism and Hypertension Susceptibility in Chinese Population: A Two-Center Case-Control Study," *BioMed Research International*, vol. 2021, Article ID 8445461, 8 pages, 2021.

## Research Article

# SOCS3 Gene Polymorphism and Hypertension Susceptibility in Chinese Population: A Two-Center Case-Control Study

Dabin Kuang,<sup>1</sup> Lichen Dong,<sup>1</sup> Lingyun Liu,<sup>2</sup> Meiling Zuo,<sup>1</sup> Yuanlin Xie,<sup>1</sup> Taoming Li,<sup>1</sup> and Zhousheng Yang<sup>3</sup> 

<sup>1</sup>The Affiliated Changsha Hospital of Hunan Normal University, Changsha, Hunan 410006, China

<sup>2</sup>Department of Pharmacy, The 921th Hospital of Joint Logistic Support Force of PLA, Hunan 410003, China

<sup>3</sup>Department of Pharmacy, The People's Hospital of Guangxi Zhuang Autonomous Region, Guangxi Academy of Medicaid Sciences, Nanning 530021, China

Correspondence should be addressed to Zhousheng Yang; yangzs117@163.com

Received 1 July 2021; Revised 26 October 2021; Accepted 3 November 2021; Published 17 November 2021

Academic Editor: Syed Sameer Aga

Copyright © 2021 Dabin Kuang et al. This is an open access article distributed under the Creative Commons Attribution License, which permits unrestricted use, distribution, and reproduction in any medium, provided the original work is properly cited.

Endothelial inflammation and vascular damage are essential risk factors contributing to hypertension. Suppressor of cytokine signaling 3 (SOCS3) is involved in the regulation of multiple inflammatory pathways. A large number of studies have shown that the anti-inflammatory effect of SOCS3 in hypertension, obesity, and allergic reactions has brought more insights into the inhibition of inflammation. Therefore, we selected a tagSNP of SOCS3 (rs8064821) to investigate whether they are contributing to the risk of hypertension in the Chinese population. In total, 532 patients with hypertension and 569 healthy controls were enrolled for two central of China. SOCS3 rs8064821 C>A polymorphism was genotyped using TaqMan assay. SOCS3 rs8064821 CA genotype was associated with an increased risk of hypertension (OR = 1.821, 95%CI = 1.276-2.600,  $P = 0.001$ ). Rs8064821 A allele was associated with higher SOCS3 mRNA level in PBMCs from healthy donors. SOCS3 rs8064821 C>A polymorphism may contribute to the risk of hypertension in the Chinese population by regulating the expression of SOCS3.

## 1. Introduction

Hypertension is the leading contributing factor to all-cause global mortality Manosroi & Williams [1]. To date, hypertension affects over 1.2 billion individuals worldwide and has become the most critical and expensive public health problem Durham & Palmer [2]; Manosroi & Williams [1]; Rossier, Bochud, & Devuyst [3]; Samson, Ayinapudi, Le Jemtel, & Oparil [4]. It is the main risk factor for stroke (ischemic and hemorrhagic) and coronary artery disease Manosroi & Williams [1]; Rossier et al. [3]. In the past decades, considerable progress has been made in understanding that hypertension is not a disease but a syndrome. Studies have shown that most cases of hypertension are affected by environmental and disease factors, including drinking, smoking, changes in daily habits, hyperlipidemia, atherosclerosis, and diabetes. At the same time, genetic association studies have shown that genetic susceptibility has a great influence on the risk and prognosis of

hypertension Kolifarhood et al. [5]. However, the genetic factors affecting hypertension are too complicated. Current research shows that it is a multigene-regulated disease. Identifying new risk sites for hypertension may help promote early diagnosis and therapeutic intervention of the disease.

Suppressor of cytokine signaling 3 (SOCS3) maps to chromosome 17q25.3 and consists of two exons Rancourt et al. [6]. SOCS3 is one of the suppressors of the cytokine signaling (SOCS) protein family. It modulates the outcome of infections and autoimmune diseases. And it has been shown to be involved in regulating signal transduction through a variety of cytokines, including insulin signaling and leptin signaling Carow & Rottenberg [7]. Recent studies have found that SOCS1 and SOCS3 are strong negative feedback regulators of cytokine signaling mediated by Janus kinase (JAK) signal transduction and transcription signal pathway activators and can play a key role in the development and progression of cancer and cardiovascular disease.



The abnormal expression of SOCS3 in cancer cells, such as breast cancer Sun et al. [8], gastric cancer Zhou, Peng, & Xu [9], and small-cell lung cancer Zhao et al. [10], is related to the disorder of cell growth, migration, and death induced by a variety of cytokines and hormones in human cancers. It has been reported that inflammatory activation can upregulate SOCS3 expression and induce cardiovascular diseases Gan et al. [11]; Park et al. [12]; Wiejak, Dunlop, Mackay, & Yarwood [13]. However, some researches also confirmed that SOCS3 has a protective effect in limiting vascular inflammation. SOCS3 can reduce the ability of IL-6 signal transduction, thereby preventing vascular inflammatory diseases, such as atherosclerosis Ortiz-Munoz et al. [14]. And decreased SOCS3 leads to excessive production of inflammatory molecules in VSMC, which leads to enhanced vascular remodeling and vasoconstriction Tian et al. [15], while the mechanism of how SOCS3 affects hypertension remains unclear.

Obesity and chronic inflammation are key factors in the occurrence of hypertension, and they mutually cause and influence each other Mouton, Li, Hall, & Hall [16]. There is no report that the polymorphism of SOCS3 is associated with the risk of hypertension. Currently, Cid-Soto et al. found that the CAT haplotype in SOCS3 is associated with metabolic syndrome in Mestizos and correlated with protection against high blood pressure Cid-Soto et al. [17]. However, many studies have found that the polymorphisms of SOCS3 are related to obesity and serum lipid levels. Obesity is strongly associated with hypertension and cardiovascular disease Rahmouni, Correia, Haynes, & Mark [18]. Tessier et al. found that SOCS3 rs6501199, rs12944581, rs4969172, and rs4436839 polymorphisms affected the BMI of various ethnic groups Tessier, Fontaine-Bisson, Lefebvre, El-Sohehy, & Roy-Gagnon [19]. And another study has found that rs4969170 in SOCS3 was significantly associated with BMI positively Li et al. [20]. Previous studies have also found that rs4969168 Talbert et al. [21] and rs12953258 Yao et al. [22] polymorphisms are related to dyslipidemia in different populations.

However, whether the SOCS3 gene polymorphism is associated with the risk of hypertension has not been studied. The purpose of this study is to determine the predictive biomarkers of hypertension risk in the Chinese population and establish an experimental basis to improve the understanding of the causes and mechanisms of hypertension.

## 2. Materials and Methods

**2.1. Study Participants.** We recruited a total of 532 patients with hypertension and 569 healthy controls from 2 hospitals in 2 provinces of China. Among them, there are 274 hypertension patients and 285 control individuals included between January 2018 and December 2020 from the First People's Hospital of Jining City, Shandong Province. And there are 248 hypertension patients and 279 control individuals included between January 2020 and April 2021 from the People's Hospital of Guangxi Zhuang Autonomous Region. Eligible patients were men and women aged 18-80 years, with clinical evidence of hypertension as demonstrated by the World Health Organization that stipulates systolic blood

pressure (SBP)  $\geq 140$  mmHg and/or diastolic blood pressure (DBP)  $\geq 90$  mmHg. Major exclusion criteria covered tumors or malignant diseases, severe hepatic or renal dysfunctions, and pregnancy. Control individuals with similar age and gender were selected from the physical examination center of the same hospital. The study protocols received approval from the People's Hospital of Guangxi Zhuang Autonomous Region. Informed consent was obtained from each participant or their guardian before the research.

**2.2. Polymorphism Selection.** Genetic polymorphisms were screened by the 1000 Genomes Project (<http://www.internationalgenome.org/>). Haploview 4.2 was used to select, and according to CHB and CHS, an unbalanced  $R^2$  value is more than 0.8, and the minimum allele frequency (MAF) was greater than 5%. F-SNP software (<http://compbio.cs.queensu.ca/F-SNP/>) was used to predict the possible functions of these selected sites. At last, we selected one site (rs8064821 C>A) of SOCS3 tagSNPs based on the above screening results and combined with the literature.

**2.3. Genomic DNA Extraction and Genotyping.** Genomic DNA was extracted from whole blood using the E.Z.N.A.<sup>™</sup> Blood DNA Midi Kit (D3494, Omega) according to the standard protocol. DNAs were stored at  $-80^{\circ}\text{C}$  until analysis. Genotype analysis was undertaken using TaqMan SNP Genotyping Assay from Applied Biosystems using 7500 Real-Time PCR System. And genotyping was performed utilizing TaqMan<sup>™</sup> Genotyping Master Mix (4371355, Thermo) and TaqMan probes (C\_43672951\_10, Thermo) as recommended by the manufacturer.

**2.4. Isolation of Peripheral Blood Mononuclear Cells (PBMCs).** 30 healthy control subjects were recruited from the People's Hospital of Guangxi Zhuang Autonomous Region. An EDTA anticoagulant tube was used to obtain 5 mL of peripheral venous blood from each subject. The blood sample was diluted with an equal volume of phosphate-buffered saline (PBS). PBMCs were stratified using an equal volume of Histopaque-1077 (Sigma-Aldrich, St. Louis, MO) and separated by centrifugation ( $400 \times g$ ) for 30 minutes at room temperature.

**2.5. RNA Isolation and Real-Time PCR.** RNAiso Plus reagents (9109, TAKARA) were utilized to extract the total RNA from PBMCs. The absorbance of the extracted RNA was measured on a spectrophotometer. Subsequently, the RNA samples were converted to cDNA using PrimeScript RT Reagent Kit (RR036A, TAKARA) according to the manufacturer's instruction. The mRNA levels of SOCS3 in the samples were quantified with ABI 7500 Real-Time PCR System using SYBR Premix EX Taq System (RR820A, TAKARA) following the manufacturer's instruction. The primer sequences involved in the experiment were as follows: SOCS3, forward, 5'-CACA TGGCACAAGCACAAGA-3'; reverse, 5'-AAGTGTCCCCT GTTTGGAGG-3'; GAPDH, forward, 5'-CTGCACCACCA ACTGCTTAG-3', reverse, 5'-AGGTCCACCCTGACA CGTT-3'. The expression of target genes was analyzed using the  $2^{-\Delta\Delta\text{Ct}}$  method.

TABLE 1: General characteristics of the hypertension patients and controls.

Characteristics	Guangxi Province			Shandong Province			Combined subjects		
	Control	Hypertension	<i>P</i>	Control	Hypertension	<i>P</i>	Control	Hypertension	<i>P</i>
Gender	279	248		290	274		569	522	
Male (%)	168 (60.2%)	152 (61.3%)		159 (54.8%)	135 (49.3%)		327 (57.5%)	287 (55.0%)	
Female (%)	111 (39.8%)	96 (38.7%)	0.801	131 (45.2%)	139 (50.7%)	0.187	242 (42.5%)	235 (45.0%)	0.408
Age (years)	53 ± 8	53 ± 8	0.231	53 ± 7	53 ± 8	0.394	53 ± 8	53 ± 8	0.146
BMI (kg/m <sup>2</sup> )	22.67 ± 1.52	25.27 ± 2.77	<0.001	23.40 ± 2.70	24.81 ± 3.61	<0.001	23.04 ± 2.23	25.02 ± 3.24	<0.001
SBP (mmHg)	121 ± 12	136 ± 20	<0.001	121 ± 11	139 ± 18	<0.001	121 ± 11	138 ± 19	<0.001
DBP (mmHg)	75 ± 7	84 ± 12	<0.001	76 ± 8	81 ± 13	<0.001	76 ± 8	82 ± 13	<0.001
Smoking history (%)	34 (12.2%)	61 (24.6%)	<0.001	46 (15.9%)	77 (28.1%)	<0.001	83 (14.6%)	138 (26.4%)	<0.001
FBG (mmol/L)	4.58 ± 0.47	5.5 ± 1.19	<0.001	4.91 ± 0.65	5.44 ± 0.83	<0.001	4.75 ± 0.59	5.46 ± 1.01	<0.001
TG (mmol/L)	1.18 ± 0.40	2.04 ± 1.32	<0.001	1.33 ± 0.79	1.45 ± 0.95	0.127	1.26 ± 0.64	1.73 ± 1.18	<0.001
TC (mmol/L)	4.56 ± 0.61	5.00 ± 0.94	<0.001	4.21 ± 1.11	4.70 ± 1.10	<0.001	4.38 ± 0.92	4.85 ± 1.04	<0.001
HDL-C (mmol/L)	1.24 ± 0.35	1.24 ± 0.51	1	1.23 ± 0.32	1.42 ± 0.57	<0.001	1.24 ± 0.33	1.33 ± 0.55	<0.001
LDL-C (mmol/L)	2.55 ± 0.64	3.07 ± 1.64	<0.001	2.17 ± 0.86	2.40 ± 0.76	0.001	2.36 ± 0.78	2.72 ± 1.30	<0.001

BMI: body mass index; SBP: systolic blood pressure; DBP: diastolic blood pressure; FBG: fasting blood glucose; TC: total cholesterol; TG: triglyceride; HDL-C: high-density lipoprotein cholesterol; LDL-C: low-density lipoprotein cholesterol.

2.6. *Statistical Assay.* All data are expressed as mean ± SD. SPSS 19.0 (version 19.0 for Windows; Chicago, IL, USA) was used for statistical analysis. Hardy-Weinberg equilibrium was compared by the  $\chi^2$  test. Unpaired two-tailed Student's *t*-test was used to determine statistical significance between two groups' normally distributed continuous variables. And for multiple group comparison, one-way ANOVA analysis was used. Logistic regression method was used to analyze the effect of SOCS3 polymorphism on the risk of hypertension adjusting for multiple cardiovascular risk factors. ORs and 95% CIs calculated from the logistic regression analysis were used to assess the strength of association between SOCS3 polymorphisms and hypertension risk. A two-sided *P* value < 0.05 was considered statistically significant.

### 3. Results

3.1. *Population Characteristics.* The basic clinical characteristics of the 532 hypertension patients and 569 healthy controls are shown in Table 1. Patients with hypertension showed significantly higher BMI, SBP, DBP, fasting blood glucose (FBG), total cholesterol (TC), high-density lipoprotein cholesterol (HDL-C), and low-density lipoprotein cholesterol (LDL-C) compared to the controls. Hypertension patients also showed a higher prevalence of smoking. No significant differences in gender and age were observed between patients and controls (*P* > 0.05).

3.2. *Association of SOCS3 rs8064821 C>A Polymorphisms and Risk for Hypertension in the South of China.* Genotype distribution of the SOCS3 rs8064821 polymorphisms in both controls and hypertension patients was in agreement with the Hardy-Weinberg equilibrium (HWE) (control: HWE = 0.347, and hypertension: HWE = 0.812). Table 2 shows the association between SOCS3 polymorphisms and hypertension risk in the south of China. Logistic regression analysis

showed that the rs8064821 TT genotypes were associated with increased risk of hypertension (additive model: AA: odds ratio (OR) = 2.558, 95%confidence interval (CI) = 1.150-5.690, *P* = 0.021; dominant model: OR = 1.509, 95%CI = 1.067-2.133, *P* = 0.020; and recessive model: OR = 2.232, 95%CI = 1.017-4.897, *P* = 0.045). And after adjustment for age, gender, BMI, smoking history, FBG, and dyslipidemia, the result was also significant (additive model: CA: odds ratio (OR) = 2.647, 95%confidence interval (CI) = 1.391-5.038, *P* = 0.003; AA: odds ratio (OR) = 5.776, 95%confidence interval (CI) = 1.613-20.682, *P* = 0.007; dominant model: OR = 2.943, 95%CI = 1.584-5.466, *P* = 0.001; and recessive model: OR = 3.729, 95%CI = 1.119-12.426, *P* = 0.032).

3.3. *Association of SOCS3 rs8064821 C>A Polymorphisms and Risk for Hypertension in the North of China.* Similar to the south of China, genotype distribution of the SNP was in accordance with HWE in the controls and patients (control: HWE = 0.607, and hypertension: HWE = 0.654, respectively). Logistic regression analyses revealed that hypertension risk was increased significantly in the CA genotype of rs8064821 polymorphism than the CC genotype (additive model: CA: OR = 1.565, 95%CI = 1.100-2.228, *P* = 0.013; dominant model: OR = 1.592, 95%CI = 1.135-2.232, *P* = 0.007) as shown in Table 3. And after adjustment, the association was still significant (additive model: CA: OR = 1.965, 95%CI = 1.210-3.191, *P* = 0.006; dominant model: OR = 1.854, 95%CI = 1.166-2.947, *P* = 0.009).

3.4. *Association of SOCS3 rs8064821 C>A Polymorphisms and Risk for Hypertension in Combined Subjects.* Then, we aggregated and analyzed all the data from the two centers in Guangxi and Shandong Province. We found that the polymorphism of rs8064821 was associated with the risk of hypertension. Logistic regression analysis showed that the rs8064821 CA and AA genotypes were associated with

TABLE 2: Association between SOCS3 rs8064821 C&gt;A polymorphism and hypertension risk in Guangxi Province.

Models	Genotypes	Control, <i>n</i> = 279 (%)	Hypertension, <i>n</i> = 248 (%)	Unadjusted OR (95% CI)	<i>P</i> value	Adjusted OR* (95% CI)	Adjusted <i>P</i> value*
rs8064821 C>A		HWE = 0.374	HWE = 0.812				
Additive	CC	171 (61.3)	127 (51.2)	1.00 (reference)		1.00 (reference)	
	CA	98 (35.1)	102 (41.1)	1.401 (0.978-2.009)	0.066	2.647 (1.391-5.038)	0.003
	AA	10 (3.6)	19 (7.7)	2.558 (1.150-5.690)	0.021	5.776 (1.613-20.682)	0.007
Dominant	CC	171 (61.3)	127 (51.2)	1.00 (reference)		1.00 (reference)	
	CA/AA	108 (38.7)	121 (48.8)	1.509 (1.067-2.133)	0.020	2.943 (1.584-5.466)	0.001
Recessive	CC/CA	269 (96.4)	229 (92.3)	1.00 (reference)		1.00 (reference)	
	AA	10 (3.6)	19 (7.7)	2.232 (1.017-4.897)	0.045	3.729 (1.119-12.426)	0.032

OR: odds ratio; CI: confidence interval. \* Adjusted for age, gender, BMI, smoking history, FBG, and dyslipidemia.

TABLE 3: Association between SOCS3 rs8064821 C&gt;A polymorphism and hypertension risk in Shandong Province.

Models	Genotypes	Control, <i>n</i> = 290 (%)	Hypertension, <i>n</i> = 274 (%)	Unadjusted OR (95% CI)	<i>P</i> value	Adjusted OR* (95% CI)	Adjusted <i>P</i> value*
rs8064821 C>A		HWE = 0.607	HWE = 0.654				
Additive	CC	187 (64.5)	146 (53.3)	1.00 (reference)		1.00 (reference)	
	CA	90 (31.0)	110 (40.1)	1.565 (1.100-2.228)	0.013	1.965 (1.210-3.191)	0.006
	AA	13 (4.5)	18 (6.6)	1.773 (0.841-3.738)	0.132	1.264 (0.456-3.502)	0.653
Dominant	CC	187 (64.5)	100 (38.0)	1.00 (reference)		1.00 (reference)	
	CA/AA	103 (35.5)	163 (62.0)	1.592 (1.135-2.232)	0.007	1.854 (1.166-2.947)	0.009
Recessive	CC/CA	277 (95.5)	256 (93.4)	1.00 (reference)		1.00 (reference)	
	AA	13 (4.5)	18 (6.6)	1.498 (0.720-3.119)	0.280	0.979 (0.361-2.659)	0.967

OR: odds ratio; CI: confidence interval. \* Adjusted for age, gender, BMI, smoking history, FBG, and dyslipidemia.

increased risk of hypertension (additive model: CA: OR = 1.479, 95%CI = 1.150-1.902,  $P = 0.002$ ; AA: OR = 2.110, 95%CI = 1.225-3.634,  $P = 0.007$ ; dominant model: OR = 1.548, 95%CI = 1.215-1.971,  $P < 0.001$ ; and recessive model: OR = 1.811, 95%CI = 1.061-3.091,  $P = 0.029$ , Table 4). However, no significant association was observed after adjustment for the recessive model, while the associations for additive and dominant models were still significant (additive model: CA: OR = 1.821, 95%CI = 1.276-2.600,  $P = 0.001$ ; AA: OR = 2.143, 95%CI = 1.042-4.410,  $P = 0.038$ ; dominant model: OR = 1.836, 95%CI = 1.326-2.619,  $P < 0.001$ ).

**3.5. Association of SOCS3 rs8064821 C>A Polymorphism with SOCS3 Expression.** In order to explore whether the genetic polymorphism of rs8064821 is associated with the mRNA expression level of SOCS3, we analyzed the relevant information in the Genotype-Tissue Expression (GTEx) database. As shown in Figure 1, rs8064821 A allele was associated with increased SOCS3 mRNA in adipose tissue, such

as adipose subcutaneous and adipose visceral (the relative expression median: CC: -0.09489, CA: 0.2325, AA: 0.4881,  $P = 2.21e - 8$ ; CC: -0.07741, CA: 0.2782, AA: -0.02204,  $P = 4.99e - 8$ , respectively). Similarly, in artery tissues, the mRNA expression level of SOCS3 has the same correlation with the rs8064821 genotype (artery aorta: CC: -0.08084, CA: 0.4946, AA: 0.05818,  $P = 1.33e - 5$ ; artery coronary: CC: -0.08208, CA: 0.2727, AA: 0.6382,  $P = 1.02e - 2$ ; and artery tibial: CC: -0.1052, CA: 0.2445, AA: 0.2314,  $P = 1.54e - 7$ , respectively). And in whole blood, the relative expression level of SOCS3 was higher in the CA and AA genotypes than in the AA genotype (CC: -0.1179, CA: 0.2184, AA: 0.3954,  $P = 4.1e - 8$ ).

To further verify the analysis results of the database, we determined the mRNA expression level of SOCS3 in 30 randomly selected healthy controls. PBMCs from 21 subjects carrying the rs8064821 CC genotype were collected, the others ( $n = 9$ ) bearing the rs8064821 CA genotype. No PBMCs from individuals with the rs8064821 AA genotype



TABLE 4: Association between SOCS3 rs8064821 C>A polymorphism and hypertension risk in combined subjects.

Models	Genotypes	Control, n = 569 (%)	Hypertension, n = 522 (%)	Unadjusted OR (95% CI)	P value	Adjusted OR* (95% CI)	Adjusted P value*
rs8064821		HWE = 0.786	HWE = 0.368				
C>A							
Additive	CC	358 (62.9)	273 (52.3)	1.00 (reference)		1.00 (reference)	
	CA	188 (33.0)	212 (40.6)	1.479 (1.150-1.902)	0.002	1.821 (1.276-2.600)	0.001
	AA	23 (4.1)	37 (7.1)	2.110 (1.225-3.634)	0.007	2.143 (1.042-4.410)	0.038
Dominant	CC	358 (62.9)	273 (52.3)	1.00 (reference)		1.00 (reference)	
	CA/AA	211 (37.1)	249 (47.7)	1.548 (1.215-1.971)	<0.001	1.863 (1.326-2.619)	<0.001
Recessive	CC/CA	546 (95.9)	485 (92.9)	1.00 (reference)		1.00 (reference)	
	AA	23 (4.1)	37 (7.1)	1.811 (1.061-3.091)	0.029	1.696 (0.839-3.428)	0.141

OR: odds ratio; CI: confidence interval. \* Adjusted for age, gender, BMI, smoking history, FBG, and dyslipidemia.

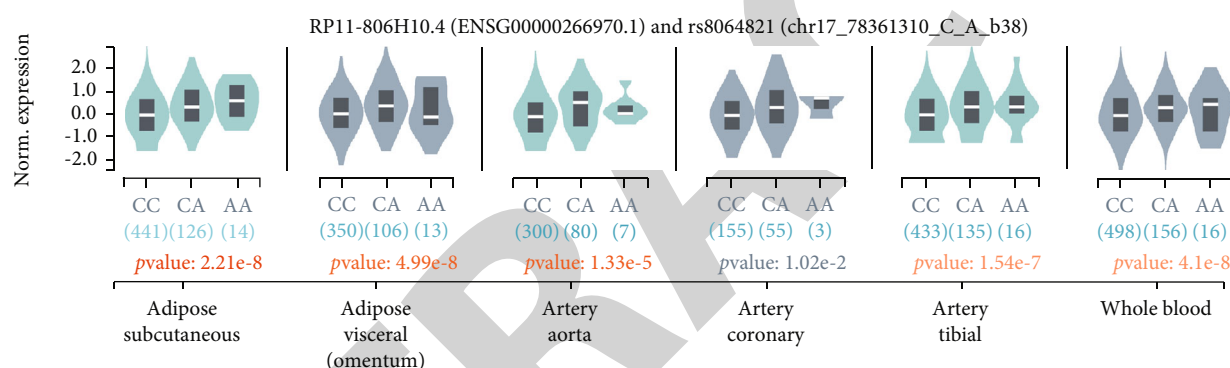


FIGURE 1: Effect of SOCS3 rs8064821 C>A polymorphism on SOCS3 mRNA expression in tissues from healthy normal donors.

were collected. As compared with PBMCs carrying the rs8064821 CC genotype, the CA genotype showed significantly higher levels of SOCS3 mRNA expression ( $P < 0.05$ , Figure 2).

#### 4. Discussion

In this study, we investigated whether SOCS3 gene polymorphism was involved in the risk of hypertension in the Chinese population using individuals from two centers. The results presented here represent that rs8064821 C>A polymorphism contributed to the risk of hypertension. Our results demonstrated that the rs8064821 CA genotype was associated with an increased risk of hypertension in the Chinese Han population. Moreover, we observed that the rs8064821 C>A polymorphism affected the expression level of SOCS3 in healthy subjects, with subjects heterozygote for the rs8064821 genotype showing significantly higher mRNA level of SOCS3 than the AA genotype in PBMCs.

SOCS protein is usually expressed at low levels under basal conditions, but it is rapidly induced by inflammatory factors. Induced SOCS3 can block IL-6/JAK/STAT activity, forming a classic negative feedback loop Moshapa, Riches-Suman, & Palmer [23]. SOCS3 inhibits the activation of

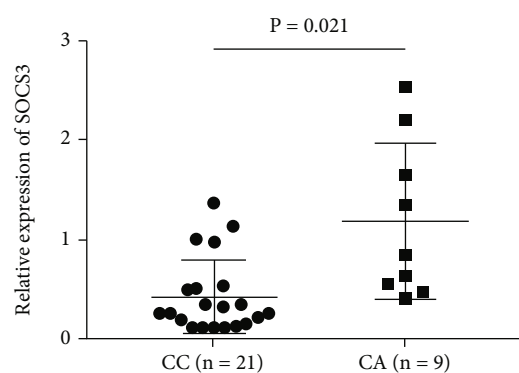


FIGURE 2: Effect of the SOCS3 rs8064821 C>A polymorphism on SOCS3 mRNA expression in PBMCs.

JAK/STAT induced by IL-6 by directly inhibiting JAK kinase activity, thereby preventing the binding of the substrate and ATP Kershaw et al. [24]. Durham and Palmer found that IL-6 activates JAK-STAT signaling to induce the transcription of proinflammatory and proantigen genes, and SOCS3 restricts IL-6 signaling, which resists the progression of pulmonary arterial hypertension (PAH) Durham & Palmer [25]. Damage to endothelial function and vascular

inflammation are key factors in the onset of hypertension. Recently, a study also found that SOCS3 expression induced by angiotensin II regulates the effect of inflammation. Knockout of SOCS3 expression in bone marrow-derived cells can prevent systemic angiotensin II-induced vascular dysfunction and then affect the angiotensin II involved in the control of blood pressure and cardiac contractility Li, Kinzenbaw, Modrick, Pewe, & Faraci [26]. SOCS3 plays an important role in maintaining the vascular function, and the correlation between the polymorphism of SOCS3 and cardiovascular disease has also been partially studied. A recent study found a significant association between SOCS3 rs7221341 and decreased risk of high blood pressure. And the SOCS3 rs7221341, rs4669168, and rs9914220 polymorphisms were associated with type 2 diabetes and high waist circumference in Mexican Amerindians Cid-Soto et al. [17]. In this study, we found that the SOCS3 rs8064821 C>A polymorphism is associated with the risk of hypertension. The risk of hypertension of the CA genotype is significantly higher than that of the CC genotype.

Some previous studies have found that the polymorphism of SOCS3 rs8064821 is related to some diseases, such as cancer and obesity. Reid-Lombardo et al. found that in patients with resection of pancreatic cancer, the SOCS3 rs8064821 C>A polymorphism was associated with a survival advantage of approximately 10 months compared with noncarriers Reid-Lombardo et al. [27], while Jiang et al. analyzed the association between the genetic polymorphism of the SOCS3 gene and the incidence and progression of hepatocellular carcinoma (HCC) Jiang et al. [28]. They confirmed that the genotype frequencies of rs12953258 and rs8064821 were not significantly different between HCC and the control group. However, for the rs4969170 polymorphism, the prevalence of GG in HCC patients was higher than that in the control group. Boyraz et al. found that SOCS3 rs8064821 G>T polymorphism is associated with obesity parameters in children. Their results showed that the GG genotype frequency at rs8064821 locus is significantly higher in the nonmetabolic syndrome obese group than in the metabolic syndrome obese group Boyraz et al. [29]. In another study, the authors did not find the correlation between rs4969169, rs12953258, and rs8064821 and general obesity and central obesity in normal female twins and also not related to the two indexes of insulin sensitivity Jamshidi et al. [30]. In this study, we found that the SOCS3 rs8064821 C>A polymorphism is associated with the risk of hypertension in the populations of the two centers. Meanwhile, the analysis after summarizing all subjects also yielded similar results. The risk of hypertension of the CA or AA genotype is about 1.8-fold than that of the CC type.

Hypertension is a disease affected by multiple factors, and the activation of inflammatory pathways plays an important role in its pathogenesis. SOCS3 modulates the inflammatory pathways responsible for vascular stability. Recently, Zhang et al. analyzed the data of blood transcriptomics in the GEO database and collected clinical subjects for verification. They found that compared with healthy controls, patients with stable coronary artery disease (CAD) and acute coronary syndrome (ACS) had significantly lower levels of SOCS3 expression. And the probe expression levels

of SOCS3 were significantly upregulated in patients with ST-segment elevation myocardial infarction (STEMI) when compared to stable CAD patients Zhang et al. [31]. Ali et al. used ELISA to detect SOCS3 levels in serum. Their results showed higher SOCS3 levels in the hypertensive group versus normotensive Ali, Ali, Farhat, & Fatima [32]. A recent study found that SOCS3 has a certain value in predicting the efficacy of pregnancy-induced hypertension by analyzing the plasma SOCS3 levels before and after being treated with nifedipine in patients with pregnancy-induced hypertension Zhao, Ai, Wu, & Dong [33]. These researches suggest that the expression level of SOCS3 may be related to the pathological process of hypertension. By analyzing the data in the GTEx database, we found that the expression level of the rs8064821 CA and AA genotype SOCS3 in adipose tissue, artery, and whole blood was significantly higher than that of the CC genotype. What is more, we found a significant upregulation of SOCS3 in the CA genotype than in the CC genotype in PBMCs. Previously, we used the F-SNP online tool to predict the function of the polymorphism of rs8064821. It was found that this site may affect the binding of transcription factors, which in turn affects the expression of SOCS3. Based on the results of this experiment, we speculate that the SOCS3 rs8064821 C>A polymorphism may affect the risk of hypertension by affecting the expression level of SOCS3.

While our results are promising, the intensity of current research is accompanied by some limitations. We would like to enlist all the limitations of the study:

- (1) Although this is a two-center study, the participants in this study are restricted to the Guangxi and Shandong populations in China. Therefore, the current research results cannot be generalized to other racial/ethnic groups. Due to the small sample size, although the calculation meets the statistical power, there may still be deviations. Therefore, large-scale, high-quality research should be conducted in the future to verify these findings
- (2) Due to the low frequency of the rs8064821 AA genotype (about 4% in healthy people), we did not collect samples of the AA genotype when studying the SOCS3 mRNA expression levels of different genotypes. We did not measure the expression levels of SOCS3 mRNA in peripheral blood PBMC cells of people with the AA genotype, thus preventing us from exploring the impact of the AA genotype on human phenotypes. These data may lead to different conclusions about the relationship between SOCS3 rs8064821 and its mRNA expression. Further research needs to expand the RNA sample to verify our conclusions
- (3) The conclusion drawn here lacks universality. In our study, the polymorphism of rs8064821 may affect the mRNA expression of SOCS3, but the mechanism is unclear. Although the previous studies have confirmed that the high expression of SOCS3 is relevant to the increase of inflammatory factors and blood lipid levels, whether the polymorphism of

rs8064821 is related to it needs further experiments to verify. Therefore, we need in vivo and in vitro studies to confirm the mechanism of the association between rs8064821 and the risk of hypertension

## 5. Conclusion

In conclusion, here, we provide the possibility of the SOCS3 rs8064821 C>A polymorphism in predicting hypertension risk. Well-designed case-control studies with large samples are needed to confirm these findings. Our study serves as a basis for future replication studies in independent populations or functional studies of SOCS3 in hypertension risk.

## Data Availability

he research data used to support the findings of this study are available from the corresponding author upon request.

## Conflicts of Interest

The authors declare that they have no competing interests.

## Authors' Contributions

DBK and ZSY conceived and designed the experiments. LCD, TML, and LYL performed the experiments. MLZ and YLX analyzed the data. DBK and LYL contributed reagents/materials/analysis tools. DBK and ZSY wrote the paper. All authors read and approved the final manuscript.

## Acknowledgments

This work was supported by research grants of the National Natural Science Foundation of China (No. 81803767), the Hunan Provincial Natural Science Foundation of China (No. 2021JJ40617), the Self-financing Scientific Research Project of Guangxi Health Commission (grant number Z20201003), and the Science and Technology Program of Changsha, China (kq1801125).

## References

- [1] W. Manosroi and G. H. Williams, "Genetics of human primary hypertension: focus on hormonal mechanisms," *Endocrine Reviews*, vol. 40, no. 3, pp. 825–856, 2019.
- [2] M. H. Forouzanfar, P. Liu, G. A. Roth et al., "Global Burden of Hypertension and Systolic Blood Pressure of at Least 110 to 115 mm Hg, 1990–2015," *JAMA*, vol. 317, no. 2, pp. 165–182, 2017.
- [3] B. C. Rossier, M. Bochud, and O. Devuyst, "The hypertension pandemic: an evolutionary perspective," *Physiology (Bethesda)*, vol. 32, no. 2, pp. 112–125, 2017.
- [4] R. Samson, K. Ayinapudi, T. H. Le Jemtel, and S. Oparil, "Obesity, hypertension, and bariatric surgery," *Current Hypertension Reports*, vol. 22, no. 7, p. 46, 2020.
- [5] G. Kolifarhood, S. Sabour, M. Akbarzadeh et al., "Genome-wide association study on blood pressure traits in the Iranian population suggests *\_ZBED9\_* as a new locus for hypertension," *Scientific Reports*, vol. 11, no. 1, p. 11699, 2021.
- [6] R. C. Rancourt, R. Ott, K. Schellong et al., "Altered SOCS3 DNA methylation within exon 2 is associated with increased mRNA expression in visceral adipose tissue in gestational diabetes," *Epigenetics*, vol. 16, no. 5, pp. 488–494, 2021.
- [7] B. Carow and M. E. Rottenberg, "SOCS3, a major regulator of infection and inflammation," *Frontiers in Immunology*, vol. 5, p. 58, 2014.
- [8] M. Sun, C. Tang, J. Liu et al., "Comprehensive analysis of suppressor of cytokine signaling proteins in human breast cancer," *BMC Cancer*, vol. 21, no. 1, p. 696, 2021.
- [9] Q. Y. Zhou, P. L. Peng, and Y. H. Xu, "MiR-221 affects proliferation and apoptosis of gastric cancer cells through targeting SOCS3," *European Review for Medical and Pharmacological Sciences*, vol. 23, no. 21, pp. 9427–9435, 2019.
- [10] G. Zhao, L. Gong, D. Su et al., "Cullin5 deficiency promotes small-cell lung cancer metastasis by stabilizing integrin  $\beta$ 1," *The Journal of Clinical Investigation*, vol. 129, no. 3, pp. 972–987, 2019.
- [11] A. M. Gan, M. M. Pirvulescu, D. Stan et al., "Monocytes and smooth muscle cells cross-talk activates STAT3 and induces resistin and reactive oxygen species and production," *Journal of Cellular Biochemistry*, vol. 114, no. 10, pp. 2273–2283, 2013.
- [12] S. J. Park, K. P. Lee, S. Kang et al., "Sphingosine 1-phosphate induced anti-atherogenic and atheroprotective M2 macrophage polarization through IL-4," *Cellular Signalling*, vol. 26, no. 10, pp. 2249–2258, 2014.
- [13] J. Wijek, J. Dunlop, S. P. Mackay, and S. J. Yarwood, "Flavonoids induce expression of the suppressor of cytokine signaling 3 (SOCS3) gene and suppress IL-6-activated signal transducer and activator of transcription 3 (STAT3) activation in vascular endothelial cells," *The Biochemical Journal*, vol. 454, no. 2, pp. 283–293, 2013.
- [14] G. Ortiz-Muñoz, J. L. Martin-Ventura, P. Hernandez-Vargas et al., "Suppressors of cytokine signaling modulate JAK/STAT-mediated cell responses during atherosclerosis," *Arteriosclerosis, Thrombosis, and Vascular Biology*, vol. 29, no. 4, pp. 525–531, 2009.
- [15] D. Tian, X. Teng, S. Jin et al., "Endogenous hydrogen sulfide improves vascular remodeling through PPAR $\delta$ /SOCS3 signaling," *Journal of Advanced Research*, vol. 27, pp. 115–125, 2021.
- [16] A. J. Mouton, X. Li, M. E. Hall, and J. E. Hall, "Obesity, hypertension, and cardiac dysfunction," *Circulation Research*, vol. 126, no. 6, pp. 789–806, 2020.
- [17] M. A. Cid-Soto, A. Martínez-Hernández, H. García-Ortiz et al., "Gene variants in *\_AKT1\_*, *\_GCKR\_* and *\_SOCS3\_* are differentially associated with metabolic traits in Mexican Amerindians and Mestizos," *Gene*, vol. 679, pp. 160–171, 2018.
- [18] K. Rahmouni, M. L. Correia, W. G. Haynes, and A. L. Mark, "Obesity-associated hypertension," *Hypertension*, vol. 45, no. 1, pp. 9–14, 2005.
- [19] F. Tessier, B. Fontaine-Bisson, J. F. Lefebvre, A. El-Sohemy, and M. H. Roy-Gagnon, "Investigating gene-gene and gene-environment interactions in the association between overnutrition and obesity-related phenotypes," *Frontiers in Genetics*, vol. 10, p. 151, 2019.
- [20] P. Li, H. K. Tiwari, W. Y. Lin et al., "Genetic association analysis of 30 genes related to obesity in a European American population," *International Journal of Obesity*, vol. 38, no. 5, pp. 724–729, 2014.

## Retraction

# Retracted: A Systematic Review and Meta-Analysis of Therapeutic Efficacy and Safety of Alirocumab and Evolocumab on Familial Hypercholesterolemia

### BioMed Research International

Received 12 March 2024; Accepted 12 March 2024; Published 20 March 2024

Copyright © 2024 BioMed Research International. This is an open access article distributed under the Creative Commons Attribution License, which permits unrestricted use, distribution, and reproduction in any medium, provided the original work is properly cited.

This article has been retracted by Hindawi following an investigation undertaken by the publisher [1]. This investigation has uncovered evidence of one or more of the following indicators of systematic manipulation of the publication process:

- (1) Discrepancies in scope
- (2) Discrepancies in the description of the research reported
- (3) Discrepancies between the availability of data and the research described
- (4) Inappropriate citations
- (5) Incoherent, meaningless and/or irrelevant content included in the article
- (6) Manipulated or compromised peer review

The presence of these indicators undermines our confidence in the integrity of the article's content and we cannot, therefore, vouch for its reliability. Please note that this notice is intended solely to alert readers that the content of this article is unreliable. We have not investigated whether authors were aware of or involved in the systematic manipulation of the publication process.

Wiley and Hindawi regrets that the usual quality checks did not identify these issues before publication and have since put additional measures in place to safeguard research integrity.

We wish to credit our own Research Integrity and Research Publishing teams and anonymous and named external researchers and research integrity experts for contributing to this investigation.

The corresponding author, as the representative of all authors, has been given the opportunity to register their agreement or disagreement to this retraction. We have kept a record of any response received.

### References

- [1] X. Ge, T. Zhu, H. Zeng et al., "A Systematic Review and Meta-Analysis of Therapeutic Efficacy and Safety of Alirocumab and Evolocumab on Familial Hypercholesterolemia," *BioMed Research International*, vol. 2021, Article ID 8032978, 16 pages, 2021.



## Review Article

# A Systematic Review and Meta-Analysis of Therapeutic Efficacy and Safety of Alirocumab and Evolocumab on Familial Hypercholesterolemia

Xiaoyue Ge,<sup>1</sup> Tiantian Zhu,<sup>2</sup> Hao Zeng,<sup>1</sup> Xin Yu,<sup>2</sup> Juan Li,<sup>1</sup> Shanshan Xie,<sup>1</sup> Jinjin Wan,<sup>1</sup> Huiyao Yang,<sup>3</sup> Keke Huang,<sup>2</sup> and Weifang Zhang<sup>1,4</sup>

<sup>1</sup>The Second Affiliated Hospital of Nanchang University, Nanchang 330006, China

<sup>2</sup>Teaching and Research Office of Clinical Pharmacology, China Department of Pharmacy, College of Pharmacy, Xinxiang Medical University, Xinxiang 453003, China

<sup>3</sup>Phase I Clinical Trial Center of Chongqing University Cancer Hospital, Chongqing 400030, China

<sup>4</sup>Medical College of Nanchang University, Nanchang 330031, China

Correspondence should be addressed to Weifang Zhang; [z\\_weifang@163.com](mailto:z_weifang@163.com)

Received 28 May 2021; Accepted 11 September 2021; Published 31 October 2021

Academic Editor: Dabin Kuang

Copyright © 2021 Xiaoyue Ge et al. This is an open access article distributed under the Creative Commons Attribution License, which permits unrestricted use, distribution, and reproduction in any medium, provided the original work is properly cited.

**Objectives.** The aim of this study was to provide the first study to systematically analyze the efficacy and safety of PCSK9-mAbs in the treatment of familial hypercholesterolemia (FH). **Methods.** A computer was used to search the electronic Cochrane Library, PubMed/MEDLINE, and Embase databases for clinical trials using the following search terms: “AMG 145”, “evolocumab”, “SAR236553/REGN727”, “alirocumab”, “RG7652”, “LY3015014”, “RN316/bococizumab”, “PCSK9”, and “familial hypercholesterolemia” up to November 2020. Study quality was assessed with the Cochrane Collaboration’s tool, and publication bias was evaluated by a contour-enhanced funnel plot and the Harbord modification of the Egger test. After obtaining the data, a meta-analysis was performed using R software, version 4.0.3. **Results.** A meta-analysis was performed on 7 clinical trials (926 total patients). The results showed that PCSK9-mAbs reduced the LDL-C level by the greatest margin, WMD  $-49.14\%$ , 95% CI:  $-55.81$  to  $-42.47\%$ , on FH versus control groups. PCSK9-mAbs also significantly reduced lipoprotein (a) (Lp (a)), total cholesterol (TC), triglycerides (TG), apolipoprotein-B (Apo-B), and non-high-density lipoprotein cholesterol (non-HDL-C) levels and increased HDL-C and apolipoprotein-A1 (Apo-A1) levels of beneficial lipoproteins. Moreover, no significant difference was found between PCSK9-mAbs treatment and placebo in common adverse events, serious events, and laboratory adverse events. **Conclusion.** PCSK9-mAbs significantly decreased LDL-C and other lipid levels with satisfactory safety and tolerability in FH treatment.

## 1. Introduction

Familial hypercholesterolemia (FH) is a common genetic disorder that causes high low-density lipoprotein cholesterol (LDL-C) level from birth, which causes atherosclerotic plaque deposition in the arteries and a markedly increased risk of coronary heart disease (CHD) at a young age [1]. In FH, the most common defect is loss-of-function mutations in LDL receptor alleles. Other more uncommon causes of FH are defects in apolipoprotein B (ApoB) and proprotein convertase subtilisin/kexin type 9 serine (PCSK9) [2]. FH

includes homozygous and heterozygous types that have different symptoms, risks, and treatments. The incidence of FH is approximately 1 in 200–500 individuals and confers a significant risk for premature cardiovascular disease (CVD) [3]. Study has reported that the risk of premature CHD is elevated approximately 20-fold in young untreated heterozygous FH men and that homozygous FH patients typically develop CHD by the second decade of life [4].

Over the past decades, lipid-lowering drugs such as statins, ezetimibe, extended-release niacin formulations, and newer bile acid sequestrants have substantially improved

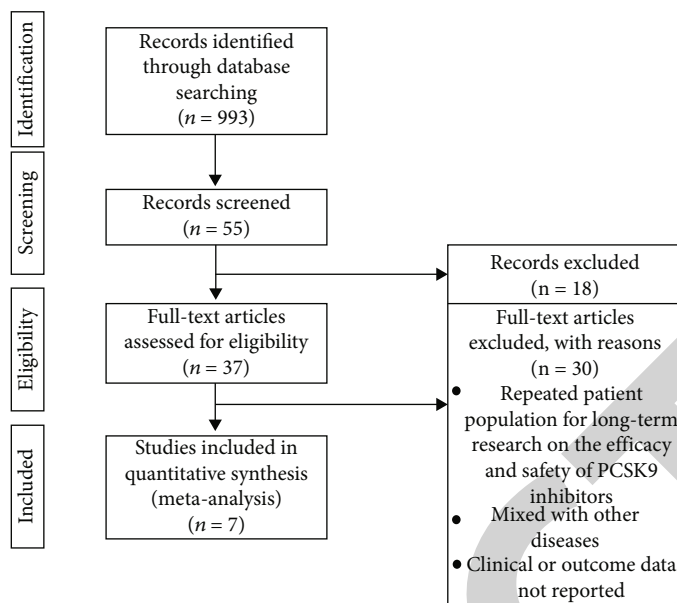


FIGURE 1: Study and patient selection.

the treatment of FH patients. However, it has been clinically observed that even if more than 50% of FH patients take high-dose statins orally, many patients still do not achieve desirable LDL cholesterol concentrations, and a high risk of CVD remains [5]. PCSK9, a major regulator of LDL-C levels, binds to the LDL receptor (LDLR) and is subsequently internalized by the receptor to enhance LDL-C degradation in endo-/lysosomal vesicles in the liver [6]. Phase 1 and 2 trials of PCSK9-mAbs have shown that the level of LDL cholesterol is further reduced by 55-60% when they are added to existing lipid-lowering treatments, for example, statins alone or statins combined with ezetimibe. Alirocumab/SAR236553/REGN727 and evolocumab/AMG145 are classic human PCSK9-mAbs. In recent years, studies have demonstrated that RG7652 [7], LY3015014 [8], and bococizumab/RN316 [9] are effective for altering the lipidome of plasma and lipoprotein fractions. However, these drug-related clinical studies were terminated.

Clinical trials have proven that PCSK9-mAbs (alirocumab and evolocumab) decrease the plasma LDL-C level in FH patients. Other lipids and lipoproteins, such as lipoprotein (a) (Lp(a)), total cholesterol (TC), triglycerides (TG), apolipoprotein-B (Apo-B), high-density lipoprotein cholesterol (HDL-C), and apolipoprotein-A1 (Apo-A1), can also benefit [10]. However, no report has comprehensively pinpointed the applicable targets of PCSK9-mAb-FH patients with sufficient clinical outcomes. To confirm the efficacy and safety of PCSK9-mAbs in FH patients, a total of 7 articles (926 patients) were assessed in this meta-analysis.

## 2. Methods

**2.1. Literature Search.** We followed the methods of our previous study described [11]. In general, we obtained individual participant data from studies identified through systematic searches of the published literature performed

using the Cochrane Library, PubMed/MEDLINE, and Embase databases (the following search terms were used: “AMG 145”, “evolocumab”, “SAR236553/REGN727”, “alirocumab”, “RG7652”, “LY3015014”, “RN316/bococizumab”, “PCSK9”, and “familial hypercholesterolemia” clinical trial) up to November 2020. We obtained articles in peer-reviewed journals for electronic searches. Additional data, especially original data not identified in the electronic databases, were collected from other data resources, and we also performed an additional search of the references of the retrieved studies. Notably, we obtained original data by contacting the corresponding authors when the data were not reported in the identified published articles.

**2.2. Selection of Studies for Inclusion in the Review.** Cohort studies were included if they met the following criteria: (1) type of study: randomized controlled trials (RCTs); (2) types of participants: FH diagnosis in accordance with clinical criteria or DNA-based analyses; (3) type of interventions: patients received PCSK9-mAbs; and (4) safety and efficacy outcomes of PCSK9-mAbs. The exclusion criteria were as follows: (1) duplicate reports describing the same cohort; (2) certain publication types, such as conference abstracts, letters, comments, case reports, and editorials; (3) repeated patient population for long-term research on the efficacy and safety of PCSK9-mAbs; and (4) non-FH subjects included in the study population.

**2.3. Data Extraction.** All studies retrieved by the search strategy were independently screened by 2 reviewers (XYG and TTZ). The initial prescreening was performed by reading the titles and abstracts to select relevant studies for further data extraction. Secondary selection was conducted by comprehensively reviewing the full text of all initially identified articles to determine whether the necessary information was reported. Basic information was extracted as follows:

TABLE 1: Baseline characteristics of trials included in the meta-analysis.

Author	Year	Patients	Mean age (y)	Number (P/C)	PCSK9-mAbs	Control	Drug regimen	Time	Area	Duration
Raal et al. [16]	2015	heFH	51	220/109	Evolocumab	Placebo	140 mg every 2 weeks, 420 mg monthly	Feb 7 to Dec 19, 2013	Australia, Asia, Europe, New Zealand, North America, and South Africa	12 weeks
Raal et al. [17]	2012	heFH	51	111/56	Evolocumab (AMG 145)	Placebo	350 mg-420 mg, every 4 weeks	Aug 2011 to Feb 2012	North America, Western Europe, Hong Kong, Singapore, and South Africa	12 weeks
Ginsberg et al. [15]	2016	heFH	50.6	72/35	Alirocumab	Placebo	150 mg, every 2 weeks	June 2012 to Jan 2015	Canada, the United States, the Netherlands, Russia, and South Africa	78 weeks
Stein et al. [14]	2012	heFH	53.4	62/15	Alirocumab (REGN727)	Placebo	150 mg, 200 mg, and 300 mg, every 4 weeks; then 150 mg every 2 weeks	Jan 18, 2011, to Nov 7, 2011	USA and Canada	12 weeks
Moriarty et al. [13]	2016	heFH	58.7	41/21	Alirocumab	Placebo	150 mg, every 2 weeks	Mar 2015 to Sep 2015	United States and Germany	18 weeks
Raal et al. (2) [18]	2015	hoFH	31	33/16	Evolocumab	Placebo	420 mg, every 4 weeks	Feb 17, 2013, to Jan 31, 2014	North America, Europe, Middle East, and South Africa	12 weeks
Stein et al. (2) [19]	2012	heFH and non-FH	45	101/32	Alirocumab	Placebo	Single-dose study: 50, 100, 150, and 250 mg; multiple-dose study: 50, 100, or 150 mg on days 1, 29, and 43	Nov 2009 to May 2011	Kansas, Miramar, Florida	148 days



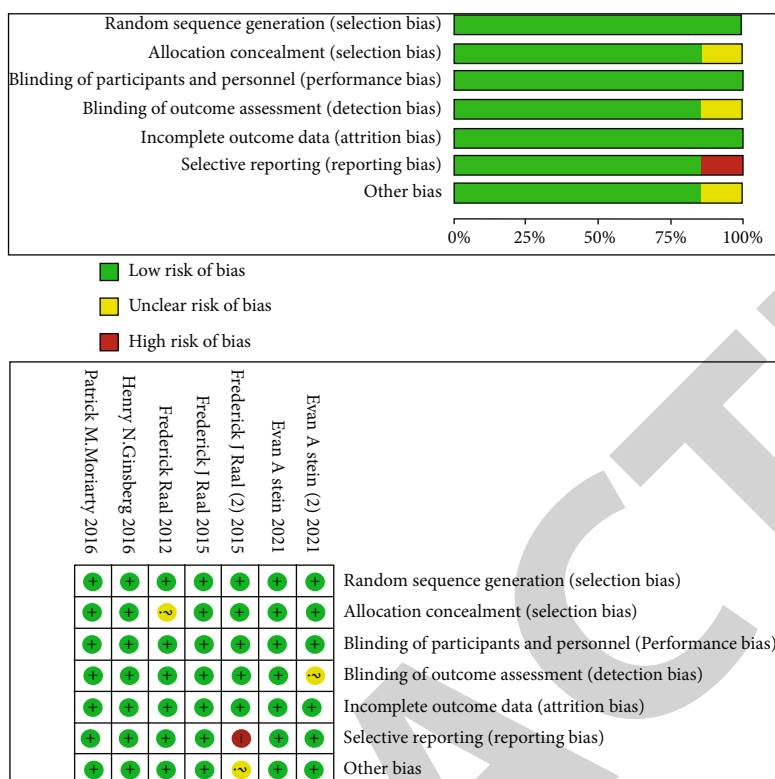


FIGURE 2: Risk-of-bias graph and summary table: review authors' judgments about each risk-of-bias item presented as percentages across all included studies.

author, year, patient number, mean age ( $\bar{y}$ ) at baseline, the type of PCSK9-mAbs, control, drug regimen, duration, study time, and area. Then, we extracted the corresponding mean differences, 95% CI or LS mean percent change, and SE from baseline of each lipid items, including LDL-C, HDL-C, non-HDL-C, TC, Apo-B and Apo-A1, TG, and Lp(a), as the primary outcomes. Safety endpoints covering the common adverse events, serious events, and laboratory adverse events were compared between the treatment and control groups.

**2.4. Quality Evaluation.** The literature quality evaluation used the Cochrane risk assessment form to conduct risk assessment on the included studies as described by "McKenzie et al." [12]. The assessment content includes (1) whether the random method is correct; (2) whether the allocation is hidden; (3) whether the implementer and participants are blinded; (4) whether the result analysis applies the blinding method; whether the data results are fully reported; (5) whether there is selective reporting; and whether there are other biases. According to specific circumstances, the risk assessment results are divided into three situations: high, low, and unclear. High-risk assessment research may lead to unsound analysis results, which are analyzed in sensitivity analysis and subgroup analysis.

**2.5. Appraisal of the Risk of Bias of the Included Studies.** Potential publication bias was evaluated by visually contour-enhanced funnel plots and Egger's test. According to the Egger methods for evaluating publication bias, a two-sided  $p$  value of 0.10 or less was regarded as significant.

**2.6. Sensitivity Analysis.** When substantial heterogeneity was noted between trials, leave-one-out sensitivity analysis was used, which means removing one study each time and repeating the analysis to determine whether exclusion of any one of the included studies altered the results.

**2.7. Statistical Analysis.** Statistical analyses were performed using R software, version 4.0.3 (R Foundation). The  $\chi^2$  statistic and independent-samples  $T$ -tests were used to assess differences in the baseline characteristics of the two groups. The risk ratio (RR) and weighted mean difference (WMD) were calculated and presented with the 95% confidence interval (CI) for summary estimates. Due to the heterogeneity among the included studies, appropriate statistical models were selected to ensure that the statistical data were estimated correctly. Statistical heterogeneity between studies was assessed using the  $\chi^2$  test, with a  $p$  value of less than 0.1 considered to indicate statistical significance, and heterogeneity was quantified using the inconsistency ( $I^2$ ) statistic. The  $I^2$  statistic describes the percentage of total variation across studies due to significant heterogeneity rather than random chance. An  $I^2$  statistic greater than 50% suggests considerable heterogeneity among the studies. Publication bias was assessed using contour-enhanced funnel plots. Because the visual interpretation of funnel plot asymmetry is inherently subjective, we also formally tested funnel plot asymmetry using the Harbord modification of Egger's test. Statistical significance was set at a  $p$  value  $< 0.05$ .

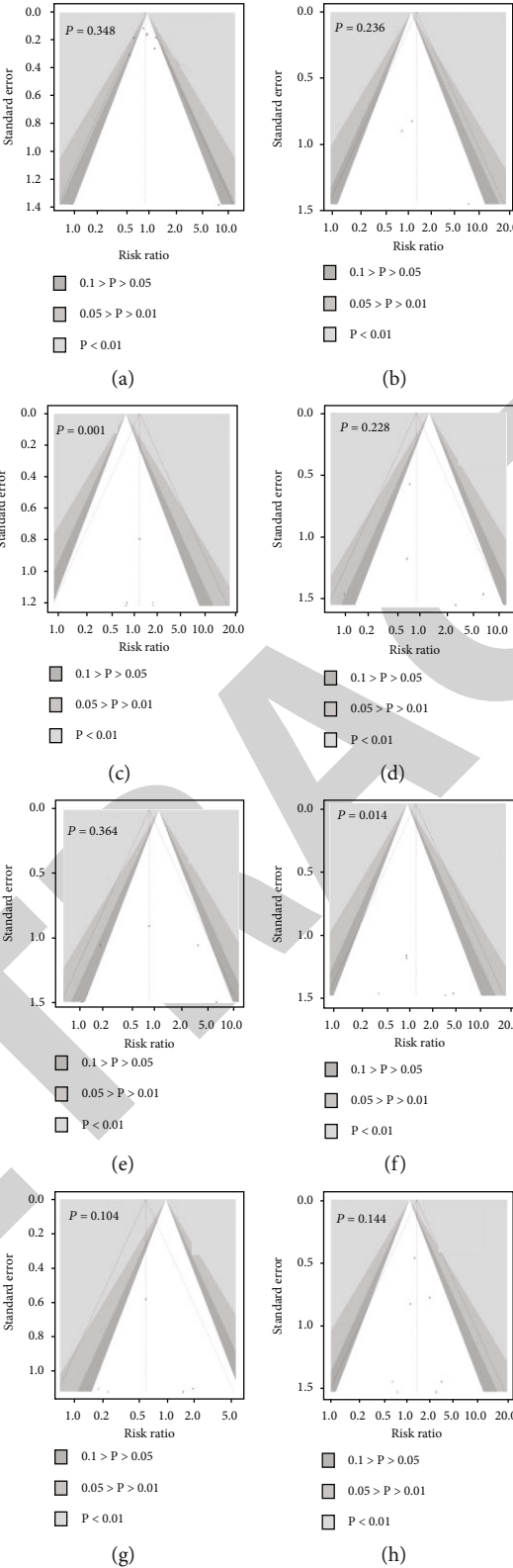


FIGURE 3: Continued.

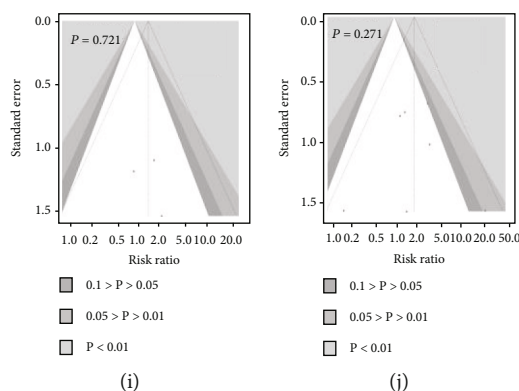


FIGURE 3: Appraisal of the risk of bias of the included studies: (a) any adverse events; (b) serious adverse events; (c) leading to treatment discontinuation; (d) adjudicated cardiovascular events; (e) nervous system disorders; (f) creatine kinase ( $CK \geq 3 \times ULN$ ); (g) headache; (h) nasopharyngitis; (i) abnormal liver function risk ( $AST/ALT \geq 3 \times ULN$ ); (j) injection site reactions.

### 3. Results

**3.1. Study Selection and Characteristics.** Literature search results and characteristics were initially obtained from 993 articles, and there were 55 clinical studies. Eighteen papers were removed after reviewing the titles and abstracts. Then, the full text of each of the remaining 37 articles was retrieved for further review to determine whether they met the predetermined criteria. Finally, 7 papers were identified and included in the present study (Figure 1). As a result, 7 studies encompassing a total of 926 patients were selected [13–19]. Among them, 3 trials used evolocumab (AMG 145), and 4 studies used alirocumab (SAR236553/-REGN727) treatment. Baseline characteristics were detailed, giving substantially similar basic values between PCSK9-mAbs and controls. The mean age of the subjects ranged from 31 to 59 years old. All trials were published between 2012 and 2016 with a follow-up period ranging from 8 to 78 weeks (Table 1) and a low risk of bias (Figure 2).

**3.2. Bias Assessment and Consistency Test.** Funnel plots were used to investigate the presence of small-study effects and publication bias. Figure 3 shows the contour-enhanced funnel plots and the Harbord modification of the Egger test of the studies included in this meta-analysis for adverse events, such as common adverse events, serious adverse events, and laboratory adverse events. There was no apparent asymmetry for the studies examining PCSK9-mAbs versus placebo for most of the adverse events, other than leading to treatment discontinuation and creatine kinase level ( $CK \geq 3 \times$  upper limit of normal (ULN)).

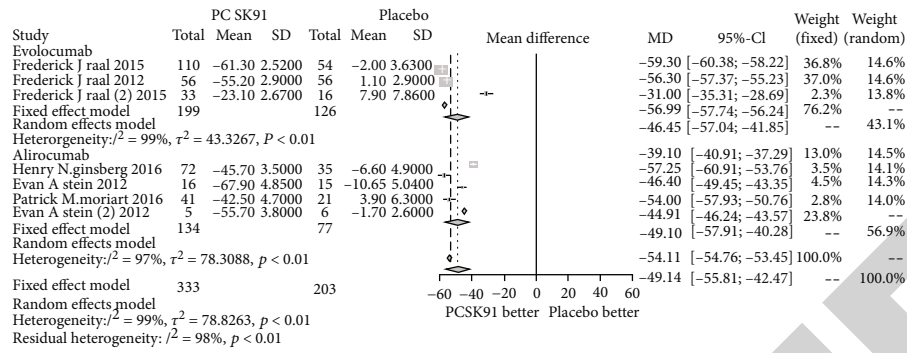
**3.3. Efficacy Outcomes of PCSK9-mAbs.** We could see from Figure 4 that PCSK9-mAbs markedly decreased the LDL-C level by -49.14%, 95% CI: -55.81 to -42.47%,  $I^2$ : 99%,  $p < 0.01$  (Figure 4(a)), and increased the level of HDL-C by 6.41%, 95% CI: 4.09 to 8.73%,  $I^2$ : 95%,  $p < 0.01$  (Figure 4(b)), and Apo-A1 by 8.27, 95% CI: 3.38 to 13.16%,  $I^2$ : 99%,  $p < 0.01$  (Figure 4(c)). They also decreased the level of Apo-B by -38.09%, 95% CI: -45.03 to 31.16%,  $I^2$ : 98%,  $p < 0.01$  (Figure 4(d)); non-HDL-C by -46.26%, 95% CI:

-53.45 to 39.06%,  $I^2$ : 93%,  $p < 0.01$  (Figure 4(e)); TC by -36.47%, 95% CI: -42.09 to 28.84%,  $I^2$ : 97%,  $p < 0.01$  (Figure 4(f)); TG by -10.26%, 95% CI: -18.68 to -1.84%,  $I^2$ : 95%,  $p < 0.01$  (Figure 4(g)); and Lp(a) by -17.65%, 95% CI: -24.75 to -10.55%,  $I^2$ : 98%,  $p < 0.01$  (Figure 4(h)).

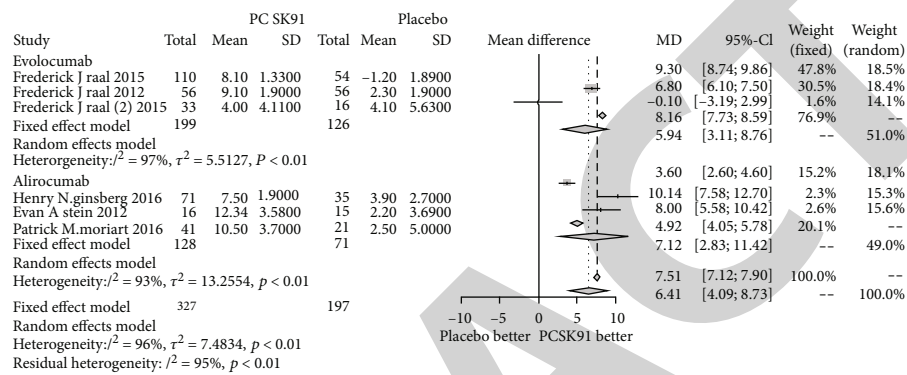
As a lipid outcome of evolocumab, a significant reduction in LDL-C level was achieved (WMD: -49.45%, 95% CI: -57.04 to -41.85%,  $I^2$ : 99%,  $p < 0.01$ , Figure 4(a)). In addition, HDL-C level obviously increased by 5.94% (95% CI: 3.11 to 8.76%,  $I^2$ : 97%,  $p < 0.01$ , Figure 4(b)), and Apo-A1 level increased by 5.20% (95% CI: -1.66 to 12.06%,  $I^2$ : 100%,  $p < 0.01$ , Figure 4(c)). Furthermore, Apo-B level obviously decreased by -40.12% (95% CI: -46.47 to -33.78%,  $I^2$ : 99%,  $p < 0.01$ , Figure 4(d)), non-HDL-C level by -54.21% (95% CI: -55.48 to -52.94%,  $I^2$ : 76%,  $p = 0.043$ , Figure 4(e)), TC level by -40.30% (95% CI: -41.08 to 39.52%,  $I^2$ : 97%,  $p < 0.01$ , Figure 4(f)), TG level by -14.07% (95% CI: -19.74 to -8.41%,  $I^2$ : 97%,  $p < 0.01$ , Figure 4(g)), and Lp(a) level by -22.56% (95% CI: -30.33 to -14.78%,  $I^2$ : 99%,  $p < 0.01$ , Figure 4(h)) versus placebo.

As a lipid outcome of alirocumab, a significant reduction in LDL-C level was achieved (mean reduction: -49.10%, 95% CI: -57.91 to -40.28%,  $I^2$ : 97%,  $p < 0.01$ , Figure 4(a)). In addition, HDL-C level obviously increased by 7.12% (95% CI: 2.83 to 11.42%,  $I^2$ : 93%,  $p < 0.01$ , Figure 4(b)) and Apo-A1 level increased by 11.43% (95% CI: 6.19 to 16.66%,  $I^2$ : 93%,  $p < 0.01$ , Figure 4(c)). Moreover, Apo-B level obviously decreased by -36.38% (95% CI: -43.75 to -29.01%,  $I^2$ : 97%,  $p < 0.01$ , Figure 4(d)), non-HDL-C level by -40.79% (95% CI: -47.00 to -34.58%,  $I^2$ : 95%,  $p < 0.01$ , Figure 4(e)), TC level by -33.80% (95% CI: -40.24 to 27.36%,  $I^2$ : 97%,  $p < 0.01$ , Figure 4(f)), TG level by -5.68% (95% CI: -5.93 to -5.43%,  $I^2$ : 0%,  $p = 0.968$ , Figure 4(g)), and Lp(a) level by -12.89% (95% CI: -20.17 to -5.61%,  $I^2$ : 94%,  $p < 0.01$ , Figure 4(h)) versus placebo.

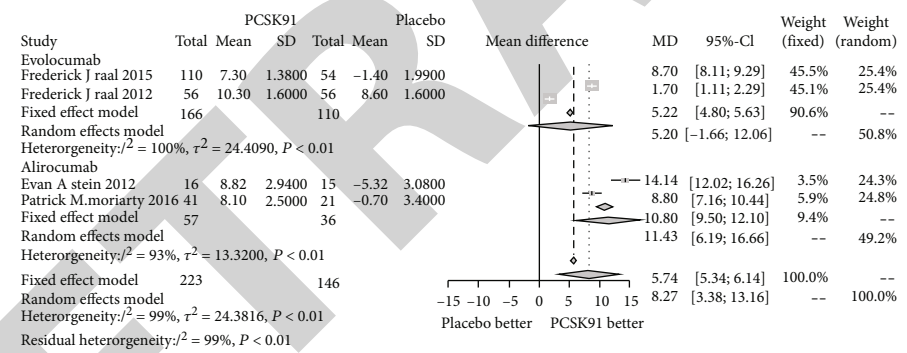
**3.4. Safety Outcomes of PCSK9-mAbs.** We compared the safety endpoints covering the common adverse events, serious events, and laboratory adverse events between the PCSK9-mAbs and control groups and found that the overall



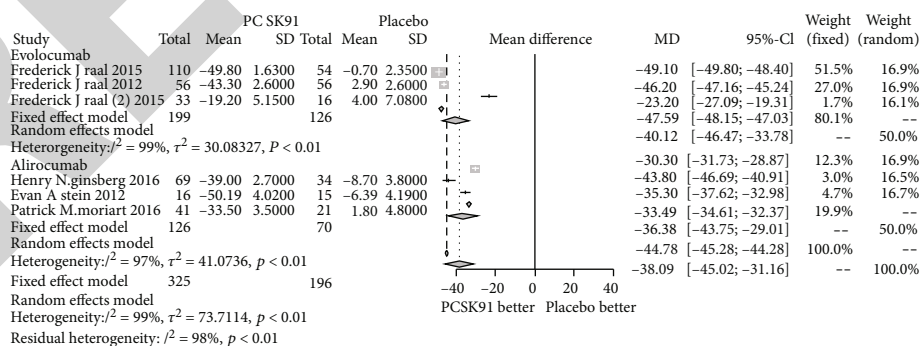
(a)



(b)

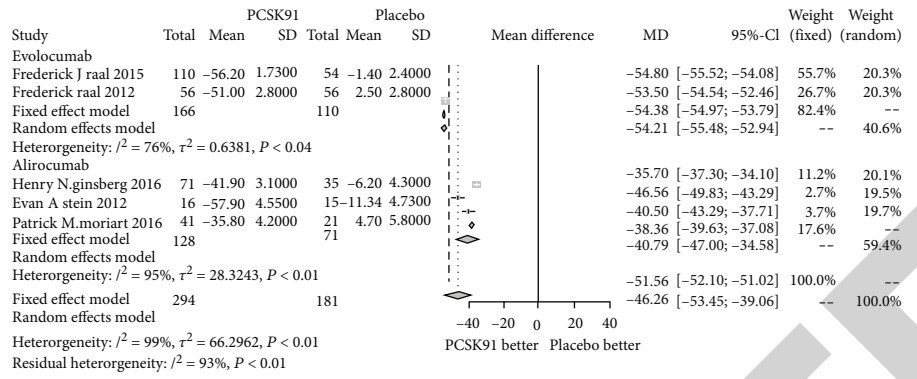


(c)

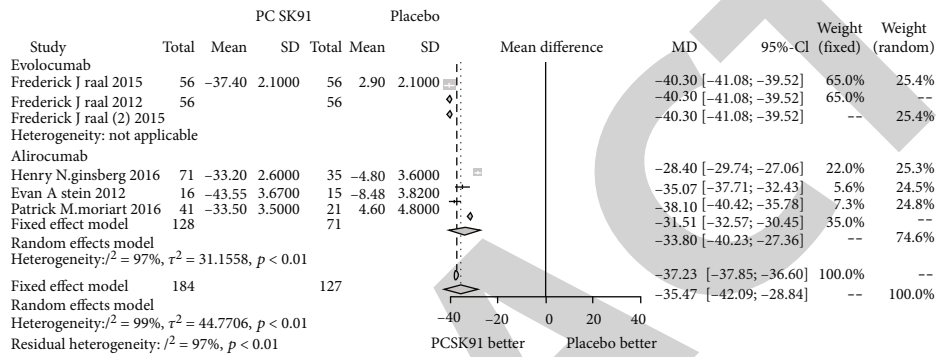


(d)

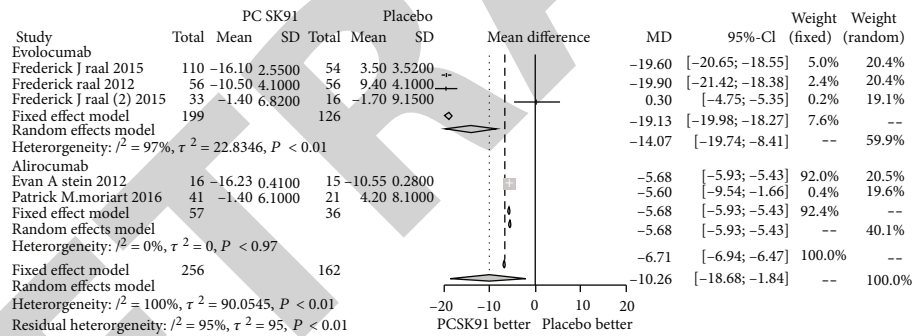
FIGURE 4: Continued.



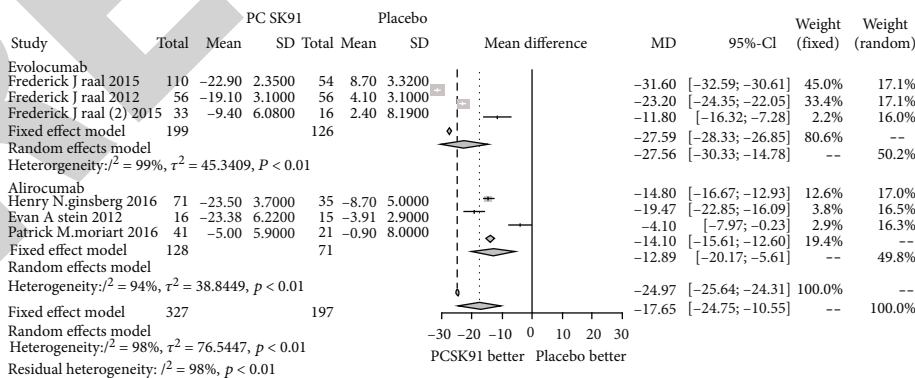
(e)



(f)



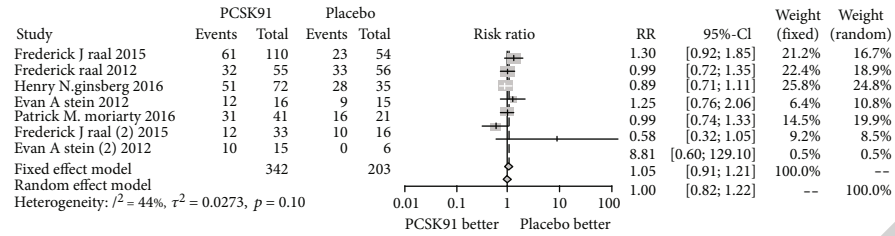
(g)



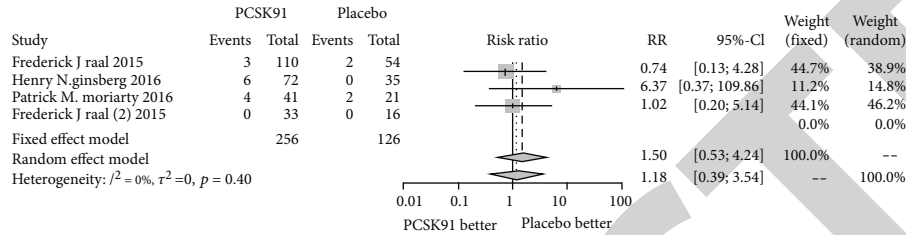
(h)

FIGURE 4: Forest plots depicting the effect of PCSK9 monoclonal antibody on FH; (a) on LDL-C; (b) on HDL-C; (c) on Apo-A1; (d) on Apo-B; (e) on non-HDL-C; (f) on TC; (g) on TG; (h) on Lp(a).

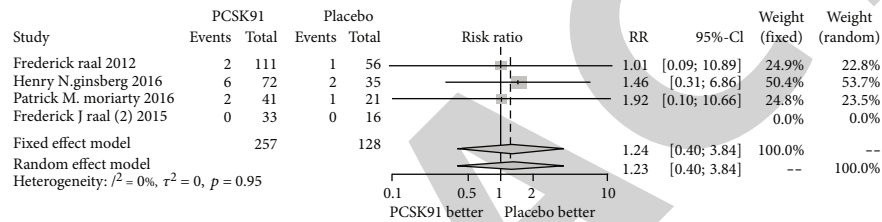




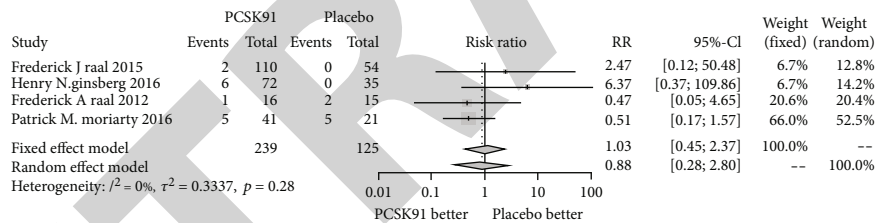
(a)



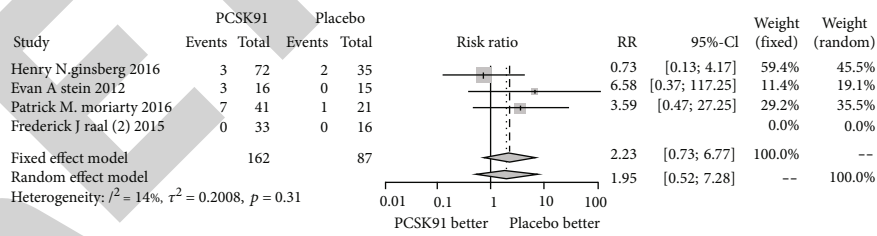
(b)



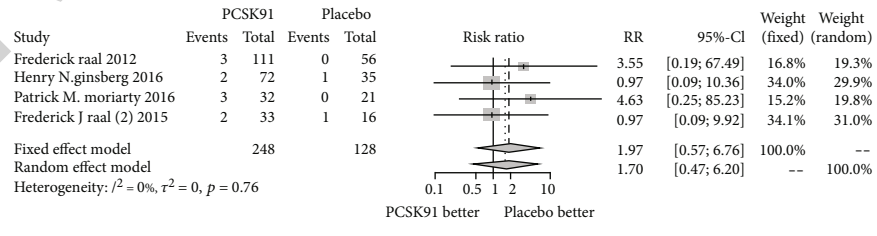
(c)



(d)



(e)



(f)

FIGURE 5: Continued.

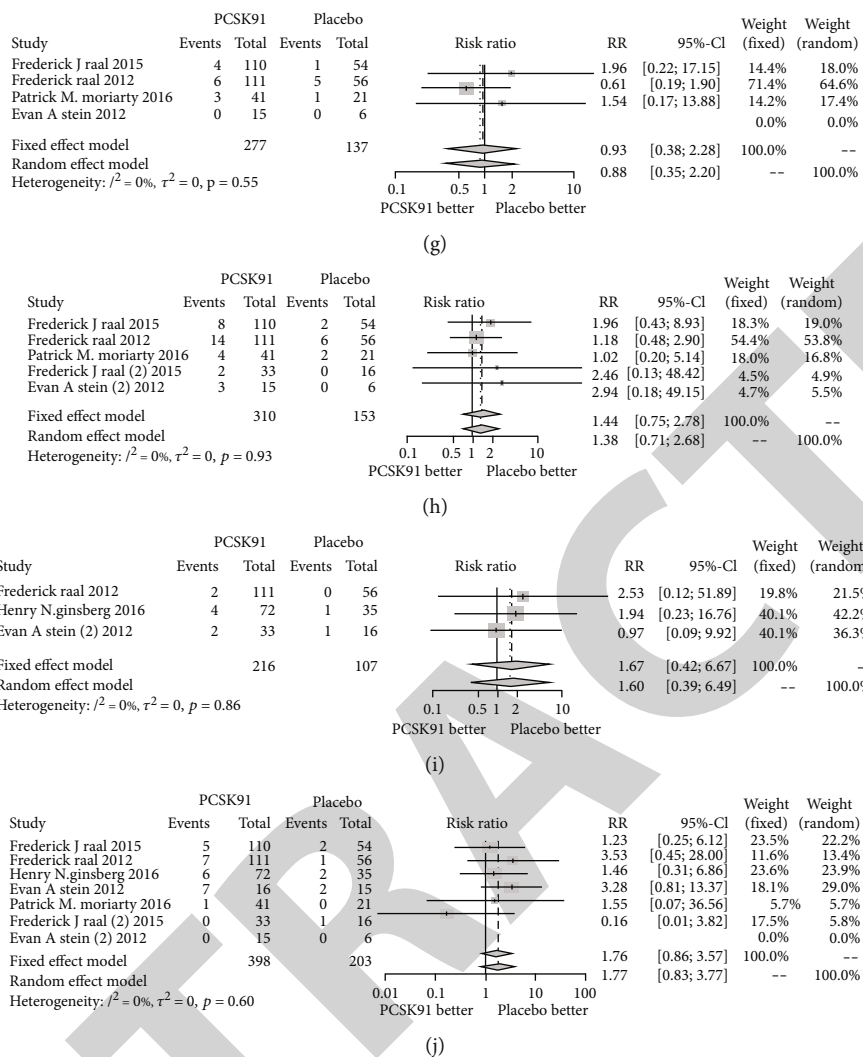
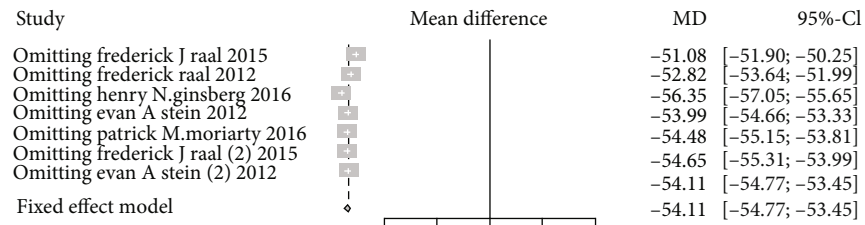


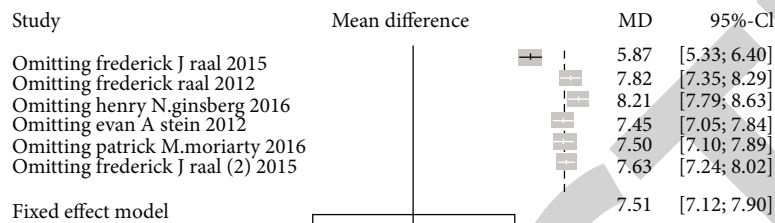
FIGURE 5: Forest plot depicting the adverse event rates of PCSK9 monoclonal antibody on FH compared with placebo controls on adverse events, serious events, and laboratory adverse events: (a) any adverse events; (b) serious adverse events; (c) leading to treatment discontinuation; (d) adjudicated cardiovascular events; (e) nervous system disorders; (f) creatine kinase (CK  $\geq 3 \times$  ULN); (g) headache; (h) nasopharyngitis; (i) abnormal liver function risk (AST/ALT  $\geq 3 \times$  ULN); (j) injection site reactions.

TABLE 2: Prespecified safety end points. No statistical differences between the PCSK9-mAbs and control groups.

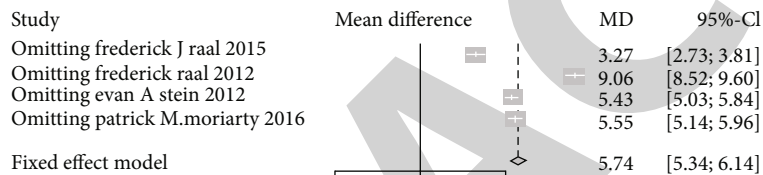
Pre-specified Safety endpoints	PCSK9-mAbs		Control		$\chi^2$	p value
	No. of patients/objects	Rate (%)	No. of patients/objects	Rate (%)		
Any adverse events	209/342	0.6111111	119/203	0.5862069	0.33	0.314
Serious adverse events	13/256	0.0507813	4/126	0.031746	0.72	0.287
Nervous system disorders	13/162	0.0802469	3/87	0.0344828	1.972	0.127
Injection site reactions	26/398	0.0653266	8/203	0.0394089	1.692	0.131
Leading to treatment discontinuation	10/257	0.0446429	4/128	0.03125	0.143	0.477
Nasopharyngitis	31/310	0.1	10/153	0.0653595	1.523	0.144
Back pain	7/151	0.0463576	2/75	0.0266667	0.508	0.377
Headache	13/277	0.0469314	7/137	0.0510949	0.035	0.513
ALT, AST, or both $\geq 3 \times$ ULN	8/216	0.037037	2/107	0.0186916	0.803	0.3
Positively adjudicated cardiovascular events	14/239	0.0585774	7/125	0.056	0.01	0.563
Creatinine kinase $\geq 3 \times$ ULN	10/248	0.0403226	2/128	0.0169492	1.667	0.164



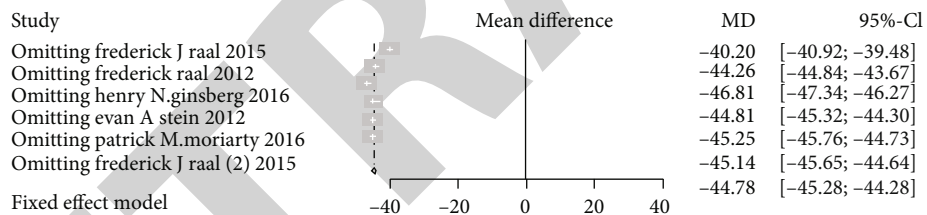
(a)



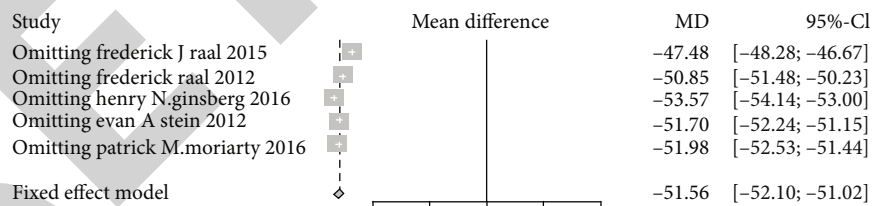
(b)



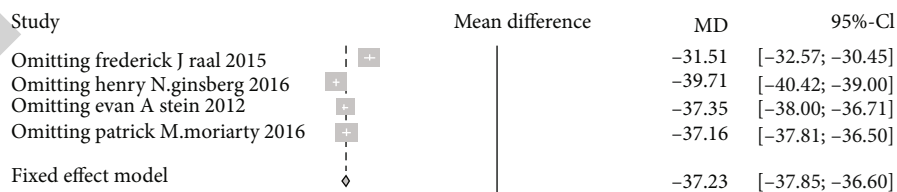
(c)



(d)



(e)



(f)

FIGURE 6: Continued.

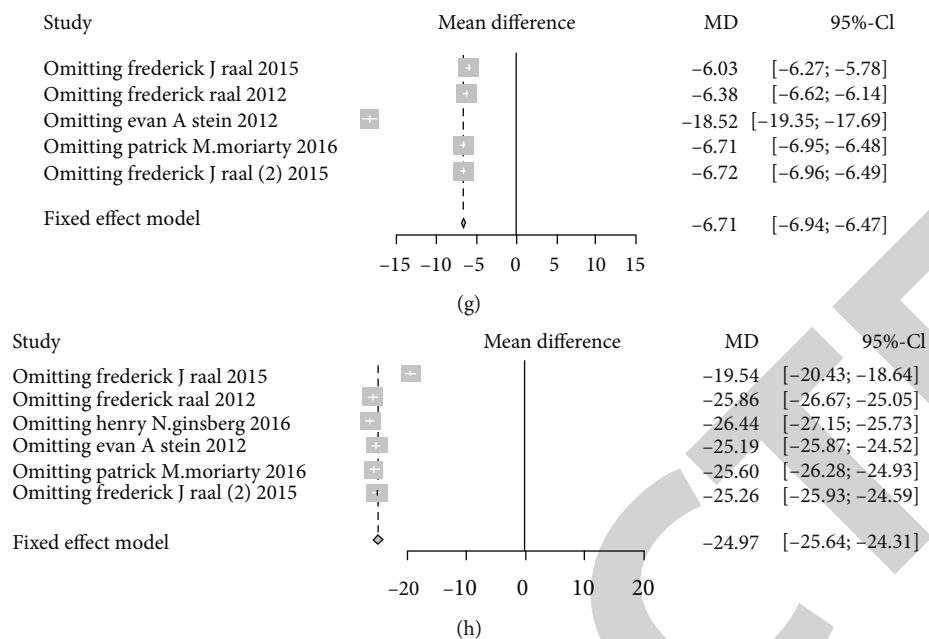


FIGURE 6: Sensitivity analysis of efficacy outcomes: (a) on LDL-C; (b) on HDL-C; (c) on Apo-A1; (d) on Apo-B; (e) on non-HDL-C; (f) on TC; (g) on TG; (h) on Lp(a).

incidence of common adverse events (RR: 1.00, 95% CI: 0.82 to 1.22,  $I^2$ : 44%,  $p$  = 0.10), serious adverse events (RR: 1.18, 95% CI: 0.39 to 3.54,  $I^2$ : 0%,  $p$  = 0.40), and leading to treatment discontinuation (RR: 1.23, 95% CI: 0.40 to 3.84,  $I^2$ : 0%,  $p$  = 0.95) implied no obvious differences versus placebo. No significant heterogeneity was found in positively adjudicated cardiovascular events by RR: 0.88, 95% CI: 0.28 to 2.80,  $I^2$ : 22%,  $p$  = 0.28; nervous system disorders by RR: 1.95, 95% CI: 0.52 to 7.28,  $I^2$ : 14%,  $p$  = 0.31; creatine kinase ( $CK \geq 3 \times ULN$ ) by RR: 1.70, 95% CI: 0.47 to 6.20,  $I^2$ : 0%,  $p$  = 0.76; headache by RR: 0.88, 95% CI: 0.35 to 2.20,  $I^2$ : 0%,  $p$  = 0.55; nasopharyngitis by RR: 1.38, 95% CI: 0.71 to 2.68,  $I^2$ : 0%,  $p$  = 0.93; abnormal liver function risk ( $AST/ALT \geq 3 \times ULN$ ) in patients by RR: 1.60, 95% CI: 0.39 to 6.49,  $I^2$ : 0%,  $p$  = 0.86; and injection site reactions by RR: 1.77, 95% CI: 0.83 to 3.77,  $I^2$ : 0%,  $p$  = 0.60, versus placebo (Figure 5).

Moreover, an additional table that describes the safety events of interest, common adverse events, and laboratory adverse events of PCSK9-mAbs was included, and we found no significant differences between the PCSK9-mAbs and control groups. A chi-square ( $\chi^2$ ) statistic was used to assess the magnitude of heterogeneity, and a  $p$  value < 0.05 was considered to be statistically significant (Table 2).

**3.5. Sensitivity Analysis.** To explain the high heterogeneity observed among all efficacy outcomes, we performed leave-one-out sensitivity analysis among the studies. We found that the statistical significance or nonsignificance of the differences between groups was not altered. This suggested that none of the included studies individually changed the overall result (Figure 6). Moreover, there was also no change in safety outcomes (Figure 7).

#### 4. Discussion

To the best of our knowledge, this is the first meta-analysis using sufficient clinical outcomes to systematically analyze the efficacy and safety of PCSK9-mAbs in the treatment of FH patients. In the present analysis, a total of 7 studies encompassing 926 patients with FH were included. The main aim is to solve whether PCSK9-mAbs treatment can reduce the levels of lipids of FH patients with satisfactory safety and tolerability.

FH is an inherited disease due to a genetic mutation and is not caused by the external environment or improper lifestyle. As mentioned before, FH includes two main subtypes: HeFH and homozygous FH. They are different in symptoms, risks, and treatments. In genetics, HeFH is caused by a pathogenic variant in one allele, while biallelic mutations in one of the known genes or compound heterozygosity for two different mutations in the same or different candidate genes cause homozygous FH. HeFH affects between one in 250 and one in 300 people worldwide, and the prevalence of homozygous FH may be 1 in 160,000 [20]. The risk of premature CHD in heterozygous FH is elevated approximately 20-fold [4], and homozygous FH patients develop CHD early by the second decade of life. In homozygous FH, valvular and supravalvular aortic stenosis induced by lipid deposition has also been reported, whereas rarely in HeFH [21]. To date, 12 meta-analysis studies have analyzed the efficacy and safety of PCSK9-mAbs in hypercholesterolemia [9, 22–32]. Among these studies, there were two in FH patients. However, one report studied the role and safety of evolocumab but did not include alirocumab [33]. In another study, although the role and safety of PCSK9-mAbs, including evolocumab and alirocumab, were discussed, the patients with

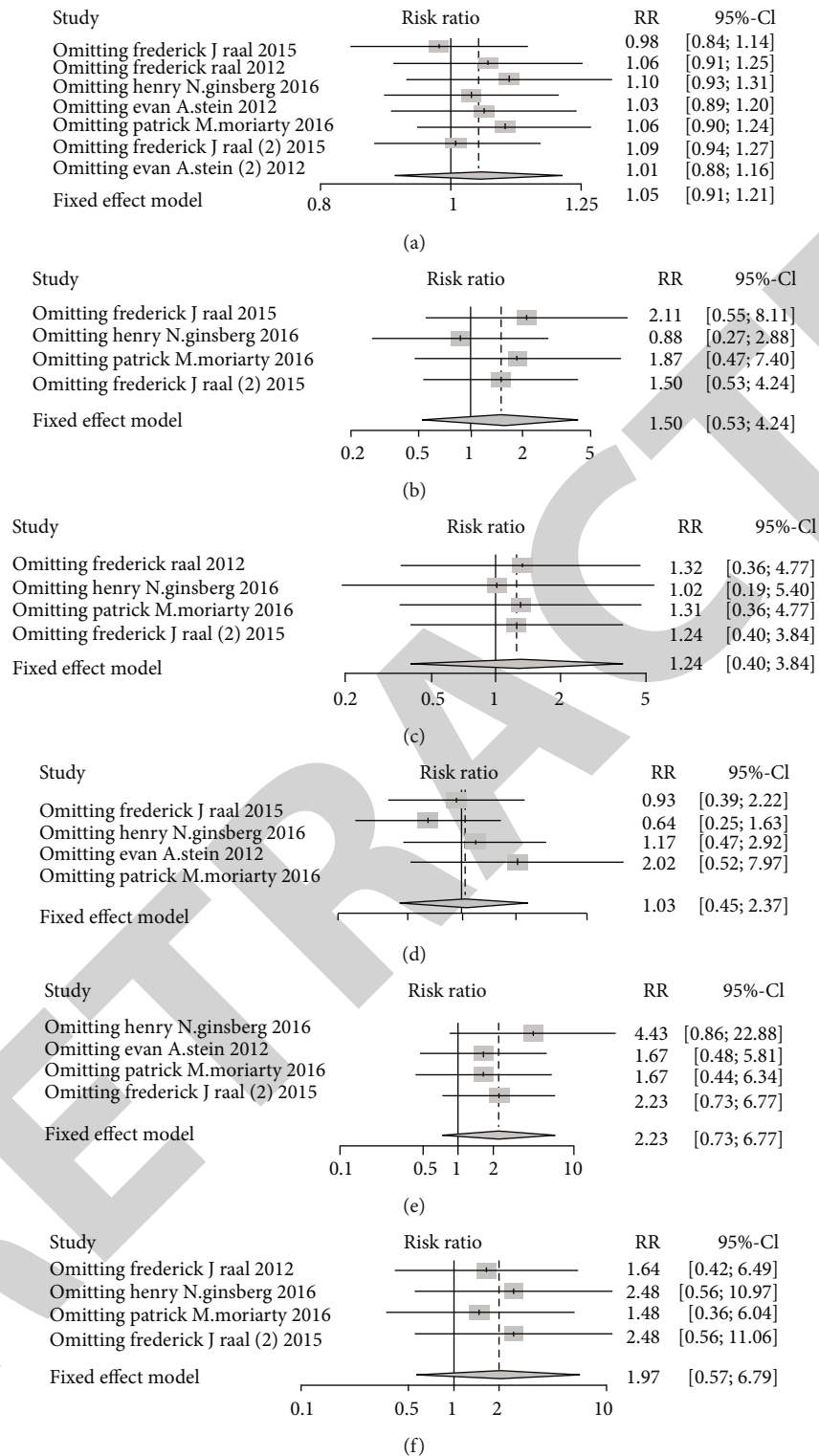


FIGURE 7: Continued.



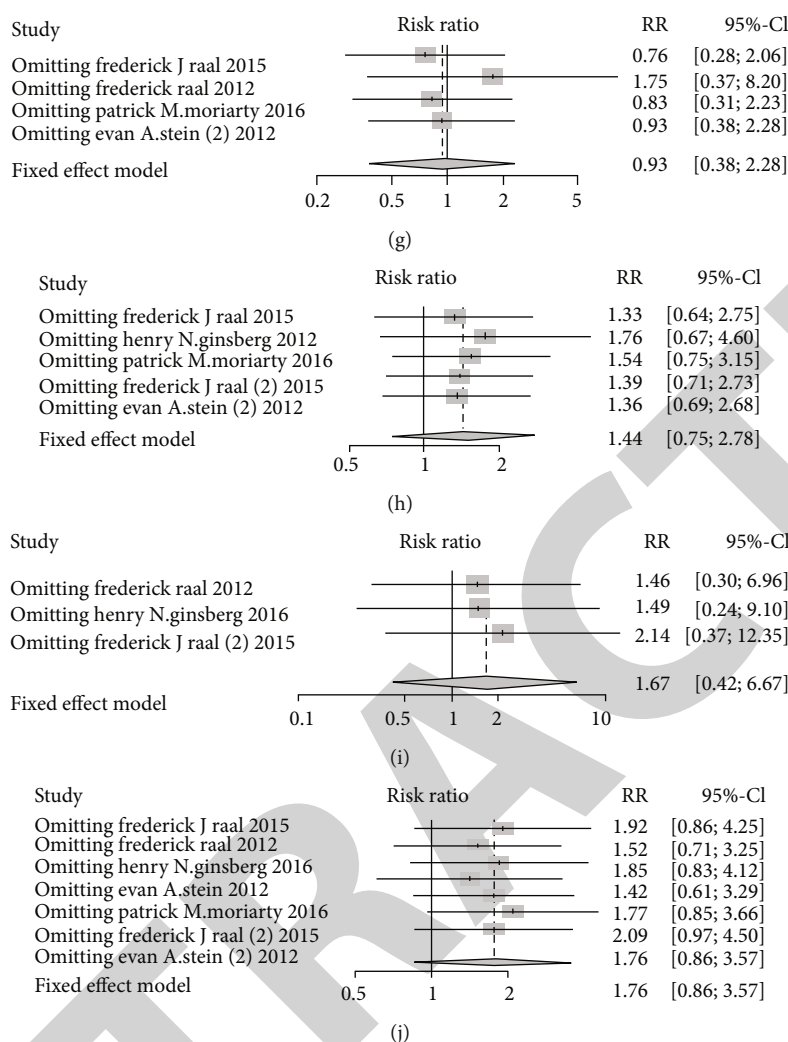


FIGURE 7: Sensitivity analysis of safety outcomes: (a) any adverse events; (b) serious adverse events; (c) leading to treatment discontinuation; (d) adjudicated cardiovascular events; (e) nervous system disorders; (f) creatine kinase ( $CK \geq 3 \times ULN$ ); (g) headache; (h) nasopharyngitis; (i) abnormal liver function risk ( $AST/ALT \geq 3 \times ULN$ ); (j) injection site reactions.

FH were controversial because the data extracted by the authors did not exclude the non-FH patients included in the clinical study [10]. Therefore, strictly speaking, our meta-analysis is the first study to systematically analyze the efficacy and safety of PCSK9-mAbs in the treatment of FH patients alone. In addition, we conducted a variety of sensitivity analyses for the included literature to ensure the reliability of the literature screening and results, including leave-one-out sensitivity analysis, contour-enhanced funnel plots, and the Harbord modification of Egger test. Moreover, we conducted a subgroup analysis of PCSK9-mAbs and analyzed the efficacy outcomes and safety outcomes of evolocumab and alirocumab in the treatment of FH, respectively.

In this study, we conducted a systematic evaluation of the efficacy and safety of PCSK9-mAbs in FH patients. The results of this study showed that PCSK9-mAbs reduced the level of the main research index LDL-C and also significantly reduced the levels of TG, TC, non-HDL-C, and Apo B, Lp(a) and increased the levels of HDL-C and Apo-A1, which are beneficial lipopro-

teins. Elevated LDL is an important pathological factor for CVD. The latest Mendelian Randomization Study Tips published by JACC based on the UK Biobank and Global Lipid Genetics Consortium (Global Lipid Genetics Consortium) demonstrated that LDL cholesterol and triglycerides induced myocardial remodeling by increasing LV mass, suggesting that they influence the development of CVD not only through atherosclerosis but also by causing adverse alterations in cardiac structure and function [34, 35]. In the present study, we showed that PCSK9-mAbs significantly reduced LDL and TG levels by -49.14% and -10.26%, respectively. The Apo-B/Apo-A1 ratio has been previously suggested to be a better risk indicator for CVD and MI than the level of lipids [36], and we demonstrated that in the PCSK9-mAbs treatment group, the level of Apo-B decreased while that of Apo-A1 increased. This result indicates that PCSK9-mAbs therapy can greatly lower the primary risk factors for heart disease with an obvious decrease in the Apo-B/Apo-A1 ratio. Recent studies have reported that Lp(a) not only serves as a "traditional"

atherosclerotic cardiovascular disease (ASCVD) risk factor but also improves the accuracy of cardiovascular risk stratification [37]. Compelling evidence from traditional epidemiological, genome-wide association, and Mendelian randomization studies has revealed that elevated plasma Lp(a) level increases the risk of acute myocardial infarction (AMI), ischemic stroke, calcific aortic valve disease, and peripheral arterial disease in non-FH patients [38]. Elevated lipoprotein (a) was found to be a significant CVD risk factor in HeFH [39], and Lp(a) level above 50 mg/dL is recently found to be an independent risk factor for calcific aortic valvulopathy among HeFH patients [40]. Safety analysis demonstrated that PCSK9-mAbs showed good safety, and the incidence of common and serious adverse reactions was basically the same as that of the placebo group in addition to abnormal liver function risk.

Several limitations should be taken into consideration. First, significant heterogeneities were observed in most of the efficacy outcomes, which may be related to the patient's baseline level, drug intervention time, the type and dose of PCSK9-mAbs, etc., but we failed to reveal the heterogeneities by dividing into subgroups or using sensitivity methods. Second, there are still a number of large-scale randomized clinical controlled studies in progress, and we should take caution in interpreting the results of the meta-analysis when combining heterogeneous data sets. Third, most of the treatment cycles included in clinical studies were between 12 and 24 weeks, and the adverse reactions that require long-term observation could not be effectively evaluated. Despite these limitations, our meta-analysis proves that PCSK9-mAbs exert significant protection from FH, including decreasing the plasma levels of LDL-C and Lp(a), TC, TG, and Apo-B and increasing the plasma levels of HDL-C and Apo-A1. Outcomes are sufficient enough to compensate our clinical guidelines. Hopefully, its long-term therapeutic efficacy, safety, and clinical outcomes should be confirmed by more RCTs.

## 5. Conclusion

In this review, we presented evidence from 7 published clinical trials and suggested that among 926 FH patients, PCSK9-mAbs significantly decreased the level of LDL-C and other lipids with satisfactory safety and tolerability.

## Conflicts of Interest

The authors have no conflicts of interest to disclose.

## Acknowledgments

This work was supported by grants from the National Natural Science Foundation of China (No. 82000062, 81960015 to WF. Zhang, and 81800051 to TT. Zhu), the Young Talents Project Foundation from Jiangxi Provincial Department of Science and Technology (20204BCJ23020), the Science Foundation for Distinguished Young Scholars of Jiangxi Province (20212ACB216008), National College Students Innovation Training Program of Henan Province (202010472010), and Research Foundation of Xinxiang Medical University (XYBSKYZZ201812).

## References

- [1] A. Onorato and A. C. Sturm, "Heterozygous familial hypercholesterolemia," *Circulation*, vol. 133, no. 14, pp. e587–e589, 2016.
- [2] A. Thedrez, D. J. Blom, S. Ramin-Mangata et al., "Homozygous familial hypercholesterolemia patients with identical mutations variably express the LDLR (low-density lipoprotein receptor): implications for the efficacy of evolocumab," *Arteriosclerosis, Thrombosis, and Vascular Biology*, vol. 38, no. 3, pp. 592–598, 2018.
- [3] C. C. Huang and M. J. Charng, "Genetic diagnosis of familial hypercholesterolemia in asia," *Frontiers in Genetics*, vol. 11, 2020.
- [4] G. F. Watts, B. Lewis, and D. R. Sullivan, "Familial hypercholesterolemia: a missed opportunity in preventive medicine," *Nature Clinical Practice. Cardiovascular Medicine*, vol. 4, no. 8, pp. 404–405, 2007.
- [5] B. G. Nordestgaard, M. J. Chapman, S. E. Humphries et al., "Familial hypercholesterolaemia is underdiagnosed and undertreated in the general population: guidance for clinicians to prevent coronary heart disease: consensus statement of the European Atherosclerosis Society," *European Heart Journal*, vol. 34, no. 45, pp. 3478–3490, 2013.
- [6] V. Blanchard, I. Khantalin, S. Ramin-Mangata, K. Chémello, B. Nativel, and G. Lambert, "PCSK9: from biology to clinical applications," *Pathology*, vol. 51, no. 2, pp. 177–183, 2019.
- [7] M. Hilvo, H. Simolin, J. Metso et al., "PCSK9 inhibition alters the lipidome of plasma and lipoprotein fractions," *Atherosclerosis*, vol. 269, pp. 159–165, 2018.
- [8] J. J. P. Kastelein, S. E. Nissen, D. J. Rader et al., "Safety and efficacy of LY3015014, a monoclonal antibody to proprotein convertase subtilisin/kexin type 9 (PCSK9): a randomized, placebo-controlled phase 2 study," *European Heart Journal*, vol. 37, no. 17, pp. 1360–1369, 2016.
- [9] P. M. Ridker, L. M. Rose, J. J. P. Kastelein et al., "Cardiovascular event reduction with PCSK9 inhibition among 1578 patients with familial hypercholesterolemia: Results from the SPIRE randomized trials of bococizumab," *Journal of Clinical Lipidology*, vol. 12, no. 4, pp. 958–965, 2018.
- [10] L. J. Qian, Y. Gao, Y. M. Zhang, M. Chu, J. Yao, and D. Xu, "Therapeutic efficacy and safety of PCSK9-mono-clonal antibodies on familial hypercholesterolemia and statin-intolerant patients: a meta-analysis of 15 randomized controlled trials," *Scientific Reports*, vol. 7, no. 1, p. 238, 2017.
- [11] X. Y. Ge, T. T. Zhu, X. Y. Zhang, Y. Liu, Y. Wang, and W. Zhang, "Gender differences in pulmonary arterial hypertension patients with BMPR2 mutation: a meta-analysis," *Respiratory Research*, vol. 21, no. 1, p. 44, 2020.
- [12] J. P. Higgins, J. Thomas, J. Chandler et al., "Cochrane handbook for systematic reviews of interventions version 6.0 (updated July 2019)," in *Cochrane*, John Wiley & Sons, 2019, <http://training.cochrane.org/handbook>.
- [13] P. M. Moriarty, K. G. Parhofer, S. P. Babirak et al., "Alirocumab in patients with heterozygous familial hypercholesterolemia undergoing lipoprotein apheresis: the ODYSSEY ESCAPE trial," *European Heart Journal*, vol. 37, no. 48, pp. 3588–3595, 2016.
- [14] E. A. Stein, D. Gipe, J. Bergeron et al., "Effect of a monoclonal antibody to PCSK9, REGN727/SAR236553, to reduce low-density lipoprotein cholesterol in patients with heterozygous familial hypercholesterolaemia on stable statin dose with or

## Review Article

# An Overview of miRNAs Involved in PASMCM Phenotypic Switching in Pulmonary Hypertension

Weifang Zhang <sup>1,2</sup>, Zeying Tao,<sup>1,3</sup> Fei Xu,<sup>1,3</sup> Qian Diao,<sup>1,3</sup> Juan Li,<sup>1,2</sup> Lu Zhou,<sup>1,3</sup> Yaxin Miao,<sup>1,3</sup> Shanshan Xie,<sup>1</sup> Jinjin Wan,<sup>1</sup> and Ruilai Xu <sup>1</sup>

<sup>1</sup>Department of Pharmacy, The Second Affiliated Hospital of Nanchang University, 330006 Nanchang, Jiangxi, China

<sup>2</sup>Department of Pharmacology, School of Pharmaceutical Science, Nanchang University, Nanchang, Jiangxi 330006, China

<sup>3</sup>Medical College of Nanchang University, Nanchang, Jiangxi 330031, China

Correspondence should be addressed to Ruilai Xu; [xruilai@163.com](mailto:xruilai@163.com)

Received 31 May 2021; Accepted 3 September 2021; Published 7 October 2021

Academic Editor: Zhousheng Yang

Copyright © 2021 Weifang Zhang et al. This is an open access article distributed under the Creative Commons Attribution License, which permits unrestricted use, distribution, and reproduction in any medium, provided the original work is properly cited.

Pulmonary hypertension (PH) is occult, with no distinctive clinical manifestations and a poor prognosis. Pulmonary vascular remodelling is an important pathological feature in which pulmonary artery smooth muscle cells (PASMCMs) phenotypic switching plays a crucial role. MicroRNAs (miRNAs) are a class of evolutionarily highly conserved single-stranded small noncoding RNAs. An increasing number of studies have shown that miRNAs play an important role in the occurrence and development of PH by regulating PASMCMs phenotypic switching, which is expected to be a potential target for the prevention and treatment of PH. miRNAs such as miR-221, miR-15b, miR-96, miR-24, miR-23a, miR-9, miR-214, and miR-20a can promote PASMCMs phenotypic switching, while such as miR-21, miR-132, miR-449, miR-206, miR-124, miR-30c, miR-140, and the miR-17~92 cluster can inhibit it. The article reviews the research progress on growth factor-related miRNAs and hypoxia-related miRNAs that mediate PASMCMs phenotypic switching in PH.

## 1. Introduction

Pulmonary hypertension (PH) is a serious cardiopulmonary disease that occurs as a primary rare disease or as a concurrent condition of various cardiac, pulmonary, or systemic diseases. PH has multiple predisposing factors, but all forms of PH show a common arteriopathy, including pulmonary vasoconstriction, vascular remodelling, and subsequent vascular lumen occlusion, although their evolution and prognosis vary depending on the aetiology. These alterations then trigger an increase in pulmonary vascular resistance and compensatory right ventricular hypertrophy, which ultimately result in mortality [1].

Pulmonary vascular remodelling involving the intima, media, and adventitia is a critical pathological change in all PH types. In the process of pulmonary vascular remodelling in patients with PH, vascular endothelial injury, vascular media hypertrophy, muscle fibrosis of peripheral

vessels, and an increase in extracellular matrix (ECM) often occur, resulting in conformational changes. As a result, the pulmonary vascular lumen will constrict, small resistant pulmonary arteries will be progressively occluded, and angioproliferative plexiform lesions will form, which regulate PH progression [2].

The overproliferation of pulmonary arterial smooth muscle cells (PASMCMs), an important component of the vascular media, caused by the disruption of the proliferation/apoptosis balance of PASMCMs and phenotypic switching is the main cause of pulmonary vascular remodelling in PH. SMCs can contract blood vessels and regulate vascular tension, blood pressure, and blood flow distribution. Under normal conditions, they are static and differentiated, showing low proliferation and low synthetic activity. However, under pathological conditions such as hypoxia and inflammation, SMCs undergo phenotypic switching, which is characterized by hyperplastic and antiapoptotic properties.

Because of the overproliferation and migration of synthetic phenotypic SMCs in a dedifferentiated state and the secretion of collagen, elastin, proteoglycan, and ECM contractile proteins, pulmonary arterioles and capillary walls become thickened or even occluded, the lumen of blood vessels becomes narrowed, and blood flow resistance increases; these changes, in turn, increase the pressure in the pulmonary arteries and promote the development of pulmonary vascular remodelling [3]. Therefore, PSMCs phenotypic switching is a key link in pulmonary vascular remodelling and is particularly important in PH. The mechanism behind phenotypic switching is complicated. Many studies have investigated the mechanism of PSMCs phenotypic switching, and some have involved various signalling pathways, such as the MAPK/ERK1/2 and PI3K/AKT signalling pathways [4, 5]. Interventions targeting the abnormal differentiation, migration, and proliferation mechanisms of PSMCs have been shown to effectively inhibit pulmonary vascular remodelling and treat PH.

MicroRNAs (miRNAs) are 18–22 nucleotides (nt) in length and are single-stranded noncoding small RNAs. Binding to the 3'-untranslated region (3'-UTR) of messenger RNAs (mRNAs) to degrade mRNA and/or inhibit target gene translation is the primary mode of action of miRNAs, which widely regulate gene expression. The discovery of miRNAs and their function constitutes a major breakthrough in the field of medicine. The role of miRNAs in various cardiovascular diseases, including ischaemia, tumour angiogenesis, and atherosclerosis (AS), has attracted considerable attention in recent decades. In particular, the abnormal expression of miRNAs in PH has attracted much recent attention among scholars. miRNAs are involved in the differentiation of vascular endothelial cells and PSMCs. Under the influence of inflammation, hypoxia, external stimuli, and other factors, miRNAs can regulate the production of cytokines, chemokines, and various growth factors by regulating the expression of related genes. These modulations further alter the biological behaviour of vascular endothelial damage, SMC proliferation, migration and phenotypic switching, and abnormal ECM deposition, which are the cellular and molecular bases of PH [6].

Despite recent progress in our understanding of the pathophysiological mechanism of PH and significant improvements in symptomatic treatment, the rapid progression and lethal course of the disease have not substantially changed [7]. There is therefore an urgent need to identify new potential therapeutic targets. The treatment of PH should not only solve the problem of vasoconstriction but also address the deeper problem of vascular remodelling. Controlling the expression of genes and proteins can fundamentally regulate the occurrence and development of PH. miRNA dysregulation is closely related to the physiopathology of PH. Consequently, miRNA-based therapeutics have constituted a new hope for the reversal of the PH process in clinical practice. In view of the key regulatory role of miRNAs in PSMCs phenotypic switching, this review describes the current research progress regarding miRNAs involved in PSMCs phenotypic switching in PH from two aspects—growth factor-related miRNAs and hypoxia-related miR-

NAs—to further clarify the pathogenesis of PH and provides an important experimental and theoretical basis for the application of miRNAs in targeted PH therapies.

## 2. Brief Description of PH, Phenotypic Switching, and their Relationship

### 2.1. Pulmonary Hypertension

**2.1.1. Overview of PH.** PH refers to a class of progressive diseases of different aetiologies. The main cause of the disease is primary pulmonary arteriolar lesions leading to increased pulmonary artery resistance and eventually to death from right heart failure [8]. PH was divided into five categories at the sixth World Symposium on Pulmonary Hypertension (WSPH): pulmonary arterial hypertension (PAH), PH associated with left heart disease, PH associated with lung disease/hypoxia, PH due to pulmonary arterial obstructions, and PH with unclear and/or multifactorial mechanisms [9]. By 2011, in all its variant presentations, PH was estimated to affect up to 100 million people worldwide [10].

Since 1973, PH has been defined as a mean pulmonary arterial pressure (mPAP)  $\geq 25$  mmHg; however, the definition was recommended to be changed to mPAP  $> 20$  mmHg at the sixth WSPH [11]. PH has previously been called an orphan disease, that is, a condition that affects relatively few individuals and is overlooked by the medical profession and pharmaceutical industry [12]. Today, PH is no longer ignored, and research on PH is intensifying. Important findings have greatly improved our understanding of this disease and have helped guide patient management. In 1891, Dr. Romberg, a famous German doctor, reported the first PH case, describing a 24-year-old patient who experienced severe dyspnoea, chronic drowsiness, and cyanosis prior to death. Romberg's autopsy report of the patient revealed vascular lesions in the small pulmonary arteries and severe right ventricular hypertrophy. Romberg, however, was unable to identify a pathological cause of the pulmonary artery lesions and ultimately described them as "pulmonary vascular sclerosis" of unknown origin [13, 14]. In the 1940s, Coumard used cardiac catheters to directly measure pulmonary artery pressure, and people began to understand PH from a haemodynamic perspective. Thereafter, Dresdale reported a patient with unexplained PH and termed it primary pulmonary hypertension (PPH). In the 1960s, aminorex caused a PH epidemic in Europe, which attracted the attention of the European medical community and even the World Health Organization (WHO). Prompted by the aminorex incident, the WHO held its first conference in Geneva in 1973 to establish an expert group on PH to define its aetiology and develop a pathological nomenclature for PH. The team of more than a dozen authoritative experts in Europe and the United States divided PH into two categories: PPH and secondary PH. Since then, the National Institutes of Health National Heart, Lung, and Blood Institute launched a nationwide multicentre PPH registration study. At the 2nd World PH Conference in 1998, PH was divided into five clinical diagnostic categories; although they are



updated every year, these five classification principles are maintained [14].

Group I PAH is the most important among the categories due to its aggressive nature, poor survival outcome, and limited treatment options. With efforts over the last three decades, the survival of patients with group I PAH has improved but is still suboptimal, and further improvement remains an unmet challenge. PAH is a dangerous disease that is nonspecific, has a poor prognosis, and lacks an effective treatment. The Registry to Evaluate Early and Long-term PAH Disease Management (REVEAL) study showed a five-year survival rate of 57% from the time of diagnostic right heart catheterization (RHC) [15]. Over the past two decades, the long-term survival of patients with PAH has markedly improved. The current average survival time of PH patients is 6 years, compared to 2.8 years in the 1980s. Similarly, the annual survival rate of PAH patients ranges from 86% to 90%, up from 65% in the 1990s. Despite these improvements, PAH still imposes a massive clinical and economic burden. While the number of PAH-related hospitalizations declined between 2001 and 2012, the average cost and length of PAH-related treatment increased, while the inpatient mortality rate did not significantly decrease and life expectancy remains low [16–18].

Because of the nonspecificity of the early symptoms, most PAH patients often delay diagnosis. The condition then worsens and finally enters the irreversible stage, where treatment is difficult and the prognosis is poor. The early diagnosis and evaluation of PAH are essential for guiding the treatment, improving prognosis, and improving the survival and quality of life of patients with PAH. Methods for the evaluation and detection of PAH have rapidly progressed in recent years. The commonly used diagnosis and treatment methods are the six-minute walk test, cardiopulmonary exercise testing, lung function testing, chest X-ray, electrocardiography, ultrasonic cardiography, chest computed tomography (CT) and CT pulmonary angiography, lung ventilation/perfusion single photon emission CT, magnetic resonance imaging, and RHC. RHC is a traumatic and invasive examination, and the procedure is complex, difficult to repeat, and has certain risks; however, it allows the direct acquisition of accurate and reliable haemodynamic data and excludes intracardiac shunts, abnormal drainage, and other serious left heart diseases to help identify the cause of PAH and test the responsiveness to therapeutic drugs. Thus, RHC remains the gold standard diagnostic method for PAH [19, 20].

Regarding treatment, in addition to the traditional comprehensive treatments of oxygen inhalation, cardiotonic agents, diuretics, anticoagulants, and vasodilators (whose effect is not favourable in patients with a negative acute pulmonary vascular response upon testing), the application of targeted drugs has brought hope for improving the quality of life and prolonging the survival of patients with advanced PH. Before 1995, clinicians used traditional medicines such as digitalis, diuretics, and potassium supplements and anti-hypertensive drugs to treat PH, but patient prognosis was poor, and the mortality rate was high. As research in PH mechanisms has progressed, targeted drugs with different

modes of action have entered the market, and PH is currently treated via the oral, inhalation, subcutaneous injection, and intravenous drip routes. The prognosis of PAH patients has thus gradually improved; the 1-, 3-, and 5-year survival rates of patients have increased from 68%, 48%, and 34% to 86%, 69%, and 61%, respectively [21, 22]. Currently, there are three main traditional categories of targeted therapeutic drugs: endothelin receptor antagonists (bosentan and ambrisentan), phosphodiesterase 5 inhibitors (sildenafil, tadalafil, and vardenafil) and prostacyclin (epoprostenol, iloprost, triprostanil, and beraprost). In addition, some novel PAH-targeted therapeutic drugs, such as the soluble guanylate cyclase activator Adempas and the prostacyclin receptor agonist Uptravi, have shown promising results.

*2.1.2. Pathophysiological Characteristics of PH.* In normal pulmonary vessels, the pulmonary arteries are the main component of the pulmonary vasculature. Pulmonary arteries have a thin wall, relatively little smooth muscle, low activity, and high compliance. In adults, the normal pulmonary artery wall thickness is 40%–70% of the normal aortic wall thickness in the same individual. The internal pulmonary arteries are generally classified as elastic pulmonary arteries, muscular pulmonary arteries, and pulmonary microvessels. Pulmonary arteries consist of three layers: the intima (a continuous layer of endothelial cells), the media (located between the inner and outer elastic membranes and consisting of SMCs, elastin, collagen, and proteoglycan), and the adventitia (composed of fibroblasts and loose collagen fibres). The outer diameter of elastic pulmonary arteries in adults is 500–1000  $\mu\text{m}$ , and the wall is composed of SMCs and abundant elastic fibres. The outer diameter of muscular pulmonary arteries is 50–100  $\mu\text{m}$ , and the inner and outer double layer elastic lamellae are composed mainly of SMCs. The average thickness of the muscle layer is 5% (3%–7%). Pulmonary microvessels are small vessels in which the precursors of SMCs can differentiate into SMCs under pathological conditions, which makes arteries less than 80  $\mu\text{m}$  appear as double-layer elastic lamellae and an intact muscle layer. This pathological change has become recognized as an important cause of PH [10, 23].

Plexiform lesions are a typical histological feature of PAH. In addition, vasoconstriction, cell proliferation, and thrombosis are thought to be central to the pathogenesis of PAH. The early stage of PAH is histologically nonspecific; the only abnormality is membrane hypertrophy and mild thickening of the intima in the pulmonary artery, and characteristic plexiform lesions do not appear until the late stage. Plexiform lesions are arteriolar lesions at the distal end of the arterial branch (usually <300  $\mu\text{m}$  in diameter). There is much debate about whether plexiform lesions are a characteristic pathological change related to pulmonary vascular disease or markers of severe PH. However, pulmonary artery hypertrophy is generally observed, and excessive proliferation, reduced apoptosis, and PASMCs phenotypic switching play an important role in medial hypertrophy.

*2.1.3. PH Pathogenesis.* Recent rapid developments in cell biology and molecular genetics have promoted further



investigations of PH pathogenesis. It is currently believed that the occurrence of PH cannot be explained by a single pathophysiological mechanism but instead results from a combination of genetic, epigenetic, and environmental factors. The endothelial cells, SMCs, fibroblasts, and platelets are abnormally involved in its formation, and that a variety of vasoactive molecules, multiple ion channels, and multiple signalling pathways play an important regulatory role [24]. Many molecular mechanisms have been studied: aberrancies in the bone-forming protein type II receptor and activator receptor-like kinase genes; DNA damage, aberrancies in miRNAs; disruption of the proliferation/apoptosis balance, including endoplasmic reticulum stress, altered mitochondrial function, peroxidase proliferator activated receptor expression, elastase activity, calcium ion concentrations, and  $K^+$  ion channel activity; and abnormal vasoconstriction involving gas signalling molecules (NO, CO, and hydrogen sulfide), prostacyclin (PGI<sub>2</sub>), endothelin, and 5-hydroxytryptamine. Overall, the molecular mechanism is highly complex, involving a variety of signalling pathways.

**2.2. Phenotypic Switching.** The phenotype of vascular smooth muscle cells (VSMCs) is characterized by diversity and variability. During embryonic development, VSMCs gradually differentiate from an undifferentiated (synthetic) phenotype into a differentiated (contractile) phenotype with mature characteristics. However, when blood vessels are damaged or stimulated by various factors, VSMCs dedifferentiate from the contractile phenotype to the synthetic phenotype. This reversible shift in response to changes in environmental stimuli is called phenotypic switching [25].

**2.2.1. Characteristics and Marker Genes of Contractile VSMCs.** In general, contractile VSMCs are smaller in size than synthetic VSMCs. Contractile VSMCs have an elongated, spindle-shaped morphology; are rich in myofilaments; express a large number of contractile-specific proteins; and have vital contractile ability. However, in these cells, DNA synthesis activity is low, and the ECM synthesis ability is poor; thus, their proliferation is very slow, and they do not migrate [26, 27]. Contractile VSMC marker genes include  $\alpha$ -smooth muscle actin ( $\alpha$ -SMA), smooth muscle myosin heavy chain (SMMHC), h1-calponin (CNh1), desmin, aortic carboxypeptidase-like protein (ACLP), metavinculin, telokin, h-caldesmon, smoothelin, and smooth muscle 22 $\alpha$  (SM22 $\alpha$ ). These genes are usually upregulated in contractile VSMCs [27, 28]. SM22 $\alpha$  has strict tissue specificity and cell phenotype specificity in smooth muscle tissue because it participates in remodelling of the actin cytoskeleton and regulates migration, contraction, and other behaviours. Caldesmon is a cytoskeletal protein that regulates cell contraction by interacting with myosin, actin, and calmodulin. It has two types, l-caldesmon and h-caldesmon, with the latter considered a specific marker for VSMC differentiation [29]. ACLP is an ECM-related secretory protein containing over 1100 types of amino acids; it can be produced by SMCs and contributes to VSMC proliferation and wound healing [30].

**2.2.2. Characteristics and Marker Genes of Synthetic VSMCs.** Synthetic VSMCs have a rhomboid/epitheloid-like morphology with a large volume, few muscle filaments, and no contractility, but they can synthesize ECM (proteins), collagen, and osteopontin-8 (OPN-8) to simultaneously enhance cell proliferation and migration [31, 32]. Their marker genes include OPN, matrix gla protein (MGP), myosin heavy chain embryonic (SMemb), and tropomyosin 4 (TM4) [27, 28]. OPN, a secretory glycoprotein, is the most widely used synthetic marker protein and can regulate the phenotypic switching of VSMCs by activating multiple intracellular signalling-level interconnecting pathways, especially the mitogen-activated protein kinase (MAPK) pathway. Relevant studies have shown that the expression of  $\alpha$ -SMA declines significantly and that of OPN increases significantly upon the conversion of contractile VSMCs into synthetic VSMCs [33]. The characteristics and marker genes of contractile VSMCs and synthetic VSMCs are summarized in Figure 1.

**2.2.3. Phenotypic Switching Mechanism.** PSMCs phenotypic switching involves a variety of complex signal transduction pathways, mainly the MAPK/ERK1/2, phosphatidylinositol 3-kinase (PI3K)/Akt, and TGF- $\beta$ /Smad pathways (see Figure 2). These signal transduction pathways regulate the differentiation direction of PSMCs by regulating the expression of SM-specific genes.

**2.2.4. MAPK/ERK1/2 Pathway.** The signal transduction pathway represented by MAPK is called the MAPK pathway and is mainly composed of three central kinases: MAPK kinase kinase (MAPKKK), MAPK kinase (MAPKK), and MAPK. Four MAPK cascades have been identified, namely, the extracellular signal-regulated kinase (ERK), p38 MAPK, JNK, and ERK5 cascades [4].

Among these pathways, the MAPK/ERK1/2 pathway is the most well-known and widely studied and is closely related to cell proliferation and differentiation. When an extracellular ligand binds to a receptor tyrosine kinase (RTK) at the plasma membrane, signal transduction is initiated. The tyrosine residues on the receptor are then phosphorylated to form the Src homology 2 (SH2) binding sites. The adaptor protein Grb2, which contains SH2 domains, can bind with the receptor. Grb2 consists of one SH2 and two SH3 domains, which function to link upstream and downstream molecules. The two SH3 domains of Grb2 bind to proline-rich sequences in the son of sevenless (SOS) protein to activate the SOS. Next, activated SOS binds to Ras (an upstream activating protein), which promotes Ras to release guanosine diphosphate (GDP) and bind to guanosine triphosphate (GTP). Ras-GDP recruits Raf. Subsequently, Raf (acting as a MAPKKK) is activated. Once Raf is activated, any Raf family member (a-Raf, b-Raf, or c-Raf) can activate MEK1/2 (acting as a MAPKK). MEK1/2, in turn, activates ERK1/2 (acting as a MAPK). This sequence constitutes the important three-level Raf/MEK/ERK signalling cascade. Activated ERK1/2 can be translocated to the nucleus to activate ternary complex factors (TCFs) and other

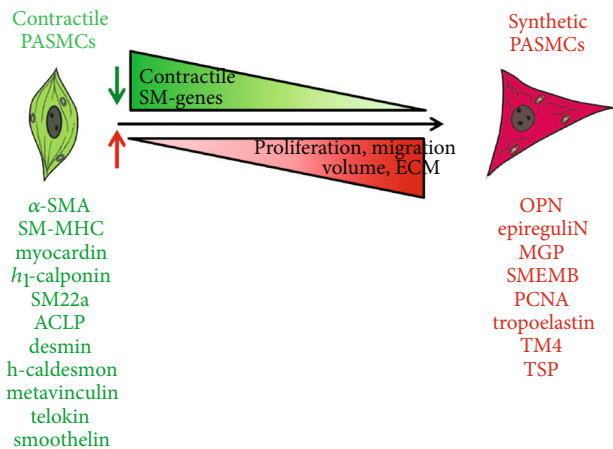


FIGURE 1: Characteristics and marker genes of contractile VSMCs and synthetic VSMCs.

factors through phosphorylation. As a result, cells produce biological substances to respond to foreign signals [4, 34].

TCFs are ternary complexes formed by the binding of MYOCD and MYOCD-related transcription factor A/B (MRTF-A/B) with serum response factor (SRF) [35]. Among these components, MYOCD, an SMC-restricted transcriptional coactivator, is the most critical transcription factor discovered to date that inhibits the phenotypic switching of VSMCs. It can physically interact with SRF to selectively induce the expression of contractile marker genes such as SMA, SM22, and CNh1 to regulate switching to the contractile phenotype [36].

**2.2.5. PI3K/Akt Signalling Pathway.** The PI3K/Akt pathway is one of the classical signalling pathways that regulates the phenotypic switching of VSMCs by regulating downstream transcription factors [37]. Insulin-like growth factor (IGF) and insulin signalling have been demonstrated to be able to inhibit VSMC dedifferentiation via the canonical PI3K/Akt pathway and maintain the contractile phenotype. Ligand-activated IGF or insulin receptors recruit insulin receptor substrates (IRS-1) and activate them by phosphorylation of the tyrosine residues. PI3K docking sites are subsequently formed, enabling PI3K to bind to its substrate, inositol phospholipids. Subsequently, PI3K converts phosphatidylinositol- (4,5-) bisphosphate (PIP<sub>2</sub>) into phosphatidylinositol- (3,4,5-) trisphosphate (PIP<sub>3</sub>). PIP<sub>3</sub> provides docking sites for phosphoinositide-dependent kinase-1 (PDK1) and mTORC2. Akt is then activated by PDK1 (by phosphorylation of Thr308) and mTORC2 (by phosphorylation of Ser473). PDK1 can only partially activate Akt. However, mTORC2 can fully activate and phosphorylate additional substrates. Finally, activated Akt plays a role by phosphorylating downstream target proteins such as FOXO4. Phosphorylation of FOXO4, the substrate of Akt, inhibits phenotypic switching by promoting the nuclear export of FOXO4 and inhibiting MYOCD activity after Akt activation [31, 38].

**2.2.6. TGF- $\beta$ /Smad Signalling Pathway.** Transforming growth factor- $\beta$  (TGF- $\beta$ ), a potent multifunctional soluble cytokine, exists in at least three isoforms: TGF- $\beta$ 1, TGF- $\beta$ 2, and TGF- $\beta$ 3. Its receptors are divided into two types, type I and type II, both of which are transmembrane serine/threonine receptors [39, 40]. TGF- $\beta$  plays an important biological function in the phenotypic switching of mature SMCs. It promotes VSMC differentiation and maintains contractile phenotypes through both Smad-dependent and Smad-independent pathways [32]. Smad is a structurally related signal effector. In vertebrates, the genome encodes eight Smads—Smad1 to Smad8. Smad2 and Smad3 are mainly activated by TGF- $\beta$  and the activin receptors T $\beta$ RI and ActRIB, while Smad1, Smad5, and Smad8 are primarily activated by ALK-1, ALK-2, BMP-RIA/ALK-3, BMP-RIB/ALK-6, and other ligands.

In the Smad-dependent pathway, TGF- $\beta$  is first activated by hydrolysis via endoproteinases. After TGF- $\beta$  is activated, it binds to TGF- $\beta$  II receptors. Next, TGF- $\beta$  II receptors bind to TGF- $\beta$  I receptors to form heterodimers. In these heterodimers, TGF- $\beta$  II receptors can autonomously phosphorylate and activate TGF- $\beta$  I receptors. Activated TGF- $\beta$ 1 receptors then recruit and activate Smad2 and Smad3. Subsequently, phosphorylated Smad2 and Smad3 form a complex with Smad4 and translocate to the nucleus to bind multiple Smad-binding elements and CarG and ultimately play related roles as transcription factors. Among the Smads, Smad3 is the primary mediator of TGF- $\beta$  signalling; Smad3 can interact with SRF and MYOCD and activate the promoters of CarG-dependent VSMC genes. In the Smad-independent pathway, TGF- $\beta$  can regulate VSMC phenotypic switching by activating the Erk, JNK, Notch, and p38 MAPK pathways [31, 39, 40].

**2.3. PH and Phenotypic Switching.** PH is a progressive pulmonary vascular disease characterized by five major features: vasoconstriction, cellular hyperplasia, high pulmonary arterial pressure, right ventricular heart hypertrophy, and vascular remodelling. It can be divided into five main groups. At present, the diagnosis and treatment of PH, especially PAH, are complex and challenging. Therefore, it is highly important to further reveal the potential molecular pathogenesis of PH and explore new therapeutic targets for PH [41, 42]. PH is a proliferative disease. As the understanding of this disease has increased, the phenotypic switching of SMCs from contractile to synthetic has attracted increasing attention. Dong et al. found that pulmonary vascular remodelling, as the core process in PH pathogenesis, is closely related to phenotypic switching [43]. Yeo et al. also noted that the PSMCs phenotypic switching induced by the loss of BMP signal transduction is an essential pathological basis of pulmonary vascular remodelling in PAH [44]. In addition, Morris et al. confirmed that VSMC phenotypes are strictly regulated by Notch3 and that abnormal Notch3 signalling plays a significant role in vascular remodelling [45]. Collectively, these results suggest that phenotypic switching plays an important role in PH. Therefore, further study of the mechanism underlying the occurrence and development of phenotypic switching is highly important for revealing the potential pathogenesis of PH.

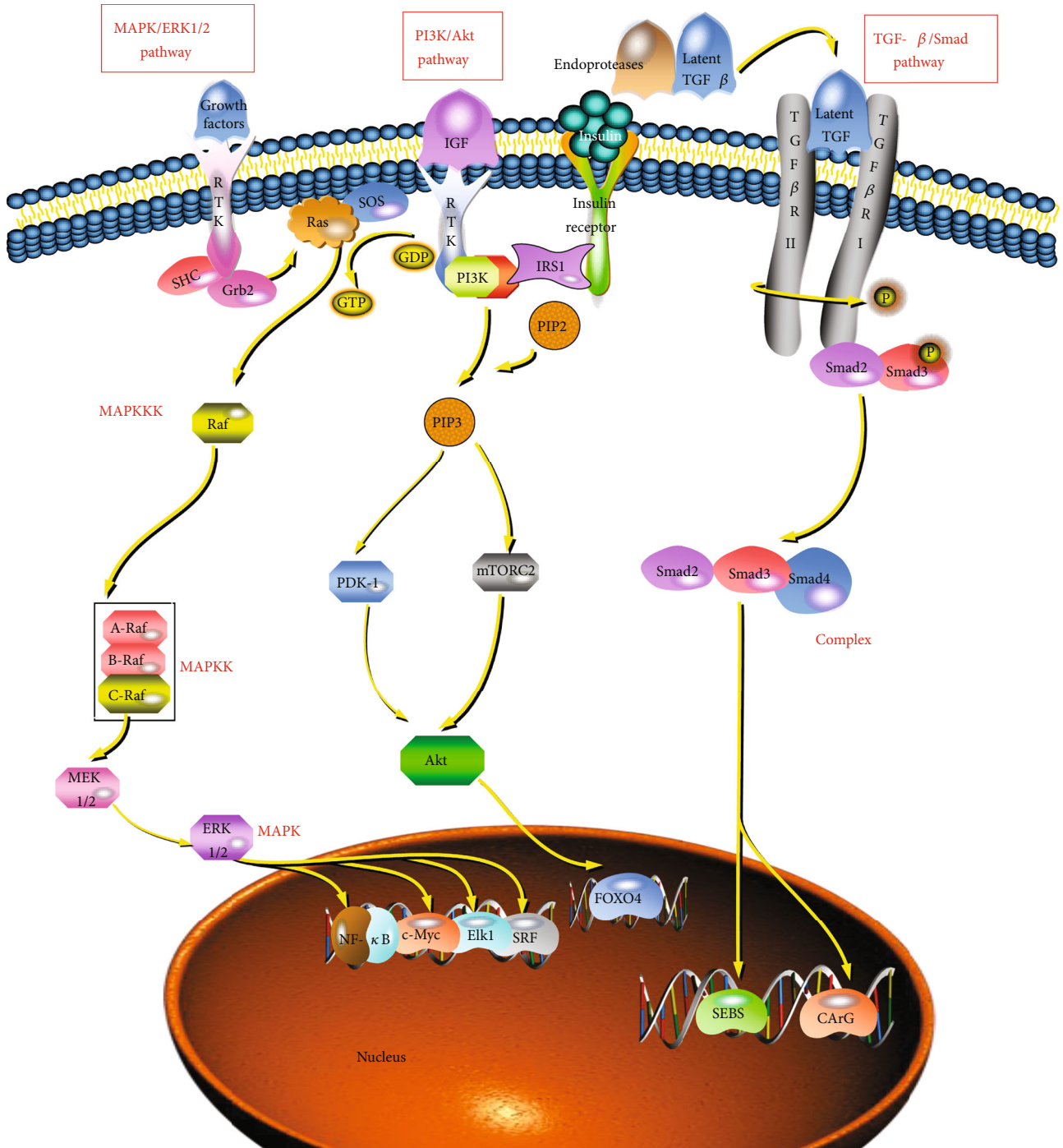


FIGURE 2: Phenotypic switching mechanism.

### 3. Effect of miRNAs on PSMCs Phenotypic Switching in PH

3.1. miRNA Biogenesis and Mechanism of Action. RNA molecules in living organisms can be grouped into two categories, coding RNAs and noncoding RNAs, which constitute a highly complex RNA regulatory network in cells. Among RNAs, miRNAs are a class of single-stranded small noncoding RNAs that are evolutionarily highly conserved and are approximately 18–22 nt in length. miRNAs can directly

degrade or repress the translation of their target mRNAs, thus negatively regulating gene expression at the posttranscriptional level.

miRNA biogenesis is a complex process. The most primitive form is the primary miRNA (pri-miRNA), which is approximately 300–1000 nt in length and is usually transcribed and synthesized by type II or type III RNA polymerase. Pri-miRNAs are first processed in the nucleus by Drosha RNase, which cleaves them into precursor miRNAs (pre-miRNAs) that contain approximately 70–90 nt and have a



stem-loop structure [46]. Pre-miRNAs are transported from the nucleus to the cytoplasm via the Ran GTP-dependent transporter exportin-5 [47]. Via Dicer, a member of the RNase III family of nucleases that specifically cleaves double-stranded RNAs, pre-miRNAs are cleaved into double-stranded miRNA intermediates that contain approximately 22 nt and have a complementary double-helix structure. One strand is the mature miRNA, and the other strand is the miRNA\* with the complementary sequence. Next, the double helix is unwound, and the mature miRNA strands are bound to the RNA-induced silencing complex (RISC) to form asymmetric RISC assembly [48]. This complex can bind to the target mRNA and cause its degradation or translational inhibition. The other strand (miRNA\*) is degraded immediately.

miRNAs can bind to their target mRNAs via two modes: complete binding and incomplete binding. In plants, miRNAs are almost completely paired with their target mRNAs and can degrade them by binding to multiple sites, including the coding region, of the target mRNAs [49]. In animals, the most common mode is incomplete complementary binding, which negatively regulates gene expression by miRNAs binding to the 3'-UTR of their target mRNAs. This binding mode generally does not affect the stability of the mRNA but can affect its translation. The biogenesis and mechanism of action are shown in Figure 3.

miRNAs are regulated by certain mechanisms. Only approximately 8% of human miRNAs are located in exons [50]. Intronic miRNAs are often regulated by their host genes and are processed from introns, but they may have distinct promoter regions, and their transcription is usually initiated by independent promoter elements. The transcription of miRNA genes can be initiated by upstream signal transduction and regulated by downstream transcription factors [51].

miRNA research has rapidly expanded in the several decades since the discovery of the first miRNA, Lin-4, in *C. elegans* by Lee et al. in 1993 and the subsequent discovery of the miRNA Let-7 [52, 53]. At least 30% of the genes in the human genome are estimated to be directly regulated by miRNAs [54]. Therefore, miRNAs are considered to be involved in almost all biological processes and play a pivotal role in various physiological processes, such as embryonic development, organogenesis, and tissue formation, as well as in many pathological processes, such as carcinogenesis, angiogenesis, and inflammation [55]. An increasing number of researchers have found that miRNAs play a unique and key role in the progression of PH by regulating PSMCs phenotypic switching, which is expected to be a potential target for the prevention of PH and related therapies [56]. Here, we review the research progress on miRNAs that regulate PSMCs phenotypic switching.

**3.2. Roles of miRNAs in PH.** miRNAs have been found to be widely involved in cardiovascular diseases such as hypertension. miRNAs are predicted to regulate various molecular mechanisms that are indispensable in the initiation, progression, and perhaps the attenuation or prevention of PH. However, the importance of only a few miRNAs in PH has

been recognized. The strategy of combining system biology with traditional experimental approaches has recently contributed to the identification of novel miRNAs and their target genes/pathways, consequently raising awareness of the significance of miRNAs in PH.

The main miRNAs that have been discovered to promote the progression of PH include miR-17, miR-20, miR-27, miR-143/145, miR-210, and miR-221, while the main miRNAs that can delay and reverse the progression of PH include miR-34, miR-140-5p, miR-223, miR-451, miR-204, miR-424, and miR-503.

The classical mechanism of miRNA involvement in PH progression mainly affects pulmonary vascular remodelling by affecting cell proliferation, apoptosis, and phenotypic switching. For instance, an miR-140-5p mimic can affect the signal transduction of bone morphogenetic protein 4 (BMP4) and/or directly target the 3'-UTR of tumour necrosis factor- $\alpha$  [57, 58], inhibit the proliferation of PSMCs, and delay PH progression.

miRNAs can also inhibit the apoptosis of PSMCs. The expression of miR-34a-3p is decreased in PAH, which in turn upregulates the expression of mitochondrial dynamic protein (MiD) in PSMCs, accelerates mitosis, and reduces apoptosis [59]. miR-29b can inhibit the proliferation and induce the apoptosis of VSMCs by targeting the myeloid leukaemia 1 and cyclin D2 proteins [60].

In addition, the mechanism of miRNA involvement in the progression of PH includes affecting cell metabolism and inducing functional alterations in pulmonary vascular endothelial cells. Caruso et al. indicated that the overexpression of miR-124 or knockdown of polypyrimidine tract binding protein (PTBP1) can normalize the pyruvate kinase muscle isoform 2 (PKM2)/PKM1 ratio in pulmonary adventitial fibroblasts [61], reprogram mitochondrial metabolism, and reduce cell proliferation, which collectively alleviate PAH progression. Endothelin-1 (ET-1) is the most potent endogenous vasoconstrictor; it strongly regulates endothelial function and is a target gene of miR-98. Hypoxia can reduce the expression of miR-98 and increase the level of ET-1, thereby promoting the proliferation of pulmonary artery endothelial cells (PAECs) [62]. The expression of miR-29 family members, which are related to energy metabolism, was found to be decreased in PSMCs after exposure to the oestrogen metabolite 16 $\alpha$ -hydroxyestrone, suggesting that miRNAs may also participate in the development of PH as hormone mediators [63].

In conclusion, miRNAs play an important and unique role in the development of PH through their complex regulatory network.

## 4. miRNAs Modulate PSMCs Phenotypic Switching

**4.1. Growth Factor-Related miRNAs.** Platelet-derived growth factor (PDGF) is a peptide growth factor that stimulates cell proliferation. It is currently considered to be the most potent growth factor that promotes the phenotypic switching of VSMCs. In PH, the amount of PDGF secreted by PAECs is

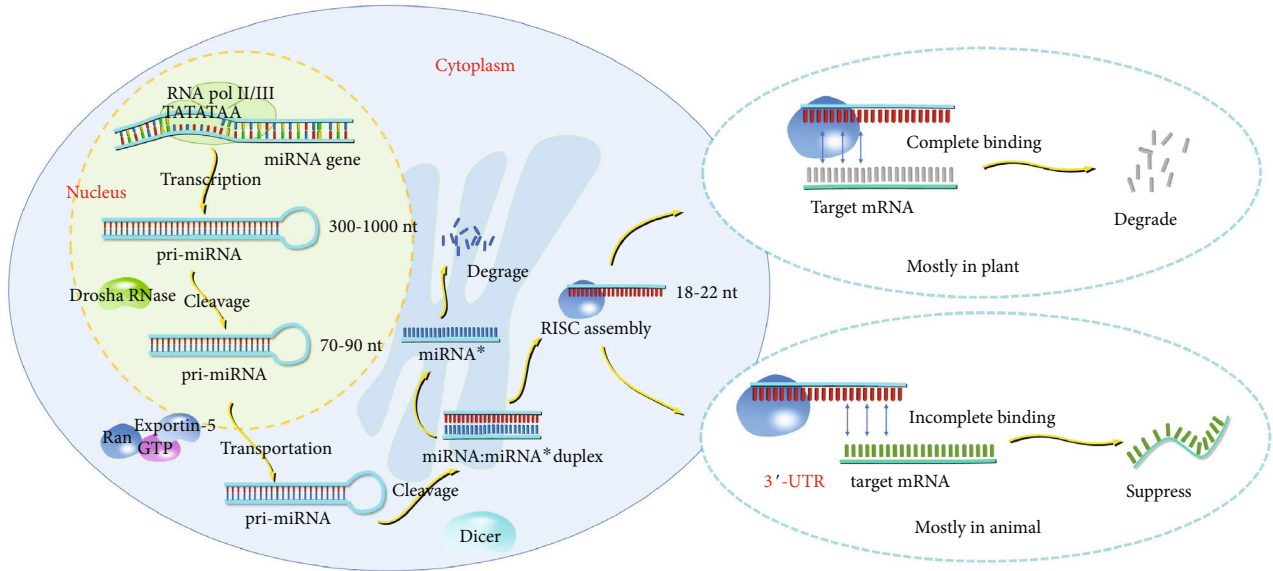


FIGURE 3: miRNA biogenesis and mechanism of action.

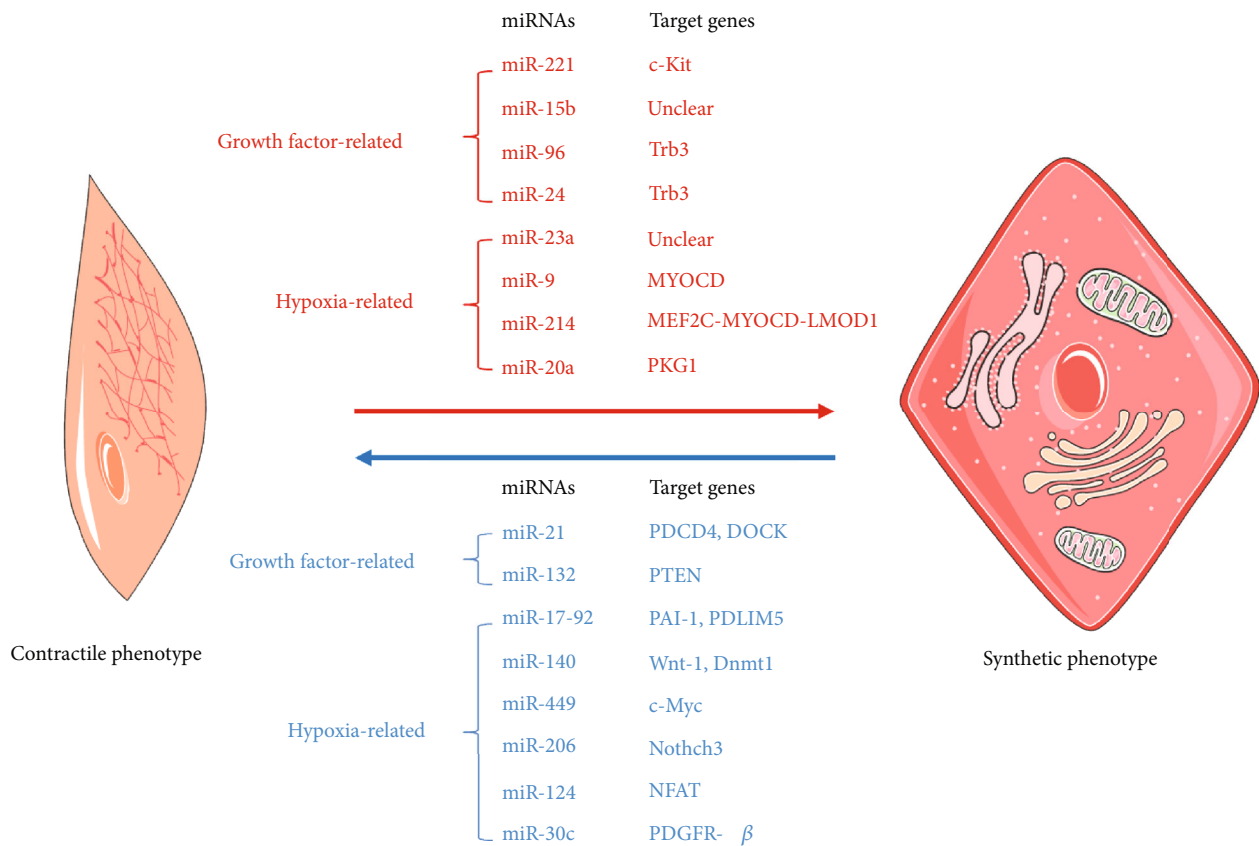


FIGURE 4: miRNAs that influence PSMC phenotypic switching.

significantly increased. PDGF treatment of PSMCs has been reported to significantly upregulate miR-221 [64], miR-15b [65], and miR-24 [66] and downregulate miR-21 [67], ultimately inducing cell phenotypic switching. Moreover, TGF-β/BMP signalling has been described as a nega-

tive regulator of the synthetic phenotype of VSMCs [32], and BMP stimulation can significantly downregulate the expression of miR-96 [68]. The mechanism by which PDGF regulates the expression of miRNAs may be related to antagonism of the BMP signalling pathway [67].



#### 4.1.1. Growth Factor-Related miRNAs That Promote Phenotypic Switching

(1) *miR-221*. The overexpression of miR-221 is associated with the proliferation of many types of tumours, such as breast and gastric cancer [69, 70]. It participates in vascular remodelling in AS by regulating angiogenesis activity and promoting the phenotypic switching of VSMCs [71]. In PH, miR-221 can promote PSMCs phenotypic switching by downregulating the target gene c-Kit. PH can cause extensive injury to small pulmonary vessels, resulting in the increased expression of PDGF ligands and receptors. Davis et al. showed that miR-221 is likely to be transcriptionally induced by PDGF signalling because they observed that both pri- and pre-miR-221 were significantly induced only 1.5 h after PDGF treatment [64]. miR-221 can directly target the 3'-UTR of the c-Kit and p27Kip1 mRNAs to mediate the differentiation and proliferation of PSMCs through distinct downstream mechanisms. Among these targets, p27Kip1 is downregulated at the translational level, which directly promotes cell proliferation. Four and a half LIM domain protein 2 (FHL2) is critical for the stabilization of MYOCD protein, which prevents MYOCD from degrading through the ubiquitin-proteasome-dependent degradation pathway [72]. The c-Kit signalling pathway may alter FHL2 gene expression or FHL2/MYOCD complex formation; these play roles in maintaining the stability of MYOCD and modulating SMC marker gene expression through direct transcriptional activation via the CARG box. PDGF treatment induces the expression of miR-221, leading to the downregulation of c-Kit mRNA expression, in turn inhibiting the transcription of SM-specific contractile genes by reducing the expression of MYOCD and thus playing a catalytic role in PSMCs phenotypic switching.

(2) *miR-15b*. The target genes of miR-15b mainly include proteins associated with cell proliferation (cyclin) [73], cell apoptosis (Bcl-2) [74], and cell invasion (NRP-2 and VEGFR-2) [75, 76]. miR-15b also participates in antiangiogenesis in the pathological process after myocardial infarction [77]. Kim and Kang showed that miR-15b is crucial for the PDGF-mediated inhibition of SM-specific genes [65]. miR-15b expression was found to be increased 1-fold within 4 h of treatment with PDGF, and the increased level of miR-15b was maintained for 24 h after PDGF stimulation, indicating that PDGF signalling regulates miR-15b expression. Previous studies have shown that miR-15b can promote the phenotypic switching of VSMCs. The inhibition of miR-15b expression under physiological conditions can promote  $\alpha$ -SMA synthesis while maintaining the contractile phenotype of VSMCs [78]. That research group further found that miR-15b also mediates PSMCs phenotypic switching, but the specific mechanism remains unclear. Further investigations of predicted targets of miR-15b and the identification of the mechanisms underlying PDGF-mediated regulation of miR-15b will provide more evidence for elucidating the pathophysiological function of miR-15b in VSMC phenotypic regulation.

(3) *miR-96*. miR-96 plays a role in the proliferation and migration of multiple tumours, such as gastric cancer and ovarian cancer [79, 80], as well as in the maintenance of embryonic stem cell pluripotency. In addition, miR-96 can inhibit postinfarct neovascularization by targeting anillin. The downregulation of miR-96 expression can improve cardiac endothelial cell growth potential [81]. Kim et al. showed that the expression of pri-miR-96 was decreased in PSMCs under BMP4 stimulation in a Smad4-dependent manner [68]. In the pulmonary arteries, miR-96 negatively regulates the target gene Tribbles-like protein 3 (Trb3), resulting in a decrease in the expression of Smads, which in turn promotes PSMCs phenotypic switching. Trb3 is a BMPRII-interacting protein. BMP stimulation can release Trb3 from BMPRII; Trb3 then interacts with Smurf1 to degrade it through the ubiquitin-proteasome pathway. The reduction of Smurf1 stabilizes Smad proteins in the BMP pathway and consequently enhances the BMP reaction [82]. miR-96 is a critical molecule that functions as a negative regulator of the BMP signalling pathway and can thus inhibit SM-specific gene expression. The inhibition of BMP4 signalling may lead to upregulated miR-96 expression, further reducing the expression of Trb3 and resulting in a decrease in Smad protein expression, ultimately promoting the synthetic phenotype of VSMCs. Hence, there may be negative feedback regulation between miR-96 and Trb3 in PSMCs.

(4) *miR-24*. miR-24 is mainly involved in haematopoietic cell differentiation [83], tumour development, and other processes and widely participates in cardiomyocyte apoptosis, myocardial fibrosis, and cardiac remodelling after acute myocardial infarction [84, 85]. The miR-24 gene contains two members: miR-24-1 and miR-24-2. The expression level of the miR-24-2 cluster, but not the miR-2 cluster, was induced 1.5-fold after PDGF treatment for 4 h [66]. Similar to miR-96, miR-24 also targets Trb3 protein, causing a decrease in the expression of Smad proteins, such as Smad1 and Smad5, which inhibits the TGF $\beta$  and BMP signalling pathways and consequently promotes the synthetic phenotype of PSMCs. The expression condition of miR-24 in PH patients needs to be further confirmed, which is hoped to provide a basis for the application of anti-miR-24 in PH treatment.

#### 4.1.2. Growth Factor-Related miRNAs That Inhibit Phenotypic Switching

(1) *miR-21*. miR-21 has long been valued for its role in tumour, cardiovascular, and lung diseases and is the most studied miRNA in PH vascular remodelling; however, the results of these studies have been contradictory. Some scholars who systematically studied miR-21 found that its expression is downregulated in the lung tissue of PH rats and in the lung tissue and plasma of idiopathic PAH (IPAH) patients. In PSMCs, PDGF significantly downregulates miR-21 expression [67, 86].

In the maintenance of the contractile phenotype in VSMCs, the BMP4 signalling pathway has always been considered to be important. Aberrant expression or inactivating

mutations in the BMP receptor (BMPR) gene can lead to VSMC dedifferentiation.

Studies have shown that miRNAs play an important role in the BMP-mediated promotion of the VSMC contraction phenotype, and miR-21 is one example [78]. Upon BMP treatment, R-Smad proteins associate with pri-miR-21 in the complex with Drosha to promote the processing of pri-miR-21 to pre-miR-21 and increase miR-21 levels [78, 87]. By inducing miR-21 expression, BMP4 leads to the down-regulation of programmed cell death 4 (PDCD4), which inhibits contractile gene expression.

In addition, Kang et al. found that in PSMCs almost all dedicator of cytokinesis (DOCK) family members are miR-21 targets [67]. BMP4-mediated upregulation of miR-21 promotes the maintenance of the PSMCs contractile phenotype and inhibits PSMCs migration by inhibiting DOCK4, -5, and -7. In addition, PDGF stimulation can promote PSMCs phenotypic switching through the miR-21/DOCK signalling pathway.

miR-21 has been identified as a biomarker of some tumours, and regulating its function is a cardioprotective strategy. Whether it is also involved in right heart failure in PH is worth further investigation.

(2) *miR-132*. miR-132 is believed to play an important role in the central nervous system and cardiovascular system. Some researchers have found that miR-132 expression is upregulated in myocardial hypertrophy, hypertension, AS, and other diseases [88–90], which suggest a strong effect of miR-132. This is closely related to its influence on the proliferation and migration of endothelial cells and VSMCs. One study found that miR-132 was upregulated in monocrotaline-(MCT-) induced PH rats and PDGF-induced PSMCs [91], and further studies found that miR-132 has a complex role in the occurrence of PH, inhibiting PSMCs proliferation and maintaining the PSMCs contraction phenotype while promoting cell migration, which was achieved by targeting phosphatase and tensor protein homology (PTEN). The anti-proliferative and phenotypic switching-inhibiting effects of miR-132 do not appear to coincide with the increase in miR-132 in MCT-induced PH rats. The cause for this may be multifaceted, and possibly PSMC proliferation is induced by other factors. Based on these results, whether inhibiting miR-132 can prevent and treat PH indeed needs further study.

**4.2. Hypoxia-Related miRNAs.** The mechanism by which hypoxia leads to changes in miRNA expression can be mediated by hypoxia inducible factor-1- (HIF-1-) dependent and HIF-1-independent pathways. Although hypoxia reportedly induces PSMCs phenotypic switching, the expression levels of miR-23a [92], miR-9 [93], miR-214 [36], and miR-20a [94] are increased, while those of miR-449 [95], miR-206 [96], miR-124 [97], miR-30c [98], and miR-140 [99] are decreased.

#### 4.2.1. Hypoxia-Related miRNAs That Promote Phenotypic Switching

(1) *HIF-1 $\alpha$ -Dependent Pathway.* HIF-1 is an important mediator of oxygen homeostasis and is a nuclear transcrip-

tion factor that plays an active role in hypoxia. HIF-1 is a heterodimer composed of an oxygen-sensitive  $\alpha$  subunit (HIF-1 $\alpha$ ) and a constitutively expressed  $\beta$  subunit (HIF-1 $\beta$ ). Under normoxic conditions, HIF-1 $\beta$  is stably expressed in the cytoplasm, while HIF-1 $\alpha$  is promptly degraded by the hydrolytic ubiquitin protease complex after its translation. In contrast, the protein level of HIF-1 $\alpha$  increases rapidly due to the inhibition of HIF-1 $\alpha$  degradation under hypoxic conditions. The physiological activity of HIF-1 mainly depends on the function and expression of the  $\alpha$  subunit; thus, HIF-1 $\alpha$  is called the active subunit of HIF-1 [100]. Many studies have confirmed that HIF-1 is upregulated and plays an important role in various types of PH, especially in hypoxic PH (HPH) [101]. In the early stage of hypoxia, HIF can activate the transcription of more than 100 genes, including miRNAs [92, 93], which affect and regulate various pulmonary vascular functions, such as reactive oxygen species generation, angiogenesis, and vascular homeostasis, including PSMCs phenotypic switching.

*miR-23a:* miR-23a is involved in the development of various cancers, promotes cardiac hypertrophy, and antagonizes muscle atrophy [102, 103]. Yan et al. showed that under hypoxic conditions the expression of miR-23a was upregulated in primary rat PSMCs through a mechanism involving HIF-1 $\alpha$  [92]. In addition, the expression of contractile protein markers was significantly downregulated, suggesting that miR-23a regulates the dedifferentiation of PSMCs. Moreover, the level of contractile protein markers was significantly downregulated after transfection of a miR-23a mimic for 48 h under normoxic conditions, while the expression of contractile protein markers in miR-23a inhibitor-transfected cells was significantly increased under hypoxic conditions. HIF-1 $\alpha$  was transcriptionally activated in PSMCs cultured under hypoxic conditions and participated in the transcriptional activation of miR-23a by binding to the regulatory element upstream of their transcription start sites (TSS), in turn downregulating the expression of contractile phenotype marker proteins in PSMCs, an effect that may be related to the enhancement of cell phenotypic switching. The downstream targets of miR-23a in the inhibition of contractile protein marker expression have not been identified.

*miR-9:* miR-9 functions in promoting or antagonizing proliferation according to cell type specificity. For instance, miR-9 promotes the proliferation of gastric carcinoma cells by targeting caudal type homeobox 2 [104, 105], while it inhibits the proliferation of nasopharyngeal, breast, and ovarian carcinoma [106–108]; reduces macrophage foam cell formation; and participates in the regulation of the AS process by targeting the human ACAT1 gene [109]. miR-9 may directly inhibit the transcription of genes encoding SM-specific proteins by targeting MYOCD, thereby promoting phenotypic switching. Shan et al. found that miR-9 was increased in primary rat PSMCs exposed to hypoxia via the activation of HIF-1 $\alpha$  [93]. HIF-1 binding motifs (5'-RCGTG-3') are located in the region within 5 kb upstream of the TSS at miR-9 loci, and HIF-1 $\alpha$  enrichment was increased at all HIF-1 binding motifs upstream of the miR-9 TSS after 24 and 48 h of hypoxia exposure.

(2) *HIF-1 $\alpha$ -Independent Pathway*. Similar to miR-9, both miR-214 and miR-20a are upregulated in HPH and promote PSMCs phenotypic switching through negative regulation of the MYOCD signalling pathway [36, 94]. However, they regulate MYOCD through different mechanisms.

*miR-214*: miR-214 participates mainly in cancer and is an important regulator of fibrosis in the liver, kidney, and myocardium. It plays a regulatory role in promoting hypertrophy in myocardial hypertrophy and heart failure [110]. miR-214 directly inhibits the MYOCD-LMOD1 signalling pathway and promotes PSMCs phenotypic switching by inhibiting the downstream target myocyte enhancer factor 2C (MEF2C) [36]. Sahoo et al. found that miR-214 was upregulated in PSMCs isolated from PAH patients and hypoxia-induced human PSMCs (hPSMCS), while leiomodulin (LMOD1), MYOCD, and MEF2C were downregulated [36]. MEF2C serves as an upstream coordinator of SMC differentiation and cooperates with MYOCD to regulate the SMC contractile phenotype [111]. LMOD1 is an SM-specific gene regulated by MYOCD at the transcriptional level and may play an important role in SMC contractile activity and actin cytoskeleton assembly through its association with tropomyosin during smooth muscle cell contraction [112]. Research has shown that MEF2C and LMOD1 are direct targets of miR-214. miR-214 directly regulates the expression of SM-specific genes at the level of LMOD1 and through the upstream disruption of the MEF2C/MYOCD pathway. Exogenous administration of a miR-214 inhibitor to hPSMCS of PH patients restored the contractile phenotype of these cells, suggesting that miR-214 plays a key role in promoting the occurrence and development of PH.

*miR-20a*: the dysregulation of miR-20a expression is involved in the development of a variety of cancers [113]. In PH, miR-20a targets PKG1, promotes the activation of Elk-1, and competes for the binding sites of MYOCD and SRF, eventually leading to the dissociation of the MYOCD-SRF complex and termination of the SM-specific gene expression programme. Zeng et al. found that miR-20a was gradually increased with prolonged exposure to hypoxia in HPH mice and in hypoxic hPSMCS [94]. Unlike miRNAs that bind to the 3'-UTR sequence of the target mRNA, miR-20a may regulate the expression of the PKG1 gene by binding to the coding region of PKG1. PKG is a serine/threonine-specific protein kinase that phosphorylates its substrate proteins to achieve signal transduction. Studies have confirmed that PKG can regulate the dedifferentiation of SMCs by promoting the expression of MYOCD, inhibiting the expression of SRF and Elk-1, and inhibiting their binding to CARG elements in SM-specific genes.

*4.2.2. Hypoxia-Related miRNAs That Inhibit Phenotypic Switching*. miR-449 [95], miR-206 [96], miR-124 [97], miR-30c [98], and miR-140 [99] are downregulated in PSMCs and in the lung vasculature of animal models of HPH and inhibit PSMCs phenotypic switching by acting on their respective targets.

(1) *miR-449*. miR-449 clusters, located in cancer susceptibility sites, inhibit tumour growth, invasion, and metastasis by acting on multiple signalling factors (including the Notch pathway, VEGF, and P53) and promoting apoptosis and differentiation. The miR-449a/c-Myc axis reportedly plays an important role in regulating PSMCs phenotypic switching and pulmonary vascular remodelling [95]. miR-449 was downregulated in rat PSMCs in hypoxia-induced PH and directly targeted c-Myc regulation to promote the expression of SM-22 $\alpha$ , calponin, and myosin, which ultimately inhibited PSMCs phenotypic switching. It is known that c-Myc expression is inhibited in resting and terminally differentiated cells, while it is temporarily activated in the initial stage of proliferation, after which it peaks rapidly and then recovers to baseline [114]. Hypoxia-induced downregulation of SM-specific genes and upregulation of OPN were significantly reversed by c-Myc knockdown. Moreover, miR-449 was found to regulate mitochondrial function in PSMCs by targeting c-Myc [95].

(2) *miR-206*. miR-206 is abnormally expressed in gastric cancer, breast cancer, liver cancer, and lung cancer and is a metastatic suppressor for many cancers. Studies have found that miR-206 targets the Notch3 gene to regulate skeletal muscle cell proliferation and cell cycle block [115]. The expression of miR-206 was significantly decreased in PSMCs from hypoxia-induced PH mice compared to control mice. The overexpression of miR-206 in hPSMCS promoted apoptosis and inhibited proliferation. Moreover, compared with the control hPSMCS,  $\alpha$ -SM actin and calponin were higher in hPSMCS overexpressing miR-206, while miR-206 downregulation decreased the expression of these proteins in hPSMCS. These findings support an important role for miR-206-mediated signalling in maintaining the differentiation phenotype of hPSMCS. Additionally, miR-206 was found to play a role by inhibiting Notch3 signalling [96].

Notch3 signalling significantly affects the development of PAH [116]. It can influence the stability of blood vessels because of the interaction between the Notch3 target gene and the BMPR target gene. Notch3 is overexpressed in VSMCs in PAH [116], but the cause of this steady-state increase is unknown. However, miR-206 downregulation in PH may be a reason for the increase in Notch3 expression in PH [96]. miR-206 can significantly increase the expression of SM-specific proteins ( $\alpha$ -SMA and calponin) in PSMCs by inhibiting the corresponding pathways. Correcting altered expression of miRNAs could be a potential therapeutic strategy for PAH.

(3) *miR-124*. miR-124 is rich in the brain, with high expression in normal tissues but low expression in many cancers (such as colorectal cancer, breast cancer, gastric cancer, and pancreatic cancer). miR-124 expression level was also lowered in diseases such as Parkinson's disease, Huntington's disease, hypertension, and PH [117]. Upregulating miRNA-124 in vivo can delay these disease processes. miR-124 may play a role in promoting contractility and



maintaining the differentiated phenotype of PSMCs by suppressing the nuclear factor of activated T cell (NFAT) pathway [97]. Studies have found that NFAT signalling is associated with PSMCs proliferation and PAH. One study showed that NFATc2 was upregulated and activated in PAH patients [118]. Additionally, the expression and activation of NFATc3 were increased in a hypoxia-induced PH mouse model, and the proliferation and migration of PSMCs are also regulated by the CAN/NFAT signalling pathway [119, 120]. It was recently reported that ectopic overexpression of three different NFAT isoforms significantly downregulates  $\alpha$ -SMA expression, indicating its role in PSMCs phenotypic switching. These results demonstrated that the NFAT-mediated signalling pathway plays a major role in the pathogenesis of PH. miR-124 inhibited NFAT signalling by suppressing both the activation and nuclear translocation of NFAT by targeting numerous genes, including NFATc1, calmodulin-binding transcription activator 1, and PTBP1 [97].

(4) *miR-30c*. miR-30c expression is reduced in various human tumour tissues, and some studies have identified it as a potential biomarker of prostate cancer, bladder cancer, and breast cancer. There are development prospects for miR-30c in the diagnosis and treatment of partial remissions. Studies have shown that hypoxia inhibits miR-30c expression in PSMCs, resulting in the proliferation of PSMCs and inhibition of their apoptosis. Moreover, a miR-30c inhibitor directly promotes PSMCs phenotypic switching from contractile to synthetic, while miR-30c mimic treatment under hypoxic conditions could reverse these effects by inhibiting the PDGF signalling pathway by targeting PDGF receptor  $\beta$  (PDGFR- $\beta$ ) [98]. PDGFR- $\beta$  plays a crucial role in the regulation of cell function. Accumulating evidence suggests that abnormalities in the PDGF/PDGFR signalling pathway are involved in PH pathogenesis [121]. In various experimental models and in humans, the upregulated expression of PDGF and PDGFRs was associated with PH [122–124]. Interestingly, miR-30c-mediated changes in PDGFR expression were found to occur only in hypoxic cells, not in PDGF-stimulated cells. In addition, miR-30c can participate in ventricular remodelling by targeting XBP1, TGF-1, and others [125], and whether it is involved in right ventricular remodelling in PH is worth exploring.

(5) *miR-140*. miR-140 was found to play an important role in breast cancer [126], non-small-cell lung cancer, and osteoarthritis [127, 128]. It can also be used as a predictor of coronary heart disease. miR-140 expression was found to be significantly downregulated in lung tissues of congenital PH and PAH patients [99]. Compared with patients without PH, patients with congenital PH have higher pulmonary artery pressure and lower miR-140 expression. Correlation analysis showed that miR-140 expression was negatively correlated with pulmonary artery pressure and the expression of Wnt signalling pathway-related proteins (Wnt-1 and  $\beta$ -catenin). Specifically, under hypoxic conditions, miR-140 expression was downregulated in hPSMCs, while Wnt-1

expression was upregulated. The upregulation of miR-140 increased the expression of SM-specific proteins; for example, it significantly increased  $\alpha$ -SMA, SM22, and calponin expression. Transfection with an miR-140 inhibitor led to an increased cell proliferation rate, increased migration, and reduced expression of contractile phenotype-related proteins, suggesting that miR-140 is necessary for maintaining the PSMCs phenotype. Further research showed that the Wnt-1 3'-UTR contains miR-140 recognition sites, suggesting that miR-140 directly targets Wnt-1 and suppresses PSMCs phenotypic switching. In addition to Wnt signalling, miR-140 also directly targets Dnmt1, decreases SOD2 expression, and inhibits phenotypic switching of hPSMCs [99]. Moreover, one study showed that delivering miR-140 into the lungs with liposomes reduced haemodynamic indicators and pulmonary vascular reconstruction in rats by suppressing Smurf1 expression [129]. The delivery of miR-140 to the lungs using liposomes may offer new possibilities for treating PH.

(6) *miR-17~92*. In the human genome, the miR-17~92 cluster, a typical polycistronic miRNA gene cluster, is located on chromosome 13. This cluster encodes and expresses six mature miRNAs, namely, miR-17, miR-20a, miR-18a, miR-19a, miR-19b, and miR-92a, each of which has its own target gene and biological function. It regulates tumour angiogenesis and widely participates in the development of lymphocytes [130]. The expression imbalance of this cluster can lead to a variety of diseases, including haematologic neoplasms, solid neoplasms, immune diseases, and cardiovascular diseases [131].

miR-19a/b and miR-17/20a are important members of the miR-17~92 cluster. The expression of miR-19a/b and miR-17/20a was downregulated in PSMCs of patients with IPAH and PAH associated with other diseases (APAH). Interestingly, in mice with HPH, miR-17~92 was found to be upregulated in the early stage of HPH but downregulated in the later stage [132]. Specific knockout of miR-17~92 in VSMCs attenuated HPH progression and pulmonary artery pressure in mice, but the effect of miR-17~92 knockout was counteracted by the addition of recombinant miR-17~92, suggesting that miR-17~92 cluster members strongly participate in pulmonary vascular remodelling in HPH. Interestingly, miR-17~92 was found to promote both proliferation and differentiation of PSMCs in vitro. Its mechanism regulating the phenotypic switching of PSMCs is independent of the MYOCD pathway but depends on the TGF- $\beta$  signal. These results suggest that miR-17~92 in PSMCs is an important participant in the pathogenesis of PH but not the absolute controller. In PSMCs, the direct downstream targets of miR-17~92 have been confirmed to include plasminogen activator inhibitor 1 (PAI-1), PDZ, LIM domain 5 (PDLIM5), and prolyl hydroxylase domain-containing 2 (PHD2).

Among the miR-17~92 cluster members, miR-19a/b can positively regulate the TGF- $\beta$ /Smad2/calponin signalling pathway by inhibiting PAI-1 in PSMCs to maintain the contraction phenotype [132]. PAI-1 can be secreted by

PASMCs and act as a major inhibitor of tissue-type and urokinase-type plasminogen activators, and it mainly regulates the plasma fibrinolysis system and cell adhesion ability. Studies show that suppression of PAI-1 can increase Smad2 and the expression of SMC markers, thus negatively regulating the PASMCs contractile phenotype and influencing its metabolism [132]. Notably, PAI-1 was not abnormally expressed in APAH and IPAHA PASMCs but was downregulated in the rat HPH model, suggesting that this pathway is regulated differently in different groups of PH.

miR-17/20a is another important member of the miR-17~92 cluster, and it can inhibit PASMCs phenotypic switching by inhibiting PDLIM5 and promoting the TGF- $\beta$ 3/Smad3 signalling pathway [133]. PDLIM5 acts as an adaptor protein to sequester transcription factors in the cytoplasm; it can also interact with kinases to exert its effects and can inhibit the expression of SMC markers through TGF- $\beta$ 3/smad3 signal transduction. Therefore, it serves as a negative regulator of the SMC contractile phenotype. miR-17/20a can directly target PDLIM5 and decrease its expression. In addition, miR-17/20a can indirectly inhibit PAI-1 by regulating PDLIM5. Further studies have shown that miR-17~92 also upregulates the expression of HIF-1 $\alpha$  by inhibiting PHD2 in PH [134], promoting the proliferation of PASMCs and enhancing pulmonary vessel remodeling. Therefore, the different effects of miR-17~92 may be closely related to the biphasic regulation of early upregulation and late downregulation during PH progression.

In summary, the miR-17~92 cluster plays a complex regulatory role in the development of PH. The regulation of PAH pathogenesis by the miR-17~92 cluster requires further study and may become a potential therapeutic direction for PH.

(7) *miR-let-7g*. miR-let-7 is widely expressed in the cardiovascular system, with abnormalities in many cardiovascular diseases, such as myocardial hypertrophy, myocardial fibrosis, myocardial infarction, angiogenesis, AS, and hypertension. Our team used miRNA network pharmacology to reveal that the let-7 family was involved in three functional pathways: TGF-/BMP, hypoxia, and inflammation. We also found that miR-let-7g was decreased in hypoxic PH rats. It can inhibit hypoxia-induced PASMCs proliferation by targeting c-Myc [135]. Considering that miR-449 can inhibit the phenotypic switching of PASMCs by targeting c-Myc [95], it is also worth exploring whether let-7g can also inhibit the phenotypic switching of PASMCs by targeting c-Myc. We also found that let-7g can negatively regulate LOX-1 expression in PH [136], and LOX-1 can promote the phenotypic switching of PASMCs through the ERK1/2-Elk-1/MRTF-A-SRF signalling pathway [25]. Additionally, it is known that after activation of the MAPK pathway, ternary complex factor (TCF) is activated and can promote the phenotypic switching of VSMCs by remodelling chromatin containing the CARG box promoter. This process isolates SRF and reduces troponin expression. Using bioinformatics prediction, our team found that let-7g targets MEKK1 to regulate the MAPK pathway. Based on the above findings, we conjecture that let-7g can likely inhibit PASMCs phenotypic switching, and this is one of our future research directions.

## 5. Conclusions and Future Directions

PH is a serious progressive cardiopulmonary disease with poor prognosis and no effective treatment. Researches worldwide have committed to exploring its pathogenesis and identifying new targets for its prevention and treatment. In recent decades, international research on miRNAs has rapidly progressed, and the discovery of miRNAs has opened a new research area to investigate mechanisms of disease occurrence and development. miRNAs play important roles in various biological systems and diseases. Recent studies have demonstrated that miRNAs can regulate many key molecular pathways that play crucial roles in the occurrence, development, and, possibly, the attenuation or prevention of PH. These miRNAs can be classified into growth factor-related miRNAs, inflammation-related miRNAs, and hypoxia-related miRNAs based on the affected signalling pathways [137]. Compared with research in other fields, research on miRNAs in the occurrence and development of PH is relatively underdeveloped. Only a few miRNAs have been proven to be suitable therapeutic targets for this disease, and almost no research has been conducted to investigate the effects of miRNAs on ion channels in PAECs and PASMCs. However, this deficit also presents a rare opportunity for us. Enhancing the study of PH-related miRNAs will help to further clarify the pathogenesis of PH, develop more effective targeted drugs, and assist in the early diagnosis. At present, clinical treatment can only reduce symptoms and cannot reverse the disease process. Although the majority of miRNA research and miRNA-based therapeutics in current clinical trials are related to cancer, they still have great prospects in the treatment of pulmonary diseases [138]. Some animal experiments have proven that drugs targeting miRNAs can delay or even reverse the PH process. For example, in a rat PH model induced by monocrotaline, an airway atomized miR-140 simulant and miR-223 simulant were shown to treat PH [57, 139]. Therefore, miRNA-based therapeutics have become a new hope for the reversal of PH symptomatology. However, further research is needed to elucidate how to accurately deliver miRNAs into lung tissue while avoiding adverse reactions in other tissues and how to maintain stability in cells. Simultaneously, the role of miRNAs in vivo is complex, and there may be multiple targets that form a network with each other. From this perspective, miRNAs that have little impact on other organs but have obvious effects in PH may be more valuable for research. Furthermore, analysing PH-related miRNAs and studying their upstream and downstream targets would also be helpful in exploring the aetiology and laying a foundation for finding new powerful targets and developing related, non-miRNA drugs. This review summarizes the role of miRNAs in pulmonary vascular remodelling in PH via the regulation of phenotypic switching and summarizes the potential target genes (see Figure 4). Researchers are expected to focus on PASMCs phenotypic switching to reveal new roles of miRNAs in PH occurrence and development. Recent reports have shown that extracellular miRNAs bind to protein complexes and are thus not readily degraded by RNases in the circulation; in addition, they exhibit stable



and abundant expression and can thus be used as potential biomarkers for the diagnosis or early detection of PH [140]. miRNA molecules have a simple structure and low molecular weight and are easy to synthesize and modify; furthermore, miRNA-based treatments can not only silence genes (and eliminate undesirable protein translation) but also restore the expression of lost proteins to physiological levels. For these reasons, drugs targeting miRNAs are expected to constitute a new generation of molecular approaches for PH treatment.

## Conflicts of Interest

The authors have no conflicts of interest to disclose.

## Acknowledgments

This project was supported by funding from the National Natural Science Foundation of China (grant nos. 82000062 and 81960015), the Science Foundation for distinguished Young Scholars of Jiangxi Province, and the Young Talents Project Foundation from Science and Technology Department of Jiangxi Province (grant nos. 20212ACB216008 and 20204BCJ23020).

## References

- [1] A. Vonk-Noordegraaf, F. Haddad, K. M. Chin et al., "Right heart adaptation to pulmonary arterial hypertension: physiology and pathobiology," *Journal of the American College of Cardiology*, vol. 62, no. 25, pp. D22–D33, 2013.
- [2] C. Guignabert and P. Dorfmüller, "Pathology and pathobiology of pulmonary hypertension," *Seminars in Respiratory and Critical Care Medicine*, vol. 38, no. 5, pp. 571–584, 2017.
- [3] M. Liu and D. Gomez, "Smooth muscle cell phenotypic diversity," *Arteriosclerosis, Thrombosis, and Vascular Biology*, vol. 39, no. 9, pp. 1715–1723, 2019.
- [4] Y. J. Guo, W. W. Pan, S. B. Liu, Z. F. Shen, Y. Xu, and L. L. Hu, "ERK/MAPK signalling pathway and tumorigenesis (Review)," *Experimental and Therapeutic Medicine*, vol. 19, no. 3, pp. 1997–2007, 2020.
- [5] Z. Fan, C. Li, C. Qin et al., "Role of the PI3K/AKT pathway in modulating cytoskeleton rearrangements and phenotype switching in rat pulmonary arterial vascular smooth muscle cells," *DNA and Cell Biology*, vol. 33, no. 1, pp. 12–19, 2014.
- [6] J. M. Miano and X. Long, "The short and long of noncoding sequences in the control of vascular cell phenotypes," *Cellular and Molecular Life Sciences*, vol. 72, no. 18, pp. 3457–3488, 2015.
- [7] H. J. Chun, S. Bonnet, and S. Y. Chan, "Translational Advances in the Field of Pulmonary Hypertension. Translating Micro-RNA Biology in Pulmonary Hypertension. It Will Take More Than "miR" Words," *American Journal of Respiratory and Critical Care Medicine*, vol. 195, no. 2, pp. 167–178, 2017.
- [8] P. McLoughlin, J. M. Hyvelin, and K. Howell, "Pulmonary hypertension," *The New England Journal of Medicine*, vol. 352, no. 4, pp. 418–419, 2005.
- [9] S. Sahay, "Evaluation and classification of pulmonary arterial hypertension," *Journal of Thoracic Disease*, vol. 11, Supplement 14, pp. S1789–S1799, 2019.
- [10] R. T. Schermuly, H. A. Ghofrani, M. R. Wilkins, and F. Grimminger, "Mechanisms of disease: pulmonary arterial hypertension," *Nature Reviews Cardiology*, vol. 8, no. 8, pp. 443–455, 2011.
- [11] G. Simonneau, D. Montani, D. S. Celermajer et al., "Haemodynamic definitions and updated clinical classification of pulmonary hypertension," *The European Respiratory Journal*, vol. 53, no. 1, article 1801913, 2019.
- [12] M. Humbert, N. Khaltaev, J. Bousquet, and R. Souza, "Pulmonary hypertension: from an orphan disease to a public health problem," *Chest*, vol. 132, no. 2, pp. 365–367, 2007.
- [13] S. A. van Wolferen, K. Grünberg, and A. Vonk-Noordegraaf, "Diagnosis and management of pulmonary hypertension over the past 100 years," *Respiratory Medicine*, vol. 101, no. 3, pp. 389–398, 2007.
- [14] A. P. Fishman, "Primary pulmonary arterial hypertension: a look back," *Journal of the American College of Cardiology*, vol. 43, no. 12, pp. S2–S4, 2004.
- [15] R. L. Benza, D. P. Miller, R. J. Barst, D. B. Badesch, A. E. Frost, and M. D. McGoon, "An evaluation of long-term survival from time of diagnosis in pulmonary arterial hypertension from the REVEAL registry," *Chest*, vol. 142, no. 2, pp. 448–456, 2012.
- [16] R. L. Benza, A. J. Foreman, W. R. Prucka et al., "Predicting survival in pulmonary arterial hypertension using the REVEAL database," in *B27. From Alpha to Omega: Assessment And Outcomes In Pulmonary Hypertension*, p. A2651, USA, 2009.
- [17] R. L. Benza, D. P. Miller, M. Gomberg-Maitland et al., "Predicting survival in pulmonary arterial Hypertension," *Circulation*, vol. 122, no. 2, pp. 164–172, 2010.
- [18] V. Anand, S. S. Roy, S. L. Archer et al., "Trends and outcomes of pulmonary arterial hypertension-related hospitalizations in the United States," *JAMA Cardiology*, vol. 1, no. 9, pp. 1021–1029, 2016.
- [19] G. Kovacs, D. Dumitrescu, A. Barner et al., "Definition, clinical classification and initial diagnosis of pulmonary hypertension: updated recommendations from the Cologne Consensus Conference 2018," *International Journal of Cardiology*, vol. 272, pp. 11–19, 2018.
- [20] N. Galiè, M. Humbert, J. L. Vachiery et al., "2015 ESC/ERS guidelines for the diagnosis and treatment of pulmonary hypertension: the joint task force for the diagnosis and treatment of pulmonary hypertension of the European Society of Cardiology (ESC) and the European Respiratory Society (ERS): endorsed by: Association for European Paediatric and Congenital Cardiology (AEPC), International Society for Heart and Lung Transplantation (ISHLT)," *The European Respiratory Journal*, vol. 46, no. 4, pp. 903–975, 2015.
- [21] D. B. Badesch, R. L. Benza, R. J. Barst, D. B. Badesch, A. E. Frost, and M. G. MD, "An evaluation of long-term survival from time of diagnosis in pulmonary arterial hypertension from the reveal registry," *Chest: The Journal of Circulation, Respiration & Related Systems*, vol. 142, no. 2, 2012.
- [22] T. Thenappan, S. J. Shah, S. Rich, L. Tian, S. L. Archer, and M. Gomberg-Maitland, "Survival in pulmonary arterial hypertension: a reappraisal of the NIH risk stratification equation," *The European Respiratory Journal*, vol. 35, no. 5, pp. 1079–1087, 2010.
- [23] R. M. Tudor, "Pulmonary vascular remodeling in pulmonary hypertension," *Cell and Tissue Research*, vol. 367, no. 3, pp. 643–649, 2017.

- [24] A. U. Fayyaz, W. D. Edwards, J. J. Maleszewski et al., "Global pulmonary vascular remodeling in pulmonary hypertension associated with Heart failure and preserved or reduced ejection Fraction," *Circulation*, vol. 137, no. 17, pp. 1796–1810, 2018.
- [25] W. Zhang, T. Zhu, W. Wu et al., "LOX-1 mediated phenotypic switching of pulmonary arterial smooth muscle cells contributes to hypoxic pulmonary hypertension," *European Journal of Pharmacology*, vol. 818, pp. 84–95, 2018.
- [26] A. Cecchetti, S. Rocchiccioli, C. Boccardi, and L. Citti, "Vascular smooth-muscle-cell activation: proteomics point of view," *International Review of Cell and Molecular Biology*, vol. 288, pp. 43–99, 2011.
- [27] M. J. Zhang, Y. Zhou, L. Chen et al., "An overview of potential molecular mechanisms involved in VSMC phenotypic modulation," *Histochemistry and Cell Biology*, vol. 145, no. 2, pp. 119–130, 2016.
- [28] B. Wu, L. Zhang, Y. H. Zhu et al., "Mesoderm/mesenchyme homeobox gene 1 promotes vascular smooth muscle cell phenotypic modulation and vascular remodeling," *International Journal of Cardiology*, vol. 251, pp. 82–89, 2018.
- [29] E. M. Smolock, D. M. Trappanese, S. Chang, T. Wang, P. Titchenell, and R. S. Moreland, "siRNA-mediated knock-down of h-caldesmon in vascular smooth muscle," *American Journal of Physiology. Heart and Circulatory Physiology*, vol. 297, no. 5, pp. H1930–H1939, 2009.
- [30] K. E. Tumelty, B. D. Smith, M. A. Nugent, and M. D. Layne, "Aortic Carboxypeptidase-like Protein (ACLP) enhances lung myofibroblast differentiation through transforming growth factor  $\beta$  receptor-dependent and -independent pathways," *The Journal of Biological Chemistry*, vol. 289, no. 5, pp. 2526–2536, 2014.
- [31] A. Frisanti, M. Philippova, P. Erne, and T. J. Resink, "Smooth muscle cell-driven vascular diseases and molecular mechanisms of VSMC plasticity," *Cellular Signalling*, vol. 52, pp. 48–64, 2018.
- [32] L. Jin, X. Lin, L. Yang et al., "AK098656, a novel vascular smooth muscle cell-dominant long noncoding RNA, Promotes Hypertension," *Hypertension*, vol. 71, no. 2, pp. 262–272, 2018.
- [33] H. Xin, Z. Wang, S. Wu et al., "Calcified decellularized arterial scaffolds impact vascular smooth muscle cell transformation via downregulating  $\alpha$ -SMA expression and upregulating OPN expression," *Experimental and Therapeutic Medicine*, vol. 18, no. 1, pp. 705–710, 2019.
- [34] D. Lake, S. A. Corrêa, and J. Müller, "Negative feedback regulation of the ERK1/2 MAPK pathway," *Cellular and Molecular Life Sciences*, vol. 73, no. 23, pp. 4397–4413, 2016.
- [35] B. N. Davis-Dusenbery, M. C. Chan, K. E. Reno et al., "Downregulation of Kruppel-like Factor-4 (KLF4) by MicroRNA-143/145 Is Critical for Modulation of Vascular Smooth Muscle Cell Phenotype by Transforming Growth Factor- $\beta$  and Bone Morphogenetic Protein 4," *The Journal of Biological Chemistry*, vol. 286, no. 32, pp. 28097–28110, 2011.
- [36] S. Sahoo, D. N. Meijles, I. Al Ghoul et al., "MEF2C-MYOCD and leiomod1 suppression by miRNA-214 promotes smooth muscle cell phenotype switching in pulmonary arterial hypertension," *PLoS One*, vol. 11, no. 5, article e0153780, 2016.
- [37] S. B. Zhu, J. Zhu, Z. Z. Zhou, E. P. Xi, R. P. Wang, and Y. Zhang, "TGF- $\beta$ 1 induces human aortic vascular smooth muscle cell phenotype switch through PI3K/AKT/ID2 signaling," *American Journal of Translational Research*, vol. 7, no. 12, pp. 2764–2774, 2015.
- [38] T. Ersahin, N. Tuncbag, and R. Cetin-Atalay, "The PI3K/AKT/mTOR interactive pathway," *Molecular BioSystems*, vol. 11, no. 7, pp. 1946–1954, 2015.
- [39] G. Wang, L. Jacquet, E. Karamariti, and Q. Xu, "Origin and differentiation of vascular smooth muscle cells," *The Journal of Physiology*, vol. 593, no. 14, pp. 3013–3030, 2015.
- [40] R. Derynck and Y. E. Zhang, "Smad-dependent and Smad-independent pathways in TGF- $\beta$  family signalling," *Nature*, vol. 425, no. 6958, pp. 577–584, 2003.
- [41] J. Gong, Z. Chen, Y. Chen et al., "Long non-coding RNA CASC2 suppresses pulmonary artery smooth muscle cell proliferation and phenotypic switch in hypoxia-induced pulmonary hypertension," *Respiratory Research*, vol. 20, no. 1, p. 53, 2019.
- [42] S. A. Mandras, H. S. Mehta, and A. Vaidya, "Pulmonary hypertension: a brief guide for clinicians," *Mayo Clinic Proceedings*, vol. 95, no. 9, pp. 1978–1988, 2020.
- [43] X. Dong, D. Wu, Y. Zhang et al., "Cathelicidin modulates vascular smooth muscle cell phenotypic switching through ROS/IL-6 pathway," *Antioxidants*, vol. 9, no. 6, p. 491, 2020.
- [44] Y. Yeo, E. S. Yi, J. M. Kim et al., "FGF12 (fibroblast growth factor 12) inhibits vascular smooth muscle cell remodeling in pulmonary arterial hypertension," *Hypertension*, vol. 76, no. 6, pp. 1778–1786, 2020.
- [45] H. E. Morris, K. B. Neves, A. C. Montezano, M. R. MacLean, and R. M. Touyz, "Notch3 signalling and vascular remodeling in pulmonary arterial hypertension," *Clinical Science (London, England)*, vol. 133, no. 24, pp. 2481–2498, 2019.
- [46] Y. Lee, C. Ahn, J. Han et al., "The nuclear RNase III Drosha initiates microRNA processing," *Nature*, vol. 425, no. 6956, pp. 415–419, 2003.
- [47] E. Lund, S. Güttinger, A. Calado, J. E. Dahlberg, and U. Kutay, "Nuclear export of microRNA precursors," *Science*, vol. 303, no. 5654, pp. 95–98, 2004.
- [48] D. S. Schwarz, G. Hutvagner, T. Du, Z. Xu, N. Aronin, and P. D. Zamore, "Asymmetry in the assembly of the RNAi enzyme complex," *Cell*, vol. 115, no. 2, pp. 199–208, 2003.
- [49] O. Voinnet, "Origin, biogenesis, and activity of plant microRNAs," *Cell*, vol. 136, no. 4, pp. 669–687, 2009.
- [50] P. W. Hsu, H. D. Huang, S. D. Hsu et al., "miRNAmap: genomic maps of microRNA genes and their target genes in mammalian genomes," *Nucleic Acids Research*, vol. 34, no. 90001, pp. D135–D139, 2006.
- [51] A. M. Mohr and J. L. Mott, "Overview of microRNA biology," *Seminars in Liver Disease*, vol. 35, no. 1, pp. 003–011, 2015.
- [52] R. C. Lee, R. L. Feinbaum, and V. Ambros, "The *C. elegans* heterochronic gene *lin-4* encodes small RNAs with antisense complementarity to *lin-14*," *Cell*, vol. 75, no. 5, pp. 843–854, 1993.
- [53] B. J. Reinhart, F. J. Slack, M. Basson et al., "The 21-nucleotide *let-7* RNA regulates developmental timing in *Caenorhabditis elegans*," *Nature*, vol. 403, no. 6772, pp. 901–906, 2000.
- [54] B. P. Lewis, C. B. Burge, and D. P. Bartel, "Conserved seed pairing, often flanked by adenosines, indicates that thousands of human genes are microRNA targets," *Cell*, vol. 120, no. 1, pp. 15–20, 2005.
- [55] M. Esteller, "Non-coding RNAs in human disease," *Nature Reviews Genetics*, vol. 12, no. 12, pp. 861–874, 2011.

- [56] O. Boucherat, F. Potus, and S. Bonnet, "microRNA and pulmonary hypertension," *Advances in Experimental Medicine and Biology*, vol. 888, pp. 237–252, 2015.
- [57] A. M. Rothman, N. D. Arnold, J. A. Pickworth et al., "MicroRNA-140-5p and SMURF1 regulate pulmonary arterial hypertension," *The Journal of Clinical Investigation*, vol. 126, no. 7, pp. 2495–2508, 2016.
- [58] T. T. Zhu, W. F. Zhang, Y. L. Yin et al., "MicroRNA-140-5p targeting tumor necrosis factor- $\alpha$  prevents pulmonary arterial hypertension," *Journal of Cellular Physiology*, vol. 234, no. 6, pp. 9535–9550, 2019.
- [59] K. H. Chen, A. Dasgupta, J. Lin et al., "Epigenetic dysregulation of the dynamin-related protein 1 binding partners MiD49 and MiD51 increases mitotic mitochondrial fission and promotes pulmonary arterial Hypertension," *Circulation*, vol. 138, no. 3, pp. 287–304, 2018.
- [60] J. Chen, Y. Li, Y. Li et al., "Effect of miR-29b on the proliferation and apoptosis of pulmonary artery smooth muscle cells by targeting Mcl-1 and CCND2," *BioMed Research International*, vol. 2018, Article ID 6051407, 10 pages, 2018.
- [61] P. Caruso, B. J. Dunmore, K. Schlosser et al., "Identification of microRNA-124 as a major regulator of enhanced endothelial cell glycolysis in pulmonary arterial hypertension via PTBP1 (polypyrimidine tract binding protein) and pyruvate kinase M2," *Circulation*, vol. 136, no. 25, pp. 2451–2467, 2017.
- [62] B. Y. Kang, K. K. Park, J. M. Kleinhenz et al., "Peroxisome proliferator-activated receptor  $\gamma$  and microRNA 98 in hypoxia-induced endothelin-1 signaling," *American Journal of Respiratory Cell and Molecular Biology*, vol. 54, no. 1, pp. 136–146, 2016.
- [63] X. Chen, M. Talati, J. P. Fessel et al., "Estrogen metabolite 16 $\alpha$ -hydroxyestrone exacerbates bone morphogenetic protein receptor type II-associated pulmonary arterial hypertension through microRNA-29-mediated modulation of cellular metabolism," *Circulation*, vol. 133, no. 1, pp. 82–97, 2016.
- [64] B. N. Davis, A. C. Hilyard, P. H. Nguyen, G. Lagna, and A. Hata, "Induction of MicroRNA-221 by Platelet-derived Growth Factor Signaling Is Critical for Modulation of Vascular Smooth Muscle Phenotype," *The Journal of Biological Chemistry*, vol. 284, no. 6, pp. 3728–3738, 2009.
- [65] S. Kim and H. Kang, "miR-15b induced by platelet-derived growth factor signaling is required for vascular smooth muscle cell proliferation," *BMB Reports*, vol. 46, no. 11, pp. 550–554, 2013.
- [66] M. C. Chan, A. C. Hilyard, C. Wu et al., "Molecular basis for antagonism between PDGF and the TGF $\beta$  family of signaling pathways by control of miR-24 expression," *The EMBO Journal*, vol. 29, no. 3, pp. 559–573, 2010.
- [67] H. Kang, B. N. Davis-Dusenbery, P. H. Nguyen et al., "Bone Morphogenetic Protein 4 Promotes Vascular Smooth Muscle Contractility by Activating MicroRNA-21 (miR-21), which Down-regulates Expression of Family of Dedicator of Cytokinesis (DOCK) Proteins," *The Journal of Biological Chemistry*, vol. 287, no. 6, pp. 3976–3986, 2012.
- [68] S. Kim, A. Hata, and H. Kang, "Down-regulation of miR-96 by bone morphogenetic protein signaling is critical for vascular smooth muscle cell phenotype modulation," *Journal of Cellular Biochemistry*, vol. 115, no. 5, pp. 889–895, 2014.
- [69] Y. Zong, Y. Zhang, X. Sun, T. Xu, X. Cheng, and Y. Qin, "miR-221/222 promote tumor growth and suppress apoptosis by targeting lncRNA GAS5 in breast cancer," *Bioscience Reports*, vol. 39, no. 1, 2019.
- [70] Q. Y. Zhou, P. L. Peng, and Y. H. Xu, "MiR-221 affects proliferation and apoptosis of gastric cancer cells through targeting SOCS3," *European Review for Medical and Pharmacological Sciences*, vol. 23, no. 21, pp. 9427–9435, 2019.
- [71] D. A. Chistiakov, I. A. Sobenin, A. N. Orekhov, and Y. V. Bobryshev, "Human miR-221/222 in physiological and atherosclerotic vascular remodeling," *BioMed Research International*, vol. 2015, Article ID 354517, 18 pages, 2015.
- [72] J. S. Hinson, M. D. Medlin, J. M. Taylor, and C. P. Mack, "Regulation of myocardin factor protein stability by the LIM-only protein FHL2," *American Journal of Physiology. Heart and Circulatory Physiology*, vol. 295, no. 3, pp. H1067–H1075, 2008.
- [73] H. Xia, Y. Qi, S. S. Ng et al., "MicroRNA-15b regulates cell cycle progression by targeting cyclins in glioma cells," *Biochemical and Biophysical Research Communications*, vol. 380, no. 2, pp. 205–210, 2009.
- [74] F. An, B. Gong, H. Wang et al., "miR-15b and miR-16 regulate TNF mediated hepatocyte apoptosis via BCL2 in acute liver failure," *Apoptosis*, vol. 17, no. 7, pp. 702–716, 2012.
- [75] X. Zheng, M. Chopp, Y. Lu, B. Buller, and F. Jiang, "MiR-15b and miR-152 reduce glioma cell invasion and angiogenesis via NRP-2 and MMP-3," *Cancer Letters*, vol. 329, no. 2, pp. 146–154, 2013.
- [76] L. S. Chan, P. Y. Yue, Y. Y. Wong, and R. N. Wong, "MicroRNA-15b contributes to ginsenoside-Rg<sub>1</sub>-induced angiogenesis through increased expression of VEGFR-2," *Biochemical Pharmacology*, vol. 86, no. 3, pp. 392–400, 2013.
- [77] Z. Liu, D. Yang, P. Xie et al., "MiR-106b and MiR-15b modulate apoptosis and angiogenesis in myocardial infarction," *Cellular Physiology and Biochemistry*, vol. 29, no. 5–6, pp. 851–862, 2012.
- [78] B. N. Davis, A. C. Hilyard, G. Lagna, and A. Hata, "Smad proteins control DROSHA-mediated microRNA maturation," *Nature*, vol. 454, no. 7200, pp. 56–61, 2008.
- [79] B. Wang, X. Liu, and X. Meng, "miR-96-5p enhances cell proliferation and invasion via targeted regulation of ZDHHC5 in gastric cancer," *Bioscience Reports*, vol. 40, no. 4, 2020.
- [80] B. Liu, J. Zhang, and D. Yang, "miR-96-5p promotes the proliferation and migration of ovarian cancer cells by suppressing Caveolae1," *Journal of Ovarian Research*, vol. 12, no. 1, p. 57, 2019.
- [81] R. F. Castellan, M. Vitiello, M. Vidmar et al., "miR-96 and miR-183 differentially regulate neonatal and adult postinfarct neovascularization," *JCI Insight*, vol. 5, no. 14, article e134888, 2020.
- [82] M. C. Chan, P. H. Nguyen, B. N. Davis et al., "A novel regulatory mechanism of the bone morphogenetic protein (BMP) signaling pathway involving the carboxyl-terminal tail domain of BMP type II receptor," *Molecular and Cellular Biology*, vol. 27, no. 16, pp. 5776–5789, 2007.
- [83] K. Y. Kong, K. S. Owens, J. H. Rogers et al., "MIR-23A microRNA cluster inhibits B-cell development," *Experimental Hematology*, vol. 38, no. 8, pp. 629–640.e1, 2010.
- [84] L. Qian, L. W. Van Laake, Y. Huang, S. Liu, M. F. Wendland, and D. Srivastava, "miR-24 inhibits apoptosis and represses Bim in mouse cardiomyocytes," *The Journal of Experimental Medicine*, vol. 208, no. 3, pp. 549–560, 2011.
- [85] J. Wang, W. Huang, R. Xu et al., "MicroRNA-24 regulates cardiac fibrosis after myocardial infarction," *Journal of Cellular and Molecular Medicine*, vol. 16, no. 9, pp. 2150–2160, 2012.



- [86] P. Caruso, M. R. MacLean, R. Khanin et al., "Dynamic changes in lung microRNA profiles during the development of pulmonary hypertension due to chronic hypoxia and monocrotaline," *Arteriosclerosis, Thrombosis, and Vascular Biology*, vol. 30, no. 4, pp. 716–723, 2010.
- [87] B. N. Davis, A. C. Hilyard, P. H. Nguyen, G. Lagna, and A. Hata, "Smad proteins bind a conserved RNA sequence to promote microRNA maturation by Drosha," *Molecular Cell*, vol. 39, pp. 373–384, 2010.
- [88] N. Choe, J. S. Kwon, J. R. Kim et al., "The microRNA miR-132 targets *Lrrfip1* to block vascular smooth muscle cell proliferation and neointimal hyperplasia," *Atherosclerosis*, vol. 229, no. 2, pp. 348–355, 2013.
- [89] A. Ucar, S. K. Gupta, J. Fiedler et al., "The miRNA-212/132 family regulates both cardiac hypertrophy and cardiomyocyte autophagy," *Nature Communications*, vol. 3, no. 1, p. 1078, 2012.
- [90] T. V. Eskildsen, P. L. Jeppesen, M. Schneider et al., "Angiotensin II regulates microRNA-132/212 in hypertensive rats and humans," *International Journal of Molecular Sciences*, vol. 14, no. 6, pp. 11190–11207, 2013.
- [91] Z. H. Zeng, W. H. Wu, Q. Peng, Y.-H. Sun, and J.-X. Liu, "MicroRNA-132 mediates proliferation and migration of pulmonary smooth muscle cells via targeting PTEN," *Molecular Medicine Reports*, vol. 19, no. 5, pp. 3823–3830, 2019.
- [92] L. Yan, H. Gao, C. Li, X. Han, and X. Qi, "Effect of miR-23a on anoxia-induced phenotypic transformation of smooth muscle cells of rat pulmonary arteries and regulatory mechanism," *Oncology Letters*, vol. 13, no. 1, pp. 89–98, 2017.
- [93] F. Shan, J. Li, and Q. Y. Huang, "HIF-1 alpha-induced up-regulation of miR-9 contributes to phenotypic modulation in pulmonary artery smooth muscle cells during hypoxia," *Journal of Cellular Physiology*, vol. 229, no. 10, pp. 1511–1520, 2014.
- [94] Y. Zeng, Y. Pan, H. Liu et al., "MiR-20a regulates the PRKG1 gene by targeting its coding region in pulmonary arterial smooth muscle cells," *FEBS Letters*, vol. 588, no. 24, pp. 4677–4685, 2014.
- [95] C. Zhang, C. Ma, L. Zhang et al., "MiR-449a-5p mediates mitochondrial dysfunction and phenotypic transition by targeting Myc in pulmonary arterial smooth muscle cells," *Journal of Molecular Medicine (Berlin, Germany)*, vol. 97, no. 3, pp. 409–422, 2019.
- [96] S. Jalali, G. K. Ramanathan, P. T. Parthasarathy et al., "Mir-206 regulates pulmonary artery smooth muscle cell proliferation and differentiation," *PLoS One*, vol. 7, no. 10, article e46808, 2012.
- [97] K. Kang, X. Peng, X. Zhang et al., "MicroRNA-124 Suppresses the Transactivation of Nuclear Factor of Activated T Cells by Targeting Multiple Genes and Inhibits the Proliferation of Pulmonary Artery Smooth Muscle Cells," *The Journal of Biological Chemistry*, vol. 288, no. 35, pp. 25414–25427, 2013.
- [98] Y. Xing, X. Zheng, G. Li et al., "MicroRNA-30c contributes to the development of hypoxia pulmonary hypertension by inhibiting platelet-derived growth factor receptor  $\beta$  expression," *The International Journal of Biochemistry & Cell Biology*, vol. 64, pp. 155–166, 2015.
- [99] Y. Zhang and J. Xu, "MiR-140-5p regulates hypoxia-mediated human pulmonary artery smooth muscle cell proliferation, apoptosis and differentiation by targeting Dnmt1 and promoting SOD2 expression," *Biochemical and Biophysical Research Communications*, vol. 473, no. 1, pp. 342–348, 2016.
- [100] G. L. Semenza, "HIF-1 and mechanisms of hypoxia sensing," *Current Opinion in Cell Biology*, vol. 13, no. 2, pp. 167–171, 2001.
- [101] J. Wang, L. Weigand, W. Lu, J. T. Sylvester, G. L. Semenza, and L. A. Shimoda, "Hypoxia inducible factor 1 mediates hypoxia-induced TRPC expression and elevated intracellular Ca<sup>2+</sup> in pulmonary arterial smooth muscle cells," *Circulation Research*, vol. 98, no. 12, pp. 1528–1537, 2006.
- [102] Z. Lin, I. Murtaza, K. Wang, J. Jiao, J. Gao, and P. F. Li, "miR-23a functions downstream of NFATc3 to regulate cardiac hypertrophy," *Proceedings of the National Academy of Sciences of the United States of America*, vol. 106, no. 29, pp. 12103–12108, 2009.
- [103] S. Wada, Y. Kato, M. Okutsu et al., "Stress responsive miR-23a attenuates skeletal muscle atrophy by targeting MAFbx/atrogin-1," *Nature Precedings*, vol. 3, 2008.
- [104] M. Shibata, H. Nakao, H. Kiyonari, T. Abe, and S. Aizawa, "MicroRNA-9 regulates neurogenesis in mouse telencephalon by targeting multiple transcription factors," *The Journal of Neuroscience*, vol. 31, no. 9, pp. 3407–3422, 2011.
- [105] P. Rotkrua, Y. Akiyama, Y. Hashimoto, T. Otsubo, and Y. Yuasa, "MiR-9 downregulates CDX2 expression in gastric cancer cells," *International Journal of Cancer*, vol. 129, no. 11, pp. 2611–2620, 2011.
- [106] J. Lu, H. Luo, X. Liu et al., "miR-9 targets CXCR4 and functions as a potential tumor suppressor in nasopharyngeal carcinoma," *Carcinogenesis*, vol. 35, no. 3, pp. 554–563, 2014.
- [107] S. D. Selcuklu, M. T. Donoghue, K. Rehmet et al., "MicroRNA-9 Inhibition of Cell Proliferation and Identification of Novel miR-9 Targets by Transcriptome Profiling in Breast Cancer Cells," *The Journal of Biological Chemistry*, vol. 287, no. 35, pp. 29516–29528, 2012.
- [108] L. He, L. Zhang, M. Wang, and W. Wang, "miR-9 functions as a tumor inhibitor of cell proliferation in epithelial ovarian cancer through targeting the SDF-1/CXCR4 pathway," *Experimental and Therapeutic Medicine*, vol. 13, no. 4, pp. 1203–1208, 2017.
- [109] J. Xu, G. Hu, M. Lu et al., "MiR-9 reduces human acyl-coenzyme A: cholesterol acyltransferase-1 to decrease THP-1 macrophage-derived foam cell formation," *Acta Biochimica et Biophysica Sinica*, vol. 45, no. 11, pp. 953–962, 2013.
- [110] Q. Duan, C. Chen, L. Yang et al., "MicroRNA regulation of unfolded protein response transcription factor XBP1 in the progression of cardiac hypertrophy and heart failure in vivo," *Journal of Translational Medicine*, vol. 13, no. 1, p. ???, 2015.
- [111] Q. Lin, J. Schwarz, C. Bucana, and E. N. Olson, "Control of mouse cardiac morphogenesis and myogenesis by transcription factor MEF2C," *Science*, vol. 276, no. 5317, pp. 1404–1407, 1997.
- [112] V. Nanda and J. M. Miano, "Leiomodin 1, a New Serum Response Factor-dependent Target Gene Expressed Preferentially in Differentiated Smooth Muscle Cells," *The Journal of Biological Chemistry*, vol. 287, no. 4, pp. 2459–2467, 2012.
- [113] Z. Z. Si, G. S. Chen, N. Zhou, T. Li, T. Li, and Z. Q. Zhang, "Restoration of miR-20a expression suppresses cell proliferation, migration, and invasion in HepG2 cells," *Oncotargets and Therapy*, vol. 9, pp. 3067–3076, 2016.

- [114] C. V. Dang, "MYC on the Path to Cancer," *Cell*, vol. 149, no. 1, pp. 22–35, 2012.
- [115] Z. Zhang, Y. Chen, B. Li et al., "Identification of a novel miR-206-Notch3 pathway regulating mouse myoblasts proliferation," *Gene*, vol. 695, pp. 57–64, 2019.
- [116] X. Li, X. Zhang, R. Leathers et al., "Notch3 signaling promotes the development of pulmonary arterial hypertension," *Nature Medicine*, vol. 15, no. 11, pp. 1289–1297, 2009.
- [117] S. Ghafouri-Fard, H. Shoorei, Z. Bahroudi, A. Abak, J. Majidpoor, and M. Taheri, "An update on the role of miR-124 in the pathogenesis of human disorders," *Biomedicine & Pharmacotherapy*, vol. 135, article 111198, 2021.
- [118] S. Bonnet, G. Rochefort, G. Sutendra et al., "The nuclear factor of activated T cells in pulmonary arterial hypertension can be therapeutically targeted," *Proceedings. National Academy of Sciences. United States of America*, vol. 104, no. 27, pp. 11418–11423, 2007.
- [119] R. Bierer, C. H. Nitta, J. Friedman et al., "NFATc3 is required for chronic hypoxia-induced pulmonary hypertension in adult and neonatal mice," *American Journal of Physiology. Lung Cellular and Molecular Physiology*, vol. 301, no. 6, pp. L872–L880, 2011.
- [120] R. L. He, Z. J. Wu, X. R. Liu, L. X. Gui, R. X. Wang, and M. J. Lin, "Calcineurin/NFAT signaling modulates pulmonary artery smooth muscle cell proliferation, migration and apoptosis in monocrotaline-induced pulmonary arterial hypertension rats," *Cellular Physiology and Biochemistry*, vol. 49, no. 1, pp. 172–189, 2018.
- [121] S. A. Antoniu, "Targeting PDGF pathway in pulmonary arterial hypertension," *Expert Opinion on Therapeutic Targets*, vol. 16, no. 11, pp. 1055–1063, 2012.
- [122] V. Balasubramaniam, T. D. Le Cras, D. D. Ivy, T. R. Grover, J. P. Kinsella, and S. H. Abman, "Role of platelet-derived growth factor in vascular remodeling during pulmonary hypertension in the ovine fetus," *American Journal of Physiology. Lung Cellular and Molecular Physiology*, vol. 284, no. 5, pp. L826–L833, 2003.
- [123] M. Humbert, G. Monti, M. Fartoukh et al., "Platelet-derived growth factor expression in primary pulmonary hypertension: comparison of HIV seropositive and HIV seronegative patients," *The European Respiratory Journal*, vol. 11, no. 3, pp. 554–559, 1998.
- [124] F. Perros, D. Montani, P. Dorfmüller et al., "Platelet-derived growth factor expression and function in idiopathic pulmonary arterial hypertension," *American Journal of Respiratory and Critical Care Medicine*, vol. 178, no. 1, pp. 81–88, 2008.
- [125] X. Zhang, S. Dong, Q. Jia et al., "The microRNA in ventricular remodeling: the miR-30 family," *Bioscience Reports*, vol. 39, no. 8, article BSR20190788, 2019.
- [126] A. Shahabi, B. Naghili, K. Ansarin, V. Montazeri, and N. Zarghami, "miR-140 and miR-196a as potential biomarkers in breast cancer patients," *Asian Pacific Journal of Cancer Prevention*, vol. 21, no. 7, pp. 1913–1918, 2020.
- [127] C. Hu, Y. Zou, and L. L. Jing, "miR-140-3p inhibits progression of non-small cell lung cancer by targeting Janus kinase 1," *Journal of Biosciences*, vol. 45, no. 1, p. 48, 2020.
- [128] T. Ren, P. Wei, Q. Song, Z. Ye, Y. Wang, and L. Huang, "MiR-140-3p ameliorates the progression of osteoarthritis < i>via</i> targeting CXCR4," *Biological & Pharmaceutical Bulletin*, vol. 43, no. 5, pp. 810–816, 2020.
- [129] A. M. Rothman, D. J. Rowlands, and A. Lawrie, "miRNA-140-5p: new avenue for pulmonary arterial hypertension drug development?," *Epigenomics*, vol. 8, no. 10, pp. 1311–1313, 2016.
- [130] M. Dews, A. Homayouni, D. Yu et al., "Augmentation of tumor angiogenesis by a Myc-activated microRNA cluster," *Nature Genetics*, vol. 38, no. 9, pp. 1060–1065, 2006.
- [131] V. Olive, I. Jiang, and L. He, "mir-17-92, a cluster of miRNAs in the midst of the cancer network," *The International Journal of Biochemistry & Cell Biology*, vol. 42, no. 8, pp. 1348–1354, 2010.
- [132] T. Chen, J. B. Huang, J. Dai, Q. Zhou, J. U. Raj, and G. Zhou, "PAI-1 is a novel component of the miR-17~92 signaling that regulates pulmonary artery smooth muscle cell phenotypes," *American Journal of Physiology. Lung Cellular and Molecular Physiology*, vol. 315, no. 2, pp. L149–L161, 2018.
- [133] T. Chen, G. Zhou, Q. Zhou et al., "Loss of microRNA-17~92 in smooth muscle cells attenuates experimental pulmonary hypertension via induction of PDZ and LIM domain 5," *American Journal of Respiratory and Critical Care Medicine*, vol. 191, no. 6, pp. 678–692, 2015.
- [134] T. Chen, Q. Zhou, H. Tang et al., "miR-17/20 controls prolyl hydroxylase 2 (PHD2)/hypoxia-inducible factor 1 (HIF1) to regulate pulmonary artery smooth muscle cell proliferation," *Journal of the American Heart Association*, vol. 5, no. 12, article e004510, 2016.
- [135] W. F. Zhang, Y. W. Xiong, T. T. Zhu, A. Z. Xiong, H. H. Bao, and X. S. Cheng, "MicroRNA let-7g inhibited hypoxia-induced proliferation of PSMCs via G<sub>0</sub>/G<sub>1</sub> cell cycle arrest by targeting c-myc," *Life Sciences*, vol. 170, pp. 9–15, 2017.
- [136] W. F. Zhang, T. T. Zhu, Y. W. Xiong et al., "Negative feedback regulation between microRNA let-7g and LOX-1 mediated hypoxia-induced PSMCs proliferation," *Biochemical and Biophysical Research Communications*, vol. 488, no. 4, pp. 655–663, 2017.
- [137] V. N. Parikh, R. C. Jin, S. Rabello et al., "MicroRNA-21 integrates pathogenic signaling to control pulmonary Hypertension," *Circulation*, vol. 125, no. 12, pp. 1520–1532, 2012.
- [138] C. Chakraborty, A. R. Sharma, G. Sharma, C. G. P. Doss, and S. S. Lee, "Therapeutic miRNA and siRNA: moving from bench to clinic as next generation medicine," *Molecular Therapy - Nucleic Acids*, vol. 8, pp. 132–143, 2017.
- [139] J. Meloche, M. Le Guen, F. Potus et al., "miR-223 reverses experimental pulmonary arterial hypertension," *American Journal of Physiology. Cell Physiology*, vol. 309, no. 6, pp. C363–C372, 2015.
- [140] C. J. Rhodes, J. Wharton, R. A. Boon et al., "Reduced microRNA-150 is associated with poor survival in pulmonary arterial hypertension," *American Journal of Respiratory and Critical Care Medicine*, vol. 187, no. 3, pp. 294–302, 2013.



## Research Article

# MicroRNA-137 Inhibited Hypoxia-Induced Proliferation of Pulmonary Artery Smooth Muscle Cells by Targeting Calpain-2

Xiao-Yue Ge,<sup>1</sup> Tian-Tian Zhu,<sup>2</sup> Mao-Zhong Yao,<sup>1</sup> Hong Liu,<sup>1</sup> Qian Wu,<sup>1</sup> Jie Qiao,<sup>1</sup> Wei-Fang Zhang <sup>3</sup> and Chang-Ping Hu <sup>1,4</sup>

<sup>1</sup>Department of Pharmacology, Xiangya School of Pharmaceutical Sciences, Central South University, Changsha, 410078 Hunan, China

<sup>2</sup>Teaching and Research Office of Clinical Pharmacology, College of Pharmacy, Xinxiang Medical University, Xinxiang, 453003 Henan, China

<sup>3</sup>Department of Pharmacy, The Second Affiliated Hospital of Nanchang University, Nanchang, 330006 Jiangxi, China

<sup>4</sup>Human Provincial Key Laboratory of Cardiovascular Research, Central South University, Changsha, 410078 Hunan, China

Correspondence should be addressed to Wei-Fang Zhang; [z\\_weifang@163.com](mailto:z_weifang@163.com) and Chang-Ping Hu; [huchangping@csu.edu.cn](mailto:huchangping@csu.edu.cn)

Received 1 July 2021; Accepted 16 August 2021; Published 1 September 2021

Academic Editor: Zhousheng Yang

Copyright © 2021 Xiao-Yue Ge et al. This is an open access article distributed under the Creative Commons Attribution License, which permits unrestricted use, distribution, and reproduction in any medium, provided the original work is properly cited.

The proliferation of pulmonary artery smooth muscle cells (PASMCs) is an important cause of pulmonary vascular remodeling in pulmonary hypertension (PH). It has been reported that miR-137 inhibits the proliferation of tumor cells. However, whether miR-137 is involved in PH remains unclear. In this study, male Sprague-Dawley rats were subjected to 10% O<sub>2</sub> for 3 weeks to establish PH, and rat primary PASMCs were treated with hypoxia (3% O<sub>2</sub>) for 48 h to induce cell proliferation. The effect of miR-137 on PASMC proliferation and calpain-2 expression was assessed by transfecting miR-137 mimic and inhibitor. The effect of calpain-2 on PASMC proliferation was assessed by transfecting calpain-2 siRNA. The present study found for the first time that miR-137 was downregulated in pulmonary arteries of hypoxic PH rats and in hypoxia-treated PASMCs. miR-137 mimic inhibited hypoxia-induced PASMC proliferation and upregulation of calpain-2 expression in PASMCs. Furthermore, miR-137 inhibitor induced the proliferation of PASMCs under normoxia, and knockdown of calpain-2 mRNA by siRNA significantly inhibited hypoxia-induced proliferation of PASMCs. Our study demonstrated that hypoxia-induced downregulation of miR-137 expression promoted the proliferation of PASMCs by targeting calpain-2, thereby potentially resulting in pulmonary vascular remodeling in hypoxic PH.

## 1. Introduction

Pulmonary hypertension (PH) is a rare vascular disorder, now defined clinically as a mean pulmonary artery pressure (mPAP) over 25 mmHg at rest or over 30 mmHg during activity. Pulmonary vascular remodeling plays an important role in PH pathology, which is mainly characterized by endothelial cell injury, smooth muscle cell proliferation, fibroblast muscularization, extracellular matrix increase, in situ thrombosis, varying degree inflammation, and plexiform arterial changes [1, 2]. In these pathological changes, the proliferation of pulmonary arterial smooth muscle cells

(PASMCs) is the most important cause of pulmonary vascular remodeling in PH. Therefore, inhibition of PASMC proliferation is expected to be a crucial pathway for PH treatment.

Calpain is a Ca<sup>2+</sup>-dependent cysteine protease that has been found to contain at least 15 subtypes, calpain-1 ( $\mu$ -calpain) and calpain-2 (m-calpain), which are the two best-characterized members of the calpain family and are ubiquitously expressed in mammals [3]. Calpain-1 and calpain-2 constitute a distinct larger catalytic subunit, and calpain-4 as a common smaller subunit is responsible for maintaining calpain activity [4]. Recent studies have linked calpain with a variety of diseases,

such as Alzheimer's and Parkinson's diseases, cancer, diabetes, atherosclerosis, and PH [5]. In hypoxia and monocrotaline-induced PH of mice and rats, the expression of calpain-1/2/4 in the lung tissues and pulmonary arteries was significantly increased [6–8]. Research focusing on the role of calpain-2 in hypoxia-induced PH becomes a meaningful work.

It has been reported that a variety of miRNAs participate in the pathogenesis of PH. For example, miR-223 [9] and miR-let-7g [10] have been found to regulate the proliferation of PSMCs participating in pulmonary vascular remodeling of PH. To fully reveal the role of miRNAs in hypoxic PH, we did the pilot microarray assay in pulmonary arteries of hypoxic PH rats and found that the expression of miR-137 was significantly downregulated. It has been reported that miR-137 inhibits the proliferation and migration of a variety of tumor cells [11, 12]. Over 1000 genes have been predicted to be targets of miR-137 by using a bioinformatic approach, and highlighted target genes are involved in a large number of pathways including neural development, cell cycle, differentiation, and proliferation [13]. However, whether miR-137 is involved in PH remains unclear. Bioinformatic analysis suggests that the 3'-UTR of calpain-2 contains a potential binding element for miR-137 with a 7-nt match to the miR-137 seed region, and miR-137 has been found to directly target calpain-2 in motoneurons [14]. We therefore hypothesize that miR-137 contributes to hypoxic PH by targeting calpain-2 and designed this study to explore the regulatory role of miR-137 in hypoxia-induced PSMC proliferation and pulmonary arterial remodeling in rat hypoxic PH, and the regulating effect of miR-137 on calpain-2 expression was also certificated.

## 2. Materials and Methods

**2.1. Animal Experiments.** About 180-220 g, male Sprague-Dawley (SD) rats were purchased from the Laboratory Animal Center of Xiangya School of Medicine, Central South University, Changsha, China (SCXK (XIANG) 2019-0014). All protocols of animal experiments (No. CSU2017009) were approved by the Central South University Veterinary Medicine Animal Care and Use Committee. Regarding the methodology, we followed the PH preclinical guidelines as previously described [15].

SD rats were randomly divided into hypoxia group and control group. Rats were exposed to continuity hypoxia (10% O<sub>2</sub>) for up to 21 days in the hypoxia group while maintained in a normal oxygen condition (21% O<sub>2</sub>) in the control group. At the 21 days after subjected to hypoxia, the rats were weighed and anesthetized by intraperitoneal injection of 2% sodium pentobarbital (60 mg/kg). A Vevo 2100 (VisualSonics, Canada) ultrasound system equipped with 21 MHz probe was used for echocardiographic assessment of pulmonary arterial acceleration/ejection time ratio (PAAT/PAET). Right-sided heart catheterization was conducted to detect right ventricular systolic pressure (RVSP) and mPAP. The right ventricle (RV) was separated from left ventricle and septum (LV+S) and weighed. The ratio of RV to (LV+S) was calculated to assess the extent of right ventricle hypertrophy. The pulmonary arterial samples were

collected for mRNA and protein expression analysis. The right lower lung was fixed in 4% paraformaldehyde for hematoxylin-eosin (HE) staining and in situ hybridization analysis of miR-137.

**2.2. HE Staining.** For HE staining, the fixed lungs were embedded in paraffin and then cut into approximately 5  $\mu$ m thick sections by microtome. HE staining of right lung was conducted in accordance to the same method used in our previous study [6].

**2.3. In Situ Hybridization.** In situ hybridization kit (Boster, Wuhan, China) was used to detect the expression of miR-137 in lung tissues according to the manufacturer's instructions. In brief, 5  $\mu$ m sections were used for sodium citrate antigen retrieval and then incubated with blocking buffer overnight with miR-137 detection probe which was labeled with 3' and 5' digoxigenin. After washed with phosphate-buffered saline (PBS) and SSC buffer, immunodetection was performed with a biotinylated anti-DIG antibody at 37°C for 60 min and the avidin-biotin-peroxidase complex (ABC kit, Vector Laboratories, Burlingame, CA) at 37°C for 20 min. After washed with PBS, the slides were detected by 3,3-diamino benzidine (DAB) staining.

**2.4. Preparation of Primary Rat PSMCs.** As our previous study described, primary rat PSMCs were extracted from the pulmonary arteries using tissue block anchorage method [10]. Dulbecco's modified Eagle's medium (DMEM) supplemented with 20% (v/v) fetal bovine serum was used to culture primary rat PSMCs at 37°C in a humidified atmosphere of 5% CO<sub>2</sub>. Smooth muscle  $\alpha$ -actin ( $\alpha$ -SMA) immunohistochemistry and immunofluorescence using anti-rat  $\alpha$ -SMA antibody (1:50, ab7817, Abcam) were used to identify PSMCs. The three to five passages of PSMCs were used for all experiments.

**2.5. Cell Transfection.** PSMCs reached 60% to 70% of confluence were starved with low serum sputum (2% FBS) for 24 h. To validate the effects of miR-137 and calpain-2 on hypoxia-induced PSMC proliferation and gene expression, the mimic and inhibitor of miR-137 and calpain-2 siRNA (Ribobio Co. Ltd., Guangzhou, China) were transiently transfected by ribo FECT™ CP transfection kit (Ribobio Co. Ltd., Guangzhou, China) according to the manufacturer's instructions. Then, the cells were maintained in hypoxia (3% O<sub>2</sub>) or normoxia chamber for up to 48 h according to grouping. Quantitative real-time polymerase chain reaction was used to detect the transfection efficiency of miR-137 mimic. Real-time PCR and Western blot were used to test the expression of calpain-2 mRNA and protein to detect the transfection efficiency of calpain-2 siRNA. The target sequences of calpain-2 siRNAs were CCAATT TGTTCAAGATCAT.

**2.6. Assay of Cell Proliferation.** For the MTS assay as described previously [10], PSMCs were seeded in 96-well culture plates (6  $\times$  10<sup>3</sup> cells/well) and then starved with low serum sputum (2% FBS) for 24 h. After treatment, the cells were washed with PBS. According to the manufacturer's

instructions, each well was added 10  $\mu$ L of MTS solution and incubated at 37°C for 2.5 h after the treatment. Colorimetric analysis was determined by an ELISA plate reader (DTX880; Beckman, Miami, FL) at 490 nm.

For EDU proliferation assay,  $5 \times 10^3$  cells/well were seeded into 96-well culture plates. According to the manufacturer's instructions, each well was added 50  $\mu$ mol/L of 5-ethynyl-2'-deoxyuridine (EDU, Ribobio, China) and incubated at 37°C for 4 h. The cells were fixed by using 4% formaldehyde for 15 min and then treated with 50  $\mu$ L 2 mg/mL glycine for 5 min at 25°C. Then, the cells were treated with 100  $\mu$ L 0.5% TritonX-100. After washing with PBS for 3 times, 100  $\mu$ L of 1 $\times$ Apollo<sup>®</sup> reaction cocktail was added in each well and reacted for 30 min. Then, the cells were stained with 100  $\mu$ L of Hoechst 33342 (5  $\mu$ g/mL) for 30 min and visualized under a fluorescent microscope.

**2.7. RNA Isolation and Real-Time PCR Analysis.** The mRNA levels of miR-137 and calpain-2 were quantified by real-time PCR. In brief, total RNA of pulmonary arteries and PSMCs was extracted by TRIzol reagent (Invitrogen, Carlsbad, CA) and the concentration and quality of RNA were confirmed by spectrophotometric method. Prime Script reverse transcription reagent Kit (DRR037S; TaKaRa) was used for RNA reverse transcription reaction. ABI Prism 7300 real-time PCR system (Applied Biosystems) with SYBR Premix Ex Taq (DRR041A; TaKaRa) was used for quantitative analysis of mRNA expression. Primers for calpain-2: (F) CCAG AAGTTGGTGAAAGGACA and (R) CTGCCGTTCTG TTAGATTTGC and  $\beta$ -actin: (F) TGTCACCAACTGGG ACGATA and (R) ACCCTCATAGATGGGCACAG. For the detection of miR-137, Bulge-Loop miRNA Primers (Ribobio) were replaced oligo and random primers during reverse transcription reaction. Data analysis was performed by comparative Ct method using the ABI software.  $\beta$ -Actin and U6 were used to normalize the expression level of mRNAs and miRNAs, respectively.

**2.8. Reverse Transcriptase Polymerase Chain Reaction (RT-PCR).** Preparation of cDNA was carried out from 2  $\mu$ g of total RNA using the TranScript One-Step gDNA Removal and cDNA Synthesis SuperMix for RT-PCR (TransGen Biotech, China) according to the manufacturer's instructions. Semiquantitative RT-PCR cDNA was amplified in a 25  $\mu$ L reaction volume containing 2.5 mM dNTPs, 10  $\mu$ M specific-primers, 10 $\times$ EasyTag buffer, and 1 U of EasyTag DNA Polymerase (TransGen Biotech, China). After initial denaturation at 94°C for 5 min, PCR was carried out for 35 cycles with denaturation for 30 s at 94°C, annealing for 30 s at 56°C for PCNA and beta-actin, and extension for 1 min at 72°C followed by a final extension of 10 min at 72°C. Primers for PCNA: (F) TACAAGCAACTTCCCATTCCA and (R) TCAGCAAACACAACCTCCTCCT and  $\beta$ -actin: (F) CCCA TCTATGAGGGTTACGC and (R) TTTAATGTACGCA CGATTTTC. The PCR products were visualized by electrophoresis with an ethidium bromide-stained 1.5% agarose gel. The densitometric analysis was conducted with UVP Bioimaging System (BioDoc, USA).

**2.9. Western Blot Analysis.** Proteins were extracted from cultured PSMCs and pulmonary arteries with RIPA buffer (contain 1% PMSF) for 30 min on ice and quantified by BCA kit (P0010, Beyotime, China). About 20~60  $\mu$ g protein of each sample was separated by 10% SDS-polyacrylamide gels and transferred onto PVDF membranes. Membranes were blocked with 5% skim milk for 1 h and then incubated with primary antibodies for calpain-2 (ab39165, Abcam, 1:1000), PCNA (A0264, ABclonal, 1:1000), and  $\beta$ -actin (AF0003, Beyotime, 1:1000) and subsequently incubated with horseradish peroxidase- (HRP-) coupled goat anti-rabbit (A0208, Beyotime, 1:1000) and HRP-coupled goat anti-mouse (A0216, Beyotime, 1:1000). The chemiluminescence signals were visualized with the Luminata<sup>TM</sup> Crescendo substrate (WBLUR0100, Millipore). The densitometric analysis was conducted with ChemiDoc XRS+ system (Bio-Rad Co. Ltd., USA).

**2.10. Luciferase Assay.** The 3'-UTR of calpain-2 mRNA with putative/mutant miR-137 binding site was cloned into the firefly luciferase reporter construct pmiR-RB-Report<sup>TM</sup> Vector (Ribobio, Guangzhou, China). Firefly luciferase (Luc) acts as a control, and renilla luciferase (Rluc) acts as a reporter. For the reporter assay, PSMCs grown in 96-well plates were cotransfected with calpain-2-3'-UTR-Luc (2  $\mu$ g) and miR-137 mimic (50 nM) by ribo FECT<sup>TM</sup> CP transfection kit. Dual-Luciferase<sup>®</sup> Reporter Assay System (E1910, Promega) was used to detect the renilla and firefly luciferase activities after incubation for 48 h.

**2.11. Statistics.** Data were shown as mean  $\pm$  S.E.M. (standard errors). Statistical analysis was performed by the permutation test when the sample size is only 3 and by Student's *t*-test for two groups or by one-way ANOVA followed by Student-Newman-Keuls test for multiple groups when the sample size is greater than 3. A value of *p* less than 0.05 was considered to be statistically significant. All statistical analyses were performed by the SPSS18.0 software, and GraphPad Prism 7 was used for drawing figures.

### 3. Results

**3.1. miR-137 Was Downregulated in Remodeled Pulmonary Arteries and Hypoxia-Treated PSMCs in Hypoxic PH.** To induce hypoxic PH, the rats were exposed to hypoxia (10% O<sub>2</sub>) for 21 days. As keeping with our previous study [10], PAAT/PAET (Figure 1(a)) was markedly decreased in the hypoxia group; meanwhile, mPAP (Figure 1(b)), RVSP (Figure 1(c)), and the right heart remodeling index RV/(LV+S) (Figure 1(d)) were significantly increased in the hypoxia group. The body weight of hypoxic PH rats was decreased compared with the control group (Figure 1(e)). HE staining demonstrated that hypoxia induced obvious thickening of the pulmonary vascular wall and the stenosis of the lumen (Figure 1(f)).

Accordance to our pilot study based on the microarray assay (mentioned in Introduction), the expression of miR-137 was measured in pulmonary arteries and PSMCs. As shown in Figures 1(g) and 1(h), hypoxia significantly

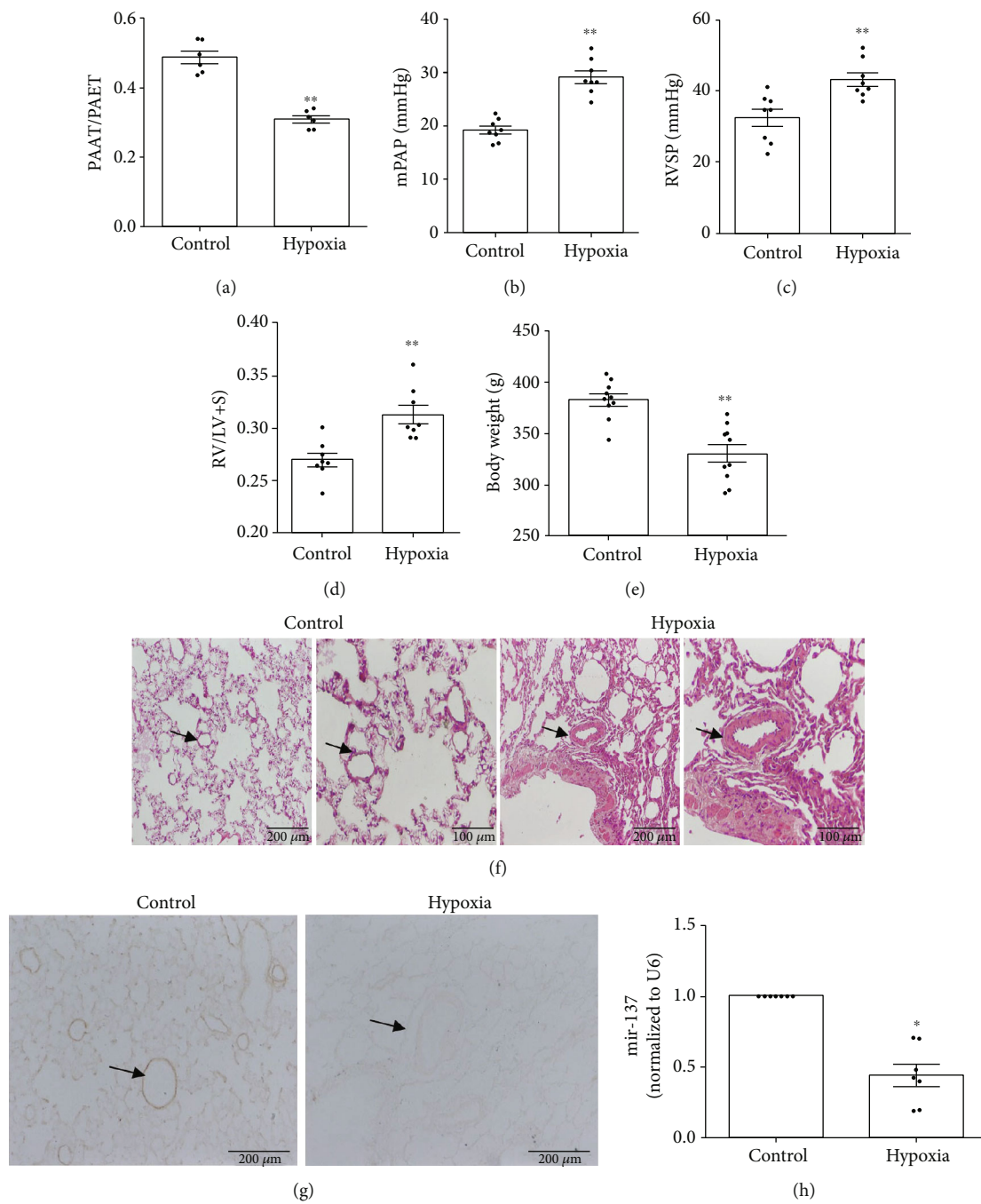


FIGURE 1: Continued.



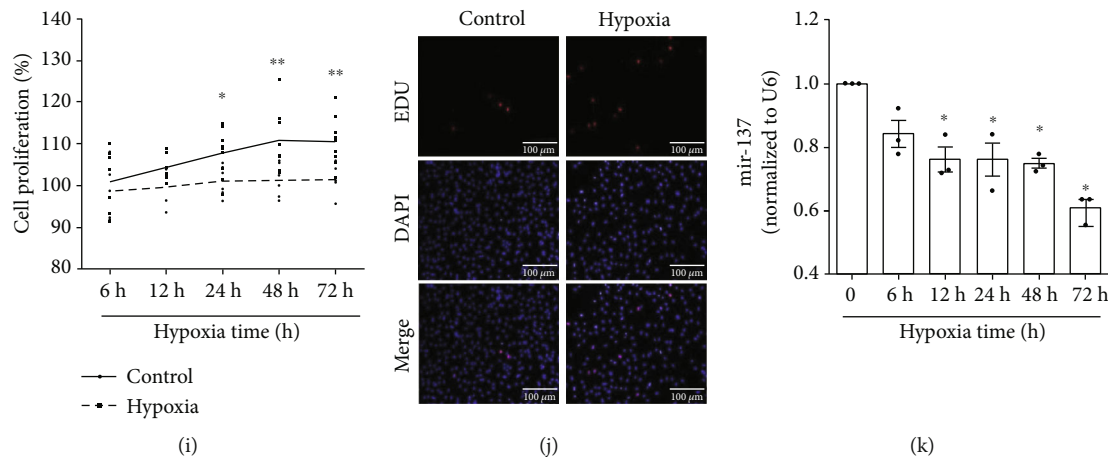


FIGURE 1: miR-137 was downregulated in remodeled pulmonary arteries and hypoxia-treated PASCs. (a) PAAT/PAET ( $n = 6$ ). (b) mPAP ( $n = 8$ ). (c) RVSP ( $n = 8$ ). (d) RV/LV+IS ( $n = 8$ ). (e) Body weight of rats ( $n = 10$ ). (f) HE staining. (g, h) The expression of miR-137 in rat pulmonary arteries was detected by in situ hybridization and real-time PCR ( $n = 7$ ). (i) The proliferation of PASCs was detected by MTS assay ( $n = 5$ ). (j) The proliferation of PASCs was detected by EDU staining. (k) The expression of miR-137 in the PASCs after hypoxia stimulation for 0, 6, 12, 24, 48, and 72 h was measured by real-time PCR ( $n = 3$ ). PAAT/PAET: pulmonary arterial acceleration/ejection time ratio; mPAP: mean pulmonary arterial pressure; RVSP: right ventricular systolic pressure; RV: right ventricle; LV: left ventricle; IS: the interventricular septum. The data are presented as means  $\pm$  S.E.M.; \* $p < 0.05$  and \*\* $p < 0.01$  vs. 0 h, control.

downregulated the expression of miR-137 in pulmonary arteries of hypoxic PH rats. As expected, PASCs exposed to 3% O<sub>2</sub> for different times (6 h, 12 h, 24 h, 48 h, and 72 h) showed significant proliferation in a time-dependent manner (Figures 1(i) and 1(j)). With the proliferation of hypoxia-induced PASCs, hypoxia also significantly downregulated the expression of miR-137 in PASCs (Figure 1(k)).

**3.2. miR-137 Inhibited Hypoxia-Induced Proliferation of PASCs.** As mentioned above, miR-137 regulates the proliferation of a variety of tumor cells [11, 12]. We therefore explored the regulatory effect of miR-137 on hypoxia-induced proliferation of PASCs by transfecting the mimic of miR-137. The results demonstrated that the transfection of miR-137 mimic significantly increased the expression of miR-137 (Figure 2(a)) and remarkably relieved hypoxia-induced the proliferation of PASCs (Figures 2(b)–2(f)).

**3.3. miR-137 Inhibitor Induced the Proliferation of PASCs.** To further confirm the role of miR-137 in the proliferation of PASCs, we transfected the inhibitor of miR-137 (100 nM) to PASCs under normoxia. As Figure 3 shown, miR-137 inhibitor decreased the expression of miR-137 (Figure 3(a)) and induced the proliferation of PASCs (Figures 3(b)–3(f)).

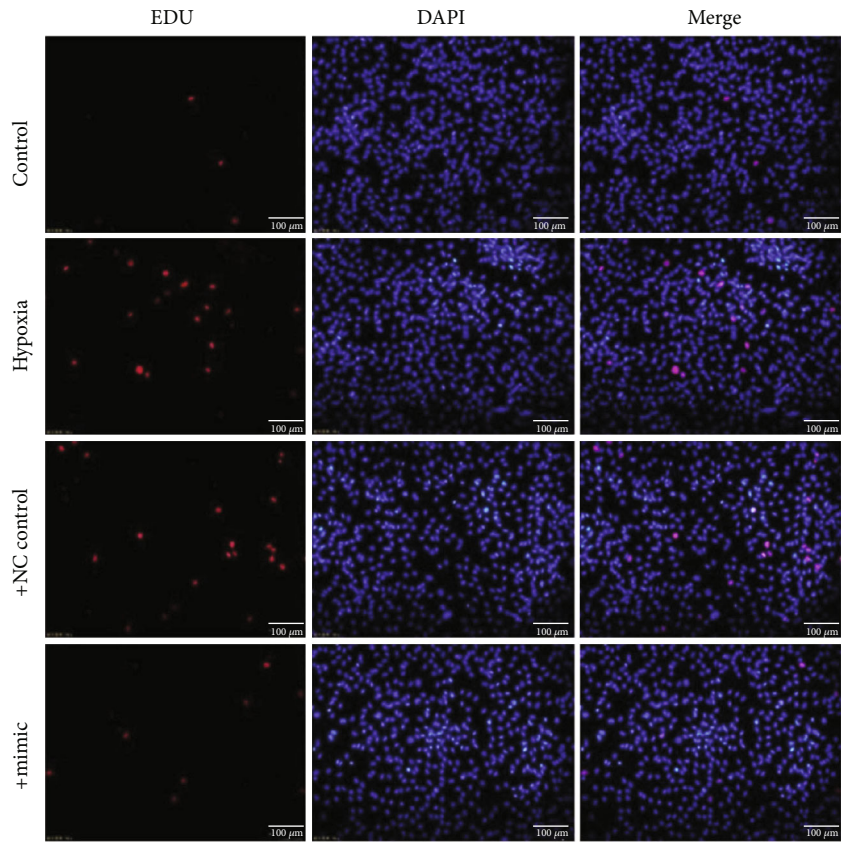
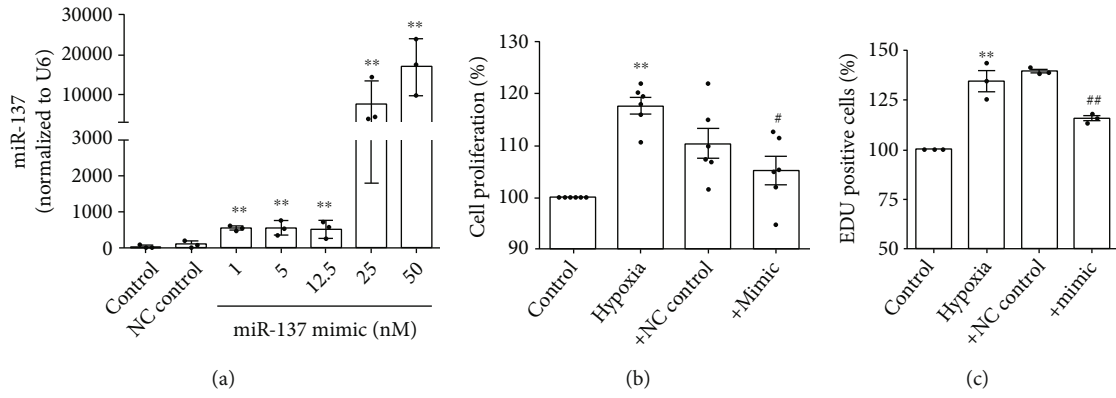
**3.4. Hypoxia Induced the Expression of Calpain-2.** It has well been documented that calpain-2 is mediated in promoting the proliferation of PASCs, thereby resulting to pulmonary arterial remodeling in hypoxic PH [6–8]. In our setting, we therefore measured the expression of calpain-2 and found that exposure of rats to continuity hypoxia (10% O<sub>2</sub>) for 21 days significantly upregulated the protein expression of calpain-2 in pulmonary arteries (Figure 4(b)) but not the expression of calpain-2 mRNA meanwhile (Figure 4(a)). Accordingly, treatment of PASCs with 3% O<sub>2</sub> for 6 h, 12 h,

24 h, and 48 h also upregulated the mRNA and protein expression of calpain-2 in a time-dependent manner (Figures 4(c) and 4(d)).

**3.5. miR-137 Inhibited Hypoxia-Induced Upregulation of Calpain-2 Expression.** It has been documented that miR-137 inhibits the mRNA of calpain-2 by directly targeting at 3'-UTR of calpain-2 [14, 16]. To explore whether miR-137 targets 3'-UTR of calpain-2 mRNA in PASCs, we mutated the putative binding site (Figure 5(a)). As shown in Figure 5(b), miR-137 mimic significantly downregulated the fluorescence values of wild-type vectors, whereas luciferase activity was unchanged using 3'-UTR binding site-mutated construct. These results indicated that miR-137 repressed the translation of calpain-2 mRNA by binding to its 3'-UTR. We then observed the effect of the transfection of miR-137 mimic on the expression of calpain-2 in PASCs and found that miR-137 mimic downregulated the expression of calpain-2 mRNA and protein expression under normoxic condition (Figures 5(c) and 5(d)). It is of note that miR-137 mimic (25 nM) reversed the upregulated expression of calpain-2 (both mRNA and protein) induced by hypoxia (Figures 5(e) and 5(f)).

**3.6. Knockdown of Calpain-2 Inhibited Hypoxia-Induced PASC Proliferation.** Inhibition of calpain-2 has been shown to attenuate proliferation of PASCs induced by PH mediators (platelet-derived growth factor [PDGF], serotonin [5-HT], and interleukin 6 [IL-6]) [17, 18]. In this study, we therefore used the calpain-2 small interfering RNA (siRNA) to knock down the expression of calpain-2 mRNA to explore whether calpain-2 mediates hypoxia-induced PASC proliferation. Different fragments and different concentrations of calpain-2 siRNA were transfected into PASCs, resulting in the decrease of calpain-2 mRNA and protein expression in PASCs, especially the effect of





(d)

FIGURE 2: Continued.

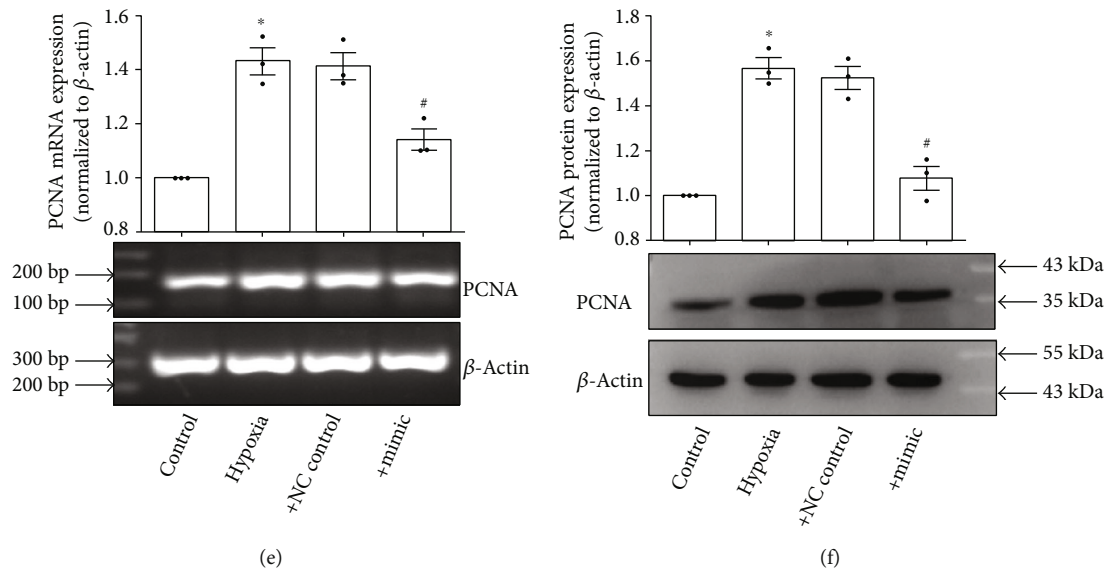


FIGURE 2: miR-137 inhibited hypoxia-induced proliferation of PSMCs. (a) PSMCs were transfected with miR-137 mimic, and the expression of miR-137 was detected by real-time PCR ( $n = 3$ ). (b) PSMCs were transfected with miR-137 mimic (25 nM), and the proliferation of PSMCs was detected by MTS assay ( $n = 6$ ). (c) Statistic diagram of EDU staining ( $n = 3$ ). (d) PSMCs were transfected with miR-137 mimic (25 nM), and the proliferation of PSMCs was detected by EDU staining. (e) PSMCs were transfected with miR-137 mimic (25 nM), and RT-PCR was used to detect the mRNA expression of PCNA, a marker of cell proliferation ( $n = 3$ ). (f) PSMCs were transfected with miR-137 mimic (25 nM), and Western blot detected the protein expression of PCNA ( $n = 3$ ). The data are presented as means  $\pm$  S.E.M.; \* $p < 0.05$  and \*\* $p < 0.01$  vs. control and # $p < 0.05$  and ## $p < 0.01$  vs. hypoxia.

fragment 2 of calpain-2 siRNAs in a concentration-dependent manner (Figures 6(a) and 6(b)). Then, we used the fragment 2 of calpain-2 siRNAs at the concentration of 40 nM for the subsequent experiments. The MTS and EDU assay showed that knockdown of calpain-2 inhibited hypoxia-induced proliferation of PSMCs (Figures 6(c)–6(e)).

#### 4. Discussion

This study represents the first evidence of the role of miR-137 in mediating hypoxia-induced proliferation of PSMCs, thereby potentially contributing to pulmonary arterial remodeling in PH. The main findings of the present study are as follows: (1) miR-137 was downregulated in pulmonary arteries of hypoxic PH rats and hypoxia-treated PSMCs; (2) miR-137 mimic inhibited hypoxia-induced proliferation of PSMCs by targeting calpain-2, and miR-137 inhibitor induced the proliferation of PSMCs under normoxia; (3) knockdown of calpain-2 by siRNA suppressed hypoxia-induced proliferation of PSMCs.

Hypoxia is one of the commonest causes of PH [19]. Hypoxia not only causes vasoconstriction by activating voltage-gated calcium channels resulting to increased cytosolic calcium of PSMCs, but also leads to pulmonary vascular remodeling by activating rho kinase and hypoxia-inducible factor- (HIF-) 1 $\alpha$  [20]. Hypoxia also compels the differential expression of miRNAs through response elements in their promoters of HIF-1 or through indirect hypoxia-associated stimulus [21]. The role of several miRNAs including miR-206 [22], miR-130/301 [23], miR-103/107 [24], miR-150 [25], miR-let-7g [6, 10], miR-17/92 [26], miR-92b-3p [27], miR-204 [28], and miR-27a [29] in

hypoxic pulmonary arterial remodeling has been reported. The present study found for the first time that miR-137 was downregulated in pulmonary arteries of hypoxic PH rats and hypoxia-treated PSMCs. Studies have reported that the downregulation of miR-137 expression is caused by the ubiquitous in hypoxic-microenvironment [30], and that miR-137 is silenced by methylation and reduction of hypermethylation of the miR-137 promoter by inhibiting DNA methyltransferase which promotes its reexpression in hypoxia condition [31, 32]. In our setting, whether these potential mechanisms are involved in hypoxia-induced, the downregulation of miR-137 expression needs further investigation.

In a variety of cancer cells, miR-137 is significantly downregulated, and transfection of miR-137 mimic to restore miR-137 expression results in significant inhibition of cell proliferation, migration, and epithelial-mesenchymal transition [11, 12, 33]. miR-137 also regulates nervous system development and synaptic plasticity [13, 34]. In high glucose-induced human umbilical vein endothelial cell injury, miR-137 is significantly upregulated and inhibition of miR-137 inhibits oxidative stress and cell apoptosis [35]. In PDGF-induced proliferation of vascular smooth muscle cells, miR-137 is significantly downregulated and overexpression of miR-137 suppresses the cell proliferation and migration by suppressing the activity of mTOR/Stat3 signaling [36]. As we described above, excessive proliferation of PSMCs is the most important cause of pulmonary vascular remodeling in PH [37]. In this study, we for the first time found that miR-137 mediated the pathogenesis of hypoxic PH by inhibiting the proliferation of PSMCs. However, the destruction of vascular intima after vascular endothelial cell injury is usually the starting point of cardiovascular

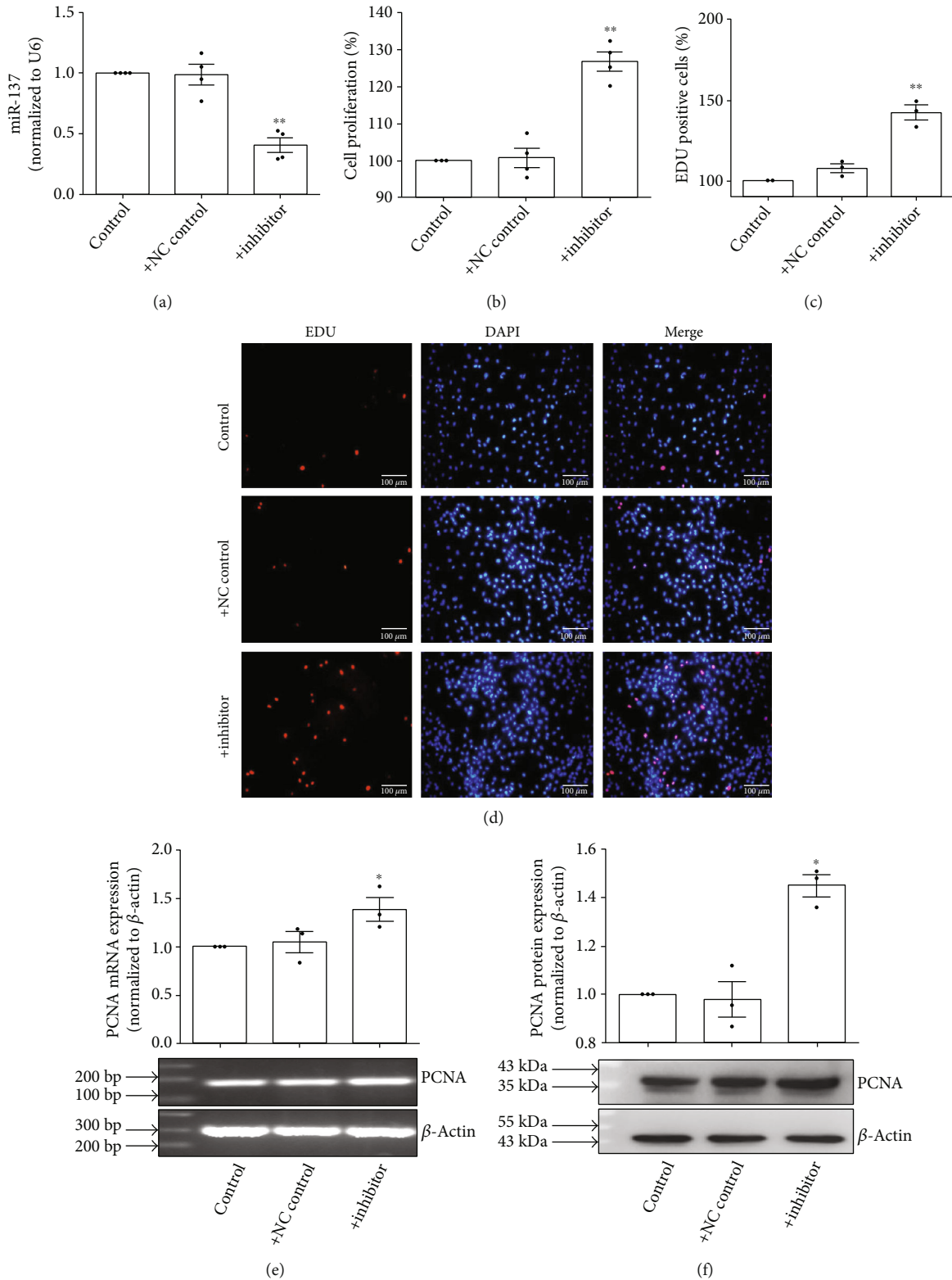


FIGURE 3: miR-137 inhibitor induced the proliferation of PSMCs. (a) PSMCs were transfected with miR-137 inhibitor (100 nM), and the expression of miR-137 was detected by real-time PCR ( $n = 4$ ). (b) PSMCs were transfected with miR-137 inhibitor (100 nM), and the proliferation of PSMCs was detected by MTS assay ( $n = 4$ ). (c) Statistic diagram of EDU staining ( $n = 3$ ). (d) PSMCs were transfected with miR-137 inhibitor (100 nM), and the proliferation of PSMCs was detected by EDU staining. (e) PSMCs were transfected with miR-137 inhibitor (100 nM), and RT-PCR was used to detect the mRNA expression of PCNA ( $n = 3$ ). (f) PSMCs were transfected with miR-137 inhibitor (100 nM), and Western blot detected the protein expression of PCNA ( $n = 3$ ). The data are presented as means  $\pm$  S.E.M.; \* $p < 0.05$  and \*\* $p < 0.01$  vs. control.

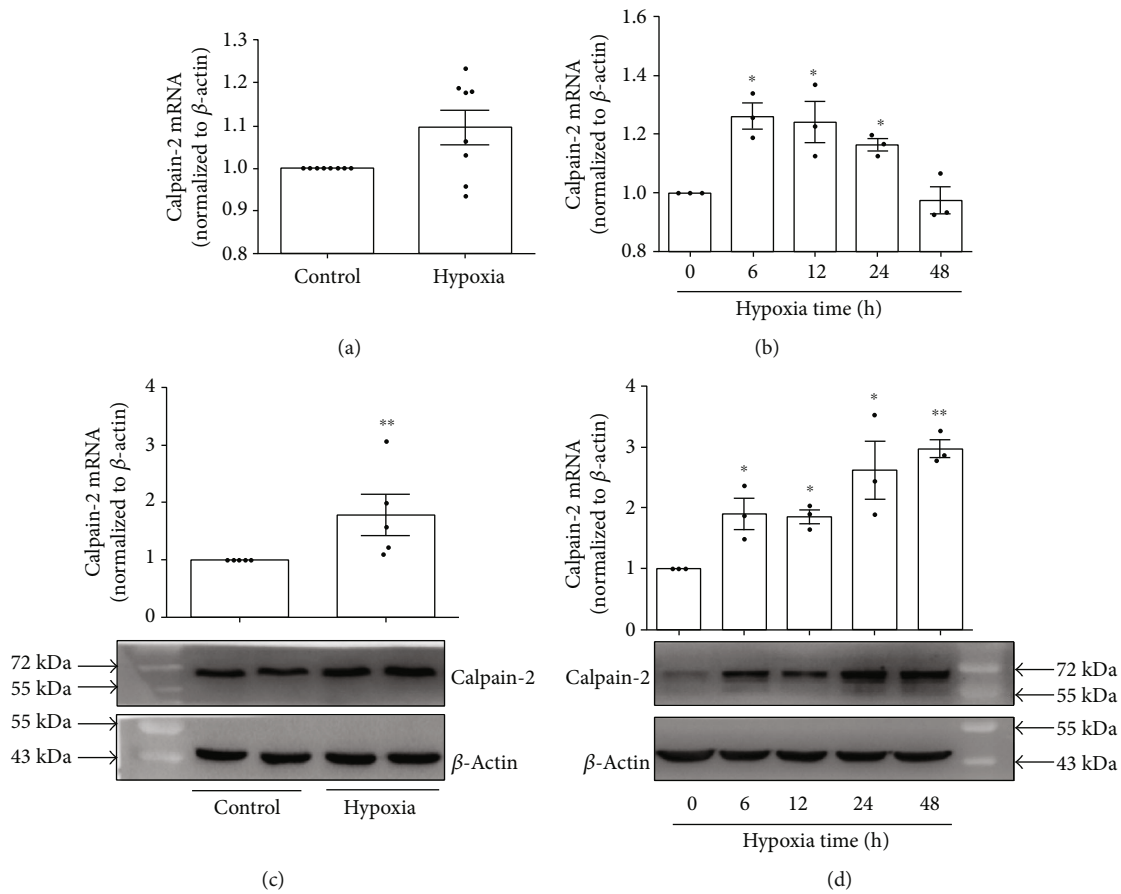


FIGURE 4: Calpain-2 was upregulated in remodeled pulmonary arteries and hypoxia-treated PSMCs. (a) The mRNA expression of calpain-2 in the pulmonary arteries of rats ( $n = 8$ ). (b) The protein expression of calpain-2 in the pulmonary arteries of rats ( $n = 8$ ). (c) The mRNA expression of calpain-2 in PSMCs ( $n = 3$ ). (d) The protein expression of calpain-2 in PSMCs ( $n = 3$ ). The data are presented as means  $\pm$  S.E.M.; \* $p < 0.05$  and \*\* $p < 0.01$  vs. 0 h, control.

diseases. In the process of PH, apoptosis, necrosis, and endothelial to mesenchymal transition occur in pulmonary arterial endothelial cells [38]. Therefore, the role of miR-137 in pulmonary arterial endothelial functions also deserves to be further studied.

miRNAs bind to the 3'-UTR of target genes, resulting in inhibition of the target genes, to participate in physiological process and the pathogenesis of diseases. Bioinformatic analysis suggests that a potential binding element for miR-137 is contained in the 3'-UTR of calpain-2. Studies have demonstrated that miR-137 binds to 3'-UTR of calpain-2 to inhibit the expression of calpain-2 [14, 16, 39]. In this study, miR-137 also suppressed the translation of calpain-2 mRNA by binding to its 3'-UTR, suggesting that the calpain-2 is a direct target of miR-137 in hypoxia which induced the proliferation of PSMCs. Moreover, as we described above, miR-137 mediates the PDGF which induced the proliferation of VSMCs by regulating the activity of mTOR/Stat3 signaling. Stat3 has been demonstrated as a key mediator of PH pathology, and the inappropriate Stat3 activation in PH has been linked to miRNA expression, such as miR-204 and

miR-17/92 [40]. Therefore, whether not only calpain-2 but also Stat3 participates in the proliferation of PSMCs mediated by miR-137 in hypoxic PH or other category of PH needs further investigation.

Calpain-2 (m-calpain) belongs to calpain family, which is activated by hypoxia-induced intracellular calcium fluxes. Our previous study found that calpain-1/2/4 expression was increased in pulmonary arteries of hypoxic PH rats, and the specific calpain inhibitor MDL28170 inhibited hypoxia-induced PSMC proliferation [7]. Others have also reported that global knockout or smooth muscle specific knockout of calpain-4 and MDL28170 prevent pulmonary vascular remodeling of MCT- or hypoxia-induced PH and EGF- and PDGF-BB-induced cell proliferation of PSMCs [8, 17, 18]. In this study, knockdown of calpain-2 by siRNA inhibited hypoxia-induced proliferation of PSMCs. Bioinformatic analysis showed that calpain-1/4 may be not targets of miR-137 (data not shown). Notably, calpain-1 has been implicated strongly in cell motility and adhesion, while calpain-2 has been implicated strongly in cell proliferation [41]. Emerging evidence has suggested an important role of calpain-2 in proliferation of PSMCs. In hyperproliferated

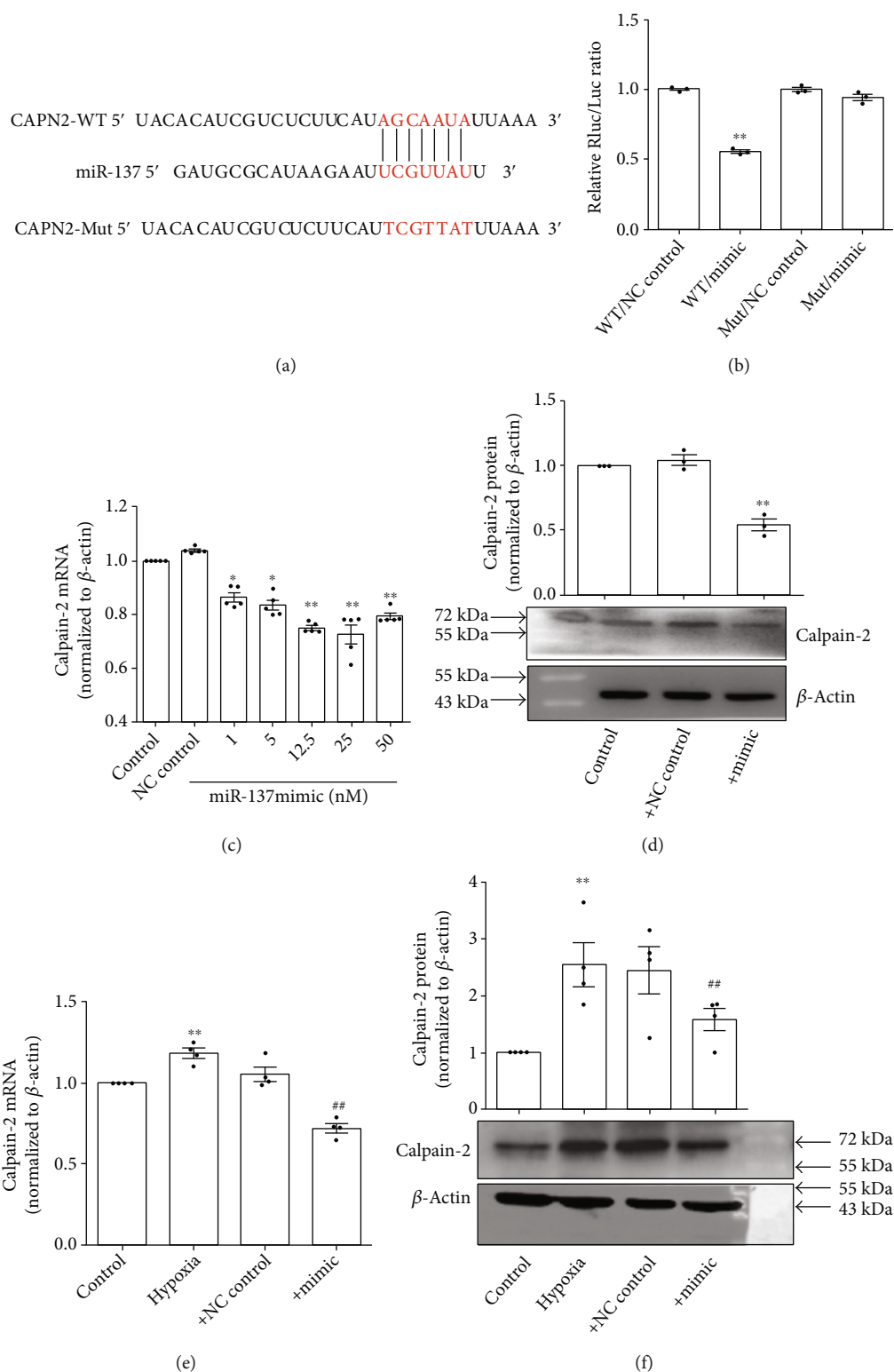


FIGURE 5: miR-137 inhibited hypoxia-induced upregulation of calpain-2 expression. (a) The putative binding site of miR-137 in 3'-UTR of calpain-2 mRNA. (b) Luciferase analysis for examining whether miR-137 targets 3'-UTR of calpain-2 mRNA ( $n = 3$ ). (c) The mRNA expression of calpain-2 in PSMCs after transfecting miR-137 mimic under normoxic condition ( $n = 5$ ). (d) The protein expression of calpain-2 in PSMCs after transfecting miR-137 mimic (25 nM) under normoxic condition ( $n = 3$ ). (e) The mRNA expression of calpain-2 in PSMCs after transfecting miR-137 mimic (25 nM) under hypoxic condition ( $n = 4$ ). (f) The protein expression of calpain-2 in PSMCs after transfecting miR-137 mimic (25 nM) under hypoxic condition ( $n = 4$ ). WT: wild type; Mut: mutant; NC: negative control. The data are presented as means  $\pm$  S.E.M.; \* $p < 0.05$  and \*\* $p < 0.01$  vs. control or WT+NC control and ## $p < 0.01$  vs. hypoxia.



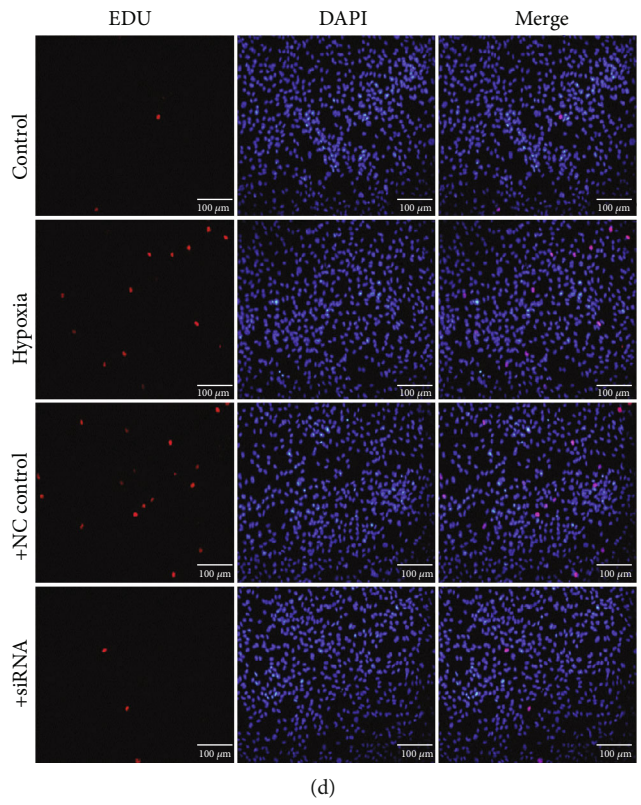
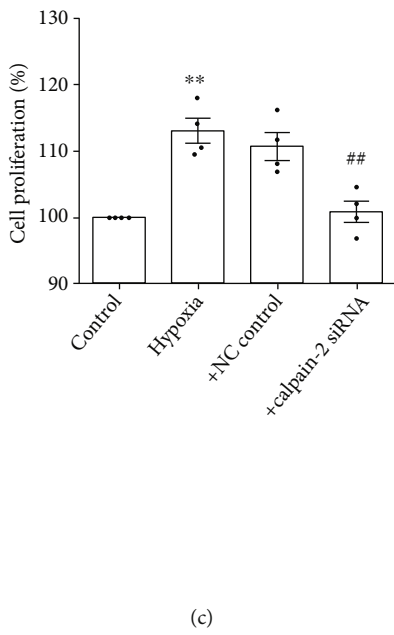
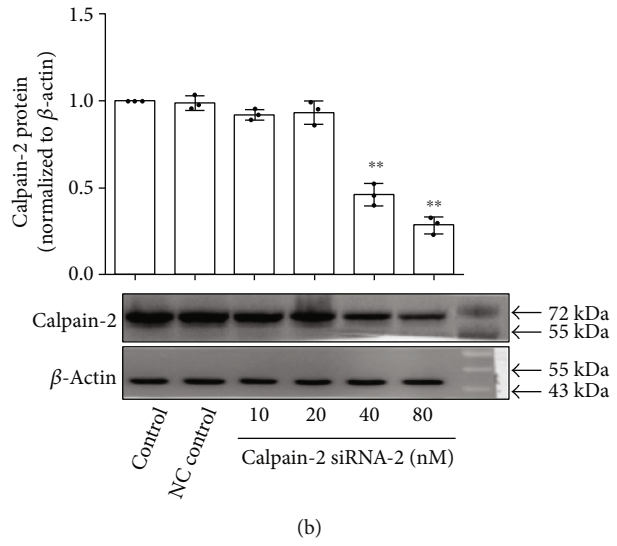
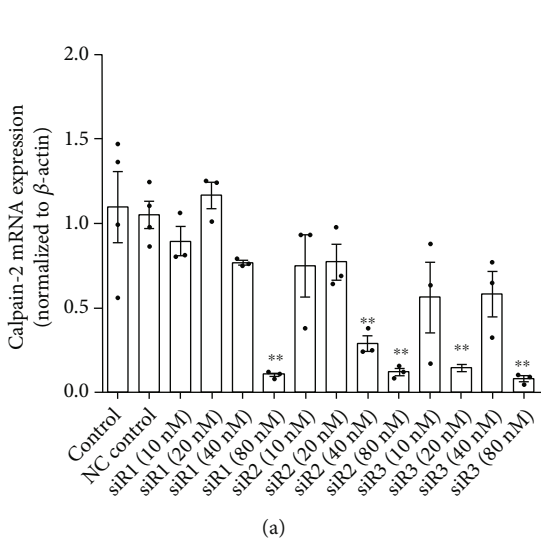


FIGURE 6: Continued.

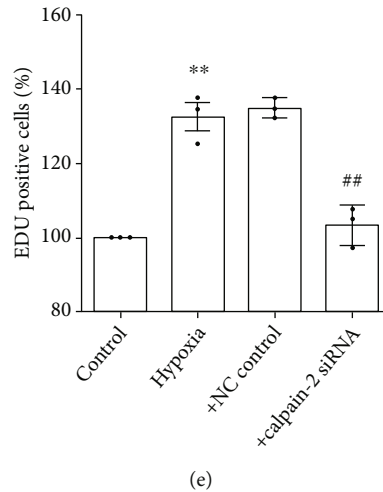


FIGURE 6: Knockdown of calpain-2 inhibited hypoxia-induced proliferation of PSMCs. (a) PSMCs were transfected with calpain-2 siRNA, and the mRNA expression of calpain-2 was detected by real-time PCR ( $n = 3$ ). (b) PSMCs were transfected with calpain-2 siRNA, and the protein expression of calpain-2 was detected by Western blot ( $n = 3$ ). (c) PSMCs were transfected with calpain-2 siRNA (40 nM), and the proliferation of PSMCs was detected by MTS assay ( $n = 4$ ). (d) PSMCs were transfected with calpain-2 siRNA (40 nM), and the proliferation of PSMCs was detected by EDU staining. (e) Statistic diagram of EDU staining ( $n = 3$ ). The data are presented as means  $\pm$  S.E.M.; \*\* $p < 0.01$  vs. control and ## $p < 0.01$  vs. hypoxia.

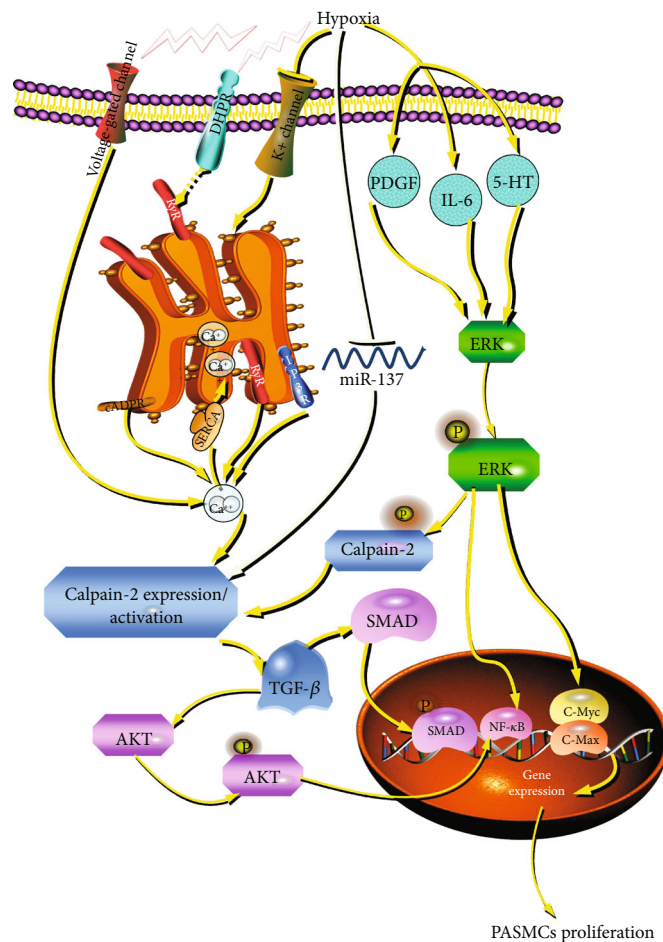


FIGURE 7: Schematic diagram of the role of miR-137 in the proliferation of PSMCs during hypoxia-induced pulmonary hypertension. Our study for the first time demonstrated that miR-137 is a novel regulator of proliferation of PSMCs in hypoxia-induced pulmonary hypertension by targeting calpain-2 pathway. DHPR: dihydropyridine receptor; RyR: ryanodine receptor; cADPR: CD38-cyclic ADP-ribose; IP3R: inositol 1,4,5-trisphosphate receptor; SERCA: sarco (endo) plasmic reticulum calcium ATPase.

PASMCs treated with PH mediators (PDGF, 5-HT, and IL-6), the extracellular signal-regulated kinase (ERK) 1/2 activated calpain-2 through phosphorylation of calpain-2 at Ser50 and ERK-1/2 inhibitor PD98059 or knockdown of calpain-2 prevented calpain activation, resulting in inhibition of proliferation of PASMCs [21, 42]. In this study, we demonstrated that miR-137 mimic reduced the expressions of calpain-2, but not measured the activity of calpain-2. However, there is a study showing that miR-137 mimic pretreatment effectively prevented the oxygen-glucose deprivation and reperfusion-induced  $[Ca^{2+}]$  increase, whereas the miR-137 inhibitor aggravated the  $[Ca^{2+}]$  increase [39]. Given that increased intracellular  $[Ca^{2+}]$  levels can activate calpain-2, we speculate that miR-137 mediates the activation of calpain-2 by regulating the concentration of  $[Ca^{2+}]$  in hypoxic PH. Calpain-2 upregulated Akt phosphorylation via an intracrine transforming growth factor- $\beta$  1 (TGF- $\beta$ 1)/mammalian target of rapamycin complex 2 (mTORC2) mechanism, resulting in proliferation of PASMCs treated with PDGF [17]. Intracrine TGF- $\beta$ 1 pathway is initiated by calpain-mediated cleavage and activation of latent TGF- $\beta$ 1 in the Golgi complex [8]. Study has reported that bone morphogenetic protein 4 (BMP4) inhibits PDGF-stimulated calpain activation and subsequent intracrine TGF- $\beta$ 1-Smad 2/3 pathway in PASMCs [43]. All findings suggest that calpain-2 is expected to be a potential therapeutic target for proliferation of PASMCs, further for PH (Figure 7).

In the present study, we found that calpain-2, as a target of miR-137, was upregulated with the downregulation of miR-137 in hypoxic PH. However, studies have also demonstrated that protein level of calpain-2 is regulated by miR-223 acting directly on the 3'-UTR of calpain-2 mRNA as well as by miR-145, which acts via an increase in histone deacetylase 2, and histone deacetylase 2 transcriptionally inhibits calpain-2 expression by hyperacetylation of the promoter of calpain-2 gene in endothelial cells [9, 44]. Therefore, whether there also exist other miRNAs targeted calpain-2 to participate in the proliferation of PASMCs in hypoxic PH or other category of PH needs further investigation. Furthermore, besides calcium channels, potassium channels have also been reported to regulate calpain activity. Potassium channel dysfunction in PASMCs is a hallmark of PH. Transient transfection of a Kv channel or a  $K^+$  channel activator increases  $K^+$  efflux to enhance PASM cell death [45, 46]. The decrease of  $K^+$  channel expression, such as Kv1.5 and Kv1.2, leads to the proliferation of PASMCs [47]. The opening of potassium channels promotes cell membrane hyperpolarization and reduces calcium overload. In a hypoxic environment, cell membrane depolarization inhibits the opening of potassium channels, which in turn promotes the increase of cytoplasmic free calcium concentration resulting in calpain-2 activation [48]. Therefore, the activation of calpain-2 may also be involved in the potassium channel-mediated proliferation of PASMCs.

In spite of the foregoing important findings, the present study has indeed some limitations. Transgenic or gene knock-out animals of miRNA-137 and calpain-2 need to be introduced to further prove the in vivo functions of miRNA-137 and calpain-2 in pulmonary vascular remodeling and further confirm the inhibitory effect of miR-137 in hypoxia-induced proliferation of PASMCs by targeting calpain-2.

In conclusion, the present study for the first time demonstrated that hypoxia-induced downregulation of miR-137 promoted PASM cell proliferation by targeting calpain-2. miR-137, a new miRNA involved in proliferation of PASMCs, further in pulmonary vascular remodeling of PH, would be a novel potential therapeutic target for PH.

## Data Availability

The research data used to support the findings of this study are available from the corresponding author upon request.

## Conflicts of Interest

The authors declare that there are no conflicts of interest.

## Acknowledgments

This work was supported by the Grants from the National Natural Science Foundation of China (No. 81872872, No. 81960015, No. 82000062, and No. 81800051), the Open Sharing Fund for the Large-scale Instruments and Equipments of Central South University (CSUZC201935), the Youth Science Foundation from Science and Technology Department of Jiangxi province (No. 2017BAB215002), the Research Foundation of Henan Province (No. 212102310319) and the Xinxiang Medical University (XYBSKYZZ201812).

## References

- [1] A. A. R. Thompson and A. Lawrie, "Targeting vascular remodeling to treat pulmonary arterial hypertension," *Trends in Molecular Medicine*, vol. 23, no. 1, pp. 31–45, 2017.
- [2] C. A. Thomas, R. J. Anderson, D. F. Condon, and V. A. de Jesus Perez, "Diagnosis and management of pulmonary hypertension in the modern era: insights from the 6th world symposium," *Pulmonary Therapy*, vol. 6, no. 1, pp. 9–22, 2019.
- [3] R. A. Hanna, R. L. Campbell, and P. L. Davies, "Calcium-bound structure of calpain and its mechanism of inhibition by calpastatin," *Nature*, vol. 456, no. 7220, pp. 409–412, 2008.
- [4] H. Sorimachi and K. Suzuki, "The structure of calpain," *Journal of Biochemistry*, vol. 129, no. 5, pp. 653–664, 2001.
- [5] S. Chakraborti, M. N. Alam, D. Paik, S. Shaikh, and T. Chakraborti, "Implications of calpains in health and diseases," *Indian Journal of Biochemistry & Biophysics*, vol. 49, no. 5, pp. 316–328, 2012.
- [6] W.-F. Zhang, T.-T. Zhu, Y.-W. Xiong et al., "Negative feedback regulation between microRNA let-7g and LOX-1 mediated hypoxia-induced PASMCs proliferation," *Biochemical and Biophysical Research Communications*, vol. 488, no. 4, pp. 655–663, 2017.
- [7] W. Zhang, T. Zhu, A. Xiong et al., "Calpain mediated pulmonary vascular remodeling in hypoxia induced pulmonary hypertension," *Zhong Nan Da Xue Xue Bao. Yi Xue Ban*, vol. 41, no. 9, pp. 929–936, 2016.
- [8] W. Ma, W. Han, P. A. Greer et al., "Calpain mediates pulmonary vascular remodeling in rodent models of pulmonary hypertension, and its inhibition attenuates pathologic features of disease," *The Journal of Clinical Investigation*, vol. 121, no. 11, pp. 4548–4566, 2011.

- [9] J. Meloche, M. le Guen, F. Potus et al., "MiR-223 reverses experimental pulmonary arterial hypertension," *American Journal of Physiology. Cell Physiology*, vol. 309, no. 6, pp. C363–C372, 2015.
- [10] W.-F. Zhang, Y.-W. Xiong, T.-T. Zhu, A.-Z. Xiong, H.-H. Bao, and X.-S. Cheng, "MicroRNA let-7g inhibited hypoxia-induced proliferation of PAMSCs via G<sub>0</sub>/G<sub>1</sub> cell cycle arrest by targeting c-myc," *Life Sciences*, vol. 170, pp. 9–15, 2017.
- [11] S. Nuzzo, S. Catuogno, M. Capuozzo et al., "Axl-targeted delivery of the oncosuppressor miR-137 in non-small-cell lung cancer," *Molecular Therapy - Nucleic Acids*, vol. 17, pp. 256–263, 2019.
- [12] C. Lei, G. Jing, W. Jichao et al., "MiR-137's tumor suppression on prolactinomas by targeting MITF and modulating Wnt signaling pathway," *The Journal of Clinical Endocrinology and Metabolism*, vol. 104, no. 12, pp. 6391–6402, 2019.
- [13] E. Mahmoudi and M. J. Cairns, "MiR-137: an important player in neural development and neoplastic transformation," *Molecular Psychiatry*, vol. 22, no. 1, pp. 44–55, 2017.
- [14] Y. Tang, R. Fu, Z.-M. Ling et al., "MiR-137-3p rescue motoneuron death by targeting calpain-2," *Nitric Oxide: Biology and Chemistry*, vol. 74, pp. 74–85, 2018.
- [15] S. Provencher, S. L. Archer, F. D. Ramirez et al., "Standards and methodological rigor in pulmonary arterial hypertension preclinical and translational research," *Circulation Research*, vol. 122, no. 7, pp. 1021–1032, 2018.
- [16] Y. Tang, Y. Li, G. Yu et al., "MicroRNA-137-3p protects PC12 cells against oxidative stress by downregulation of calpain-2 and nNOS," *Cellular and Molecular Neurobiology*, vol. 41, no. 6, pp. 1373–1387, 2021.
- [17] P. Abeyrathna, L. Kovacs, W. Han, and Y. Su, "Calpain-2 activates Akt via TGF- $\beta$ 1-mTORC2 pathway in pulmonary artery smooth muscle cells," *American Journal of Physiology. Cell Physiology*, vol. 311, no. 1, pp. C24–C34, 2016.
- [18] L. Kovacs, W. Han, R. Rafikov et al., "Activation of calpain-2 by mediators in pulmonary vascular remodeling of pulmonary arterial hypertension," *American Journal of Respiratory Cell and Molecular Biology*, vol. 54, no. 3, pp. 384–393, 2016.
- [19] A. C. Oliveira, E. M. Richards, and M. K. Raizada, "Pulmonary hypertension: pathophysiology beyond the lung," *Pharmacological Research*, vol. 151, article 104518, 2020.
- [20] K. J. Dunham-Snary, D. Wu, E. A. Sykes et al., "Hypoxic pulmonary vasoconstriction: from molecular mechanisms to medicine," *Chest*, vol. 151, no. 1, pp. 181–192, 2017.
- [21] V. Mohsenin, "The emerging role of microRNAs in hypoxia-induced pulmonary hypertension," *Sleep & Breathing*, vol. 20, no. 3, pp. 1059–1067, 2016.
- [22] J. Yue, J. Guan, X. Wang et al., "MicroRNA-206 is involved in hypoxia-induced pulmonary hypertension through targeting of the HIF-1  $\alpha$  /Fhl-1 pathway," *Laboratory Investigation*, vol. 93, no. 7, pp. 748–759, 2013.
- [23] T. Bertero, Y. Lu, S. Annis et al., "Systems-level regulation of microRNA networks by miR-130/301 promotes pulmonary hypertension," *The Journal of Clinical Investigation*, vol. 124, no. 8, pp. 3514–3528, 2014.
- [24] B. Deng, J. du, R. Hu et al., "MicroRNA-103/107 is involved in hypoxia-induced proliferation of pulmonary arterial smooth muscle cells by targeting HIF-1 $\beta$ ," *Life Sciences*, vol. 147, pp. 117–124, 2016.
- [25] M. Chen, C. Shen, Y. Zhang, and H. Shu, "MicroRNA-150 attenuates hypoxia-induced excessive proliferation and migration of pulmonary arterial smooth muscle cells through reducing HIF-1 $\alpha$  expression," *Biomedicine & Pharmacotherapy*, vol. 93, pp. 861–868, 2017.
- [26] T. Chen, J. B. Huang, J. Dai, Q. Zhou, J. U. Raj, and G. Zhou, "PAI-1 is a novel component of the miR-17~92 signaling that regulates pulmonary artery smooth muscle cell phenotypes," *American Journal of Physiology-Lung Cellular and Molecular Physiology*, vol. 315, no. 2, pp. L149–L161, 2018.
- [27] J. Lee, J. Heo, and H. Kang, "MiR-92b-3p-TSC1 axis is critical for mTOR signaling-mediated vascular smooth muscle cell proliferation induced by hypoxia," *Cell Death and Differentiation*, vol. 26, no. 9, pp. 1782–1795, 2019.
- [28] T. Liu, X.-Z. Zou, N. Huang et al., "Down-regulation of miR-204 attenuates endothelial-mesenchymal transition by enhancing autophagy in hypoxia-induced pulmonary hypertension," *European Journal of Pharmacology*, vol. 863, p. 172673, 2019.
- [29] T. Liu, X.-Z. Zou, N. Huang et al., "MiR-27a promotes endothelial-mesenchymal transition in hypoxia-induced pulmonary arterial hypertension by suppressing BMP signaling," *Life Sciences*, vol. 227, pp. 64–73, 2019.
- [30] D.-M. Li, Q.-D. Chen, G.-N. Wei et al., "Hypoxia-induced miR-137 inhibition increased glioblastoma multiforme growth and chemoresistance through LRP6," *Frontiers in Oncology*, vol. 10, p. 611699, 2021.
- [31] K. Kozaki, I. Imoto, S. Mogi, K. Omura, and J. Inazawa, "Exploration of tumor-suppressive microRNAs silenced by DNA hypermethylation in oral cancer," *Cancer Research*, vol. 68, no. 7, pp. 2094–2105, 2008.
- [32] R. Steponaitiene, J. Kupcinskas, C. Langner et al., "Epigenetic silencing of miR-137 is a frequent event in gastric carcinogenesis," *Molecular Carcinogenesis*, vol. 55, no. 4, pp. 376–386, 2016.
- [33] X. Ding, J. Zhang, Z. Feng, Q. Tang, and X. Zhou, "MiR-137-3p inhibits colorectal cancer cell migration by regulating a KDM1A-dependent epithelial-mesenchymal transition," *Digestive Diseases and Sciences*, vol. 66, no. 7, pp. 2272–2282, 2021.
- [34] K. T. Thomas, B. R. Anderson, N. Shah et al., "Inhibition of the schizophrenia-associated microRNA miR-137 disrupts Nrg1 $\alpha$  neurodevelopmental signal transduction," *Cell Reports*, vol. 20, no. 1, pp. 1–12, 2017.
- [35] J. Li, J. Li, T. Wei, and J. Li, "Down-regulation of microRNA-137 improves high glucose-induced oxidative stress injury in human umbilical vein endothelial cells by up-regulation of AMPK $\alpha$ 1," *Cellular Physiology and Biochemistry*, vol. 39, no. 3, pp. 847–859, 2016.
- [36] J. Pan, K. Li, W. Huang, and X. Zhang, "MiR-137 inhibited cell proliferation and migration of vascular smooth muscle cells via targeting IGFBP-5 and modulating the mTOR/STAT3 signaling," *PLoS ONE*, vol. 12, no. 10, article e0186245, 2017.
- [37] D. Wang, P. Uhrin, A. Mocan et al., "Vascular smooth muscle cell proliferation as a therapeutic target. Part 1: molecular targets and pathways," *Biotechnology Advances*, vol. 36, no. 6, pp. 1586–1607, 2018.
- [38] B. Ranchoux, L. D. Harvey, R. J. Ayon et al., "Endothelial dysfunction in pulmonary arterial hypertension: an evolving landscape (2017 Grover Conference Series)," *Pulmonary Circulation*, vol. 8, no. 1, p. 2045893217752912, 2018.
- [39] H. Wang, Q. Yu, Z.-L. Zhang, H. Ma, and X.-Q. Li, "Involvement of the miR-137-3p/CAPN-2 interaction in ischemia-reperfusion-induced neuronal apoptosis through modulation




- of p35 cleavage and subsequent caspase-8 overactivation,” *Oxidative Medicine and Cellular Longevity*, vol. 2020, Article ID 2616871, 17 pages, 2020.
- [40] R. Paulin, J. Meloche, and S. Bonnet, “STAT3 signaling in pulmonary arterial hypertension,” *JAK-STAT.*, vol. 1, no. 4, pp. 223–233, 2012.
- [41] A. Glading, R. J. Bodnar, I. J. Reynolds et al., “Epidermal growth factor activates m-calpain (calpain II), at least in part, by extracellular signal-regulated kinase-mediated phosphorylation,” *Molecular and Cellular Biology*, vol. 24, no. 6, pp. 2499–2512, 2004.
- [42] L. Kovacs, Y. Cao, W. Han et al., “PFKFB3 in smooth muscle promotes vascular remodeling in pulmonary arterial hypertension,” *American Journal of Respiratory and Critical Care Medicine*, vol. 200, no. 5, pp. 617–627, 2019.
- [43] P. Cai, L. Kovacs, S. Dong, G. Wu, and Y. Su, “BMP4 inhibits PDGF-induced proliferation and collagen synthesis via PKA-mediated inhibition of calpain-2 in pulmonary artery smooth muscle cells,” *American Journal of Physiology-Lung Cellular and Molecular Physiology*, vol. 312, no. 5, pp. L638–L648, 2017.
- [44] D. Siuda, V. Randriamboavonjy, and I. Fleming, “Regulation of calpain 2 expression by miR-223 and miR-145,” *Biochimica et Biophysica Acta - Gene Regulatory Mechanisms*, vol. 1862, no. 10, p. 194438, 2019.
- [45] E. D. Burg, C. V. Remillard, and J. X.-J. Yuan, “Potassium channels in the regulation of pulmonary artery smooth muscle cell proliferation and apoptosis: pharmacotherapeutic implications,” *British Journal of Pharmacology*, vol. 153, Supplement 1, pp. S99–S111, 2008.
- [46] S. Krick, O. Platoshyn, M. Sweeney et al., “Nitric oxide induces apoptosis by activating K<sup>+</sup> channels in pulmonary vascular smooth muscle cells,” *American Journal of Physiology. Heart and Circulatory Physiology*, vol. 282, no. 1, pp. H184–H193, 2002.
- [47] Y. Lv, L. Fu, Z. Zhang et al., “Increased expression of microRNA-206 inhibits potassium voltage-gated channel subfamily a member 5 in pulmonary arterial smooth muscle cells and is related to exaggerated pulmonary artery hypertension following intrauterine growth retardation in rats,” *Journal of the American Heart Association*, vol. 8, no. 2, article e010456, 2019.
- [48] D. E. Goll, V. F. Thompson, H. Li, W. Wei, and J. Cong, “The calpain system,” *Physiological Reviews*, vol. 83, no. 3, pp. 731–801, 2003.



## Research Article

# miR-129 Attenuates Myocardial Ischemia Reperfusion Injury by Regulating the Expression of PTEN in Rats

Zhao-Hui Dai,<sup>1,2</sup> Zhi-Ming Jiang,<sup>1,2</sup> Hua Tu,<sup>1</sup> Li Mao,<sup>3</sup> Gui-Lin Song,<sup>1,4</sup>  
Zhong-Bao Yang ,<sup>1,4</sup> Fang Liu,<sup>1,5</sup> and Md Sayed Ali Sheikh<sup>6</sup>

<sup>1</sup>The Affiliated Changsha Hospital of Hunan Normal University, Changsha, Hunan 410006, China

<sup>2</sup>Chest Pain Center of Changsha, Changsha, China

<sup>3</sup>Department of Basic Medicine, Changsha Health Vocational College, Changsha, Hunan 410600, China

<sup>4</sup>Institute of Emergency and Critical Care Medicine of Changsha, Changsha, China

<sup>5</sup>College of Medicine, Hunan Normal University, Changsha, Hunan 410006, China

<sup>6</sup>Internal Medicine Department, Cardiology, College of Medicine, Jouf University, Sakaka, Aljouf, Saudi Arabia

Correspondence should be addressed to Zhong-Bao Yang; [yzb55@yahoo.com](mailto:yzb55@yahoo.com)

Received 27 February 2021; Revised 13 May 2021; Accepted 22 July 2021; Published 16 August 2021

Academic Editor: Lei Chen

Copyright © 2021 Zhao-Hui Dai et al. This is an open access article distributed under the Creative Commons Attribution License, which permits unrestricted use, distribution, and reproduction in any medium, provided the original work is properly cited.

PTEN/AKT signaling plays pivotal role in myocardial ischemia reperfusion injury (MIRI), and miRNAs are involved in the regulation of AKT signaling. This study was designed to investigate the interaction between miR-129 and PTEN in MIRI. A MIRI rat model and a hypoxia reoxygenation (H/R) H9C2 cell model were constructed to simulate myocardial infarction clinically. TTC staining, creatine kinase (CK) activity, TUNEL/Hoechst double staining, Hoechst staining and flow cytometer were used for evaluating myocardial infarction or cell apoptosis. miR-129 mimic transfection experiment and luciferase reporter gene assay were conducted for investigating the function of miR-129 and the interaction between miR-129 and PTEN, respectively. Real-time PCR and western blotting were performed to analyze the gene expression. Compared to the control, MIRI rats presented obvious myocardial infarction, higher CK activity, increased expression of caspase-3 and PTEN, decreased expression of miR-129, and insufficient AKT phosphorylation. Consistently, H/R significantly increased the apoptosis of H9C2 cells, concomitant with the downregulation of miR-129, upregulation of PTEN and caspase-3, and insufficient phosphorylation of AKT, while miR-129 mimic obviously inhibited the expression of PTEN and caspase-3, increased the AKT phosphorylation, and decreased the cell apoptosis. Additionally, miR-129 mimic obviously decreased the relative luciferase activity in H9C2 cells. To our best knowledge, this study firstly found that the low expression of miR-129 accelerates the myocardial cell apoptosis by directly targeting 3' UTR of PTEN. miR-129 is an important biomarker for MIRI, as well as a potential therapy target.

## 1. Introduction

myocardial infarction is one of the leading causes of death worldwide, especially in elder population, which was characterized by the blockage of blood to coronary artery and consequently resulting in dysfunction of myocardial cell, even death [1]. Restoration of blood to the coronary artery by pharmacological or surgery approaches was the common and effective therapy clinically. However, besides the benefits to the affected heart, blood reperfusion will paradoxically be harmful to the heart at certain stage, which was called myocardial ischemia/reperfusion injury (MIRI) [2]. The common

and worst consequence of MIRI is myocardial cell death that was associated with the inhibition of antiapoptotic signaling pathways [3]. Among them, Akt signaling pathways are involved in many cellular physiological processes and have important roles in cell survival [4]. Amounted evidences demonstrated that MIRI contributes to the decrease of phosphorylation of AKT in myocardial cell [4, 5]. Thereby, elucidation of the molecular mechanism of decreased AKT phosphorylation in MIRI is very important for the knowing of myocardial infarction as well as its therapy. As an upstream molecule of the AKT signaling pathway, PTEN plays a pivotal role in AKT phosphorylation regulation.

Previous studies have found that higher expression levels of PTEN were, at least partially, the cause of insufficiency of AKT phosphorylation in myocardial cells in pathological state caused by MIRI [6]. Although there are many experiments designed to study the expression regulation mechanism of PTEN in MIRI and got many findings, its detail mechanism still needs to be elucidated.

miRNAs are a class of conserved noncoding RNAs of about 22 nt in length and have many biological functions; for example, it can suppress gene expression [7]. Previous studies have proved that one miRNA can target several different genes and one gene can be targeted by several different miRNAs. [7] For its broad biological functions, miRNAs play key roles in the development and progress of diseases, such as myocardial infarction and tumor. [8, 9] Accumulated evidence show that abnormal expression of miRNAs was associated with the process of MIRI, for example, miR-494, miR-26a-5p, and miR-199a [10–12]. In addition, Xing et al. have demonstrated that PTEN is a target gene of miR-26a-5P [10]. This suggested that miRNAs are involved in MIRI, at least partly, by regulating of PTEN. However, few of the present studies were designed to explore the role of the miRNAs/PTEN axis in MIRI. For better understanding the role of miRNA in PTEN expression regulation in MIRI, more target miRNAs of PTEN need to be confirmed. miR-129 was proved to be a multifunction molecule and involving in the development and progression of many diseases, such as cerebral ischemia reperfusion injury and MIRI [13–15]. We recently found that miR-129 is a putative target miRNA of PTEN based on bioinformation analysis and prediction. Thus, explicating the interrelationship between miR-129 and PTEN is of great importance in understanding MIRI.

This study was designed to investigate the role of miR-129 in MIRI. To our best knowledge, this was the first time to observe the interaction of miR-129 and PTEN and it will provide a novel target for MIRI therapy.

## 2. Materials and Methods

**2.1. Animals' Experiments.** A total of 24 male Sprague-Dawley rats (8 weeks old, 250–260 g) were purchased from the Hunan SJA Laboratory Animal Co., Ltd. Animals were housed in conditions (24°C, 60% humidity, and 12 h light/dark cycle) with free access to water and food. The rats were randomly divided into three groups (the control group, sham group, and I/R injury group; 8 per group). A rat MIRI model was established following a previously described surgical method [10]. Firstly, the rats were intraperitoneally injected with 3% pentobarbital sodium (40 mg/kg) for light anesthesia. Then, the hair of the neck was removed and an endotracheal intubation was performed. After that, a rodent ventilator (R407, RWD Life Science, China) and an electrocardiograph (Beheart R3, Mindray, China) were used for monitoring the rats' respiratory rate and electrocardiogram, respectively. Before carrying out left lateral thoracotomy and exposing the heart, the skin along the left edge of the sternum was incised and the muscle between the third and fourth ribs was separated. An 8–0 atraumatic suture was used to ligate the left anterior descending coronary artery

(LADCA) to produce occlusions. When the ST segment in ECG was notably upgraded indicated that the coronary artery was successfully blocked. After 30 min of occlusion, the suture was released and the blood to the heart was restored. During the reperfusion process, there is an obvious decline in the ST segment. Thus, the myocardial I/R model was successfully constructed. Next, the pneumothorax was evacuated manually, and the chest and skin were closed using a 6–0 Prolene suture. For analgesia, buprenorphine (0.1 mg/kg body weight) was administered ip. Additionally, the sham group of rats subjected to the same procedure except the ligation of LADCA.

**2.2. Measurement of Creatine Kinase (CK) Activity.** A CK activity test kit (Beijing Solarbio Science & Technology Co., Ltd.) was used for CK activity measurement. According to the manufacture's instruction, 0.1 g of heart tissues and 1 mL extraction solution were mixed to prepare homogenate at 0°C. Then, the homogenate was centrifuged at 10000 g, 4°C for 15 min and the supernatant was collected. The CK activity was determined using a spectrophotometer (colorimetric method). Briefly, a 1000  $\mu$ L reaction mix was prepared by mixing 200  $\mu$ L supernatant, 450  $\mu$ L working solution, and 350  $\mu$ L water. Then, the absorption value was read at 340 nm. The CK activity was calculated as the following formula:  $CK (U/g) = 268 \times \Delta A \div W$ . ( $\Delta A =$  (the absorption value of sample at the time of 190 s – the absorption value of sample at the time of 10s) – (the absorption value of control at the time of 190 s – the absorption value of control at the time of 10s)).

**2.3. Determination of Infarction Area.** At the end of 2 h reperfusion, all rats (16 rats) were sacrificed by decapitation after loss of consciousness following anesthesia via intraperitoneal injection of 3% pentobarbital sodium (40 mg/kg weight). The heart was immediately excised and stored at –20°C. Prior to TTC staining, heart slices were prepared by coronally cutting heart tissues into sections with a thickness of 0.2–0.3 cm. Then, the slices were immersed in 2% TTC and maintained in dark (37°C) for 0.5 h. The sample pictures were captured. The infarct area was assessed using ImageJ software (version 1.4; National Institutes of Health). The myocardial infarct size is reported as the infarct area.

**2.4. Cell Culture.** The H9C2 cell line was purchased from the Committee on Type Culture Collection of Chinese Academy of Sciences of Shanghai and maintained in a cell incubator with conditions as 37°C, 5% CO<sub>2</sub>, and 95% air. DMEM culture (Thermo Fisher Scientific, Inc.) supplemented with 10% FBS and penicillin/streptomycin (100 U/mL) was used for cell culture. Cells ( $5 \times 10^5$ ) were cultured with 12-well plates for miRNA functional assays and the luciferase reporter gene experiment.

**2.5. Cell Model of Hypoxia/Reoxygenation (H/R).** An in vitro H9C2 cell H/R model was established following the methods of Mao et al. to mimic myocardial ischemia reperfusion injury [16]. When cells grow to a 70% area of a plate, the DMEM culture was removed and cells were washed twice using PBS to remove the residual culture. Following that,

the cells were incubated with Dulbecco's phosphate-buffered saline (DPBS; Sigma-Aldrich; Merck KGaA) at 37°C in a hypoxic condition (95% N<sub>2</sub> and 5% CO<sub>2</sub>) for 5 h. Then, the DPBS was dumped and replaced with an addition of DMEM culture, and the cells were maintained at 37°C in a standard condition (5% CO<sub>2</sub> and 95% air) for 20 h reoxygenation. The attempts of hypoxia/reoxygenation (5 h/20 h) were to get an apoptosis rate of H9C2 cells greater than 40%.

**2.6. Bioinformatics Prediction.** TargetScan (<http://www.targetscan.org/vert-72/>) and miRBase (<http://www.mirbase.org/>) were used to predict the target miRNAs of PTEN.

**2.7. Cell Transfection.** miR-129-5p mimic and negative controls (NC) miRNA were synthesized from Shanghai Gene Pharma Co., Ltd. (China). To investigate the function of miR-129 in a cardiomyocyte, H9C2 cells were transfected with miR-129 mimics (final concentration 100 nm) by Lipofectamine 2000 (Ruibio, China).

**2.8. Luciferase Reporter Assay.** Luciferase reporter assay was performed following the methods of Mao et al. to observe the interaction between PTEN and miR-129 [16]. A luciferase reporter gene plasmid (pGL6; Promega Corporation) was constructed and designated as PTEN-WT or PTEN-MU according to the sequence of 3'UTR of PTEN cloned into the plasmid whether it contains the wild-type (WT) binding sites of miR-129-5p "CAAAAAA" or mutant (MUT) "CAAGAAA". These plasmids were verified by electrophoresis (figure S1). The plasmids and miR-129-5p mimic were cotransfected into the H9C2 cell via Lipofectamine® 2000 (Ruibio, China). After 24 h of transfection, the relative luciferase activity of H9C2 cells was determined using a dual luciferase reporter gene assay kit (Beyotime Institute of Biotechnology). Firefly luciferase activities were normalized to Renilla luciferase activities.

**2.9. TUNEL/Hoechst Double-Labeling.** TUNEL/Hoechst double-labeling was performed following the methods of Mao et al. to evaluate the apoptosis of the myocardial tissues [16]. Firstly, heart sections were fixated with 4% w/v formaldehyde solution for 10 min at 25°C and then rinsed with PBS. Subsequently, the sections were postfixed in formaldehyde and acetic acid at 4°C (5 min) and then washed with PBS. An equilibration buffer and working strength deoxynucleotide transferase were then added successively, and the sections were maintained at 37°C for 1 h. Following washing, the sections were immersed into Hoechst 33342 at 25°C (5 min). Negative control was just added a TUNEL reaction mixture. The examination of slides was performed at ×200 magnification, and photographs were obtained with an epifluorescence microscope (Nikon Eclipse 80i). The TUNEL-positive cells are expressed as the percentage.

**2.10. Hoechst Staining.** Hoechst staining was performed following the methods of Mao et al. to evaluate the apoptosis of H9C2 cells [16]. First, the cells were fixed with formaldehyde (4%) at 25°C for 10 min. After that, the formaldehyde was removed and the cells were rinsed twice with PBS. Then, the cells were incubated with Hoechst 33258 (Beyotime Insti-

tute of Biotechnology) at 25°C for 5 min. Following that, pictures of cell apoptosis were taken using a fluorescent microscope (Olympus; magnification: ×200) and cellular apoptotic percentage was evaluated as the following formula: Number of apoptosis bodies/(number of apoptotic cells + number of cells).

**2.11. Flow Cytometry Analysis.** Flow cytometry was used for assessing the apoptosis of H9C2 cells following the methods established by Mao et al. [16] First, H9C2 cells were treated with FITC-conjugated Annexin V (C1062M, Beyotime Institute of Biotechnology, 2.5%, v/v) and propidium iodide (PI) (5%, v/v) in dark at 25°C for 20 min. Thereafter, the cellular apoptosis and death of H9C2 cells were analyzed using flow cytometry (BD FACSCalibur; BD Biosciences). Cell apoptosis was analyzed using CellQuest Pro software (BD FACSCalibur; BD Biosciences; US): Cell death percentage = the percentage of early plus late apoptotic cells.

**2.12. Real-Time PCR.** Real-time PCR analysis was performed following the methods of Mao et al. [16] Total RNAs from myocardial tissues or H9C2 cells were extracted using TRIzol (Takara Biotechnology Co., Ltd.). The purity and concentration of RNA were determined using NanoDrop One spectrophotometer (ThermoFisher). Prior to PCR, the cDNAs were obtained using a reverse transcription kit (cat. no. DRR037A; Takara Bio, Inc.). Real-time PCR was conducted with ABI 7300 plus system (Applied Biosystems; Thermo Fisher Scientific, Inc.) using SYBR™ Green PCR Kit (Takara Bio, Inc.).  $\beta$ -Actin was defined as the internal reference. The  $2^{-\Delta\Delta Cq}$  method was used for data analysis, and results were expressed as the ratio of NOX2 mRNA to  $\beta$ -actin mRNA or miR-532-3p to U6 [17]. The following primers were used: miR-26a-5p forward: 5'-CGGCGGTTTTTGCGGTCTGGGCT-3', reverse: 5'-GTGCAGGGTCCGAGGT-3'; PTEN forward: 5'-AAGACCATAACCCACCACAGC-3', reverse: 5'-ACCAGTTCGTCCCTTTCCAG-3';  $\beta$ -actin forward, 5'-CCCATCTATGAGGGTTACGC-3' and reverse, 5'-TTTATGTCACGCACGATTTTC-3'.

**2.13. Western Blotting.** Western blotting analysis was performed following the methods of Mao et al. [16] Total protein from heart tissues or H9C2 cells was extracted using a cell lysis buffer (cat. no. P0013; Beyotime Institute of Biotechnology), and the protein concentration was determined using the bicinchoninic acid protein assay kit (cat. no. P0009; Beyotime Institute of Biotechnology). 40  $\mu$ g of protein from each sample was used for western blotting analysis. First, the protein was separated via 10% SDS-PAGE and transferred to PVDF membranes. Then, the membranes were occluded with 5% fat-free milk for 2 h and rinsed twice with PBS, each 5 min. After that, the PVDF membranes were incubated with primary antibodies (1:1000) against rabbit anti-PTEN (Santa Cruz Biotechnology, Inc.) or anti-caspase-3 (Santa Cruz Biotechnology, Inc.) or anti-AKT or anti-p AKT or  $\beta$ -actin (Santa Cruz Biotechnology, Inc.) for 16 h at 4°C in dark. Then, these membranes were rinsed twice with water (each 5 min) and incubated with a horseradish peroxidase-conjugated goat anti-rabbit secondary antibody (Beyotime



Institute of Biotechnology; 1:2000) for 2 h at 25°C. Then, enhanced chemiluminescence solutions (BeyoECL Plus kit; Amersham; Cytiva) and a ChemiDox XRS+ Imaging System (Bio-Rad Laboratories, Inc.) were used for protein visualization and imaging. ImageJ 1.43 (NIH) was used for densitometric analysis of protein bands. Results were expressed as the ratio to  $\beta$ -actin.

**2.14. Statistical Analysis.** Data are reported as means  $\pm$  SD and were assessed by GraphPad Prism Software (version 7, USA). Each experiment was performed repeatedly at least three times. The difference between two groups was evaluated by Student's *t*-test, and the comparison between more than two groups was analyzed by one-way ANOVA with Bonferroni's multiple comparisons test. A value of  $P = 0.05$  was regarded as a significant difference.

### 3. Results

**3.1. I/R Injury Contribute to Myocardial Infarction and Apoptosis.** To simulate myocardial ischemia clinically, we established a rat MIRI model. As Figures 1(a) and 1(b) show, the rats subjected to MIRI presented significant myocardial infarction (TTC staining of heart tissues is white). Then, we measured the activity of creatine kinase (CK) which is an important biomarker of acute myocardial infarction and found that rats underwent MIRI with higher CK activity when compared with control (Figure 1(c)). This suggested that MIRI caused myocardial cell death. Consistently, heart tissues subjected to MIRI with higher expression of cleaved caspase-3 (Figure 1(d)). Similarly, the TUNEL/Hoechst staining indicated that I/R obviously increased the apoptosis of heart tissues when compared to the control (Figures 1(e) and 1(f)). These data above indicated that MIRI resulted in cell apoptosis.

**3.2. The Effect of I/R on PTEN/AKT Signaling.** As AKT signaling is an important prosurvival pathway, its abnormal was closely associated with cell apoptosis. Our next experiment was designed to observe the effect of MIRI on PTEN/AKT signaling. Compared to the control group, the expression level of PTEN was significantly increased at both mRNA and protein in MIRI rats (Figures 2(a)–2(c)). Consistently, the phosphorylation of AKT in MIRI rats was significantly decreased, compared to the control group (Figures 2(b) and 2(d)). These data suggested that the high expression of PTEN contributed to insufficient of AKT phosphorylation was one of the main causes of MIRI.

**3.3. Bioinformatics Analysis and the Effect of I/R on the Expression of miR-129.** Considering that miRNAs has an important role in gene expression and is involved in many cellular functions, such as cell apoptosis, we then focused on the role of miRNA in PTEN expression regulation. Through bioinformatics analysis, we found that PTEN is a putative target of miR-129 (Figure 3(a)). As the present data show, compared to the control, the expression of miR-129 was significantly decreased in MIRI rats (Figure 3(b)). This indicated that there is a reverse relationship between the expression level of miR-129 and PTEN.

**3.4. The Effect of miR-129 on the Relative Luciferase Activity.** To further confirm the relationship between miR-129 and PTEN, we then performed a dual luciferase activity experiment. As shown in Figure 4, miR-129 mimics significantly decreased the relative luciferase activity of cells transfected with wild-type plasmid PTEN-WT (containing a wild seed sequence "UAAAAA" of PTEN 3'UTR), but not cells transfected with mutated plasmid PTEN-MU (containing a mutated seed sequence "UAAGAAA" of PTEN 3'UTR). Additionally, NC miRNA did not affect the relative luciferase activity of cells transfected with PTEN-WT or PTEN-MU plasmid. These data suggested that PTEN is a target of miR-129.

**3.5. miR-129 Mimics Reversed the Effect of H/R on PTEN/AKT Signaling in H9C2 Cells.** To simulate MIRI in vitro, H9C2 cells were subjected to H/R according to the methods described above. Consistent with the rat MIRI model, H/R significantly decreased the expression level of miR-129 in H9C2 cells (Figure 5(a)), accompanied with an increased expression level of PTEN (Figures 5(b)–5(d)) and insufficient phosphorylation of AKT (Figures 5(c) and 5(e)). Our next experiments were designed to observe whether miR-129 mimics can reverse the effect of H/R on PTEN/AKT signaling. As shown in Figure 5(a), miR-129 mimic (not NC miRNA) transfection significantly increased the expression level of miR-129 in H9C2 cells. This suggested that miR-129 mimics were successfully transfected into cells and work properly. As expected, miR-129 mimics significantly reversed the phenomenon that H/R induced an increase of PTEN expression in H9C2 cells, as well as decrease of AKT phosphorylation (Figures 5(b)–5(d)).

**3.6. miR-129 Mimics Reversed the Effect of H/R on Apoptosis in H9C2 Cells.** We then observed the effect of miR-129 mimics on apoptosis of H9C2 cells. As shown in Figures 6(a) and 6(b), compared with the control, H/R significantly increased the expression level of cleaved caspase-3. Consistently, the Hoechst staining results show that miR-129 mimics significantly inhibited the H/R-induced apoptosis in H9C2 cells (Figures 6(c) and 6(d)). Similarly, as shown in Figures 6(e) and 6(f), the apoptosis of H/R-induced H9C2 cells was obviously inhibited by miR-129 mimics. These data indicated that miR-129 is an important molecule related to the apoptosis of myocardial cell or a potential drug for the myocardial infarction therapy.

### 4. Discussion

Myocardial ischemia reperfusion injury is a common pathophysiological process in clinic, and its detailed mechanism is still need to be elucidated. In this study, we established in vivo and in vitro models to simulate MIRI clinically and found that PTEN/AKT signaling abnormal was closely associated with myocardial cell apoptosis. We found that low expression of miR-129 accelerates the myocardial cell apoptosis by directly targeting 3'UTR of PTEN. This suggested that miR-129 may be an important biomarker for MIRI and a target for its treatment.



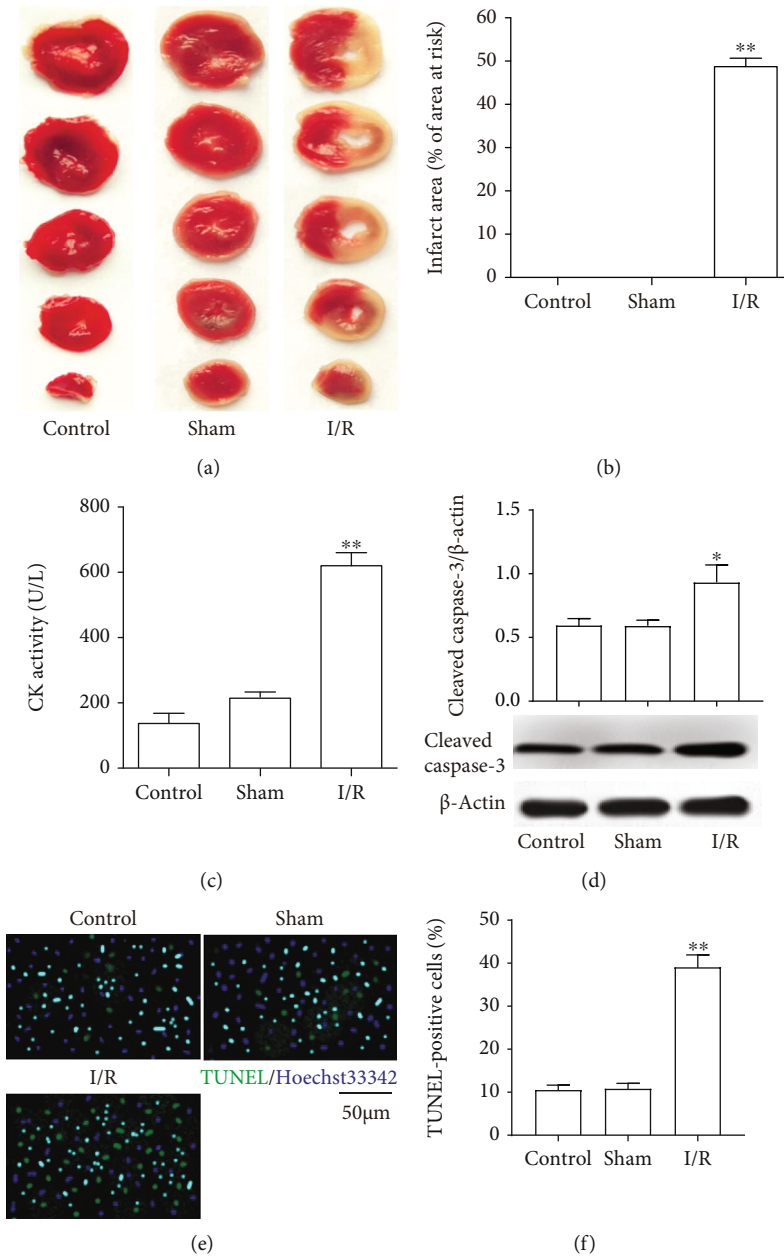


FIGURE 1: I/R injury contribute to myocardial infarction and apoptosis. (a) TTC staining. (b) Infarction area. (c) CK activity. (d) Cleaved caspase-3 protein expression. (e) TUNEL/Hoechst double staining. (f) TUNEL-positive cell counting. The differences of the values between the groups were analyzed by one-way ANOVA. All experiments were repeated 3 times, and all data are mean ± standard deviation. \* $P < 0.05$  vs. the control; \*\* $P < 0.01$  vs. the control.

PTEN, an upstream molecule of AKT signaling, involves in the development and progress of many diseases, such as tumor, stroke, and acute myocardial infarction [14, 15, 18]. A great many of studies have found that low expression of PTEN was closely associated with tumor cell viability, proliferation, migration, invasion, and drug resistance and found that inhibition of PTEN pharmacologically promotes tumors cell apoptosis [15, 19, 20]. Different from cancer, studies related to ischemic stroke and myocardial ischemia injury have found that high expression of PTEN was closely associated with neural cell or cardiomyocyte death and that knock-down of PTEN protects the neuron or cardiomyocyte from

ischemia injury [21, 22]. These data indicated that PTEN was a target for disease therapy (including cancer and stroke) or for drug development. Therefore, elucidating the detail mechanism of PTEN expression regulation becoming the most interested events in fundamental research or clinical research. In the past decades, a great many of studies were designed to investigate the role of miRNAs in PTEN expression regulation since miRNAs were found have crucial roles in gene expression. According to the report by Wei et al., in clinical specimens of multiple human cancers (breast cancer and bladder cancer), the expression of miR-130 family members correlated inversely with PTEN expression [23]. In

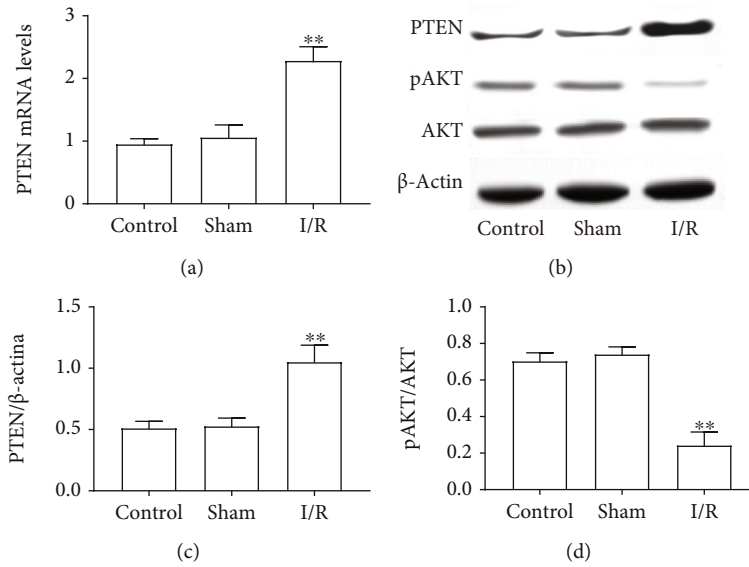


FIGURE 2: The effect of I/R on PTEN/AKT signaling. (a) mRNA level of PTEN. (b) Protein expression of PTEN, AKT, and pAKT. (c) The ratio of PTEN to  $\beta$ -actin. (d) The ratio of pAKT to AKT. The differences of the values between the groups were analyzed by one-way ANOVA. All experiments were repeated 3 times, and all data are mean  $\pm$  standard deviation. \*\* $P < 0.01$  vs. the control.

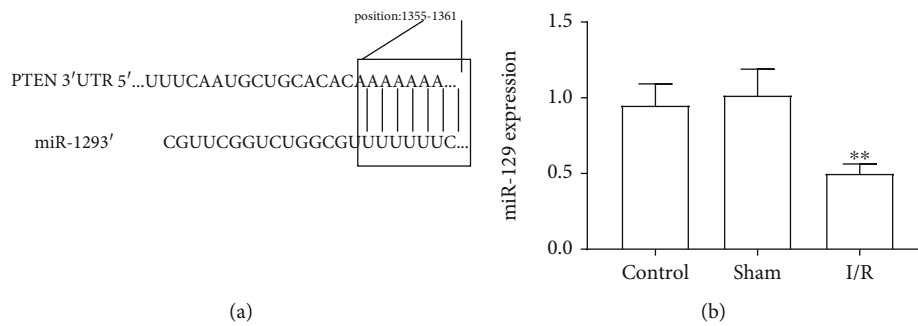


FIGURE 3: Bioinformatics analysis and the effect of I/R on the expression of miR-129. (a) Schematic diagram of bioinformatics analysis. (b). miR-129 expression level. The differences of the values between the groups were analyzed by one-way ANOVA. All experiments were repeated 3 times, and all data are mean  $\pm$  standard deviation. \*\* $P < 0.01$  vs. the control.

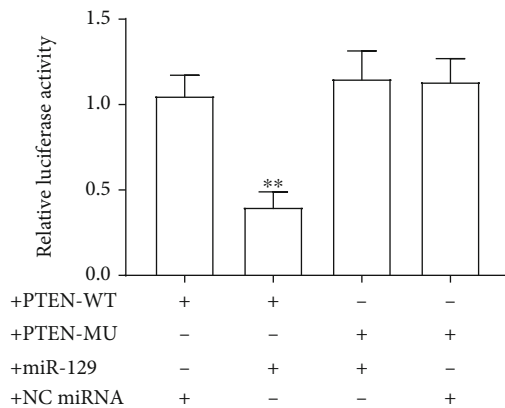


FIGURE 4: The effect of miR-129 on the relative luciferase activity. Relative luciferase activity. The differences of the values between the groups were analyzed by one-way ANOVA. All experiments were repeated 3 times, and all data are mean  $\pm$  standard deviation. \*\* $P < 0.01$  vs. the PTEN-WT+NC miRNA.

another study carried out by Zheng et al., they found that miR-130a exerts neuroprotective effects against ischemic stroke through the PTEN/PI3K/AKT pathway [24]. Besides miR-130a, in fact, more and more miRNAs were found negatively regulating the expression of PTEN, such as miR-301, miR-26, miR-19, miR-29, miR-140, miR-142, and miR-200 [18, 19, 25–27]. However, most of these studies were performed on cancer, and few were down on myocardial ischemia reperfusion injury. To further understand the miRNAs/PTEN axis in MIRI, therefore, more investigations should be performed to observe the interaction between miRNAs and PTEN in myocardial ischemia reperfusion injury.

During the process of MIRI, the expression of many miRNAs was found altered (downregulated or upregulated) in myocyte, for example, miR-130a, miR-26, and miR-193, and these miRNAs were biomarkers for MIRI. In this study, we focused on miR-129 and found that the expression of miR-129 was significantly downregulated in rats subjected to MIRI or in H9C2 cells subjected to H/R. In fact, miR-129 was a multifunctional biomolecule involving in the

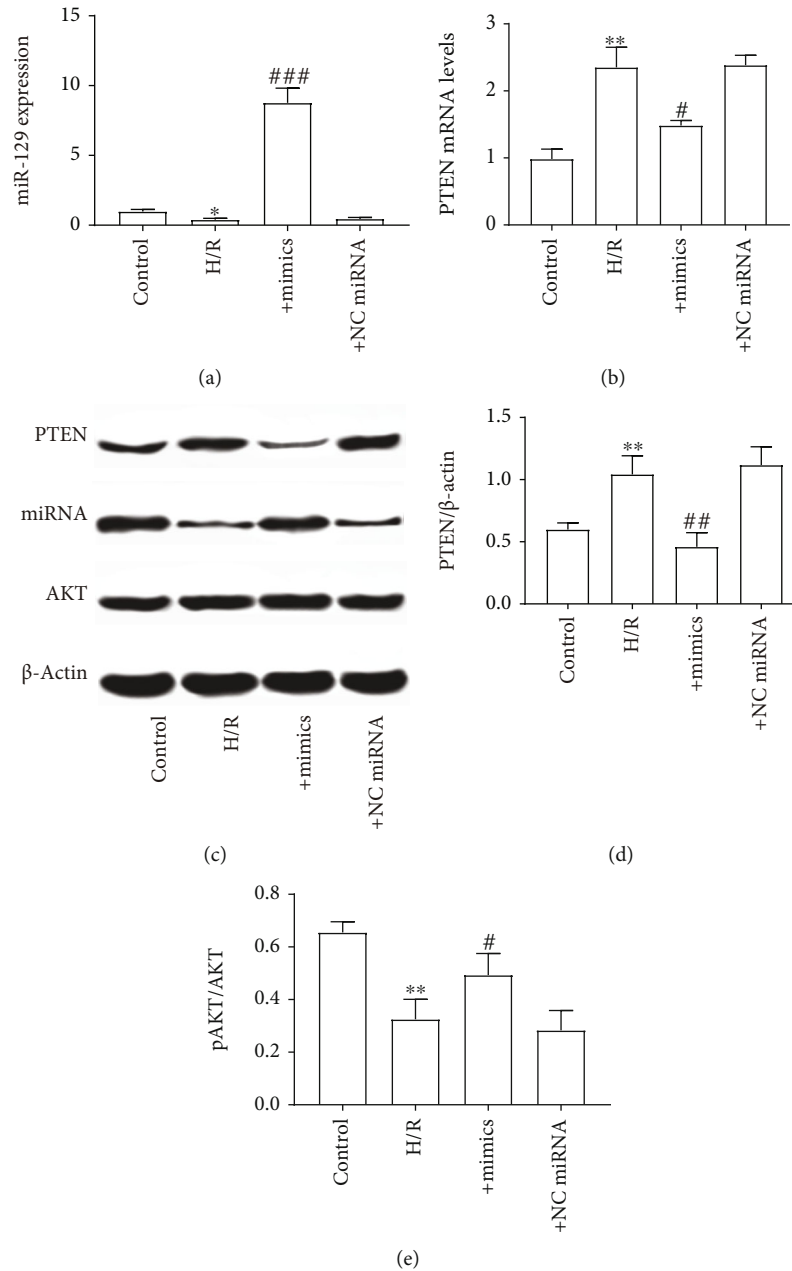


FIGURE 5: miR-129 mimics reversed the effect of H/R on PTEN/AKT signaling in H9C2 cells. (a) miR-129 expression level. (b) mRNA level of PTEN. (c) Protein expression of PTEN, AKT, and pAKT. (d) The ratio of PTEN to  $\beta$ -actin. (e) The ratio of pAKT to AKT. The differences of the values between the groups were analyzed by one-way ANOVA. All experiments were repeated 3 times, and all data are mean  $\pm$  standard deviation. \* $P < 0.05$  vs. the control; # $P < 0.05$  vs. H/R. \*\* $P < 0.01$  vs. H/R. ### $P < 0.001$  vs. H/R.

development and progression of many diseases, such as tumor [20, 28]. Recent studies found that miR-129 plays crucial roles in cardiovascular and cerebrovascular diseases, especially in myocardial ischemia reperfusion injury; for example, Chen et al. have found that miR-129-5p protects against myocardial ischemia-reperfusion injury via targeting HMGB1, and Ma et al. found that miR-129-5p alleviates myocardial injury by targeting suppressor of cytokine signaling 2 after ischemia/reperfusion [29, 30]. In addition, Zou et al. found that miR-129 is involved in the process of inflammation and apoptosis in cardiomyocytes by directly targeting

Smad3 [31]. These data above indicated that miR-129 is a potential biomarker for MIRI and a therapy target for myocardial infarction. Interestingly, the present study found that the expression of miR-129 (downregulated) was inversely correlated with the expression of PTEN (upregulated) in both the MIRI rat model and H/R cell model; this suggested that PTEN is a putative target of miR-129, and it was confirmed by miR-129 mimic transfection experiment and luciferase reporter gene experiment. As the results presented, miR-129 mimic significantly reversed the expression of PTEN in H/R-induced H9C2 cells, as well as the phosphorylation of

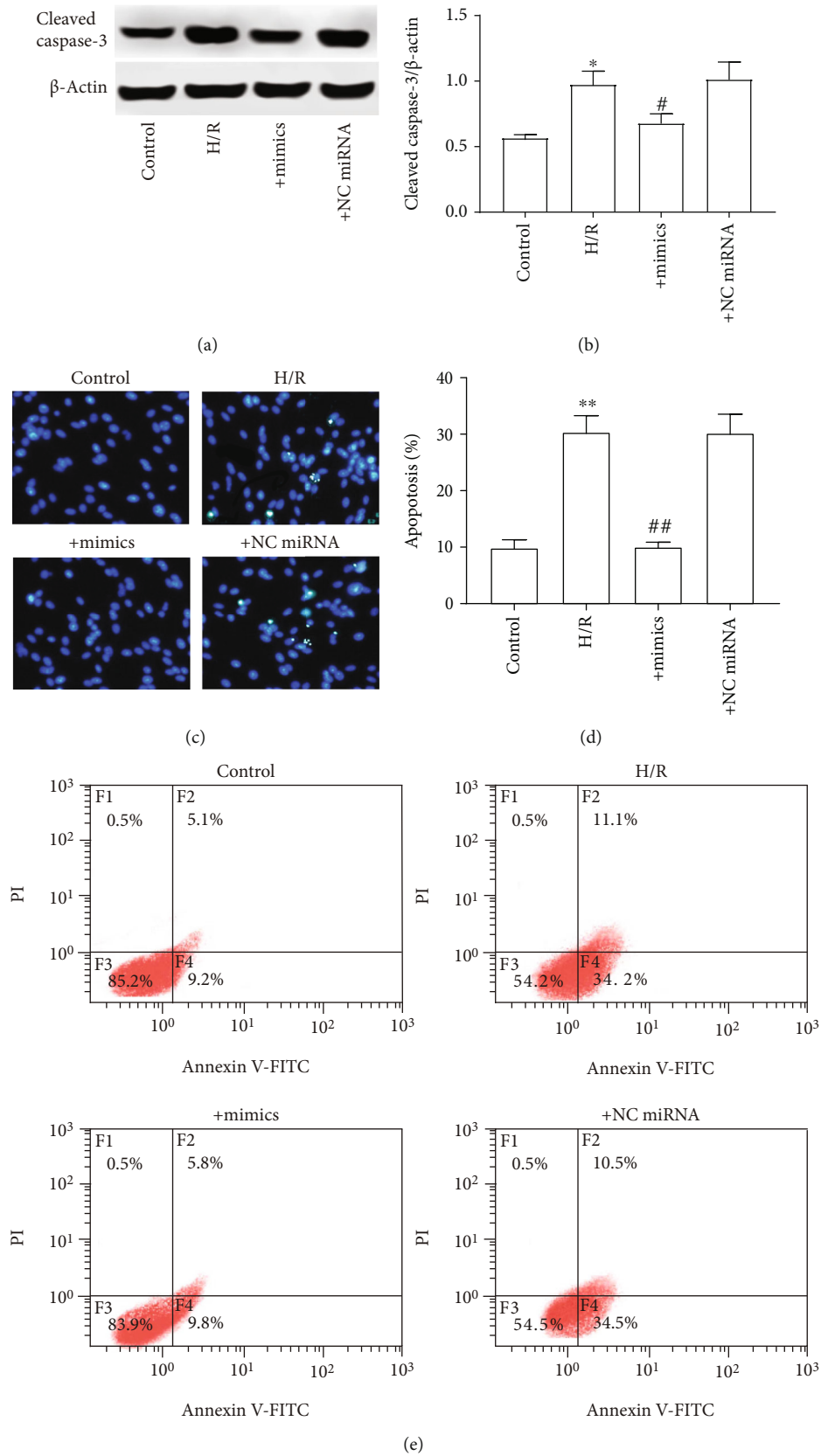


FIGURE 6: Continued.



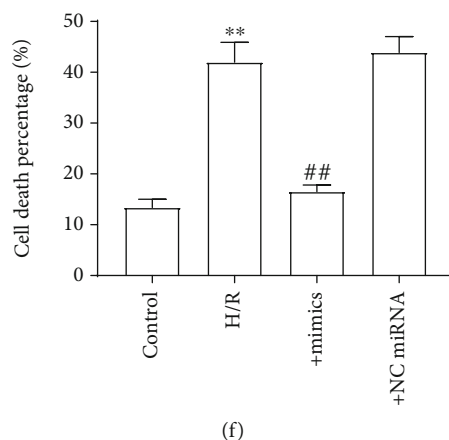


FIGURE 6: miR-129 mimics reversed the effect of H/R on apoptosis in H9C2 cells. (a) Cleaved caspase-3 protein expression. (b) The ratio of cleaved caspase-3 to  $\beta$ -actin. (c) Hoechst staining. (d) Apoptosis rate. (e) Presentative images of cell apoptosis by flow cytometer. (f) The percentage of cell death. The differences of the values between the groups were analyzed by one-way ANOVA. All experiments were repeated 3 times, and all data are mean  $\pm$  standard deviation. \* $P < 0.05$  vs. the control; \*\* $P < 0.01$  vs. the control; # $P < 0.05$  vs. H/R; and ## $P < 0.01$  vs. H/R.

AKT. Moreover, miR-129 mimic significantly decreased the relative luciferase activity. These data demonstrated that miR-129 is involved in MIRI by directly targeting PTEN. However, different from our findings, Xie et al. have found that miR-129 can inhibit the phosphorylation of AKT by binding to the 3'UTR of PI3KCA and LINC00198 as a sponge of miR-129 play roles in PTEN expression inhibition by regulating the formation of REST, RCOR1, and HDAC2 [32]. This suggested that miR-129 can regulate AKT phosphorylation from many ways. In addition, considering mTOR is the direct downstream of PTEN-Akt signaling and a key protein responsible for the regulation of many signaling pathway, such as proliferation- and apoptosis-related pathways, we predict miR-129 may be a potential target for salvage of myocardial ischemia in the future [33]. However, before miR-129 as a drug or therapy used clinically, there are a lot of works still need to be done. There are many limitations of this study; for example, the function study of miR-129 only performed in an in vitro model and whether it also come into play in vivo model are still not known. In addition, MIRI is a pathological process that was closely associated with metabolism dysfunction of the myocardium. So, whether miR-129 is involved in the mitochondrial oxidative phosphorylation process deserved further exploring.

This study firstly demonstrated that miR-129 ameliorates myocardial cell apoptosis by directly target 3'UTR of PTEN. This suggested that the miR-129/PTEN axis is a potential target for MIRI therapy.

## Data Availability

The dataset used and/or analyzed during the current study are available from the corresponding author on reasonable request.

## Conflicts of Interest

These authors declared no conflict of interest.

## Authors' Contributions

Zhi-Ming Jiang, Fang Liu, Hua Tu, and Li Mao performed the experiments. Fang Liu and Md Sayed Ali Sheikh contributed to the data analysis and manuscript drafting. Zhao-Hui Dai, Gui-Lin Song, and Zhong-Bao Yang contributed to the design of the experiments and drafting of the manuscript. All authors have read and approved the manuscript. Zhi-Ming Jiang and Fang Liu contributed equally to this work.

## Acknowledgments

This work was supported by the HuNan Provincial Science and Technology Department (No. 2020JJ5384 to Zhong-Bao Yang), Education Department of HuNan Province (No. 18C1853 to Li Mao), and ChangSha Science & Technology Bureau (No. kq2004153 to Zhong-Bao Yang).

## Supplementary Materials

Figure S1: image of plasmids electrophoresis. Representative image of plasmid electrophoresis. pGL6: vector plasmid; PTEN-WT: plasmid containing the wild-type (WT) binding sites of miR-129-5p; PTEN-MU: plasmid containing the mutant (MUT) binding sites of miR-129-5p; control: water. (*Supplementary Materials*)

## References

- [1] L. M. Buja, "Myocardial ischemia and reperfusion injury," *Cardiovascular pathology*, vol. 14, no. 4, pp. 170–175, 2005.
- [2] A. Frank, M. Bonney, S. Bonney, L. Weitzel, M. Koeppen, and T. Eckle, "Myocardial ischemia reperfusion injury: from basic science to clinical bedside," *Seminars in Cardiothoracic and Vascular Anesthesia*, vol. 16, no. 3, pp. 123–132, 2012.
- [3] Z. Liu, B. Tao, S. Fan, Y. Pu, H. Xia, and L. Xu, "MicroRNA-145 protects against myocardial ischemia reperfusion injury via CaMKII-mediated antiapoptotic and anti-inflammatory

- pathways," *Oxidative medicine and cellular longevity*, vol. 2019, Article ID 8948657, 14 pages, 2019.
- [4] B.-F. Guan, X.-F. Dai, Q.-B. Huang et al., "Icariside II ameliorates myocardial ischemia and reperfusion injury by attenuating inflammation and apoptosis through the regulation of the PI3K/AKT signaling pathway," *Molecular Medicine Reports*, vol. 22, no. 4, pp. 3151–3160, 2020.
  - [5] W. Xu, L. Zhang, S. Ma et al., "TRAF5 protects against myocardial ischemia reperfusion injury via AKT signaling," *Journal de Pharmacologie*, vol. 878, article 173092, 2020.
  - [6] C.-M. Li, S.-W. Shen, T. Wang, and X.-H. Zhang, "Myocardial ischemic post-conditioning attenuates ischemia reperfusion injury via PTEN/Akt signal pathway," *International Journal of Clinical and Experimental Medicine*, vol. 8, no. 9, pp. 15801–15807, 2015.
  - [7] T. X. Lu and M. E. Rothenberg, "MicroRNA," *Journal of allergy and clinical immunology*, vol. 141, no. 4, pp. 1202–1207, 2018.
  - [8] B. C. Bernardo, J. Y. Y. Ooi, R. C. Y. Lin, and J. R. McMullen, "miRNA therapeutics: a new class of drugs with potential therapeutic applications in the heart," *Future medicinal chemistry*, vol. 7, no. 13, pp. 1771–1792, 2015.
  - [9] Y. S. Lee and A. Dutta, "MicroRNAs in cancer," *Annual Review of Pathology*, vol. 4, no. 1, pp. 199–227, 2009.
  - [10] X. Xing, S. Guo, G. Zhang et al., "miR-26a-5p protects against myocardial ischemia/reperfusion injury by regulating the PTEN/PI3K/AKT signaling pathway," *Brazilian Journal of Medical and Biological Research*, vol. 53, no. 2, article e9106, 2020.
  - [11] X. Wang, X. Zhang, X.-P. Ren et al., "MicroRNA-494 targeting both proapoptotic and antiapoptotic proteins protects against ischemia/reperfusion-induced cardiac injury," *Circulation*, vol. 122, no. 13, pp. 1308–1318, 2010.
  - [12] D.-W. Liu, Y.-N. Zhang, H.-J. Hu, P.-Q. Zhang, and W. Cui, "Downregulation of microRNA-199a-5p attenuates hypoxia/reoxygenation-induced cytotoxicity in cardiomyocytes by targeting the HIF-1 $\alpha$ -GSK3 $\beta$ -mPTP axis," *Molecular Medicine Reports*, vol. 19, no. 6, pp. 5335–5344, 2019.
  - [13] Q. Gao and Y. Wang, "Long noncoding RNA MALAT1 regulates apoptosis in ischemic stroke by sponging miR-205-3p and modulating PTEN expression," *American Journal of Translational Research*, vol. 12, no. 6, pp. 2738–2748, 2020.
  - [14] S. Cheng, X. Zhang, Q. Feng et al., "Astragaloside IV exerts angiogenesis and cardioprotection after myocardial infarction via regulating PTEN/PI3K/Akt signaling pathway," *Life Sciences*, vol. 227, pp. 82–93, 2019.
  - [15] X. Xia, K. Zhang, G. Luo et al., "Downregulation of miR-301a-3p sensitizes pancreatic cancer cells to gemcitabine treatment via PTEN," *American Journal of Translational Research*, vol. 9, no. 4, pp. 1886–1895, 2017.
  - [16] L. Mao, M.-I. Zuo, A.-P. Wang et al., "Low expression of miR-532-3p contributes to cerebral ischemia/reperfusion oxidative stress injury by directly targeting NOX2," *Molecular Medicine Reports*, vol. 22, no. 3, pp. 2415–2423, 2020.
  - [17] K. J. Livak and T. D. Schmittgen, "Analysis of Relative Gene Expression Data Using Real-Time Quantitative PCR and the 2<sup>- $\Delta\Delta$</sup> -C<sub>T</sub> Method," *Methods*, vol. 25, no. 4, pp. 402–408, 2001.
  - [18] N. Chalhoub and S. J. Baker, "PTEN and the PI3-kinase pathway in cancer," *Annual Review of Pathology*, vol. 4, no. 1, pp. 127–150, 2009.
  - [19] L. R. Zeitels, A. Acharya, G. Shi et al., "Tumor suppression by miR-26 overrides potential oncogenic activity in intestinal tumorigenesis," *Genes & Development*, vol. 28, no. 23, pp. 2585–2590, 2014.
  - [20] X. Wang, J. Li, X. Xu, J. Zheng, and Q. Li, "miR-129 inhibits tumor growth and potentiates chemosensitivity of neuroblastoma by targeting MYO10," *Biomedicine & Pharmacotherapy*, vol. 103, pp. 1312–1318, 2018.
  - [21] Q. Cui, J. Wang, X. Liu, X. Wang, and G. Su, "Knockout of PTEN improves cardiac function and inhibits NLRP3-mediated cardiomyocyte pyroptosis in rats with myocardial ischemia-reperfusion," *Xi Bao Yu Fen Zi Mian Yi Xue Za Zhi*, vol. 36, no. 3, pp. 205–211, 2020.
  - [22] A. P. Shabanzadeh, P. M. D'Onofrio, M. Magharious, K. A. B. Choi, P. P. Monnier, and P. D. Koeberle, "Modifying PTEN recruitment promotes neuron survival, regeneration, and functional recovery after CNS injury," *Cell death & disease*, vol. 10, no. 8, p. 567, 2019.
  - [23] H. Wei, R. Cui, J. Bahr et al., "miR-130a deregulates PTEN and stimulates tumor growth," *Cancer Research*, vol. 77, no. 22, pp. 6168–6178, 2017.
  - [24] T. Zheng, Y. Shi, J. Zhang et al., "MiR-130a exerts neuroprotective effects against ischemic stroke through PTEN/PI3K/AKT pathway," *Biomedicine & Pharmacotherapy*, vol. 117, article 109117, 2019.
  - [25] G.-F. Zhang, J.-M. Zhong, L. Lin, and Z.-H. Liu, "MiR-19 enhances pancreatic cancer progression by targeting PTEN through PI3K/AKT signaling pathway," *European Review for Medical and Pharmacological Sciences*, vol. 24, no. 3, pp. 1098–1107, 2020.
  - [26] R. Yin, J. Jiang, H. Deng, Z. Wang, R. Gu, and F. Wang, "miR-140-3p aggregates osteoporosis by targeting PTEN and activating PTEN/PI3K/AKT signaling pathway," *Human cell*, vol. 33, no. 3, pp. 569–581, 2020.
  - [27] H. Li, J. Tang, H. Lei et al., "Decreased miR-200a/141 suppress cell migration and proliferation by targeting PTEN in Hirschsprung's disease," *Cellular Physiology and Biochemistry*, vol. 34, no. 2, pp. 543–553, 2014.
  - [28] Q. Wang and J. Yu, "MiR-129-5p suppresses gastric cancer cell invasion and proliferation by inhibiting COL1A1," *Biochemistry and Cell Biology*, vol. 96, no. 1, pp. 19–25, 2018.
  - [29] Z.-X. Chen, D. He, Q.-W. Mo et al., "MiR-129-5p protects against myocardial ischemia-reperfusion injury via targeting HMGB1," *European Review for Medical and Pharmacological Sciences*, vol. 24, no. 8, pp. 4440–4450, 2020.
  - [30] R. Ma, X. Chen, Y. Ma, G. Bai, and D.-S. Li, "MiR-129-5p alleviates myocardial injury by targeting suppressor of cytokine signaling 2 after ischemia/reperfusion," *The Kaohsiung Journal of Medical Sciences*, vol. 36, no. 8, pp. 599–606, 2020.
  - [31] Y. Zou and M. Kong, "Tetrahydroxy stilbene glucoside alleviates palmitic acid-induced inflammation and apoptosis in cardiomyocytes by regulating miR-129-3p/Smad3 signaling," *Cellular & Molecular Biology Letters*, vol. 24, no. 1, p. 5, 2019.
  - [32] Y. Xie and Y. Cheng, "LINC01198 facilitates gliomagenesis through activating PI3K/AKT pathway," *RNA Biology*, vol. 17, no. 7, pp. 1040–1052, 2020.
  - [33] T. Li, J. Gu, O. Yang, J. Wang, Y. Wang, and J. Kong, "Bone marrow mesenchymal stem cell-derived exosomal miRNA-29c decreases cardiac ischemia/reperfusion injury through inhibition of excessive autophagy via the PTEN/Akt/mTOR signaling pathway," *Circulation Journal*, vol. 84, no. 8, pp. 1304–1311, 2020.

## Review Article

# Roles of MicroRNAs in Peripheral Artery In-Stent Restenosis after Endovascular Treatment

Mo Wang,<sup>1,2</sup> Weichang Zhang,<sup>1,2</sup> Lei Zhang,<sup>1,2</sup> Lunchang Wang,<sup>1,2</sup> Jiehua Li,<sup>1,2</sup>  
Chang Shu,<sup>1,2,3</sup> and Xin Li <sup>1,2</sup>

<sup>1</sup>Department of Vascular Surgery, The Second Xiangya Hospital, Central South University, Changsha, Hunan, China 410011

<sup>2</sup>The Institute of Vascular Diseases, Central South University, Changsha, Hunan, China 410011

<sup>3</sup>State Key Laboratory of Cardiovascular Diseases, Center of Vascular Surgery, Fuwai Hospital, National Center for Cardiovascular Diseases, Chinese Academy of Medical Science and Peking Union Medical College, Beijing, China 100037

Correspondence should be addressed to Xin Li; [lixin1981@csu.edu.cn](mailto:lixin1981@csu.edu.cn)

Received 13 March 2021; Accepted 13 July 2021; Published 28 July 2021

Academic Editor: Burak Durmaz

Copyright © 2021 Mo Wang et al. This is an open access article distributed under the Creative Commons Attribution License, which permits unrestricted use, distribution, and reproduction in any medium, provided the original work is properly cited.

Endovascular repair including percutaneous transluminal angioplasty (PTA) and stent implantation has become the standard approach for the treatment of peripheral arterial disease; however, restenosis is still the main limited complication for the long-term success of the endovascular repair. Endothelial denudation and regeneration, inflammatory response, and neointimal hyperplasia are major pathological processes occurring during in-stent restenosis (ISR). MicroRNAs exhibit great potential in regulating several vascular biological events in different cell types and have been identified as novel therapeutic targets as well as biomarkers for ISR prevention. This review summarized recent experimental and clinical studies on the role of miRNAs in ISR modification, with the aim of unraveling the underlying mechanism and potential therapeutic strategy of ISR.

## 1. Introduction

Peripheral arterial disease (PAD) affects approximately 12-14% of the general population, and its prevalence increased to 15-20% in patients over 70 years. The prevalence of symptomatic intermittent claudication reaching 6% in patients over 60 years, 5-10% of patients with PAD will eventually progress to critical limb ischemia [1, 2]. PAD is a part of a diffuse atherosclerosis of the whole vasculature including coronary arteries, and it has been classified as a coronary heart disease risk equivalent, i.e., the PAD patients are at an exceptionally high risk for cardiovascular events.

There are various revascularization strategies to treat PAD, including percutaneous transluminal angioplasty (PTA), stent implantation, atherectomy, thrombectomy and interposition of the venous, and arterial or synthetic bypass graft. Endovascular treatment, including PTA and stent implantation, has become the standard approach for the femoropopliteal arterial occlusive disease [3]. Compared to PTA alone, stent implantation can prevent early elastic recoil

and late constrictive remodeling. It can effectively maintain lumen volume when encountering residual stenosis or flow-limiting dissection after PTA. Therefore, stent implantation in PAD is highly prevalent especially for a longer and more complex femoropopliteal arterial lesion. However, the high incidence of in-stent restenosis (ISR) restricts the development of endovascular techniques, and it became the major cause of endovascular treatment failure and reintervention. Approximately 20-40% of PAD patients treated with bare metal stent develop ISR depending on complexity and severity, localization, and length of the lesion [4].

Bare metal stent (BMS) has been widely applied to PAD endovascular treatment; its metal scaffold implantation undoubtedly will lead to severe target vessel injury and provoke pathobiological cascade leading to neointimal hyperplasia. Compare to BMS, drug-eluted stent (DES) provides localized antiproliferative drug delivery and can effectively reduce the incidence of neointimal hyperplasia and ISR. However, the nonselective drugs also inhibit reendothelialization and healing of the injured artery and lead to fatal late

phase thrombosis, therefore still far from optimized and fail to eliminate ISR [5]. As such, a cell-specific therapy targeting ISR is imperatively needed. And miRNA-based strategy may offer an alternative approach for preventing ISR. In this review, we discussed the roles of miRNAs in ISR and explored the underlying mechanism and potential therapeutic miRNA-based strategy of ISR

## 2. The Pathophysiology of In-Stent Restenosis (ISR)

Once a stent was inserted into an obstructive arterial lesion, it induces an acute mechanical injury to the diseased blood vessel. The initial events immediately after stent implantation are endothelium denudation, a crush of the plaque, often accompanied with dissection into media, even adventitia, the stretch of the entire artery [6, 7]. Endothelium act as a selectively permeable barrier between the tunica media, and blood flow participates in the regulation of vascular tone and suppression of neointimal hyperplasia mainly caused by the underlying vascular smooth muscle cells (VSMCs). This alternation of endothelium is followed by the deposition of a layer of platelets and fibrin at the injured site and initiates a cascade of inflammatory response. Activated platelet expressed adhesion molecules such as P-selectin which attach to and recruit circulating leukocytes to the injured vessel. A component of leucocyte secretory granules, Mac-1 [8], promotes leukocyte that binds tightly to the surface of injured endothelial cells (ECs). The migration of leukocytes across the platelet-fibrin layer and into the tissue (i.e., leukocyte infiltration) is driven by a group of chemoattractant cytokines produced by SMCs, ECs, and resident leukocytes, such as monocyte chemoattractant protein-1 (MCP-1) and interleukin- (IL-) 8. Next is an SMC proliferation and migration phase. Growth factors, such as fibroblast growth factor (FGF), platelet-derived growth factor (PDGF), vascular endothelial growth factor (VEGF), and transforming growth factor-beta (TGF- $\beta$ ), released from platelets, leukocytes, and SMCs, stimulate proliferation and migration of SMC from the media into the neointima, leading to neointimal thickening consequently. The resultant neointima consists of SMCs, extracellular matrix (ECM) synthesis by SMCs, and macrophages recruited over several weeks [6, 7]. Compared to balloon angioplasty alone, stent implantation results in an increased and sustained inflammatory response and larger neointimal growth ultimately [7]. The late phase of ISR is vascular remodeling involving ECM protein degradation and resynthesis. There is a shift towards greater ECM synthesis rather than SMC proliferative activity [9]. ECM is composed of various collagen subtypes and proteoglycans and constitutes the major component of the mature restenotic plaque [10]. Besides, there is eventual reendothelialization (i.e., the regeneration and regrowth of the denuded endothelium) of at least part of the injured vessel surface. The reendothelialization is originated from remaining locally derived ECs and circulating endothelial progenitor cells from the blood, and it is always found to be inadequate in terms of both barrier integrity and functionality with impaired endothelium-dependent vasodilation and increased perme-

ability [11]. An integrated view of pathophysiology of ISR has been shown in Figure 1.

## 3. General Introduction to MicroRNA

MicroRNAs (miRNAs) are short (17-25 nucleotides long), single-stranded, generally noncoding RNAs. Through the binding to miRNA-response elements (MREs) within the 3'-untranslated regions (3-UTRs) of target genes, miRNAs regulate their gene expression via posttranscriptional degradation or translational repression [12]. Most miRNA genes are located in intronic regions; they are commonly transcribed into primary-miRNA (pri-miRNA) by RNA polymerase II in the nucleus. Then, the enzyme complex of Drosha-Dgcr8 facilitates the processing of pri-miRNAs into a ~60-70 hairpin-structured precursor miRNA (pre-miRNA). Pri-miRNAs are transported to the cytoplasm from nucleus via exportin 5, the RanGTPdependent nuclear export factor. In the cytoplasm, pro-miRNAs are further processed by the RNase III enzyme complex into mature duplex miRNA. One strand of the mature microRNA is incorporated into the miRNA-induced silencing complex (miRISC), while the other strand is usually degraded [13].

A single miRNA can regulate multiple genes, and a single gene can be regulated by multiple miRNAs. Moreover, miRNAs interact with each other to form a cotargeting network, which allows miRNAs to play an essential role in the powerful and fine regulation of almost every vascular biology. Numerous studies unravel miRNAs that act as potential biomarkers or therapeutic targets of many cardiovascular diseases [13, 14]. Of which, miRNAs have been associated with ISR-related process, such as neointimal hyperplasia, inflammatory response, and regeneration of endothelial layer (Table 1 and Figure 1).

## 4. miRNAs Involved in Neointimal Formation

Restenosis is defined as the arterial wall's healing response to mechanical injury. The key pathophysiologic phenomenon responsible for restenosis after stent implantation is the neointimal formation which consists of VSMC proliferation, migration, and ECM deposition [6, 15]. The metallic scaffold of BMS prevents vessel shrinkage (i.e., elastic recoil and negative remodeling), however, induces an enhanced neointimal hyperplasia response [6].

VSMCs within adult blood vessels are highly specialized, and they play an important role in regulating blood vessel tone, blood pressure, and blood flow distribution. Under normal conditions, VSMCs proliferate at a very low rate, exhibit low synthetic activity, and express a repertoire of contractile proteins, ion channels, and signaling molecules required for its contractile function. Although fully differentiated, VSMCs retain remarkable plasticity. In response to vascular injury induced by stent implantation, VSMCs dramatically increase their rate of cell proliferation, migration, and synthetic capacity, transiently modify their phenotype to a high "synthetic" phenotype, hence starting to proliferate and migrate to the vessel interior, causing the lumen reduction. Kearney et al. [16] retrieved in-stent restenotic tissue by directional



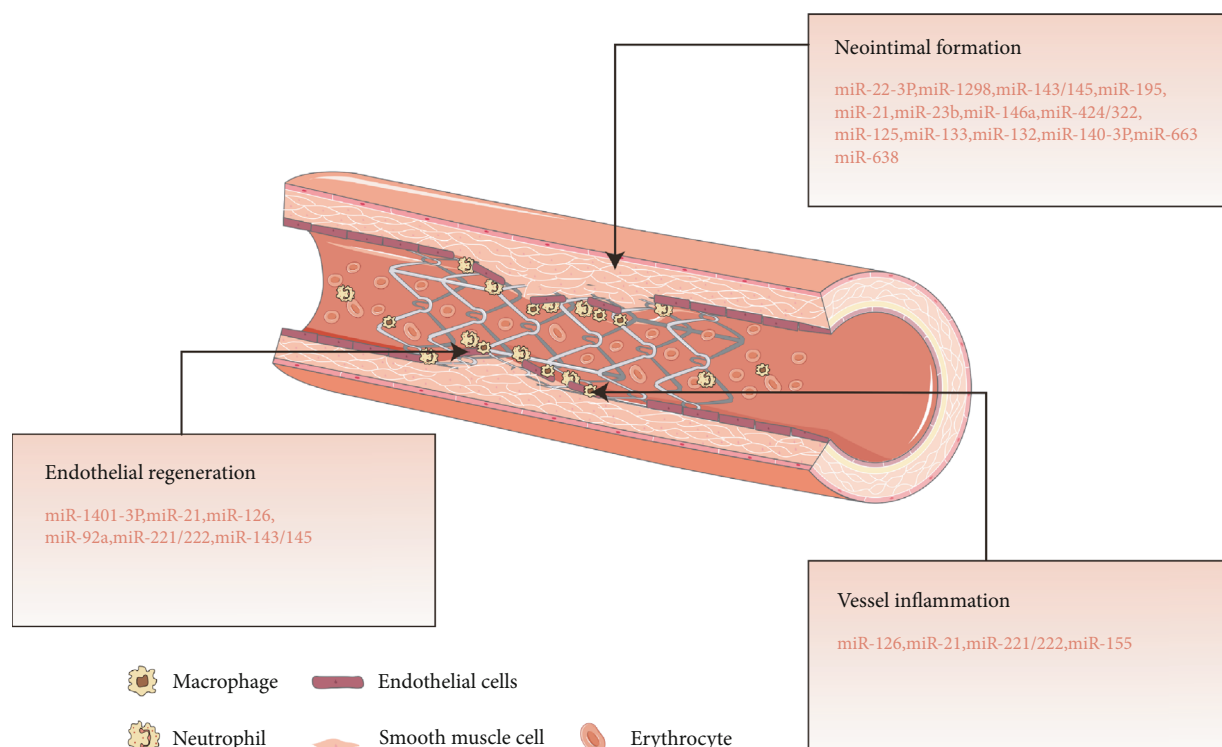


FIGURE 1: miRNA involved in in-stent restenosis (ISR). The schematic depicts the pathophysiology of ISR. Vessel inflammation, neointimal formation, and endothelial regeneration are three key processes of ISR, regulated by multiple miRNAs, respectively (see text and Table 1 for details on mechanism of all displayed miRNAs).

atherectomy from 10 patients after percutaneous revascularization of PAD and demonstrated that the in-stent restenotic tissue composed predominantly of SMCs. Upon resolution of injury, VSMCs reacquire their contractile phenotype [17, 18].

Among several miRNAs, the miR-143/-145 cluster is highly expressed in VSMCs and is known as an essential mediator of SMC proliferation, differentiation, and phenotypic switching [19]. miR-143 and miR-145 are located on human chromosome 5, and they were cotranscribed as a bicistronic unit. They cooperatively target a network of transcription factors, including Kruppel-like factor- (Klf-) 4, Klf-5, Elk-1, myocardin, angiotensin converting enzyme (ACE), calmodulin kinase II  $\delta$ , fascin, and myocardin-related transcription factor-beta (MRTF- $\beta$ ) [19, 20]. Vascular injury leads to downregulation of miR-145 in VSMCs; the downregulated miR-145 results in increased Klf-5 expression, which miR-145 directly targeting, as well as decreased myocardin and VSMC differentiation markers, e.g., smooth muscle alpha-actin, calponin, and smooth muscle myosin heavy chain (SM-MHC), inhibits migration but promotes differentiation of VSMCs [21]. miR-143 also contributes to the maintenance of VSMC contractile phenotype and suppression of VSMC proliferation, mainly through targeting Elk-1 [19].

miR-195 is also involved in the modulation of VSMC physiology. The overexpression of miR-195 inhibited VSMC proliferation and migration and therefore suppressed the neointimal hyperplasia after vascular injury through downregulating Cdc42 and its downstream mediator cyclinD1 (CCND1), which are responsible for cell cycle regulation

and cell growth [22]. Similarly, miR-125a-5p is downregulated after a vascular injury caused by angioplasty. Its expression level is inversely correlated to the proliferative status: when miR-125a-5p is overexpressed, proliferation and migration of VSMCs are reduced. On the other hand, miR-125a-5p is positively correlated to the expression of Alpha Smooth Muscle Actin 2 (ACTA2), Myosin Heavy Chain 11 (MYH11), and Smooth Muscle 22 alpha (SM22 $\alpha$ ) which characterizes the contractile phenotype of VSMCs: these marker gene expressions are decreased during VSMC phenotypic switch from contractile to synthesis. Of note, miR-125a-5p is directly target to E26 transformation specific-1 (ETS-1), an important transcriptional factor of VSMC proliferation and migration, and is crucial in PDGF-BB pathway in VSMCs. With the stimuli of vascular injury, miR-125a-5p is downregulated, and ETS-1 upregulated consequently, promoting VSMC phenotypic switch mediated by PDGF-BB, a potent mitogen for VSMCs [23, 24]. Recently, miR-125-3p downregulation was detected in VSMC of patient suffer PAD. miR-125-3p exhibits an antiproliferative effect on VSMC via targeting mitogen-activated protein kinase (MAPK) 1, a common hub of the MAPK signaling pathway and the insulin signaling pathway [25].

miR-23b is a member of gene cluster consisting of miR-23b, miR-27b, and miR-24-1 [26]. miR-23b is downregulated after vascular injury in vivo. The experimental study showed that miR-23b overexpression is responsible for the upregulation of ACTA2 and MYH11, the markers of the contractile phenotype of VSMC, and consequently inhibits VSMC

TABLE 1: miRNAs involved in ISR progression.

(a)

miRNAs	Expressed cell type	Up (↑) and down (↓) regulation after vascular injury	Function regulated	Target gene(s)	Preclinical model	Ref
miR-143/145	VSMC	↓	Differentiation, migration, proliferation	Klf-4, Klf-5, Elk-1	Carotid artery balloon injury model in Sprague-Dawley rat	[19, 21]
miR-195	VSMC	↓	Proliferation, migration	Cdc-42, CCND1	Carotid artery balloon injury model in Sprague-Dawley rat	[22]
miR-125	VSMC	↓	Proliferation, migration	ETS-1, MAPK1	Carotid artery balloon injury model in Sprague-Dawley rat and Wistar rat	[23, 25]
miR-23b	VSMC	↓	Proliferation, migration	uPA, Smad3, FOXO4	Carotid artery balloon injury model in Wistar rat	[27]
miR-663	VSMC	↓	Proliferation, migration	JunB, Myl9	Carotid artery ligation injury model in C57BL/6N mice	[30]
miR-140-3p	VSMC	↓	Proliferation, apoptosis	c-Myb, Bcl-2	Carotid artery restenosis model in Sprague-Dawley rat	[31]
miR-22-3p	VSMC	↓ (in ASO)	Proliferation, migration	HMGBl	Carotid artery balloon injury model in rat	[32]
miR-1298	VSMC	↓ (in ASO)	Proliferation, migration	Cx43	Carotid artery balloon injury model in rat	[33]
miR-21	VSMC	↑	Proliferation, migration, apoptosis	PTEN, Bcl-2	Thoracic aorta stent implantation in mice	[35, 46]

(b)

miRNAs	Expressed cell type	Up (↑) and down (↓) regulation after vascular injury	Function regulated	Target gene(s)	Preclinical model	Ref
miR-146	VSMC	↑	Proliferation	Klf-4, Klf-5	Carotid artery balloon injury model in rat	[37]
miR-424/322	VSMC	↑	Proliferation, migration, apoptosis	CCND1, STIM1	Carotid artery balloon injury model in rat	[38]
miR-133	VSMC	↓ (in early phase), ↑ (in late phase)	Proliferation, migration	Sp-1, moesin	Carotid artery balloon injury model in rat	[39]
miR-132	VSMC	↓ (in early phase), ↑ (in late phase)	Proliferation, migration, apoptosis, survival	LRRFIP1	Carotid artery injury model in rat	[40]
miR-638	VSMC	—	Proliferation, migration	NORI	—	[41]
miR-126	EC	—	Proliferation, migration	Spred-1, VCAM-1	Iliac artery neointimal formation model in rabbit	[51]
miR-92a	EC	↑	Proliferation, migration, NO release	BMPr2, Klf-4, MKK4	Carotid artery balloon injury model in Wistar rat	[53, 55]
miR-221/222	VSMC and EC	↑	Proliferation in VSMC, proliferation, migration, apoptosis in EC	p27 (Kip1), p57 (Kip2), c-kit, ETS-1, ICAM-1	Carotid artery balloon injury model in rat	[47, 56, 57]

proliferation, migration, and neointimal formation after stent implantation. And this effect is mediated by miR-23b directly targets to urokinase plasminogen activator (uPA), Smad3, and Forkhead box O4 (FOXO4) which are the essential modulators of VSMC proliferation, migration, and phenotypic switch [27–29]. Similarly, the other members of the cluster, miR-27b and miR-24-1, are downregulated after vascular injury, suggesting that this cluster participates in regulation of VSMC phenotypic switch [27]. miR-663 is a novel regulator of VSMCs in the phenotypic switch. Overexpression of miR-663 is associated with increased expression of VSMC contractile phenotypic markers, such as SM22 $\alpha$  and MYH11. Furthermore, miR-663 effectively inhibits VSMC proliferation and migration in vitro, and vascular injury induced neointimal hyperplasia in a mice carotid artery ligation model, through targeting the transcription factor JunB and its downstream Myl9 [30].

Recent studies reveal miR-140-3p's potential as the therapeutic target for preventing ISR in PAD [31]. miR-140-3p is mainly distributed in artery media rather than in endothelium or adventitia, and it is mainly expressed in SMCs. miR-140-3p was prominently downregulated in VSMCs with ISR. Increasing expression of miR-140-3p repressed cell proliferation via directly targeting c-Myb while promoted cell apoptosis via targeting c-Myb and Bcl-2. Intriguingly, miR-140-3p does not affect cell SMC migration [31]. In vivo study showed delivery of miR-140-3p into rat carotid artery after balloon angioplasty leads to reduction of neointimal hyperplasia. Another two miRNAs downregulated in VSMC of the patient with arteriosclerosis obliterans (ASO) are miR-22-3p and miR-1298. miR-22-3p upregulation results in attenuation of VSMC proliferation and migration in vitro via directly targeting and negatively regulating high mobility group box-1 (HMGB1). Consistent with the antiproliferative and antimigrative effect of miR-22-3p in vitro, miR-22-3p inhibits neointimal hyperplasia in balloon-injured rat carotid arteries in vivo, also by targeting HMGB1 [32]. The downregulation of miR-1298 in ASO is associated with the higher DNA methylation of its upstream CpG sites. In vitro study showed that miR-1298 suppresses VSMC proliferation and migration without affecting apoptosis [33]. These cellular effects are mediated via directly targeting connexin 43 which has been proved that its downregulation suppress VSMC phenotypic switching from contractile to synthesis [34]. In vivo study confirmed that overexpression of miR-1298 inhibits neointimal hyperplasia in an injured artery.

Besides miRNAs mentioned above, which are downregulated in response to vascular injury, there are several miRNAs upregulated after stent implantation induced vascular injury. miR-21 is one of the most upregulated miRNAs. Inhibition of miR-21 reduces VSMC proliferation while enhances VSMC apoptosis via targeting phosphatase and tensin homolog (PTEN) and Bcl-2, two crucial signaling molecules involved in VSMC growth and apoptosis [35]. Utilizing a humanized in vivo model which mimics human ISR, Wang et al. demonstrate that the miR-21 expression increased during ISR. Anit-miR-21 inhibits

VSMC proliferation, while miR-21 overexpression induced proproliferative response of VSMC. This effect of anti-miR-21 is modulated through derepression of PTEN. Besides, miR-21 also regulates VSMC cell shape via directly targeting Tropomyosin-1 [36]. miR-146a exhibits a potent capacity to promote VSMC proliferation in vitro and neointimal hyperplasia in vivo. miR-146a targets and inhibits Klf-4, which plays an antiproliferative role in the regulation of VSMC biology, while Klf-4 binding to miR-146a promoter inhibits miR-146a transcription. This feedback loop of miR-146a and Klf-4 regulates each other's expression and VSMC proliferation. Additionally, Klf-5 competitively binds to miR-146a promoter to promote miR-146a transcription as a Klf-4 competitor [37]. Human miR-424 or its rat ortholog miR-322 (miR-424/322) upregulated in proliferative VSMC in vitro and after vascular injury in vivo; however, it exhibits antiproliferative effect. Overexpression of miR-424/322 induced an increase in the expression of several differentiation markers such as ACTA2, calponin-1, and MYH11, inhibited VSMC proliferation and migration without affecting VSMC apoptosis by directly targeting CCND1 known as a regulator of cell cycle transition, Ca<sup>2+</sup>-regulating proteins calumenin and by indirectly targeting stromal interaction molecule 1 (STIM1). This suggested that miR-424/322 has protective effect against neointimal hyperplasia [38].

miR-133 and miR-132 expression transiently decreased in early phase and prominently increased in a late phase of vascular injury. MAPK/ERK1/2 is the major upstream signaling to regulation miR-133. ERK1/2 activation is responsible for miR-133 downregulation. Overexpression of miR-133 significantly reduces VSMC proliferation and migration, prevents VSMC phenotype switch from contractile to synthesis, and ultimately results in inhibition of neointimal hyperplasia. These effects are modulated via directly targeting to Sp-1 and moesin and repressing the expression of these two transcriptional factors since Sp-1 regulates VSMC phenotypic switch and moesin modulates VSMC migration both in vitro and in vivo [39]. Delivery miR-132 to a rat carotid artery injury model induces increasing expression of p27 and Bax which have the proapoptosis effect, as well as expression of VSMC differentiation marker smooth muscle  $\alpha$ -actin, and decreasing expression of Bcl-2, an antiapoptotic protein. These effects are modulated by miR-132 targets to leucine-rich repeat (in Flightless 1) interacting protein-1 (LRRFIP1), which is documented to affect cancer cell proliferation and migration. miR-132 inhibits VSMC survival and growth while promotes its apoptosis and attenuates neointimal hyperplasia conclusively [40].

miR-638 is enriched in human aortic SMC. PDGF-BB stimulation, as one of the most potent stimulants for VSMC proliferation and migration, leads to sharply decreased expression of miR-638. MAPK/ERK1/2 serves as an upstream signaling molecule that involved in the regulation of PDGF-BB-induced miR-638 decreasing. Overexpression of miR-638 leads to inhibition of VSMC proliferation and migration, as well as decrease of the CCND1 expression by directly targeting NOR1 [41].

## 5. miRNAs Involved in Vessel Inflammation

Inflammation plays a pivotal role in ISR, linking early vascular injury to the eventual consequence of neointimal hyperplasia and lumen compromise. Leukocyte recruitment and infiltration are characteristics of restenosis induced by stent implantation, trigger the subsequent neointimal formation [7]. There is mounting evidence for the role of inflammation in restenosis. Moreno and colleagues found primary lesions that develop restenosis after coronary atherectomy have more macrophages and SMCs than primary lesions that do not develop restenosis, provide evidence linking leukocytes and restenosis [42]. Cipollone et al. demonstrated significantly elevated levels of MCP-1, a potent chemoattractant of monocytes, in restenotic patients after percutaneous transluminal coronary angioplasty [43]. Tenaka et al. proved a sustained upregulation of vascular adhesion molecules-1 (VCAM-1), intercellular adhesion molecule-1 (ICAM-1), and major histocompatibility complex class II antigens in a balloon injured rabbit model [44].

Recent studies have reported that miRNAs are involved in the process of inflammatory response. miR-126 is an endothelial cell-specific miRNA. It targets to VCAM-1, which regulates leukocyte trafficking to sites of inflammation, and suppresses the VCAM-1 expression. Decreased miR-126 leads to an increase in the TNF-stimulated VCAM-1 expression and promotes leukocyte adherence to endothelial cells consequently [45]. miR-21 is also involved in the modulation of vascular inflammatory response. miR-21 is abundantly expressed in inflammatory cells. Loss of miR-21 represses macrophage activation, therefore reduces inflammatory response after vascular injury aroused by stent implantation [46]. Both miR-221/222 and miR-155 can also regulate endothelial inflammation by regulating endothelial adhesion molecules. Overexpression of miR-155 and miR-221/222 downregulated ETS-1, a critical transcription factor of vascular inflammation and remodeling, and its downstream signaling VCAM1, MCP-1, and FLT1, thus attenuate the adhesion of Jurkat T cells to ECs [47]. Additionally, miR-195 reduced synthesis of proinflammatory biomarkers, IL-1 $\beta$ , IL-6, and IL-8, suggesting that it could be a potential regulator of ISR because of its anti-inflammatory effect [22].

## 6. miRNAs Involved in Endothelial Regeneration

Endothelium, the inner layer of the integrated vessel wall, acts as a selectively permeable barrier between the rest of the vessel wall and blood flow and participates in regulation of vascular tone and suppression of neointimal hyperplasia by inhibiting inflammation, thrombus formation, and VSMC proliferation and migration. Compared to angioplasty, stent implantation results in severe injury because the metal scaffold provides a nonphysiological surface for adhesion and generates perturbations in blood flow and hinders the following reendothelialization as well. The reendothelialization, that is the regeneration and regrowth of the denuded endothelium, retrieved mainly from the remaining endothelial cells. However, this process after stent implantation is found to be inadequate in both structural and

functional integrity with impaired endothelium-dependent vasodilation and increased permeability [11, 48].

Endothelial denudation acts as a trigger of ISR; the consequent delayed endothelial recovery and endothelial dysfunction are the major contributing factors of late stent thrombosis [49]. The antiproliferative drugs of DES have nonselective effect on both SMC and EC, thus prevent both neointimal hyperplasia and reendothelialization. Taking together, these observations confirmed the essential role of endothelium in the process of ISR, implied that promoting rather than blocking the healing process by stimulating reendothelialization seems the most natural approach to prevent restenosis after DES implantation. Experimental studies showed that delivery of miR-140-3p into rat carotid artery after balloon angioplasty leads to the reduction of neointimal hyperplasia; meanwhile, it has no adverse effect on reendothelialization. Similarly, anti-miR-21 effectively attenuates neointimal hyperplasia and ISR without impeding reendothelialization, and anti-miR-21 did not inhibit EC proliferation *in vitro* [50]. Thus, application of miRNAs might be a novel, cell-specific perspective in this challenging problem.

miR-126 is an EC-specific microRNA. It has been proved that miR-126 plays an irreplaceable role in the maintenance of endothelial integrity and angiogenesis. miR-126 mutant mice express severe systemic edema, multifocal hemorrhages, ruptured blood vessel, and partial embryonic lethality [51]. miR-126 targets to Spred-1, a negative regulator of MAPK signaling, therefore promotes VEGF- and FGF-mediated endothelial cell migration and angiogenesis by repressing Spred-1. Although miR-126 is not expressed in VSMCs, it participates in the regulation of VSMC function. By targeting and downregulating insulin receptor substrate-1 (IRS-1), miR-126 reduces VSMC proliferation and migration. Moreover, Taglin and Acta2, which indicate VSMC differentiation, were upregulated by miR-126 in VSMCs [52].

miR-92a is another essential mediator of endothelial functions and angiogenesis which is selectively expressed in EC but not in SMC [53]. Inhibition of miR-92a induced increased phosphorylation of ERK1/2 and c-jun N-terminal kinases/stress-activated protein kinases (JNK/SAPK), as well as increased serum response factor (SRF) protein level, and therefore enhances EC proliferation and migration *in vitro*. Moreover, inhibition of miR-92a also induced increased Klf-4 expression, which regulates endothelial hemostasis, and thus enhances the eNOS expression and its nitric oxide (NO) production in EC. Not only maintain the endothelial integrity, the EC released NO also negatively regulates SMC proliferation and migration and consequently inhibits neointimal hyperplasia [54]. Importantly, functional inhibition of miR-92a *in vivo* prominently reduced neointimal hyperplasia and accelerated the reendothelialization after vascular injury and stent implantation, indicating that regulation of miR-92a could be a novel therapeutic approach to prevent ISR [53]. miR-92 is a member of the miR17-92 cluster, a polycistronic unit encoding miR-17, miR-18a, miR-19a/b, miR-20a, and miR-92a. All the members of the miR17-92 cluster are expressed in EC and known to participate in VSMC proliferation and neointimal hyperplasia of carotid artery



restenosis [55]. miR17-92 cluster members are upregulated in carotid artery restenosis; they mediate the crosstalk of two TGF- $\beta$  signaling pathway, smad3 and bone morphogenetic protein receptor type II (BMP2). Smad3 activates miR17-92, therefore downregulated BMP2 which directly target to miR17-92, and consequently promotes neointimal hyperplasia and carotid artery restenosis [55].

miR221 and miR222 are highly expressed in both EC and VSMC. In VSMC, miR221 and miR222 exhibit strong proliferative effects. After vascular injury induced by angioplasty, the miR221 and miR222 expressions are increased and promote VSMC proliferation and neointimal hyperplasia via inhibits their target gene p27 (Kip1) and p57 (Kip2) [56]. On the contrary, in EC, upregulated miR221 and miR222 suppress EC proliferation/migration, promote EC apoptosis, and lead to decreased reendothelialization after angioplasty via inhibiting c-kit, which expressed in EC, but not VSMC [57]. The opposite effects of miR221 and miR222 expression on EC and VSMC may partly due to differential target gene expression in different cell types. And this imply that inhibit miR221 and miR222 could repress neointimal hypoplasia while enhance reendothelialization, which are responsible for ISR reducing.

miR-143/-145 is undetectable in endothelial cells; however, its expression increased in response to shear stress and Klf-2, the shear-responsive transcription factor. It has been proved that Klf-2 expressed endothelial cell transfer miR-143/-145 enriched extracellular vesicles to SMCs, influencing SMC functions in a paracrine manner [58]. Furthermore, when coculture VSMC and EC, the cell-to-cell contact induces miR-143/-145 transfer from SMC to EC via tunneling nanotubes [59]. These cell-to-cell crosstalk studies illustrate that miR-143/-145 acts as a signaling transmitter to communicate VSMCs and ECs and regulate their functions consequently.

## 7. Interaction with lncRNA in the Vasculature

Long noncoding RNAs (lncRNAs) are nonprotein coding transcripts with a length of more than 200 nt. lncRNAs are highly versatile; they can be regulated by miRNA and the reciprocal. Generally, the mechanism of microRNAs and lncRNA interactions can be summarized in 3 ways [60]. First, lncRNAs bind and compete with microRNAs (lncRNA-microRNA sponge) to reduce microRNA function with cells and alleviate mRNA repressions. Besides, lncRNAs host microRNAs within their exons and introns. Finally, microRNAs bind lncRNAs and regulate their stability.

LncRNA 362 was identified as one of the angiotensin II (Ang II-) responsive RNAs [61], and it acts as host gene for miR-221 and miR-222 which has been identified as regulators of VSMC proliferation and migration [56]. Knocking-down of LncRNA 362 results in decreased miR-221/222 expression and subsequent inhibition of VSMC proliferation. It suggested that the coregulation of LncRNA362 and miR-221/222 could promote VSMC proliferation and neointimal hyperplasia [60, 62].

LncRNA-H19 modulates let-7 availability, which have been indicated to protect VSMC from oxidative damage, by acting as a molecular sponge [63, 64]. Also, LncRNA-H19 is a primary

precursor for miR-675. It has been proved that both of LncRNA-H19 and miR-675 expression are increased after vascular injury. LncRNA-H19 accelerates VSMC proliferation in a miR-675 dependent manner by directly targets to PTEN [65].

LncRNA LINC00341 acts as the sponge of miR-214 and therefore promotes its target protein FOXO4 expression, and transcription factor FOXO4 activates the transcription of LINC00341. LINC00341 promotes the proliferation and migration of VSMCs via this positive feedback loop [66]. Tian et al.'s study revealed that the lncRNA UCA1, which is known to play an important role in cardiovascular injury, acts as a sponge of miR-26a and downregulates miR-26a expression, thereby alleviates smooth muscle cell proliferation against atherosclerosis [67]. Recently, Zhang et al. discovered that the lncRNA POU3F3 expression increased in ISR patients after PCI. POU3F3 promotes VSMC proliferation, migration, and phenotypic transformation via POU3F3/miR-449a/KLF4 signaling pathway [68].

LncRNA MALAT1 expressed in ECs, and it reciprocally interacts with miR-320a. In human umbilical vein endothelial cells (HUVECs), knockdown of MALAT1 induced increasing of miR-320a expression and decreasing of FOXM1 expression, consequently inhibited HUVEC proliferation [69].

## 8. Circulating miRNAs as Biomarkers for ISR

miRNAs can be found in the blood circulation in an extraordinary stable form, and they are susceptible to sensitive detection through qPCR, thus were identified as potential biomarkers of many cardiovascular disease, predicting the response of therapeutic interventions, such as ISR [70].

A case-control study reveals that circulating miR-21 level increased while miR-100, miR143, and miR145 decreased in patients with ISR compared to healthy people and non-ISR patient and demonstrate these miRNAs as potential biomarkers of ISR. Interestingly, they can discriminate between diffuse ISR and local ISR [71]. miR-93-5p was able to discriminate between patients with stable coronary artery disease (CAD) and those with no CAD; furthermore, it is a powerful independent predictor of coronary ISR [72]. A recent study found that miR-19a, miR-126, miR-210, and miR-378 independently correlated with lower restenosis occurrence, demonstrating that these four miRNAs had good value in predicting restenosis risk [73].

There are also several studies performed to explore the predict value of miRNAs in PAD restenosis. Circulating microRNA-320a and microRNA-572 in PAD patients with ISR had significantly higher expression levels than it from non-ISR and healthy volunteers [74]. miR-195 is a PAD-specific miRNA that has potential diagnostic value to discriminate patients with PAD from healthy population [75]. Moreover, it is a strong and independent predictor of adverse atherothrombotic events and target vessel revascularization following angioplasty and stenting for PAD, and it could become a valuable and easily accessible biomarker for risk stratification after endovascular revascularization procedures [76].

## 9. Future Perspectives and Conclusion

The invasive endovascular repair including PTA and stent implantation has become the standard approach for both CAD and PAD. Despite the development of DES significantly reduced the rate of restenosis compared to BMS and PTA alone, ISR is still the major drawback of endovascular repair. DES failed to completely obliterate ISR, and it induced risk of late stent thrombosis, hindered endothelial healing and inflammatory response due to nonselective inhibition of endothelial and SMC proliferation by the antiproliferative drugs [77]. Therefore, based on the comprehensive understanding of ISR pathophysiology, an ideal therapeutic target to prevent ISR should be able to inhibit SMC proliferation induced neointimal hyperplasia and facilitate endothelial healing simultaneously.

The recent development of gene-eluting stent is a major breakthrough in stent technology. Paul and colleagues developed a nanobiohybrid hydrogel-based endovascular stent device to prevent ISR [78]. In this study, the hydrogel works as a reservoir to carry, protect, and simultaneously deliver proangiogenic, VEGF, and Angiopoietin-1 genes to the target site. And the results showed enhancement in reendothelialization, attenuation of stenosis, and prevention of neointimal formation. Yang et al. reported a stent coated with bilayered poly (lactide-co-glycolide) (PLGA) nanoparticles containing VEGF plasmid in the outer layer and paclitaxel in the inner core (VEGF/PTX NPs), demonstrating that the VEGF/PTX NP-coated stent promotes early endothelium healing while inhibits SMC proliferation through sequential release of the VEGF gene and paclitaxel, resulted in significant suppression of ISR [79]. These studies inspired us that restenosis could be prevented at the molecular level by administering gene expression, and miRNA-eluting stent could be a promising therapy because miRNA can inhibit ISR via more than one pathway. One of the challenging puzzles is choosing appropriate target miRNA. The miR-195, miR-92a, and miR-221/222 are potential targets of the miRNA-eluting stent, because miR-195 effectively prevents ISR by inhibiting VSMC proliferation and migration while reducing inflammatory response as well, whereas miR-92a and miR-221/222 showed different effects on VSMCs and ECs.

As for miRNA-based therapy, silencing miR-122 leads to long-lasting suppression of hepatitis C virus (HCV) viremia maybe be the first human therapy [80]. However, compared to reach up to liver, specific miRNA delivery to the vascular system can be more challenging. Santulli et al. used an adenoviral vector that encodes p27 with target sequences for EC-specific miR-126-3p at the 3' end, demonstrating the potential of using a miRNA-based strategy as a therapeutic approach to specifically inhibit vascular restenosis while preserving EC function [81]. Wang et al. reported application of anti-21-coated stents effectively reduced ISR, whereas no significant off-target effects could be observed [50].

Despite the therapeutic implication of some miRNA in restenosis has entered clinical trials by integrating them in microsphere-integrated stent, adenovirus, or nanoparticles [82], there are still many problems need to be solved. For

example, since miRNA controls multiple pathways in different tissue types, how to avoid the unwanted effects accompanied with miRNA inhibition is of importance. Some miRNAs might have an ambivalent effect that is both a beneficial therapeutic effect in terms of angiogenesis and a detrimental promotion of tumor angiogenesis.

In conclusion, miRNAs exhibit great therapeutic potential for ISR treatment. Fully understand the molecular mechanisms underlying miRNA regulated ISR is of paramount importance to promote the realization of miRNA-based strategy, despite there is still a long way to go before clinical application of miRNA-eluting stent.

## Abbreviations

3-UTRs:	3'-Untranslated regions
ACE:	Angiotensin converting enzyme
ACTA2:	Alpha Smooth Muscle Actin 2
ASO:	Arteriosclerosis obliterans
BMPR2:	Bone morphogenetic protein receptor type II
BMS:	Bare metal stent
CAD:	Coronary artery disease
CCND1:	CyclinD1
DES:	Drug-eluted stent
ECs:	Endothelial cells
ECM:	Extracellular matrix
ETS-1:	E26 transformation specific-1
FGF:	Fibroblast growth factor
FOXO4:	Forkhead box O4
HCV:	Hepatitis C virus
HMGB-1:	High mobility group box-1
ICAM-1:	Intercellular adhesion molecule-1
IL:	Interleukin
IRS-1:	Insulin receptor substrate-1
ISR:	In-stent restenosis
JNK/SAPK:	c-Jun N-terminal kinases/stress-activated protein kinases
Klf:	Kruppel-like factor
lncRNA:	Long noncoding RNA
LRRFIP1:	Leucine-rich repeat (in Flightless 1) interacting protein-1
MCP-1:	Monocyte chemoattractant protein-1
MAPK:	Mitogen-activated Protein Kinase
miRNA:	MicroRNAs
miRISC:	miRNA-induced silencing complex
MREs:	miRNA-response elements
MRTF- $\beta$ :	Myocardin-related transcription factor-beta
MYH11:	Myosin Heavy Chain 11
NO:	Nitric oxide
PAD:	Peripheral arterial disease
PDGF:	Platelet-derived growth factor
PLGA:	Poly(lactide-co-glycolide)
PTA:	Percutaneous transluminal angioplasty
PTEN:	Phosphatase and tensin homolog
SM22 $\alpha$ :	Smooth Muscle 22 alpha
SM-MHC:	Smooth muscle myosin heavy chain
SRF:	Serum response factor
STIM1:	Stromal interaction molecule 1
TGF- $\beta$ :	Transforming growth factor-beta

uPA: Urokinase plasminogen activator  
 VCAM-1: Vascular adhesion molecules-1  
 VEGF: Vascular endothelial growth factor  
 VSMCs: Vascular smooth muscle cells.

## Data Availability

All relevant data are within the paper and its supporting information files.

## Conflicts of Interest

The authors have no conflicts of interest to declare.

## References

- [1] L. Norgren, W. R. Hiatt, J. A. Dormandy, M. R. Nehler, K. A. Harris, and F. G. R. Fowkes, "Inter-Society Consensus for the Management of Peripheral Arterial Disease (TASC II)," *J Vasc Surg*, vol. 45, no. 1, Supplement S, pp. S5–S67, 2007.
- [2] N. W. Shammass, "Epidemiology, classification, and modifiable risk factors of peripheral arterial disease," *Vascular Health and Risk Management*, vol. 3, no. 2, pp. 229–234, 2007.
- [3] K. J. Ho and C. D. Owens, "Diagnosis, classification, and treatment of femoropopliteal artery in-stent restenosis," *Journal of Vascular Surgery*, vol. 65, no. 2, pp. 545–557, 2017.
- [4] A. Abizaid, R. Kornowski, G. S. Mintz et al., "The influence of diabetes mellitus on acute and late clinical outcomes following coronary stent implantation," *Journal of the American College of Cardiology*, vol. 32, no. 3, pp. 584–589, 1998.
- [5] M. I. Papafaklis, Y. S. Chatzizisis, K. K. Naka, G. D. Giannoglou, and L. K. Michalis, "Drug-eluting stent restenosis: effect of drug type, release kinetics, hemodynamics and coating strategy," *Pharmacology & Therapeutics*, vol. 134, no. 1, pp. 43–53, 2012.
- [6] M. A. Costa and D. I. Simon, "Molecular basis of restenosis and drug-eluting stents," *Circulation*, vol. 111, no. 17, pp. 2257–2273, 2005.
- [7] F. G. Welt and C. Rogers, "Inflammation and restenosis in the stent era," *Arteriosclerosis, Thrombosis, and Vascular Biology*, vol. 22, no. 11, pp. 1769–1776, 2002.
- [8] T. Inoue, Y. Sakai, K. Hoshi, I. Yaguchi, T. Fujito, and S. Morooka, "Lower expression of neutrophil adhesion molecule indicates less vessel wall injury and might explain lower restenosis rate after cutting balloon angioplasty," *Circulation*, vol. 97, no. 25, pp. 2511–2518, 1998.
- [9] A. K. Mitra and D. K. Agrawal, "In stent restenosis: bane of the stent era," *Journal of Clinical Pathology*, vol. 59, no. 3, pp. 232–239, 2006.
- [10] R. Riessen, J. M. Isner, E. Blessing, C. Loushin, S. Nikol, and T. N. Wight, "Regional differences in the distribution of the proteoglycans biglycan and decorin in the extracellular matrix of atherosclerotic and restenotic human coronary arteries," *The American Journal of Pathology*, vol. 144, no. 5, pp. 962–974, 1994.
- [11] A. Cornelissen and F. J. Vogt, "The effects of stenting on coronary endothelium from a molecular biological view: time for improvement?," *Journal of Cellular and Molecular Medicine*, vol. 23, no. 1, pp. 39–46, 2019.
- [12] A. Wronska, I. Kurkowska-Jastrzebska, and G. Santulli, "Application of microRNAs in diagnosis and treatment of cardiovascular disease," *Acta Physiologica (Oxford, England)*, vol. 213, no. 1, pp. 60–83, 2015.
- [13] S. De Rosa, A. Curcio, and C. Indolfi, "Emerging role of microRNAs in cardiovascular diseases," *Circulation Journal*, vol. 78, no. 3, pp. 567–575, 2014.
- [14] K. Stellos and S. Dimmeler, "Vascular microRNAs: from disease mechanisms to therapeutic targets," *Circulation Research*, vol. 114, no. 1, pp. 3–4, 2014.
- [15] C. Gareri, S. De Rosa, and C. Indolfi, "MicroRNAs for restenosis and thrombosis after vascular injury," *Circulation Research*, vol. 118, no. 7, pp. 1170–1184, 2016.
- [16] M. Kearney, A. Pieczek, L. Haley et al., "Histopathology of in-stent restenosis in patients with peripheral artery disease," *Circulation*, vol. 95, no. 8, pp. 1998–2002, 1997.
- [17] G. K. Owens, "Regulation of differentiation of vascular smooth muscle cells," *Physiological Reviews*, vol. 75, no. 3, pp. 487–517, 1995.
- [18] G. K. Owens, M. S. Kumar, and B. R. Wamhoff, "Molecular regulation of vascular smooth muscle cell differentiation in development and disease," *Physiological Reviews*, vol. 84, no. 3, pp. 767–801, 2004.
- [19] K. R. Cordes, N. T. Sheehy, M. P. White et al., "miR-145 and miR-143 regulate smooth muscle cell fate and plasticity," *Nature*, vol. 460, no. 7256, pp. 705–710, 2009.
- [20] W. Zhao, S. P. Zhao, and Y. H. Zhao, "MicroRNA-143/-145 in cardiovascular diseases," *BioMed Research International*, vol. 2015, Article ID 531740, 9 pages, 2015.
- [21] Y. Cheng, X. Liu, J. Yang et al., "MicroRNA-145, a novel smooth muscle cell phenotypic marker and modulator, controls vascular neointimal lesion formation," *Circulation Research*, vol. 105, no. 2, pp. 158–166, 2009.
- [22] Y. S. Wang, H. Y. Wang, Y. C. Liao et al., "MicroRNA-195 regulates vascular smooth muscle cell phenotype and prevents neointimal formation," *Cardiovascular Research*, vol. 95, no. 4, pp. 517–526, 2012.
- [23] C. Gareri, C. Iaconetti, S. Sorrentino, C. Covelto, S. De Rosa, and C. Indolfi, "miR-125a-5p modulates phenotypic switch of vascular smooth muscle cells by targeting ETS-1," *Journal of Molecular Biology*, vol. 429, no. 12, pp. 1817–1828, 2017.
- [24] F. Dandré and G. K. Owens, "Platelet-derived growth factor-BB and Ets-1 transcription factor negatively regulate transcription of multiple smooth muscle cell differentiation marker genes," *American Journal of Physiology. Heart and Circulatory Physiology*, vol. 286, no. 6, pp. H2042–H2051, 2004.
- [25] W. Hu, G. Chang, M. Zhang et al., "MicroRNA-125a-3p affects smooth muscle cell function in vascular stenosis," *Journal of Molecular and Cellular Cardiology*, vol. 136, pp. 85–94, 2019.
- [26] C. Bang, J. Fiedler, and T. Thum, "Cardiovascular importance of the microRNA-23/27/24 family," *Microcirculation*, vol. 19, no. 3, pp. 208–214, 2012.
- [27] C. Iaconetti, S. De Rosa, A. Polimeni et al., "Down-regulation of miR-23b induces phenotypic switching of vascular smooth muscle cells in vitro and in vivo," *Cardiovascular Research*, vol. 107, no. 4, pp. 522–533, 2015.
- [28] Y. Kiyani, A. Limbourg, R. Kiyani et al., "Urokinase receptor associates with myocardin to control vascular smooth muscle cells phenotype in vascular disease," *Arteriosclerosis, Thrombosis, and Vascular Biology*, vol. 32, no. 1, pp. 110–122, 2012.
- [29] S. Tsai, S. T. Hollenbeck, E. J. Ryer et al., "TGF- $\beta$  through Smad3 signaling stimulates vascular smooth muscle cell proliferation and neointimal formation," *American Journal of*



- Physiology-Heart and Circulatory Physiology*, vol. 297, no. 2, pp. H540–H549, 2009.
- [30] P. Li, N. Zhu, B. Yi et al., “MicroRNA-663 regulates human vascular smooth muscle cell phenotypic switch and vascular neointimal formation,” *Circ Res*, vol. 113, no. 10, pp. 1117–1127, 2013.
- [31] Z. R. Zhu, Q. He, W. B. Wu et al., “MiR-140-3p is involved in in-stent restenosis by targeting C-Myb and BCL-2 in peripheral artery disease,” *Journal of Atherosclerosis and Thrombosis*, vol. 25, no. 11, pp. 1168–1181, 2018.
- [32] S. C. Huang, M. Wang, W. B. Wu et al., “Mir-22-3p inhibits arterial smooth muscle cell proliferation and migration and neointimal hyperplasia by targeting HMGB1 in arteriosclerosis obliterans,” *Cellular Physiology and Biochemistry*, vol. 42, no. 6, pp. 2492–2506, 2017.
- [33] W. Hu, M. Wang, H. Yin et al., “MicroRNA-1298 is regulated by DNA methylation and affects vascular smooth muscle cell function by targeting connexin 43,” *Cardiovascular Research*, vol. 107, no. 4, pp. 534–545, 2015.
- [34] C. E. Chadjichristos, S. Morel, J. P. Derouette et al., “Targeting connexin 43 prevents platelet-derived growth factor-BB-induced phenotypic change in porcine coronary artery smooth muscle cells,” *Circulation Research*, vol. 102, no. 6, pp. 653–660, 2008.
- [35] R. Ji, Y. Cheng, J. Yue et al., “MicroRNA expression signature and antisense-mediated depletion reveal an essential role of MicroRNA in vascular neointimal lesion formation,” *Circulation Research*, vol. 100, no. 11, pp. 1579–1588, 2007.
- [36] M. Wang, W. Li, G. Q. Chang et al., “MicroRNA-21 regulates vascular smooth muscle cell function via targeting tropomyosin 1 in arteriosclerosis obliterans of lower extremities,” *Arteriosclerosis, Thrombosis, and Vascular Biology*, vol. 31, no. 9, pp. 2044–2053, 2011.
- [37] S. G. Sun, B. Zheng, M. Han et al., “miR-146a and Krüppel-like factor 4 form a feedback loop to participate in vascular smooth muscle cell proliferation,” *EMBO Reports*, vol. 12, no. 1, pp. 56–62, 2011.
- [38] E. Merlet, F. Atassi, R. K. Motiani et al., “miR-424/322 regulates vascular smooth muscle cell phenotype and neointimal formation in the rat,” *Cardiovascular Research*, vol. 98, no. 3, pp. 458–468, 2013.
- [39] D. Torella, C. Iaconetti, D. Catalucci et al., “MicroRNA-133 controls vascular smooth muscle cell phenotypic switch in vitro and vascular remodeling in vivo,” *Circulation Research*, vol. 109, no. 8, pp. 880–893, 2011.
- [40] N. Choe, J. S. Kwon, J. R. Kim et al., “The microRNA miR-132 targets Lrrfip1 to block vascular smooth muscle cell proliferation and neointimal hyperplasia,” *Atherosclerosis*, vol. 229, no. 2, pp. 348–355, 2013.
- [41] P. Li, Y. Liu, B. Yi et al., “MicroRNA-638 is highly expressed in human vascular smooth muscle cells and inhibits PDGF-BB-induced cell proliferation and migration through targeting orphan nuclear receptor NOR1,” *Cardiovascular Research*, vol. 99, no. 1, pp. 185–193, 2013.
- [42] P. R. Moreno, V. H. Bernardi, J. Lo’pez-Cue’llar et al., “Macrophage infiltration predicts restenosis after coronary intervention in patients with unstable angina,” *Circulation*, vol. 94, no. 12, pp. 3098–3102, 1996.
- [43] F. Cipollone, M. Marini, M. Fazio et al., “Elevated circulating levels of monocyte chemoattractant protein-1 in patients with restenosis after coronary angioplasty,” *Arteriosclerosis, Thrombosis, and Vascular Biology*, vol. 21, no. 3, pp. 327–334, 2001.
- [44] H. Tanaka, G. K. Sukhova, S. J. Swanson et al., “Sustained activation of vascular cells and leukocytes in the rabbit aorta after balloon injury,” *Circulation*, vol. 88, no. 4, pp. 1788–1803, 1993.
- [45] T. A. Harris, M. Yamakuchi, M. Ferlito, J. T. Mendell, and C. J. Lowenstein, “MicroRNA-126 regulates endothelial expression of vascular cell adhesion molecule 1,” *Proceedings of the National Academy of Sciences of the United States of America*, vol. 105, no. 5, pp. 1516–1521, 2008.
- [46] R. A. McDonald, C. A. Halliday, A. M. Miller et al., “Reducing in-stent restenosis: therapeutic manipulation of miRNA in vascular remodeling and inflammation,” *Journal of the American College of Cardiology*, vol. 65, no. 21, pp. 2314–2327, 2015.
- [47] N. Zhu, D. Zhang, S. Chen et al., “Endothelial enriched microRNAs regulate angiotensin II-induced endothelial inflammation and migration,” *Atherosclerosis*, vol. 215, no. 2, pp. 286–293, 2011.
- [48] H. M. van Beusekom, D. M. Whelan, S. H. Hofma et al., “Long-term endothelial dysfunction is more pronounced after stenting than after balloon angioplasty in porcine coronary arteries,” *Journal of the American College of Cardiology*, vol. 32, no. 4, pp. 1109–1117, 1998.
- [49] M. Joner, A. V. Finn, A. Farb et al., “Pathology of drug-eluting stents in humans: delayed healing and late thrombotic risk,” *Journal of the American College of Cardiology*, vol. 48, no. 1, pp. 193–202, 2006.
- [50] D. Wang, T. Deuse, M. Stubbendorff et al., “Local microRNA modulation using a novel anti-miR-21-eluting stent effectively prevents experimental in-stent restenosis,” *Arteriosclerosis, Thrombosis, and Vascular Biology*, vol. 35, no. 9, pp. 1945–1953, 2015.
- [51] S. Wang, A. B. Aurora, B. A. Johnson et al., “The endothelial-specific microRNA miR-126 governs vascular integrity and angiogenesis,” *Developmental Cell*, vol. 15, no. 2, pp. 261–271, 2008.
- [52] M. Izuwara, Y. Kuwabara, N. Saito et al., “Prevention of neointimal formation using miRNA-126-containing nanoparticle-conjugated stents in a rabbit model,” *PLoS One*, vol. 12, no. 3, article e0172798, 2017.
- [53] C. Iaconetti, A. Polimeni, S. Sorrentino et al., “Inhibition of miR-92a increases endothelial proliferation and migration in vitro as well as reduces neointimal proliferation in vivo after vascular injury,” *Basic Research in Cardiology*, vol. 107, no. 5, p. 296, 2012.
- [54] C. Indolfi, D. Torella, C. Coppola et al., “Physical training increases eNOS vascular expression and activity and reduces restenosis after balloon angioplasty or arterial stenting in rats,” *Circulation Research*, vol. 91, no. 12, pp. 1190–1197, 2002.
- [55] T. Luo, S. Cui, C. Bian, and X. Yu, “Crosstalk between TGF- $\beta$ /Smad3 and BMP/BMP2 signaling pathways via miR-17-92 cluster in carotid artery restenosis,” *Molecular and Cellular Biochemistry*, vol. 389, no. 1-2, pp. 169–176, 2014.
- [56] X. Liu, Y. Cheng, S. Zhang, Y. Lin, J. Yang, and C. Zhang, “A necessary role of miR-221 and miR-222 in vascular smooth muscle cell proliferation and neointimal hyperplasia,” *Circulation Research*, vol. 104, no. 4, pp. 476–487, 2009.
- [57] X. Liu, Y. Cheng, J. Yang, L. Xu, and C. Zhang, “Cell-specific effects of miR-221/222 in vessels: molecular mechanism and therapeutic application,” *Journal of Molecular and Cellular Cardiology*, vol. 52, no. 1, pp. 245–255, 2012.



- [58] E. Hergenreider, S. Heydt, K. Tréguer et al., "Atheroprotective communication between endothelial cells and smooth muscle cells through miRNAs," *Nature Cell Biology*, vol. 14, no. 3, pp. 249–256, 2012.
- [59] M. Climent, M. Quintavalle, M. Miragoli, J. Chen, G. Condorelli, and L. Elia, "TGF $\beta$  triggers miR-143/145 transfer from smooth muscle cells to endothelial Cells, Thereby Modulating Vessel Stabilization," *Circulation Research*, vol. 116, no. 11, pp. 1753–1764, 2015.
- [60] M. D. Ballantyne, R. A. McDonald, and A. H. Baker, "lncRNA/MicroRNA interactions in the vasculature," *Circulation Research*, vol. 99, no. 5, pp. 494–501, 2016.
- [61] A. Leung, C. Trac, W. Jin et al., "Novel long noncoding RNAs are regulated by angiotensin II in vascular smooth muscle cells," *Circulation Research*, vol. 113, no. 3, pp. 266–278, 2013.
- [62] H. Li, H. Zhu, J. Ge, and R. N. A. Noncoding, "Long Noncoding RNA: Recent updates in atherosclerosis," *International Journal of Biological Sciences*, vol. 12, no. 7, pp. 898–910, 2016.
- [63] Z. Ding, X. Wang, L. Schnackenberg et al., "Regulation of autophagy and apoptosis in response to ox-LDL in vascular smooth muscle cells, and the modulatory effects of the microRNA hsa-let-7g," *International Journal of Cardiology*, vol. 168, no. 2, pp. 1378–1385, 2013.
- [64] A. N. Kallen, X. B. Zhou, J. Xu et al., "The imprinted H19 lncRNA antagonizes let-7 microRNAs," *Molecular Cell*, vol. 52, no. 1, pp. 101–112, 2013.
- [65] J. Lv, L. Wang, J. Zhang et al., "Long noncoding RNA H19-derived miR-675 aggravates restenosis by targeting PTEN," *Biochemical and Biophysical Research Communications*, vol. 497, no. 4, pp. 1154–1161, 2018.
- [66] X. Liu, B. D. Ma, S. Liu, J. Liu, and B. X. Ma, "Long noncoding RNA LINC00341 promotes the vascular smooth muscle cells proliferation and migration via miR-214/FOXO4 feedback loop," *American Journal of Translational Research*, vol. 11, no. 3, pp. 1835–1842, 2019.
- [67] S. Tian, Y. Yuan, Z. Li, M. Gao, Y. Lu, and H. Gao, "LncRNA UCA1 sponges miR-26a to regulate the migration and proliferation of vascular smooth muscle cells," *Gene*, vol. 673, pp. 159–166, 2018.
- [68] J. Zhang, F. Gao, T. Ni et al., "Linc-POU3F3 is overexpressed in in-stent restenosis patients and induces VSMC phenotypic transformation via POU3F3/miR-449a/KLF4 signaling pathway," *American Journal of Translational Research*, vol. 11, no. 7, pp. 4481–4490, 2019.
- [69] J. Y. Sun, Z. W. Zhao, W. M. Li et al., "Knockdown of MALAT1 expression inhibits HUVEC proliferation by upregulation of miR-320a and downregulation of FOXM1 expression," *Oncotarget*, vol. 8, no. 37, pp. 61499–61509, 2017.
- [70] N. Varela, F. Lanás, L. A. Salazar, and T. Zambrano, "The current state of microRNAs as restenosis biomarkers," *Frontiers in Genetics*, vol. 10, p. 1247, 2020.
- [71] M. He, Y. Gong, J. Shi et al., "Plasma microRNAs as potential noninvasive biomarkers for in-stent restenosis," *PLoS One*, vol. 9, no. 11, article e112043, 2014.
- [72] J. F. O'Sullivan, A. Neylon, E. F. Fahy, P. Yang, C. McGorrian, and G. J. Blake, "MiR-93-5p is a novel predictor of coronary in-stent restenosis," *Heart Asia*, vol. 11, no. 1, article e011134, 2019.
- [73] R. Dai, Y. Liu, Y. Zhou et al., "Potential of circulating pro-angiogenic microRNA expressions as biomarkers for rapid angiographic stenotic progression and restenosis risks in coronary artery disease patients underwent percutaneous coronary intervention," *Journal of Clinical Laboratory Analysis*, vol. 34, no. 1, article e23013, 2020.
- [74] L. Yuan, J. Dong, G. Zhu et al., "Diagnostic value of circulating microRNAs for in-stent restenosis in patients with lower extremity arterial occlusive disease," *Scientific Reports*, vol. 9, no. 1, p. 1402, 2019.
- [75] P. W. Stather, N. Sylvius, J. B. Wild, E. Choke, R. D. Sayers, and M. J. Bown, "Differential microRNA expression profiles in peripheral arterial disease," *Circulation: Cardiovascular Genetics*, vol. 6, no. 5, pp. 490–497, 2013.
- [76] S. Stojkovic, M. Jurisic, C. W. Kopp et al., "Circulating microRNAs identify patients at increased risk of in-stent restenosis after peripheral angioplasty with stent implantation," *Atherosclerosis*, vol. 269, pp. 197–203, 2018.
- [77] I. Iakovou, T. Schmidt, E. Bonizzoni et al., "Incidence, predictors, and outcome of thrombosis after successful implantation of drug-eluting stents," *Journal of the American Medical Association*, vol. 293, no. 17, pp. 2126–2130, 2005.
- [78] A. Paul, W. Shao, D. Shum-Tim, and S. Prakash, "The attenuation of restenosis following arterial gene transfer using carbon nanotube coated stent incorporating TAT/DNA<sup>Ang1+Vegf</sup> nanoparticles," *Biomaterials*, vol. 33, no. 30, pp. 7655–7664, 2012.
- [79] J. Yang, Y. Zeng, C. Zhang et al., "The prevention of restenosis in vivo with a VEGF gene and paclitaxel co-eluting stent," *Biomaterials*, vol. 34, no. 6, pp. 1635–1643, 2013.
- [80] R. E. Lanford, E. S. Hildebrandt-Eriksen, A. Petri et al., "Therapeutic silencing of microRNA-122 in primates with chronic hepatitis C virus infection," *Science*, vol. 327, no. 5962, pp. 198–201, 2010.
- [81] G. Santulli, A. Wronska, K. Uryu et al., "A selective microRNA-based strategy inhibits restenosis while preserving endothelial function," *Journal of Clinical Investigation*, vol. 124, no. 9, pp. 4102–4114, 2014.
- [82] S. Liu, Y. Yang, S. Jiang et al., "Understanding the role of non-coding RNA (ncRNA) in stent restenosis," *Atherosclerosis*, vol. 272, pp. 153–161, 2018.

## Retraction

# Retracted: Atomic Scale Interactions between RNA and DNA Aptamers with the TNF- $\alpha$ Protein

### BioMed Research International

Received 12 March 2024; Accepted 12 March 2024; Published 20 March 2024

Copyright © 2024 BioMed Research International. This is an open access article distributed under the Creative Commons Attribution License, which permits unrestricted use, distribution, and reproduction in any medium, provided the original work is properly cited.

This article has been retracted by Hindawi following an investigation undertaken by the publisher [1]. This investigation has uncovered evidence of one or more of the following indicators of systematic manipulation of the publication process:

- (1) Discrepancies in scope
- (2) Discrepancies in the description of the research reported
- (3) Discrepancies between the availability of data and the research described
- (4) Inappropriate citations
- (5) Incoherent, meaningless and/or irrelevant content included in the article
- (6) Manipulated or compromised peer review

The presence of these indicators undermines our confidence in the integrity of the article's content and we cannot, therefore, vouch for its reliability. Please note that this notice is intended solely to alert readers that the content of this article is unreliable. We have not investigated whether authors were aware of or involved in the systematic manipulation of the publication process.

Wiley and Hindawi regrets that the usual quality checks did not identify these issues before publication and have since put additional measures in place to safeguard research integrity.

We wish to credit our own Research Integrity and Research Publishing teams and anonymous and named external researchers and research integrity experts for contributing to this investigation.

The corresponding author, as the representative of all authors, has been given the opportunity to register their agreement or disagreement to this retraction. We have kept a record of any response received.

### References

- [1] H. Asadzadeh, A. Moosavi, G. Alexandrakis, and M. R. K. Mofrad, "Atomic Scale Interactions between RNA and DNA Aptamers with the TNF- $\alpha$  Protein," *BioMed Research International*, vol. 2021, Article ID 9926128, 11 pages, 2021.

## Research Article

# Atomic Scale Interactions between RNA and DNA Aptamers with the TNF- $\alpha$ Protein

Homayoun Asadzadeh,<sup>1</sup> Ali Moosavi ,<sup>1</sup> Georgios Alexandrakis,<sup>2</sup> and Mohammad R. K. Mofrad<sup>3</sup>

<sup>1</sup>Center of Excellence in Energy Conversion (CEEC), School of Mechanical Engineering, Sharif University of Technology, Azadi Avenue, P.O. Box 11365-9567, Tehran 11365-9567, Iran

<sup>2</sup>Department of Bioengineering, University of Texas at Arlington, Arlington, TX 76019, USA

<sup>3</sup>Molecular Cell Biomechanics Laboratory, Departments of Bioengineering and Mechanical Engineering, University of California, Berkeley, CA, USA

Correspondence should be addressed to Ali Moosavi; [moosavi@sharif.edu](mailto:moosavi@sharif.edu)

Received 1 April 2021; Accepted 5 July 2021; Published 17 July 2021

Academic Editor: Lei Chen

Copyright © 2021 Homayoun Asadzadeh et al. This is an open access article distributed under the Creative Commons Attribution License, which permits unrestricted use, distribution, and reproduction in any medium, provided the original work is properly cited.

Interest in the design and manufacture of RNA and DNA aptamers as apta-biosensors for the early diagnosis of blood infections and other inflammatory conditions has increased considerably in recent years. The practical utility of these aptamers depends on the detailed knowledge about the putative interactions with their target proteins. Therefore, understanding the aptamer-protein interactions at the atomic scale can offer significant insights into the optimal apta-biosensor design. In this study, we consider one RNA and one DNA aptamer that were previously used as apta-biosensors for detecting the infection biomarker protein TNF- $\alpha$ , as an example of a novel computational workflow for selecting the aptamer candidate with the highest binding strength to a target. We combine information from the binding free energy calculations, molecular docking, and molecular dynamics simulations to investigate the interactions of both aptamers with TNF- $\alpha$ . The results reveal that the RNA aptamer has a more stable structure relative to the DNA aptamer. Interaction of aptamers with TNF- $\alpha$  does not have any negative effect on its structure. The results of molecular docking and molecular dynamics simulations suggest that the RNA aptamer has a stronger interaction with the protein. Also, these findings illustrate that basic residues of TNF- $\alpha$  establish more atomic contacts with the aptamers compared to acidic or pH-neutral ones. Furthermore, binding energy calculations show that the interaction of the RNA aptamer with TNF- $\alpha$  is thermodynamically more favorable. In total, the findings of this study indicate that the RNA aptamer is a more suitable candidate for using as an apta-biosensor of TNF- $\alpha$  and, therefore, of greater potential use for the diagnosis of blood infections. Also, this study provides more information about aptamer-protein interactions and increases our understanding of this phenomenon.

## 1. Introduction

Severe blood infections leading to sepsis are one of the major causes of death, especially among hospitalized patients [1, 2]. Patients suffering from blood infections are characterized by complex pathophysiology and heterogeneous phenotypes with respect to response to treatment, symptoms, and outcomes. Blood infections are clinically difficult to diagnose due to the multiple factors contributing to their emergence

[3], and definitive diagnosis techniques, risk determination tools, treatment selections, and evaluation methods, or outcome prediction procedures are to be found for these infections [4]. Biomarkers are recognized as natural molecules, genes, or characteristics that can be used as a basis for the detection of specific physiologic or pathologic processes. Clinically speaking, biomarkers are deemed valuable only when they can contribute to decision making. Ideal biomarkers are characterized by fast kinetics, high affinity and

specificity, detectability by automated technologies, and inexpensive bedside testing [4]. Many protein biomarkers have been identified that can be used to detect blood infections, such as C-reactive protein (CRP) [5], Interleukin 6 (IL-6) [6], Procalcitonin (PCT) [7], Interleukin 10 (IL-10) [8], Interferon-gamma (IFN- $\gamma$ ) [8], and tumor necrosis factor-alpha (TNF- $\alpha$ ) [9–11].

The multiple proinflammatory cytokines are identified as possible biomarkers of blood infection [11], and TNF- $\alpha$  is one of the most promising candidates [10], as its serum levels increase significantly during an infection [9]. Tumor necrosis factor- $\alpha$  (TNF- $\alpha$ ) is an important proinflammatory cytokine that contributes to acute phase reaction. Although TNF- $\alpha$  can be secreted by many cell types such as NK cells eosinophils, neurons, CD4+ lymphocytes, neutrophils, and mast cells, it is secreted primarily by macrophages [12]. TNF- $\alpha$  is a subordinate member of the TNF superfamily which embodies different types of transmembrane proteins with a homology domain [13]. Mature human TNF- $\alpha$  is secreted after cleavage of a 76-residue peptide from the amino terminus of the prohormone and the mature protein contains single intramolecular disulfide bridge [14]. Previous studies have shown TNF- $\alpha$  to be a trimer in solution [14, 15]. The several crystal forms in which the molecule has been obtained have either crystallographic or noncrystallographic 3-fold symmetry, suggesting that the cytokine forms trimers in the solid-state as well [16, 17]. The TNF- $\alpha$  subunit is a  $\beta$ -sheet sandwich constructed almost entirely of antiparallel  $\beta$ -strands.

Due to the known involvement of TNF- $\alpha$  in sepsis, many bioassays have been targeting its molecular structure with various probes to reveal its presence in serum [18]. TNF- $\alpha$ , including fluorescence immunoassay, enzyme-linked immunosorbent assay (ELISA), radioimmunoassay, and time-resolved immune-fluorometric assay, is, thanks to a number of commonly used traditional immunoassays, easy to detect and quantify [19, 20]. Nevertheless, creation of sandwich immunoassays in the traditional methods is dependent on antibody pairs. Moreover, these methods are characterized by multiple washing steps and high-cost readout signal development procedures.

Aptamers are single-stranded DNA or RNA oligonucleotides that have been developed as powerful and reasonably priced alternatives to traditional antibodies for TNF- $\alpha$  targeting. Aptamers are actually recognized as high-affinity and high-specificity biomolecule binding agents. These oligonucleotides are characterized by their modifiability and their potential to introduce affinity and signal transducing moieties into the same molecule. Aptasensors with analyte capturing and signal transducing potential have already been addressed in the literature [21, 22]. Detection of aptasensor-based cell biomarkers has received a lot of attention over the last few years [23, 24].

Analytical and numerical methods can provide further insight into observed biologically oriented experiments or biological phenomenon, which are difficult to study experimentally [25–29]. Among these available techniques, molecular dynamics and docking technique which are strong computational tools that provide valuable complementary

to experiment information about the details of the atomistic interactions in biological phenomena has attracted attention recently. Up to now, various researches have been performed a lot of research regarding the molecular dynamic and docking simulation to investigate the behavior of protein, aptamer, ligands, and peptides in the atomic scale [30, 31]. In 2021, He et al. [32] performed molecular docking simulations for an electrochemical impedimetric sensing platform based on a peptide aptamer, and they found the binding capacity of peptide aptamers by molecular docking and demonstrated that docking was an effective tool to screen peptide aptamers for amino acid-binding capacity.

In this study, we investigate the interactions of TNF- $\alpha$ , with aptamer candidates (DNA and RNA) via molecular dynamics (MD) method. For this purpose, two-dimensional (2D) and three-dimensional (3D) structures of aptamers were calculated and were optimized through a 200 ns MD simulation. In the next step, the interactions of these aptamers with different sides of the TNF- $\alpha$  protein were investigated using molecular docking and MD simulations and binding free energy calculations. The results of this study provide useful information for identifying an aptasensor with high selectivity and affinity to TNF- $\alpha$ .

## 2. Method and Materials

*2.1. Preparation and Calculation the Input Structural Files.* In this study, we studied the interactions of two DNA and RNA aptamers with TNF- $\alpha$ . The structure of TNF- $\alpha$  was obtained from the RCSB database (PDB id: 1TNF) [14]. The missing residues of TNF- $\alpha$  were modeled by the SWISS-MODEL web tool and, then, simulated for 200 ns [33, 34]. On the basis of previous experimental studies, we selected two aptamers that specifically interact with TNF- $\alpha$  [35, 36]. The sequence of aptamers is illustrated in the following:

25-mer DNA: 5'-TGGTGGATGGCGCAGTCGGCG ACAA-3'.

28-mer RNA: 5'-GGAGUAUCUGAUGACAAUUCG GAGCUCC-3'.

The secondary structures of DNA and RNA aptamers were predicted by the use of the Mfold [37] web server and ViennaRNA [38] web services, respectively. The SimRNA [39] web server was used to predict the 3D structure of RNA aptamers from the 2D pattern. Furthermore, the 3D structure of DNA aptamer was modeled using the method of Iman Jeddi and colleagues [40]. Finally, each 3D structure model of DNA and RNA aptamers was modeled for 200 ns, and the final data were employed for docking with the equilibrated TNF- $\alpha$  conformation.

*2.2. Molecular Docking.* In order to obtain the basic information about the possible binding locations of aptamers to protein, we performed molecular shape complementarity docking using the PatchDock [41] web server. Prepared Protein Data Bank (PDB) files of aptamers and receptor were provided to a PatchDock server at a default value of 4.0 for clustering Root-Mean-Square Deviation (RMSD) and default complex types. PatchDock represents the Connolly's surface of docking as flat, convex, and concave patches and conforms



them to produce candidate transformations [41]. For each aptamer-protein complex, we extracted two select cluster with higher score for using as the initial set of coordinates in the MD simulations [42–44].

**2.3. Molecular Dynamics (MD) Simulation.** All the simulations in the present investigation were performed via the GROMACS 5.1.4 package [45]. Also, the Amber ff99SB-ILDN force fields were used in this study [46]. In order to neutralize the system, we add the appropriate number of the ions (sodium and chloride) that were added to the system. The periodic boundary conditions (PBCs) were applied to each system in all the spatial directions [47]. Additionally, to solvate the system, the transferable intermolecular potential 3-point (TIP3P) water model was utilized [48]. Using LINCS algorithms, all of the covalent bonds lengths were constrained [49]. Simulations were performed using a short-distance electrostatic interplay and a distance cutoff of 1.2 nm for the van der Waals interaction. Using the Particle Mesh Ewald algorithm (PME), the long-range electrostatic forces were calculated [50]. All systems' energy was minimized via the steepest descent algorithm. The considered cases were then allowed to reach the equilibrium state by a subsequent NVT 500 ps run. After that, all the cases equilibrated through the NPT ensemble. Using Nose-Hoover algorithm temperature [51], the temperature was maintained at 310 K in this process [52, 53]. Over the course of the NPT equilibration, the Parrinello-Rahman barostat was used to maintain the pressures at 101.3 kPa via [54]. Complementary details about simulation systems are provided in Table 1.

**2.4. The  $g\_mmpbsa$  Method.** The interactions between the protein (nonpolar and polar) can be determine via the binding free-energy evaluation and other biological macromolecules. The binding free-energy was calculated by using the MM-PBSA method and the  $g\_mmpbsa$  tool [55–58].

By adding the nonpolar ( $\Delta G_{\text{nonpolar}}$ ) and the polar ( $\Delta G_{\text{polar}}$ ) interaction free-energy differences, the overall binding free-energy ( $\Delta G$ ) was obtained as the following:

$$\Delta G_{\text{total}} = \Delta G_{\text{polar}} + \Delta G_{\text{nonpolar}}, \quad (1)$$

where  $\Delta G_{\text{polar}}$  and  $\Delta G_{\text{nonpolar}}$  are given by

$$\Delta G_{\text{polar}} = \Delta G_{\text{ps}} + \Delta G_{\text{elec}}, \quad (2)$$

$$\Delta G_{\text{nonpolar}} = \Delta G_{\text{nps}} + \Delta G_{\text{vdW}}, \quad (3)$$

where  $\Delta G_{\text{ps}}$  and  $\Delta G_{\text{nps}}$  are the difference of the polar and nonpolar solvation energies, respectively. Also,  $\Delta G_{\text{vdW}}$  is the difference of the energy related to the van der Waals interactions, and  $\Delta G_{\text{elec}}$  stands for the difference of the energy associated with the electrostatic interactions. 500 snapshots taken from the last 100 ns of each aptamer-protein complex simulation were used in these binding free-energy calculations.

TABLE 1: List of abbreviations and key physical parameter values for the performed simulations. In all states, the length of simulation and the temperature are 200 ns and 310 K, respectively.

Simulation compounds	Acronym	No. of water molecules
TNF- $\alpha$	TNF	30260
RNA aptamer	RNA	10004
TNF-RNA-1	TR1	31425
TNF-RNA-2	TR2	30581
DNA aptamer	DNA	7674
TNF-DNA-1	TD1	30681
TNF-DNA-2	TD2	29451

### 3. Results and Discussion

**3.1. Elucidation of the Structure and Dynamics of Individual Aptamers and TNF- $\alpha$  Proteins.** Based on the previous studies, we selected two aptamers that have specific interactions with TNF- $\alpha$  [35, 36]. These RNA and DNA aptamers were 28 and 25 nucleotides in length, respectively. In the next step, the secondary structure and folding of each aptamer were predicted using the Mfold [38] web server and ViennaRNA [38] web services. The Gibbs free energy of folding for DNA and RNA, respectively, and suggest the folding pattern with the most favorable energy. Then, the 3D structure of aptamers predicted based on the folding pattern that calculated in the previous step. Finally, in order to validate the obtained 3D structure, 200 ns molecular dynamics simulation performed on modeled structures. In Figure 1, the 2D, 3D, and equilibrated 3D structures are shown. The  $\Delta G$  energy of folding for DNA and RNA aptamers is -4.81 kcal/mol and -10.6 kcal/mol, respectively. Many previous computational studies used the RMSD as a parameter to illustrate the equilibration of the system. Hence, in order to investigate the stability of conformations arrived at by our MD simulations, the RMSD value was computed for C- $\alpha$  in TNF- $\alpha$  and the backbone atoms of aptamers. The resulting RMSD time trajectories are illustrated in Figure 2. As shown in Figure 2(a), after about 20 ns, the structural fluctuation of the protein became stable and RMSD values plateaued. Furthermore, aptamers had higher fluctuations in their structure than TNF- $\alpha$ , due to their structural features that make them more flexible than proteins [59].

In Figure 2(b), the DNA aptamer has higher fluctuation in own structure than the RNA aptamer. These results are in line with the value of  $\Delta G$  energy of folding. In total, the RNA aptamer has a more stable structure than the DNA aptamer. Also, previous experimental works have shown that the RNA folded structure has more stability than the single-strand DNA folded structure [60]. Furthermore, some researchers have employed the MD and docking simulation in their studies. In 2016, Torabi et al. [61] conducted a MD and docking simulation to achieve a better understanding of specific binding interactions of the target protein (RBP4) and RBA. They computed RMSD as a function of time and compare them for the two states, one lone RBA and RBA in the complex with RBP4, and second lone RBP4 backbone and RBP4 backbone in the complex with RBA. The resulting

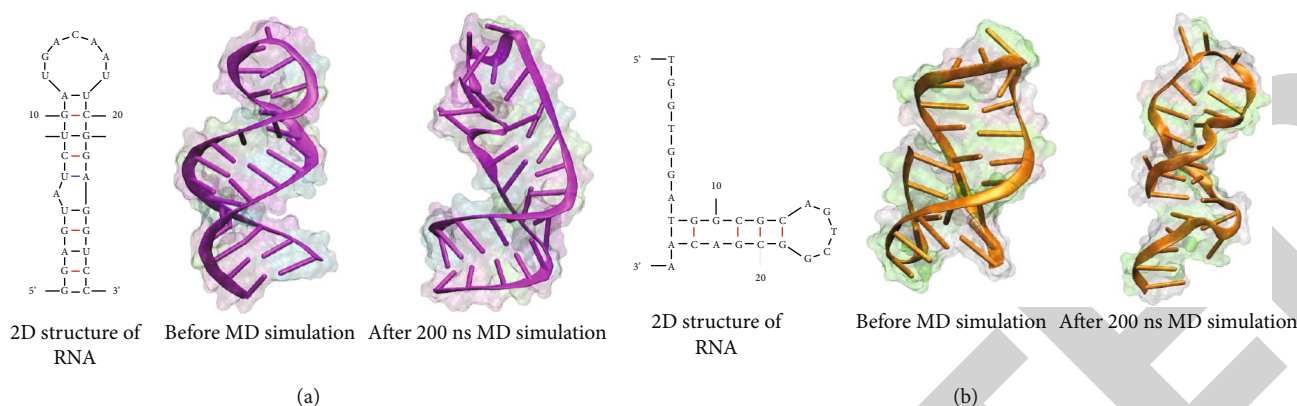


FIGURE 1: The 2D, 3D (presimulation), and equilibrated 3D (postsimulation) structures of (a) RNA and (b) DNA aptamers.

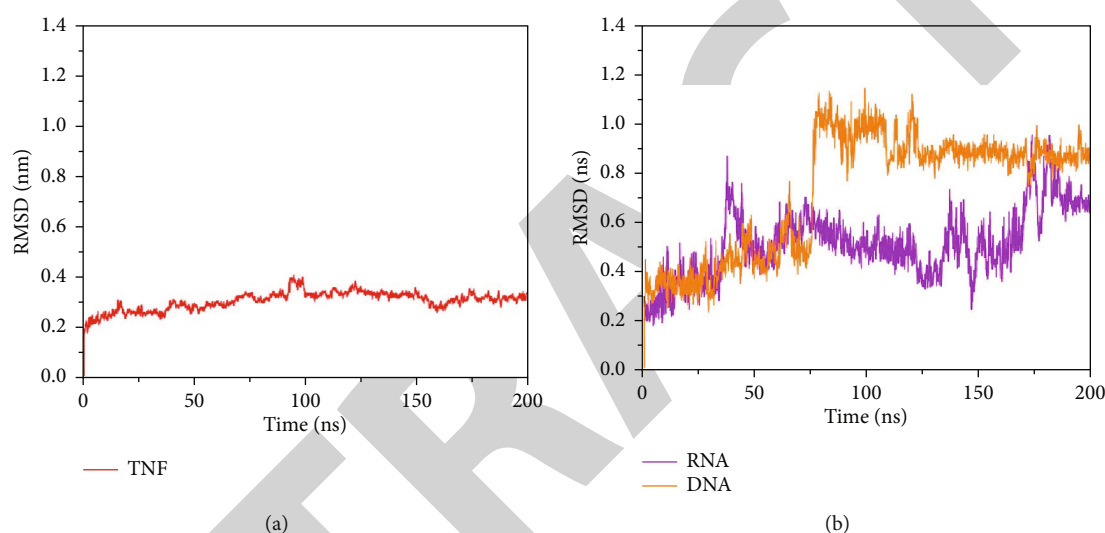


FIGURE 2: Time course of RMSD during the MD simulations for (a) TNF- $\alpha$  and (b) aptamers. The RMSD value of each chain of TNF- $\alpha$  was computed separately, and only their average is reported.

RMSD time trajectories are shown that after about 20 ns, the structural fluctuation of the protein became stable, and it can be concluded that the RBA has more fluctuation than the RBA in the complex with the RBP4. Also, in 2018, Autiero et al. [62] conducted a research via the MD and docking simulation technique and evaluated the dynamics of the complex between the S8 protein and the aptamer. The RMSD values of trajectory structures vs. complex, aptamer, and protein was computed and compared with each other. The RMSD time trajectories shown that the overall system undergoes a little rearrangement after 50 ns, whereas both the protein and the aptamer remain virtually unchanged. Thus, according to these results and our study, it can be concluded that RMSD in MD simulation is an important parameter which can demonstrate the equilibration of the system [30–58].

**3.2. Studying Protein-Aptamer Interactions by Molecular Docking Simulations.** To investigate further the interactions of aptamers with TNF- $\alpha$  in terms of identifying the possible binding locations of aptamers to the protein, we performed molecular docking computations using the PatchDock server. Many previous studies have used the PatchDock

TABLE 2: Results of the molecular docking calculations between aptamers and TNF- $\alpha$ .

	Geometric shape complementarity score [68]	Approximate interface area of the complex ( $\text{\AA}^2$ ) (area)	Atomic contact energy [69] (kcal/mol) (ACE)
TR1	13160	1870.90	-235.58
TR2	12876	1736.30	-166.63
TD1	10865	1532.40	-153.24
TD2	9864	1498.80	-142.57

server to investigate the interaction of nucleic acids with proteins [63–65]. The coordinates of TNF- $\alpha$ , RNA aptamer, and DNA aptamer were extracted from the last snapshot of the prior MD simulations and used for performing docking computations. For each RNA-protein and DNA-protein complex, we selected two clusters with a higher score relative to other clusters. More detailed information from the docking computation results is shown in Table 2, with both clusters of RNA aptamer having a higher binding affinity to TNF- $\alpha$

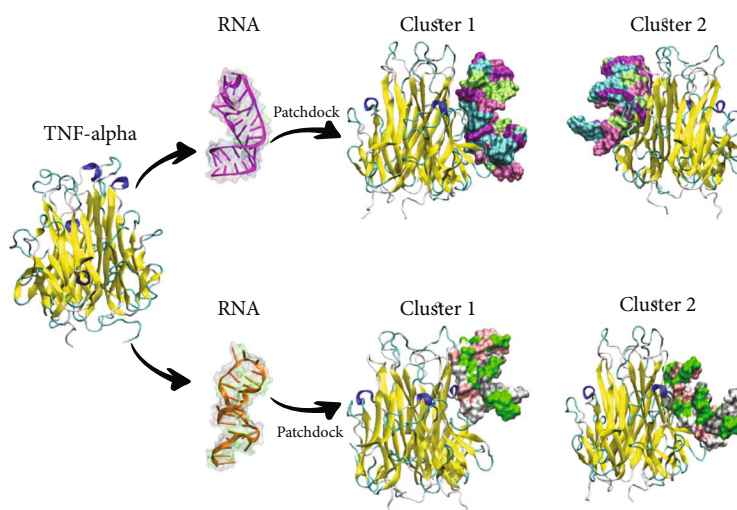


FIGURE 3: Graphical representation of the aptamer-TNF- $\alpha$  complexes computed by PatchDock.

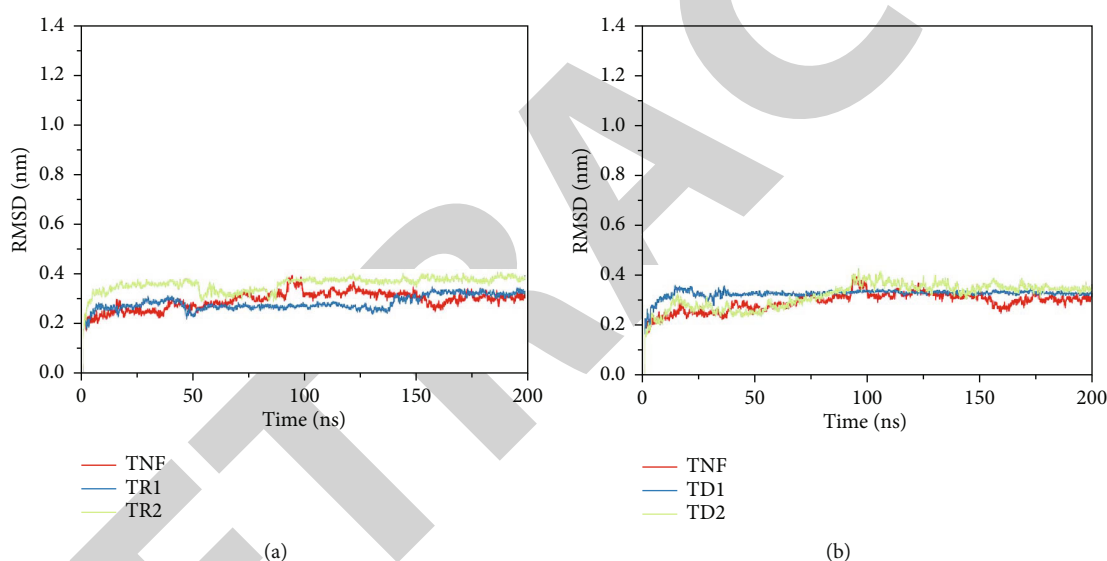


FIGURE 4: The RMSD value of TNF- $\alpha$  during interactions with (a) an RNA aptamer and (b) a DNA aptamer. To better represent the effect of aptamers on the protein structure, the RMSD plot of TNF- $\alpha$  alone was shown in both graphs.

than the DNA clusters. The RNA aptamer had more interface area with TNF- $\alpha$ , which shows that more nucleotides of the aptamer are in the direct contacts with protein. Also, the RNA aptamer had higher binding energy with TNF- $\alpha$  than the DNA aptamer. The results of docking calculations are in agreement with previous experimental studies that have illustrated the RNA molecules to have stronger interactions with proteins due to the Ribose carbohydrate in their backbone [66, 67].

As shown in Figure 3, the binding locations of aptamers onto the protein surface differed in each cluster. Furthermore, the orientation of aptamers was different in clusters. Both aptamers in cluster 1 interacted with two side chains of TNF- $\alpha$ , but aptamers in cluster 2 interacted with one chain only. This is probably why the aptamers in cluster 2 had a smaller interface area with TNF- $\alpha$  relative to the aptamers in cluster 1.

**3.3. Molecular Dynamics Simulations.** The atomic coordinates of aptamer-protein complexes obtained by molecular docking calculations were used as initial conditions for subsequent molecular dynamics simulations of 200 ns duration to help refine further our understanding of aptamer-TNF- $\alpha$  interactions.

**3.4. Structural Analyses of Aptamer-Protein Complexes through MD Simulation.** To investigating the effects of the conformational fluctuations of aptamers and TNF- $\alpha$  on the structural stability of the complexes they formed, the RMSD values of each entity were computed during their interactions over 200 ns MD simulation trajectories. First, we studied the fluctuations of the TNF- $\alpha$  structure during interactions with aptamers. As shown in Figure 4, the interactions of aptamers with TNF- $\alpha$  had no major effect on the structure of the protein. For each interaction pair, the RMSD value of three TNF-

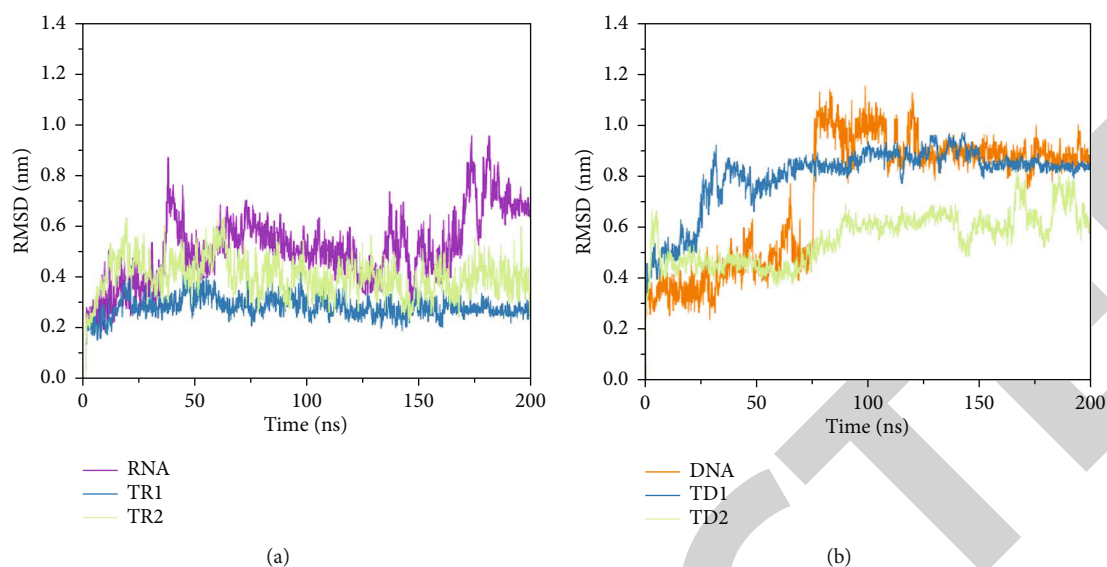


FIGURE 5: RMSD plots in (a) RNA-contained simulation systems and (b) DNA-contained simulation systems.

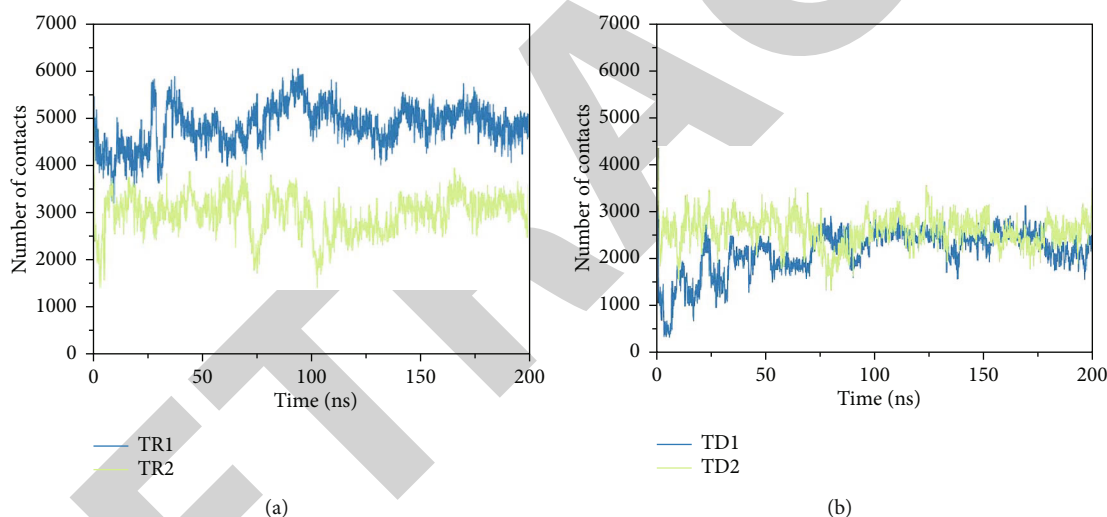


FIGURE 6: The number of contacts in (a) RNA-contained systems and (b) DNA-contained systems during 200 ns MD simulation trajectories (>0.6 nm).

$\alpha$  chains was calculated separately, and the average value was reported. All interaction pairs reached stable states after about 15 ns, and the fluctuations of TNF- $\alpha$  structure in all simulation systems were almost equal and in the range of 0.2 nm to 0.4 nm. Hence, we can conclude that bound aptamers to the protein did not have any major effect on the structure of TNF- $\alpha$ . These findings are in line with other experimental and computational studies [70, 71].

Furthermore, the RMSD value of aptamers during interactions with TNF- $\alpha$  was also calculated. The RMSD was computed for only the backbone atoms of the aptamers. The results show that interactions with TNF- $\alpha$  reduced the structural fluctuations of the RNA aptamer (Figure 5(a)). In RNA-contained simulations, we can see that the fluctuations of free RNA aptamer are about 0.7 nm at the end of the simulation, but in the TR1 and TR2 systems, the structural fluctuations

are 0.2 nm and 0.4 nm, respectively. By comparing these results with the docking results, we can conclude that the interactions between aptamer and TNF- $\alpha$  are stronger, and as a result, the structural fluctuations of the aptamer are reduced. For instance, the fluctuations of RNA aptamer in the TR1 system are lower than the fluctuation of the RNA aptamer in the TR2 system (Figure 5(a)), because the aptamer-protein complex in the TR1 system has a stronger binding affinity (Table 2). When the aptamer binds to the protein surface, the strong electrostatic interactions between basic residues of protein and negatively charged nucleotides make the structural fluctuations of the protein restrained. For the DNA-contained systems, similar behavior was observed (Figure 5(b)).

### 3.5. Aptamer-Protein Interactions during MD Simulations.

For explaining the affinity binding of aptamers to TNF- $\alpha$ ,



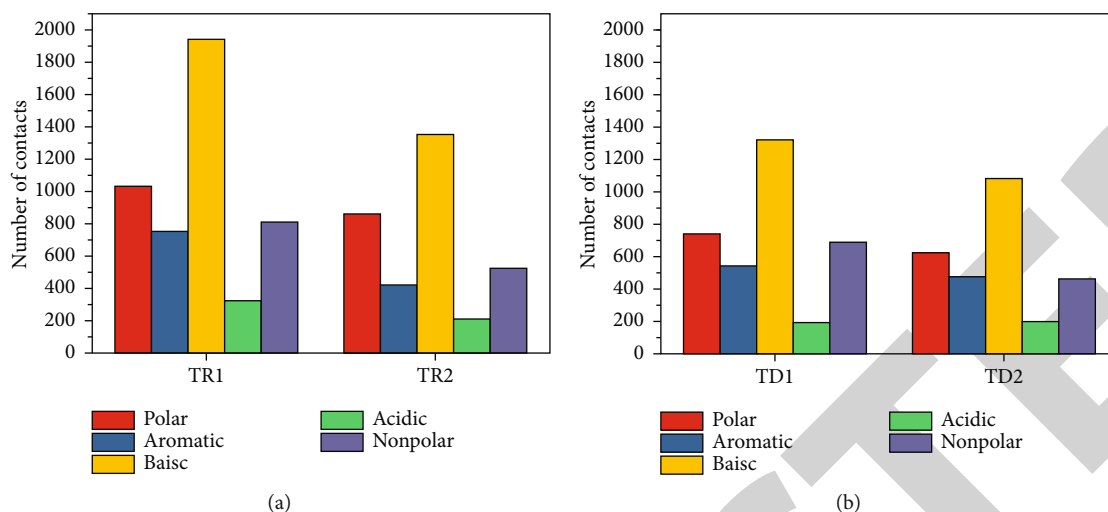


FIGURE 7: Average number of contacts between different types of residues and aptamers in (a) RNA-contained systems and (b) DNA-contained systems (>0.6 nm).

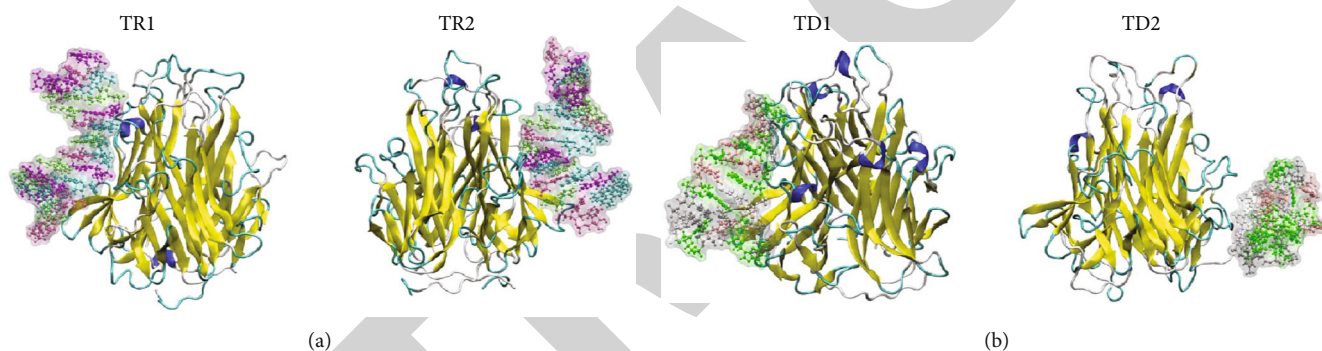


FIGURE 8: Graphical representation of aptamer-protein complexes at the end of the 200 ns MD simulations for (a) RNA-contained systems and (b) DNA-contained systems.

the contact numbers between aptamers and protein were calculated during the simulation trajectories (Figure 6). Furthermore, to determine the role of different types of protein residues in interactions with aptamers, the average number of contacts between different types of residue (polar, nonpolar, aromatic, basic, and acidic) and each aptamer was computed (Figure 7). As shown in Figure 6, the RNA aptamer in both clusters has a higher number of contacts with TNF- $\alpha$  than the DNA aptamer. Also, the RNA aptamer in the TR1 system had the highest number of contacts between all simulation systems (Figure 6(a)). These findings are in good agreement with the results of our molecular docking computations and illustrate that the RNA aptamer had stronger interactions with protein relative to the DNA aptamer. The latter had almost equal number of contacts with protein in both clusters (Figure 6(b)).

Moreover, the results of the contact number analyses have shown the significant role of the basic residues of TNF- $\alpha$  that have in the interactions with aptamers. Previous investigations indicate that in the interactions with anionic molecules such as antimicrobial peptides and nucleic acids the basic residues in the proteins play a major role [72, 73].

In Figure 7, it has shown that in all systems, the basic residues had the highest number of contacts with aptamers which is due to the strong electrostatic interactions with negatively charged nucleotides. The basic residues of the TNF- $\alpha$  had higher numbers of contacts with the RNA and DNA aptamers. These findings also provide the insight that RNA aptamer interacted more strongly with TNF- $\alpha$  compared to DNA ones due to the more polar and less basic nature of the residues in the latter, while the number of aptamer contacts with TNF- $\alpha$  was comparable in both cases.

To provide a better understanding of aptamer-protein complexes, the graphical representation of complexes at the end of the simulation was illustrated Figure 8. As shown in Figure 8, aptamers in cluster 2 could not maintain their positions on the protein's surface and settled at some distance from protein, especially their terminal nucleotides. On the other hand, in cluster 1 systems, aptamers could conserve their interactions with TNF- $\alpha$  and have a higher number of contacts which are in line with results of our molecular docking computations (Table 2). In total, we can interpret from the results of MD simulation section that RNA aptamer can make stronger interaction with TNF- $\alpha$ . Taken together, the

TABLE 3: Binding free energy calculations of the aptamer-protein interactions. (kJ/mol).

Simulation systems	Nonpolar binding free energy		Polar binding free energy		Total binding free energy
	Van der Waals energy	SASA energy	Electrostatic energy	Polar solvation energy	
TR1	-475.247	-48.14	-7291.523	74.127	-7740.783
TR2	-287.586	-25.481	-5761.594	63.842	-6010.819
TD1	-362.815	-29.648	-5634.128	41.479	-5985.112
TD2	-259.483	-18.87	-4861.243	48.275	-5091.321

number of contacts, free energy, and docking, all support the conclusion of stronger interactions with RNA. Our simulation findings are therefore congruent with the results of the previous experimental studies demonstrating the feasibility of using RNA aptamers as apta-biosensors tailored to bind target proteins with high specificity and at very low concentrations [36, 74].

**3.6. Binding Free Energy Calculations.** Previous investigations have revealed that electrostatic interactions play a key role in biological macromolecule interactions, especially when these have opposite charges [56, 71, 75–77]. To get more information about the interaction of aptamers with the TNF- $\alpha$  via the `g_mmpbsa` tool (Table 3), the nonpolar, polar, and total binding free energy between the aptamers and the protein were computed. The table shows that the van der Waals (vdW) energy had a major contribution in nonpolar energy, while SASA energy had a small contribution. The vdW energy has a significant effect on the interactions between the aptamer and the protein, especially in TR1 and TR2 simulation systems. This is probably due to the favorable hydrophobic interactions of aptamers with protein. This is possibly due to the electrostatic interaction between the basic residues of TNF- $\alpha$  and the negatively charged nucleotides. The strongest electrostatic energy was found in TR1 and the weakest one in TD2. The polar solvation energy was positive in all the simulations. In total, by taking into account the total binding energy as a parameter to represent the strength of aptamer-protein complexes, the TR1 was the strongest complex and TD2 was the weakest. The results of these binding free energy calculations are in close agreement with the previous results and confirm that the RNA aptamer had stronger interactions with TNF- $\alpha$  than the DNA aptamer.

## 4. Conclusion

In this study, we investigated the interactions of RNA and DNA aptamers with TNF- $\alpha$  at the atomic scale by binding free energy calculations, molecular docking, and MD simulations. It was observed that the folding process of the RNA aptamer had more negative  $\Delta G$  energy than the folding process of the DNA aptamer. Furthermore, the results of molecular docking calculations showed that the RNA aptamer had stronger interactions with TNF- $\alpha$  and got a higher score relative to the DNA aptamer. Computational structural analyses illustrated that during interactions, the aptamers did not have any negative effect on the TNF- $\alpha$  structure. Furthermore, the structural fluctuations of aptamers were reduced during interactions with the protein. The results of binding

free energy calculations and MD simulations showed that the RNA aptamer had stronger interactions with protein than the DNA aptamer. The results revealed that basic residues of TNF- $\alpha$  had more contacts at the atomic scale with aptamer relative to other residue types. RNA aptamers, in turn, created more contacts with protein and thermodynamically had more favorable binding energy with TNF- $\alpha$ . Collectively, these findings illustrated that RNA aptamers are a more suitable candidate, compared to DNA aptamers, to use for constructing an apta-biosensor for sensing the presence of TNF- $\alpha$  in a biological sample, which is in agreement with previous experimental studies [40]. It is also important to point out that the computational methodologies workflow developed in this work could be generalizable to the design of other apta-biosensors to their target proteins.

## Data Availability

In order to obtain the basic information about the possible binding locations of aptamers to protein, we performed molecular shape complementarity docking using the PatchDock web server: “Schneidman-Duhovny, D., Inbar, Y., Nussinov, R., Wolfson, H. J. (2005), Patchdock and symmdock: servers for rigid and symmetric docking, Nucleic acids research, 33, W363-W367”.

## Disclosure

The funding sources had no involvement in the study design, collection, analysis, or interpretation of data, writing of the manuscript, or in the decision to submit the manuscript for publication.

## Conflicts of Interest

We declare no conflict of interest.

## Acknowledgments

The authors acknowledge the high performance computing center in the Department of Computer Engineering and the Micro- and Nanofluidic Lab in the School of Mechanical Engineering at the Sharif University of Technology (SUT) for their assistance and authorization to access supercomputers to fulfill advanced computations and simulations of the current study.

## References

- [1] S. A. Novosad, M. R. Sapiano, C. Grigg et al., "Vital signs: epidemiology of sepsis: prevalence of health care factors and opportunities for prevention," *Morbidity and Mortality Weekly Report*, vol. 65, no. 33, pp. 864–869, 2016.
- [2] J. L. Vincent, J. Rello, J. Marshall et al., "International study of the prevalence and outcomes of infection in intensive care units," *JAMA*, vol. 302, no. 21, pp. 2323–2329, 2009.
- [3] J. Rello, F. Valenzuela-Sanchez, M. Ruiz-Rodriguez, and S. Moyano, "Sepsis: a review of advances in management," *Advances in Therapy*, vol. 34, no. 11, pp. 2393–2411, 2017.
- [4] J. Cohen, J.-L. Vincent, N. K. Adhikari et al., "Sepsis: a roadmap for future research," *The Lancet Infectious Diseases*, vol. 15, no. 5, pp. 581–614, 2015.
- [5] P. Póvoa, A. M. Teixeira-Pinto, A. H. Carneiro, and the Portuguese Community-Acquired Sepsis Study Group (SACiUCI), "C-reactive protein, an early marker of community-acquired sepsis resolution: a multi-center prospective observational study," *Critical Care*, vol. 15, no. 4, article R169, 2011.
- [6] T. Hou, D. Huang, R. Zeng, Z. Ye, and Y. Zhang, "Accuracy of serum interleukin (IL)-6 in sepsis diagnosis: a systematic review and meta-analysis," *International Journal of Clinical and Experimental Medicine*, vol. 8, article 15238, 2015.
- [7] A. L. Vijayan, S. Ravindran, R. Saikant, S. Lakshmi, and R. Kartik, "Procalcitonin: a promising diagnostic marker for sepsis and antibiotic therapy," *Journal of Intensive Care*, vol. 5, no. 1, p. 51, 2017.
- [8] Q. Ye, L. Z. du, W. X. Shao, and S. Q. Shang, "Utility of cytokines to predict neonatal sepsis," *Pediatric Research*, vol. 81, no. 4, pp. 616–621, 2017.
- [9] B. G. Sood, S. Shankaran, R. L. Schelonka et al., "Cytokine profiles of preterm neonates with fungal and bacterial sepsis," *Pediatric Research*, vol. 72, no. 2, pp. 212–220, 2012.
- [10] A. Gordon, A. Lagan, E. Aganna et al., "Tnf and Tnfr polymorphisms in severe sepsis and septic shock: a prospective multi-centre study," *Genes & Immunity*, vol. 5, no. 8, pp. 631–640, 2004.
- [11] A. Deasy and R. C. Read, "Genetic variation in pro-inflammatory cytokines and meningococcal sepsis," *Current Opinion in Infectious Diseases*, vol. 23, no. 3, pp. 255–258, 2010.
- [12] B. Beutler, D. Greenwald, J. Hulmes et al., "Identity of tumour necrosis factor and the macrophage-secreted factor cachectin," *Nature*, vol. 316, no. 6028, pp. 552–554, 1985.
- [13] R. M. Locksley, N. Killeen, and M. J. Lenardo, "The Tnf and Tnf receptor superfamilies: integrating mammalian biology," *Cell*, vol. 104, no. 4, pp. 487–501, 2001.
- [14] M. J. Eck and S. R. Sprang, "The structure of tumor necrosis factor- $\alpha$  at 2.6 Å resolution: implications for receptor binding," *Journal of Biological Chemistry*, vol. 264, no. 29, pp. 17595–17605, 1989.
- [15] P. Wingfield, R. H. Pain, and S. Craig, "Tumour necrosis factor is a compact trimer," *FEBS Letters*, vol. 211, no. 2, pp. 179–184, 1987.
- [16] H.-J. Schoenfeld, B. Poeschl, J. R. Frey et al., "Efficient purification of recombinant human tumor necrosis factor beta from escherichia coli yields biologically active protein with a trimeric structure that binds to both tumor necrosis factor receptors," *Journal of Biological Chemistry*, vol. 266, no. 6, pp. 3863–3869, 1991.
- [17] E. Jones, D. Stuart, and N. Walker, "Structure of tumour necrosis factor," *Nature*, vol. 338, no. 6212, pp. 225–228, 1989.
- [18] M. A. Palladino, F. R. Bahjat, E. A. Theodorakis, and L. L. Moldawer, "Anti-Tnf- $\alpha$  therapies: the next generation," *Nature Reviews Drug Discovery*, vol. 2, no. 9, pp. 736–746, 2003.
- [19] S. Cesaro-Tadic, G. Dernick, D. Juncker et al., "High-sensitivity miniaturized immunoassays for tumor necrosis factor  $\alpha$  using microfluidic systems," *Lab on a Chip*, vol. 4, no. 6, pp. 563–569, 2004.
- [20] K. Zeman, J. Kantorski, E. M. Paleolog, M. Feldmann, and H. Tchórzewski, "The role of receptors for tumour necrosis factor- $\alpha$  in the induction of human polymorphonuclear neutrophil chemiluminescence," *Immunology Letters*, vol. 53, no. 1, pp. 45–50, 1996.
- [21] Y. Xiao, R. Y. Lai, and K. W. Plaxco, "Preparation of electrode-immobilized, redox-modified oligonucleotides for electrochemical DNA and aptamer-based sensing," *Nature Protocols*, vol. 2, no. 11, pp. 2875–2880, 2007.
- [22] E. E. Ferapontova, E. M. Olsen, and K. V. Gothelf, "An Rna aptamer-based electrochemical biosensor for detection of theophylline in serum," *Journal of the American Chemical Society*, vol. 130, no. 13, pp. 4256–4258, 2008.
- [23] Y. Wang, Z. Li, D. Hu, C.-T. Lin, J. Li, and Y. Lin, "Aptamer/graphene oxide nanocomplex for in situ molecular probing in living cells," *Journal of the American Chemical Society*, vol. 132, no. 27, pp. 9274–9276, 2010.
- [24] W. Zhao, S. Schafer, J. Choi et al., "Cell-surface sensors for real-time probing of cellular environments," *Nature Nanotechnology*, vol. 6, no. 8, pp. 524–531, 2011.
- [25] E. Ghazimirsaeed, M. Madadelahi, M. Dizani, and A. Shamloo, "Secondary flows, mixing, and chemical reaction analysis of droplet-based flow inside serpentine microchannels with different cross sections," *Langmuir*, vol. 37, no. 17, pp. 5118–5130, 2021.
- [26] M. Boodaghi and A. Shamloo, "Effects of wax boundaries in combination with evaporation on dynamics of fluid flow in paper-based devices," *Surfaces and Interfaces*, vol. 21, article 100684, 2020.
- [27] A. Lafzi, A. H. Raffiee, and S. Dabiri, "Inertial migration of a deformable capsule in an oscillatory flow in a microchannel," *Physical Review E*, vol. 102, no. 6, article 063110, 2020.
- [28] S. Razavi Bazaz, A. Mashhadian, A. Ehsani, S. C. Saha, T. Krüger, and M. Ebrahimi Warkiani, "Computational inertial microfluidics: a review," *Lab on a Chip*, vol. 20, no. 6, pp. 1023–1048, 2020.
- [29] A. Shamloo and A. Mashhadian, "An inertial microfluidic device for targeted cell separation," *New Biotechnology*, vol. 44, article S129, 2018.
- [30] H. Asadzadeh and A. Moosavi, "Investigation of the interactions between Melittin and the PLGA and PLA polymers: molecular dynamic simulation and binding free energy calculation," *Material Research Express*, vol. 6, no. 5, article 055318, 2019.
- [31] H. Asadzadeh, A. Moosavi, and J. H. Arghavani, "The effect of chitosan and PEG polymers on stabilization of GF-17 structure: a molecular dynamics study," *Carbohydrate Polymer*, vol. 237, article 116124, 2020.
- [32] Y. He, L. Zhou, L. Deng, Z. Feng, Z. Cao, and Y. Yin, "An electrochemical impedimetric sensing platform based on a peptide aptamer identified by high-throughput molecular docking for sensitive l-arginine detection," *Bioelectrochemistry*, vol. 137, p. 107634, 2021.



- [33] A. Waterhouse, M. Bertoni, S. Bienert et al., "Swiss-model: homology modelling of protein structures and complexes," *Nucleic Acids Research*, vol. 46, no. W1, pp. W296–W303, 2018.
- [34] S. Bienert, A. Waterhouse, T. A. de Beer et al., "The Swiss-model repository—new features and functionality," *Nucleic Acids Research*, vol. 45, no. D1, pp. D313–D319, 2017.
- [35] Y. Liu, Q. Zhou, and A. Revzin, "An Aptasensor for electrochemical detection of tumor necrosis factor in human blood," *Analyst*, vol. 138, no. 15, pp. 4321–4326, 2013.
- [36] E. W. Orava, N. Jarvik, Y. L. Shek, S. S. Sidhu, and J. Gariépy, "A short DNA aptamer that recognizes Tnfa and blocks its activity in vitro," *ACS Chemical Biology*, vol. 8, no. 1, pp. 170–178, 2013.
- [37] M. Zuker, "Mfold web server for nucleic acid folding and hybridization prediction," *Nucleic Acids Research*, vol. 31, no. 13, pp. 3406–3415, 2003.
- [38] A. R. Gruber, R. Lorenz, S. H. Bernhart, R. Neuböck, and I. L. Hofacker, "The vienna Rna suite," *Nucleic Acids Research*, vol. 36, no. Web Server, pp. W70–W74, 2008.
- [39] M. J. Boniecki, G. Lach, W. K. Dawson et al., "Simrna: a coarse-grained method for Rna folding simulations and 3d structure prediction," *Nucleic Acids Research*, vol. 44, no. 7, pp. e63–e63, 2016.
- [40] I. Jeddi and L. Saiz, "Three-dimensional modeling of single stranded DNA hairpins for aptamer-based biosensors," *Scientific Reports*, vol. 7, pp. 1–13, 2017.
- [41] D. Schneidman-Duhovny, Y. Inbar, R. Nussinov, and H. J. Wolfson, "Patchdock and symmdock: servers for rigid and symmetric docking," *Nucleic Acids Research*, vol. 33, no. Web Server, pp. W363–W367, 2005.
- [42] A. Mollahosseini, S. Argumeedi, A. Abdelrasoulab, and A. Shoker, "A case study of poly (aryl ether sulfone) hemodialysis membrane interactions with human blood: molecular dynamics simulation and experimental analyses," *Computer Methods and Programs in Biomedicine*, vol. 197, article 105742, 2020.
- [43] K. Al-Khafajia and T. T. Tok, "Molecular dynamics simulation, free energy landscape and binding free energy computations in exploration the anti-invasive activity of amygdalin against metastasis," *Computer Methods and Programs in Biomedicine*, vol. 195, article 105660, 2020.
- [44] R. Maleki, H. Hassanzadeh Afrouzi, M. Hosseini, D. Davood Toghrai, and S. Sara Rostami, "Molecular dynamics simulation of Doxorubicin loading with N-isopropyl acrylamide carbon nanotube in a drug delivery system," *Computer Methods and Programs in Biomedicine*, vol. 184, article 105303, 2020.
- [45] D. Van Der Spoel, E. Lindahl, B. Hess, G. Groenhof, A. E. Mark, and H. J. Berendsen, "Gromacs: fast, flexible, and free," *Journal of Computational Chemistry*, vol. 26, no. 16, pp. 1701–1718, 2005.
- [46] K. Lindorff-Larsen, S. Piana, K. Palmo et al., "Improved side-chain torsion potentials for the amber F99sb protein force field," *Proteins: Structure, Function, and Bioinformatics*, vol. 78, no. 8, pp. 1950–1958, 2010.
- [47] S. Jahromi, E. Amani, and S. Movahed, "An improved hybrid continuum-atomistic four-way coupled model for electrokinetics in nanofluidics," *Electrophoresis*, vol. 40, no. 12-13, pp. 1678–1690, 2019.
- [48] W. L. Jorgensen, J. Chandrasekhar, J. D. Madura, R. W. Impey, and M. L. Klein, "Comparison of simple potential functions for simulating liquid water," *The Journal of Chemical Physics*, vol. 79, no. 2, pp. 926–935, 1983.
- [49] B. Hess, "P-Lincs: a parallel linear constraint solver for molecular simulation," *Journal of Chemical Theory and Computation*, vol. 4, no. 1, pp. 116–122, 2008.
- [50] T. Darden, D. York, and L. Pedersen, "Particle mesh ewald: an N-log(N) method for ewald sums in large systems," *The Journal of Chemical Physics*, vol. 98, no. 12, pp. 10089–10092, 1993.
- [51] H. Shirzadi Jahromi, F. Mehdipour, and G. Firoozi, "Fracture analysis of vacancy defected nitrogen doped graphene sheets via MD simulations," *Mapta Journal of Mechanical and Industrial Engineering*, vol. 5, no. 1, pp. 18–23, 2021.
- [52] W. G. Hoover, "Canonical dynamics: equilibrium phase-space distributions," *Physical Review A*, vol. 31, no. 3, pp. 1695–1697, 1985.
- [53] S. Nosé, "A molecular dynamics method for simulations in the canonical ensemble," *Molecular Physics*, vol. 52, no. 2, pp. 255–268, 1984.
- [54] M. Parrinello and A. Rahman, "Polymorphic transitions in single crystals: a new molecular dynamics method," *Journal of Applied Physics*, vol. 52, no. 12, pp. 7182–7190, 1981.
- [55] R. Kumari, R. Kumar, Open Source Drug Discovery Consortium, and A. Lynn, "G\_Mmpbsa— a Gromacs tool for high-throughput Mm-Pbsa calculations," *Journal of Chemical Information and Modeling*, vol. 54, no. 7, pp. 1951–1962, 2014.
- [56] H. Gouda, I. D. Kuntz, D. A. Case, and P. A. Kollman, "Free energy calculations for theophylline binding to an Rna aptamer: comparison of Mm-Pbsa and thermodynamic integration methods," *Biopolymers: Original Research on Biomolecules*, vol. 68, no. 1, pp. 16–34, 2003.
- [57] H. Freedman, L. P. Huynh, L. Le, T. E. Cheatham III, J. A. Tuszyński, and T. N. Truong, "Explicitly solvated ligand contribution to continuum solvation models for binding free energies: selectivity of theophylline binding to an Rna aptamer," *The Journal of Physical Chemistry B*, vol. 114, no. 6, pp. 2227–2237, 2010.
- [58] S. Jahangiri, M. Jafari, M. Arjomand, and F. Mehrnejad, "Molecular insights into the interactions of Gf-17 with the gram-negative and gram-positive bacterial lipid bilayers," *Journal of Cellular Biochemistry*, vol. 119, no. 11, pp. 9205–9216, 2018.
- [59] S. Niazi, M. Purohit, A. Sonawani, and J. H. Niazi, "Revealing the molecular interactions of aptamers that specifically bind to the extracellular domain of HER2 cancer biomarker protein: An in silico assessment," *Journal of Molecular Graphics and Modelling*, vol. 83, pp. 112–121, 2018.
- [60] E. A. Lesnik and S. M. Freier, "Relative thermodynamic stability of DNA, Rna, and DNA: Rna hybrid duplexes: relationship with base composition and structure," *Biochemistry*, vol. 34, no. 34, pp. 10807–10815, 1995.
- [61] R. Torabi, K. Bagherzadeh, H. Ghourchian, and M. Massoud Amanlou, "An investigation on the interaction modes of a single-strand DNA aptamer and RBP4 protein: a molecular dynamic simulations approach," *Organic & Biomolecular Chemistry*, vol. 14, no. 34, pp. 8141–8153, 2016.
- [62] I. Autiero, M. Ruvo, R. Roberto Improta, and L. Vitagliano, "The intrinsic flexibility of the aptamer targeting the ribosomal protein S8 is a key factor for the molecular recognition," *Biochimica et Biophysica Acta (BBA) - General Subjects*, vol. 1862, no. 4, pp. 1006–1016, 2018.
- [63] R. Ahirwar, S. Nahar, S. Aggarwal, S. Ramachandran, S. Maiti, and P. Nahar, "In silico selection of an aptamer to estrogen



## Research Article

# Inhibition of miR-214-3p Protects Endothelial Cells from ox-LDL-Induced Damage by Targeting GPX4

Min Xie,<sup>1</sup> Panhao Huang,<sup>2</sup> Tian Wu,<sup>2</sup> Li Chen ,<sup>3</sup> and Ren Guo <sup>2</sup>

<sup>1</sup>Department of Operating Room, The Third Xiangya Hospital, Central South University, Changsha, 410013 Hunan, China

<sup>2</sup>Department of Pharmacy, The Third Xiangya Hospital, Central South University, Changsha, 410013 Hunan, China

<sup>3</sup>Department of Infectious Diseases, The Third Xiangya Hospital, Central South University, Changsha, 410013 Hunan, China

Correspondence should be addressed to Li Chen; [chenli2020@yeah.net](mailto:chenli2020@yeah.net) and Ren Guo; [grfw2012@aliyun.com](mailto:grfw2012@aliyun.com)

Received 11 March 2021; Revised 3 June 2021; Accepted 22 June 2021; Published 6 July 2021

Academic Editor: Dabin Kuang

Copyright © 2021 Min Xie et al. This is an open access article distributed under the Creative Commons Attribution License, which permits unrestricted use, distribution, and reproduction in any medium, provided the original work is properly cited.

It is generally believed that excessive production of reactive oxygen species (ROS) during cardiovascular diseases impairs endothelial function. In this study, we aimed to investigate whether miR-214-3p is involved in the endothelial dysfunction induced by oxidized low-density lipoprotein (ox-LDL). In cultured vascular endothelial cells (VECs), the effects of miR-214-3p on endothelial injury induced by 100 mg/L ox-LDL were evaluated by knockdown of miR-214-3p. Western blotting was used to determine the expression of glutathione peroxidase 4 (GPX4) and endothelial nitric oxide synthase (eNOS) in VECs under different conditions. A luciferase reporter assay was used to identify GPX4 as the target of miR-214-3p. Our data showed that 100 mg/L ox-LDL significantly decreased the expression of GPX4 and eNOS, which was associated with increases in ROS levels and impairments of VEC viability and migration. Knockdown of miR-214-3p could partially reduce the increase in ROS, restore the decreased expression of GPX4 and eNOS, and thus rescue the impaired endothelial function caused by ox-LDL. Our data demonstrated that ox-LDL could induce upregulation of miR-214-3p and result in suppression of GPX4 in VECs. Downregulation of miR-214-3p could protect VECs from ROS-induced endothelial dysfunction by reversing its inhibitory effect on GPX4 expression.

## 1. Introduction

At present, the incidence rates of chronic diseases such as coronary heart disease, hypertension, and diabetes are on the rise all over the world, seriously endangering human health [1]. Many studies have shown that these cardiovascular diseases are closely associated with endothelial dysfunction [2, 3]. Vascular endothelial cells (VECs) mainly locate in the inner surface of the vasculatures; they consist of a tightly connected layer to act as a barrier between the blood and vascular walls. The basic function of VECs is to act as a barrier between the blood and vascular walls. In addition, VECs can synthesize and release a variety of vasoactive mediators that can regulate vascular permeability, VEC-specific chemotaxis, vasoconstriction and vasodilatation, and platelet aggregation. It has been evident that many factors such as oxidized low-density lipoprotein (ox-LDL), angiotensin II (Ang II), and interleukin-6 (IL-6) can impair the barrier

and secretion functions of VECs in different cardiovascular diseases, leading to an acceleration of disease progression [4]. For example, oxidative stress injury caused by ox-LDL is the most common mechanism of endothelial damage [5]. On the other hand, ox-LDL can also impair endothelial nitric oxide synthase (eNOS) function, leading to a reduction in the production of NO. VECs synthesize and release a series of vasoactive factors by sensing changes in the internal environment to maintain endothelial function and vascular homeostasis. The most widely studied of these protective factors secreted by VECs is NO, which is produced by eNOS through catalysis of L-arginine. NO exerts a strong effect on relaxing blood vessels and maintaining vascular physiological function. In cardiovascular disease studies, the expression of eNOS is often used as an important indicator to evaluate endothelial function [6].

Reactive oxygen species (ROS) are important components of free radicals necessary for cell biological behaviors,

but excessive ROS production under pathological conditions often leads to endothelial dysfunction [7]. In the long process of evolution, the human body has developed an antioxidant system to protect cells from the damage caused by excessive ROS production. Glutathione peroxidase (GPX) is one of the three main nonenzymatic antioxidants in the human body [8]. Seven types of GPXs have been identified in humans, and GPX4 is the most researched type, showing the strongest antioxidative capacity [9]. The main oxidizing substrate of GPX4 is phospholipid hydroperoxide, which is present in biofilms. In addition, GPX4 can catalyze  $H_2O_2$  and different lipid hydroperoxides, such as free fatty acid hydroperoxides, thymidine hydroperoxides, cholesterol, and cholesterol ester hydroperoxides. GPX4 has been shown to be associated with cardiovascular diseases, whereby overexpression of GPX4 in apolipoprotein E-deficient mice and in a myocardial ischemia/reperfusion mouse model inhibits the development of atherosclerosis and protects cardiac contractile function, respectively [10, 11]. Ectonucleotide pyrophosphatase 2 (ENPP2) is a lipid kinase that protects cardiomyocytes from erastin-induced ferroptosis by enhancing the expression of GPX4 [12].

MicroRNAs (miRNAs) are a class of small noncoding RNAs composed of 19–25 nucleotides. By recognizing and binding to the 3'-untranslated regions (UTRs) of target genes, miRNAs cause the degradation or block the translation of target genes. A large number of studies have confirmed that miRNAs are closely related to cell growth, differentiation, apoptosis, neural development, and oxidative stress. Abnormal expression of certain miRNAs in the circulation leads to a variety of diseases, such as atherosclerosis, tumors, diabetes, and Parkinson's disease [13–16]. Previous studies have documented that many miRNAs, such as miR-145 and miR-590, participate in the progression of vascular injury [17–19]. In our research, we found that miR-214-3p was also significantly upregulated in ox-LDL-induced VECs. Furthermore, by using bioinformatics methods, we found that GPX4 may be a direct target of miR-214-3p. Although miR-214-3p has been reported to play a role in colorectal cancer and the inflammatory pathogenesis of Parkinson's disease [20, 21], the mechanism by which miR-214-3p exerts its effects on VECs remains unclear. In this study, we aimed to investigate the relationship between miR-214-3p and GPX4 in an ox-LDL-induced VEC damage model.

## 2. Materials and Methods

**2.1. Cell Culture.** The human VEC line (human umbilical vein endothelial cell (HUVEC)) was purchased from the Cell Lab of Central South University and was cultured in Dulbecco's modified Eagle medium (DMEM, Gibco, USA) containing 10% fetal bovine serum (Gibco, USA) in a 5%  $CO_2$  incubator at 37°C. Subsequently, after 3 passages, the cells were placed in serum-free medium for 12 h prior to the experiment and then divided into different groups to receive different treatments. ox-LDL was purchased from Yiyuan Biotechnology (Guangzhou, China, No. YB-002). VECs were treated with 100 mg/L ox-LDL for 24 h to induce endothelial damage.

**2.2. Transfection.** First, the transfection complex was prepared as follows: 10× riboFECT buffer (RiboBio, China) was diluted 10 times, and then, 20  $\mu$ L miR-214-3p mimic or inhibitor was diluted in 120  $\mu$ L diluted riboFECT buffer to obtain the nucleic acid dilution. The sequences of miRNA-214-3p mimic and inhibitor are presented as follows: miR-214-3p mimics: 5'-ACAGCAGGCACAGACAGGCAG U-3' (sense), 5'-UGCCUGUCUGUGCCUG CU GUUU-3' (antisense); miR-214-3p inhibitor: 5'-ACUGCC UGUCUGUGCCUGCUGU-3' (sense), 5'-CAGUACUUU UGUGUAG UACAA-3' (antisense). Twelve microliters of transfection reagent was slowly added to the nucleic acid solution to obtain the transfection complex. To overexpress or knock down the expression of miR-214-3p, the transfection complexes with miR-214-3p mimic or inhibitor were added to the cell culture medium, and then, the cells were incubated in a 5%  $CO_2$  incubator at 37°C for 24 h. 50 nmol/L miR-214-3p mimic and 100 nmol/L miR-214-3p inhibitor were used to treating VECs.

**2.3. Real-Time PCR.** Total RNA from VECs was extracted for reverse transcription and real-time quantitative PCR. Real-time PCR was performed according to the manufacturer's instructions using the ABI 7500 real-time PCR system with SYBR Green reagents. The primers for miR-214-3p are listed as follows: miR-214-3p-F: ACAGCAGGCACAGACAGGCAG; miR-214-3p-R: GTGCAGGGTCCGAGGTAT TC. The CT values of each sample were normalized to the U6 values as an internal reference, and the expression levels of miR-214-3p were calculated by the  $2^{-\Delta\Delta CT}$  method. All amplification reactions were performed in triplicate.

**2.4. Western Blotting.** Protein was extracted from VECs using RIPA buffer and phenylmethanesulfonyl fluoride (PMSF). Then, 40  $\mu$ g of total protein was separated by 10% SDS-PAGE, and the protein bands were then transferred to a polyvinylidene difluoride membrane (Millipore, USA). After blocking with 5% nonfat milk in TBST, the membrane was incubated overnight with rabbit anti-human GPX4 (polyclonal antibody, Sigma, USA, Catalog Number: SAB2108670) and eNOS antibodies (polyclonal antibody, Sigma, USA, Catalog Number: SAB4502013) overnight. Immunoreactive bands were visualized by electrochemiluminescence (Bio-Rad, USA) after incubation with a horseradish peroxidase-conjugated anti-mouse secondary antibody. The ratio of the protein of interest to GAPDH was used for statistical analysis.

**2.5. Dual-Luciferase Reporter Assay.** Two human GPX4 3'-UTR sequences containing predicted miR-214-3p target sites and the mutant 3'-UTR of GPX4 were synthesized and inserted into the pGL3 control vector (Promega, USA). For the reporter assay, VECs were seeded into 24-well plates and cotransfected with 200 ng pGL3-GPX4-3'-UTR with 100 nmol/L miR-214-3p mimics or a negative control. Cells cotransfected with 200 ng pGL3-mut-GPX4-3'-UTR plasmid with 100 nmol/L miR-214-3p mimics or negative control were used as controls. X-tremeGENE HP DNA Transfection

Reagent (Roche, Switzerland) was used for transfection of pGL3 report plasmid into VECs. After incubation for 24 h, luciferase activities were measured using a dual-luciferase reporter assay kit (Promega, USA) according to the manufacturer's instructions.

**2.6. Cell Viability Test.** VECs were cultured to logarithmic growth phase and seeded on 96-well plates at a cell density of  $10^4$  and then cultured in a constant temperature incubator at  $37^\circ\text{C}$  and 5%  $\text{CO}_2$  for 24 h. A  $50\ \mu\text{L}$   $1\times$  MTT solution was added to each well, and the plate was placed in a cell incubator at  $37^\circ\text{C}$  for 4 h. The cell supernatants were discarded,  $150\ \mu\text{L}$  DMSO was added to each well, and the plate was vibrated for 10 min on an oscillator. The absorbance value (OD) of each well was detected by a Bio-Rad 680 microplate analyzer at a wavelength of 570 nm, and the average OD value of three replicate wells was taken.

**2.7. ROS Detection.** An ROS kit from Beyotime Biotechnology was used to detect the ROS level in cells following the manufacturer's instructions. First,  $10^6$  cells were seeded on a plate and incubated in a 5%  $\text{CO}_2$  incubator at  $37^\circ\text{C}$  for 24 h. Then, DCFH-DA was diluted 1:1000 with serum-free medium to a final concentration of  $10\ \mu\text{mol/L}$ . An appropriate volume of diluted DCFH-DA was added to the cell culture medium. Then, the cell culture plate was placed into a  $37^\circ\text{C}$  incubator for 20 min. The cells were washed with serum-free cell culture solution 3 times to remove the DCFH-DA that did not enter the cells. Finally, flow cytometry (Beckman, USA) was used to detect the intensity of intracellular green fluorescence. FlowJo software was used to quantize the fluorescence intensity to evaluate the ROS level.

**2.8. Statistical Analysis.** SPSS software (version 16.0) was used for the statistical analysis. The data are expressed as the mean  $\pm$  SD. The differences among the groups were compared using one-way ANOVA.  $P < 0.05$  was considered to be statistically significant.

### 3. Results

**3.1. ox-LDL Induced an Increase in miR-214-3p Expression and a Decrease in GPX4 Expression.** To determine the changes in miR-214-3p after 100 mg/L ox-LDL stimulation and its influence on VECs, we first measured the expression of miR-214-3p in VECs after ox-LDL treatment. Real-time PCR revealed that ox-LDL caused an approximately 8-fold increase in miR-214-3p expression compared with the control treatment (Figure 1(a)). We also observed that ox-LDL treatment did not cause significant changes in miR-145 but significantly reduced the expression level of miR-590 (Figures 1(b) and 1(c)). Since the endothelial protective effect of miR-590 has been elucidated in the paper by Wu et al., our study mainly focused on miR-214-3p [19]. Interestingly, we also observed a significant decrease in GPX4 protein expression upon ox-LDL treatment of VECs (Figure 1(d)). Together, these results suggest that both miR-214-3p and GPX4 are involved in ox-LDL-induced damage to VECs.

**3.2. GPX4 Is a Target of miR-214-3p.** We used the online software TargetScan 7.2 to explore the possible association of miR-214-3p with GPX4. As shown in Figure 2(a), the 3'-UTR of GPX4 contained possible binding sites for miR-214-3p. Then, 100 nmol/L miR-214-3p mimic was used to overexpress miR-214-3p in VECs. As shown in Figures 2(b) and 2(c), overexpression of miR-214-3p by the miR-214-3p mimic significantly decreased GPX4 expression at both the mRNA and protein levels. Furthermore, a luciferase activity assay showed that the miR-214-3p mimic significantly inhibited the luciferase activity of the wild-type but not the mutant 3'-UTR of the GPX4 gene in VECs (Figure 2(d)). These data suggest that GPX4 is a direct target of miR-214-3p.

**3.3. Suppression of miR-214-3p Rescues VEC Viability upon ox-LDL Treatment.** Because the process of ox-LDL-induced endothelial damage was accompanied by the upregulation of miR-214-3p expression, we next determined the influence of miR-214-3p on the ox-LDL-induced inhibition of endothelial activity by reducing the level of miR-214-3p. The MTT test demonstrated that 100 mg/L ox-LDL caused a significant decrease in VEC viability, whereas pretreatment of VECs with 200 nmol/L miR-214-3p inhibitor partially rescued the impaired VEC growth in comparison with the control treatment (Figure 3).

**3.4. Inhibition of miR-214-3p Reverses the Decreased Expression of GPX4 and eNOS upon ox-LDL Treatment.** GPX4 expression and activity are crucial for inhibiting the level of vascular oxidative stress. eNOS is the primary enzyme that produces NO and is also very important for the maintenance of normal vasodilation function. Therefore, in this study, we also investigated the effect of miR-214-3p on GPX4 and eNOS after ox-LDL stimulation. Treatment of VECs with ox-LDL for 24 h decreased the expression of GPX4 and eNOS, whereas miR-214-3p inhibitor-mediated depletion of miR-214-3p partially restored the expression of GPX4 and eNOS compared with that in the control group (Figures 4(a) and 4(b)).

**3.5. Inhibition of miR-214-3p Restores the Impaired VEC Migration Induced by ox-LDL.** In addition to cell viability, we also observed VEC migration under different treatments. As shown in Figure 5, ox-LDL treatment of VECs significantly impaired the migration ability of VECs within 24 h, as indicated by the longer distance between the isolated cells. However, compared with the control treatment, miR-214-3p inhibitor-mediated depletion of miR-214-3p partially restored the migration ability of VECs.

**3.6. miR-214-3p Affects ROS Levels in VECs upon ox-LDL Treatment.** High levels of ROS are often associated with endothelial dysfunction, so we also explored whether knock-down of miR-214-3p could affect ROS levels in VECs stimulated by ox-LDL. Our data indicated that ox-LDL induced a dramatic increase in ROS levels in VECs, and pretreatment of VECs with the miR-214-3p inhibitor could partially lower the increased ROS levels compared with those in the control group (Figure 6).

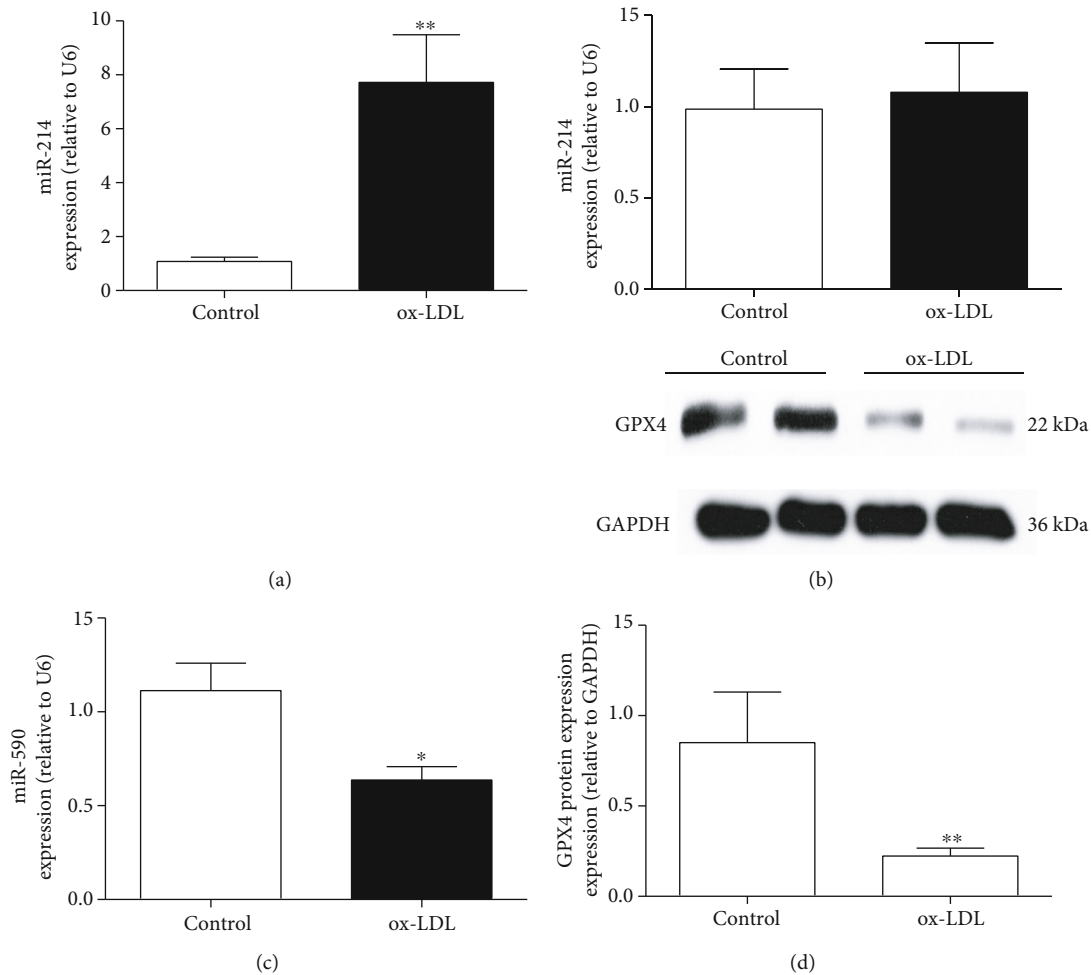


FIGURE 1: The expression of miR-214-3p and GPX4 in ox-LDL-stimulated VECs. The expressions of miR-214 (a), miR-145 (b), and miR-590 (c) after treatment with 100 mg/L ox-LDL in VECs. All values are expressed as the mean  $\pm$  SD,  $n = 3$ . \* $P < 0.05$  and \*\* $P < 0.01$ , compared with the control group.

#### 4. Discussion

In this study, we used ox-LDL to establish an endothelial damage model. It is generally believed that ox-LDL-induced endothelial damage is the initial event of atherosclerosis and is involved in the entire process of atherosclerosis, including the formation and rupture of atherosclerotic plaques. Our data suggest that 100  $\mu\text{g}/\text{mL}$  ox-LDL significantly increased the ROS level and impaired the viability and migration of cultured VECs. To determine the potential mechanism by which ox-LDL triggers the increase in ROS levels, GPX4 expression was detected because of its important role in the antioxidant system. As expected, treatment of VECs with ox-LDL decreased GPX4 expression, which was accompanied by VEC dysfunction and increased ROS levels. Although many studies have revealed that the normal expression and activity of GPX4 are critical for maintaining oxidative homeostasis in different cell types [22–24], one study also showed that the mRNA levels of GPX1, GPX3, and GPX4 were significantly upregulated in patients with acute coronary syndrome (ACS) [25]. It is known that ox-LDL, TNF- $\alpha$ , IL-6, and other atherosclerosis stimuli remain at a

high level in ACS patients for a long time, which may lead to the adaptive upregulation of the expression and activity of antioxidant enzymes in the affected cells. However, this adaptive regulation of GPX4 is not sufficient to effectively remove the excessive levels of ROS.

After determining the decreased expression of GPX4 in VECs induced by ox-LDL, we next attempted to find the factor responsible for the decreased GPX4 expression upon stimulation with ox-LDL. Previous studies have demonstrated that many miRNAs exhibit oxidative stress-related expression changes in atherosclerosis and hypertension [18]. Therefore, in this study, we detected several miRNAs with previously reported vasoprotective effects, including miR-145, miR-590, and miR-214-3p. Our data showed that treatment of VECs with ox-LDL triggered significant decreases in miR-590 and miR-214-3p expression levels. Previously, Wu and his colleagues reported that miR-590 could protect VECs from Ang II-induced damage by inhibiting the expression of CD40 [19]. Therefore, we mainly focused on the association of miR-214-3p with GPX4 during ox-LDL-induced endothelial dysfunction. Interestingly, by using the online software TargetScanHuman 7.1, we found that



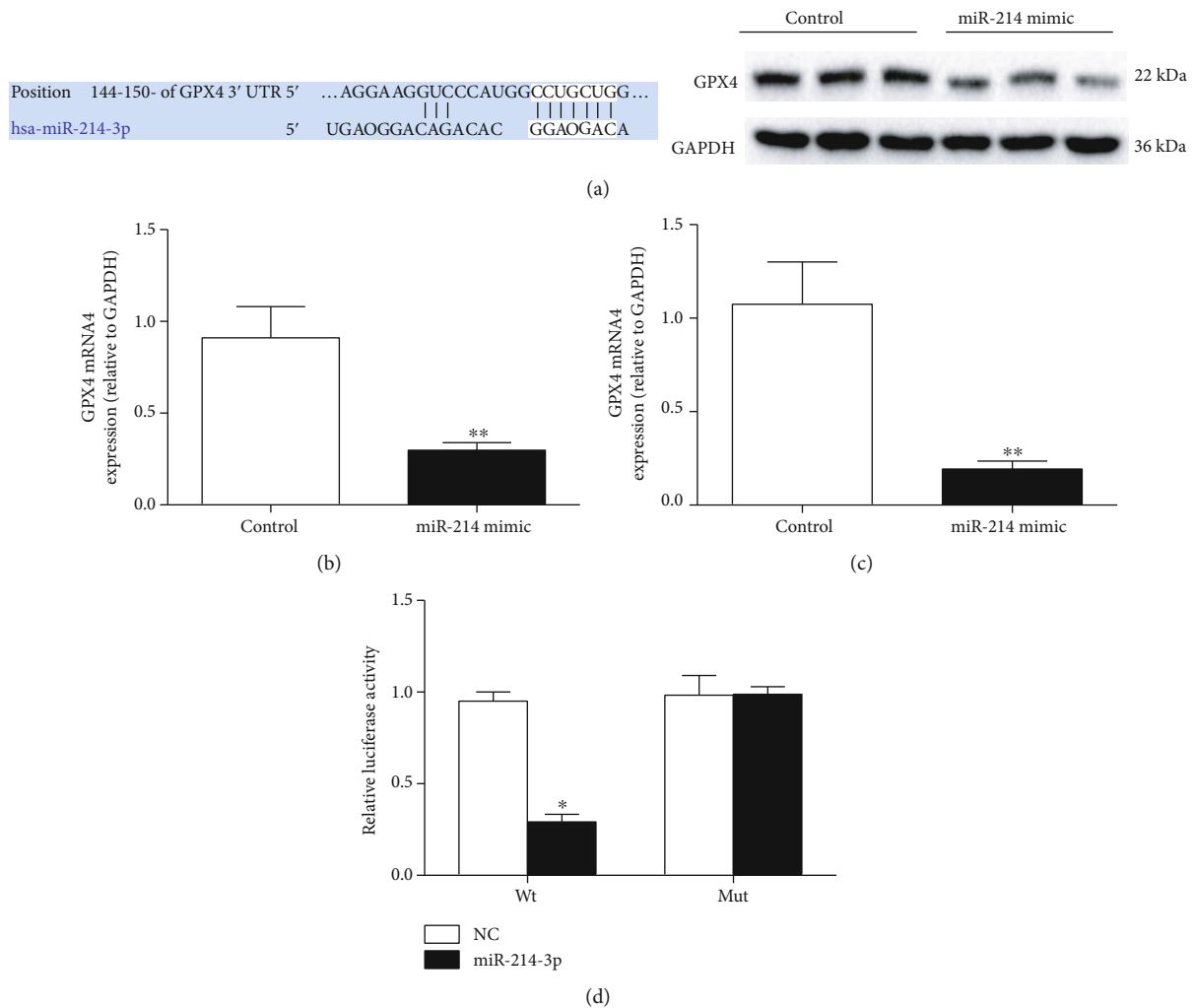


FIGURE 2: GPX4 is a target of miR-214-3p. (a) Predicted binding sites of miR-214-3p to GPX4; (b) real-time PCR measurement after miR-214-3p mimic treatment; (c) representative Western blot and statistical analyses of GPX4 in VECs treated with 100 nmol/L miR-214-3p mimic; (d) luciferase activity assay after miR-214-3p mimic treatment. All values are expressed as the mean  $\pm$  SD,  $n = 3$ . \* $P < 0.05$  and \*\* $P < 0.01$ , compared with the control group.

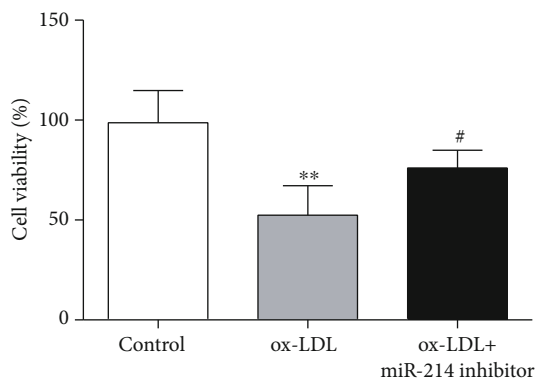


FIGURE 3: Suppression of miR-214-3p rescues VEC viability upon ox-LDL treatment. All values are expressed as the mean  $\pm$  SD,  $n = 3$ . \* $P < 0.05$ , compared with the control group; # $P < 0.05$ , compared with the ox-LDL treatment group.

GPX4 may be a target gene of miR-214-3p. To determine the regulation of GPX4 by miR-214-3p, we overexpressed miR-214-3p by using a miR-214-3p mimic to investigate its effect on GPX4 expression. Our results indicated that miR-214-3p overexpression significantly decreased GPX4 expression in normal conditions but not in ox-LDL-induced conditions, which is likely because the strong suppression of GPX4 exerted by ox-LDL masks the effect of miR-214-3p overexpression. Furthermore, in our luciferase reporter assay, we found that miR-214-3p inhibited the luciferase activity of the wild-type but not the mutant 3'-UTR of the GPX4 gene in VECs, which provided direct evidence that GPX4 is a target gene of miR-214-3p.

Having demonstrated that GPX4 is a direct target gene of miR-214-3p, we sought to determine whether inhibiting miR-214-3p expression could be a feasible way to rescue the impaired endothelial function upon ox-LDL stimulation. Excessive ROS production in cardiovascular diseases often causes endothelial dysfunction, which is manifested as

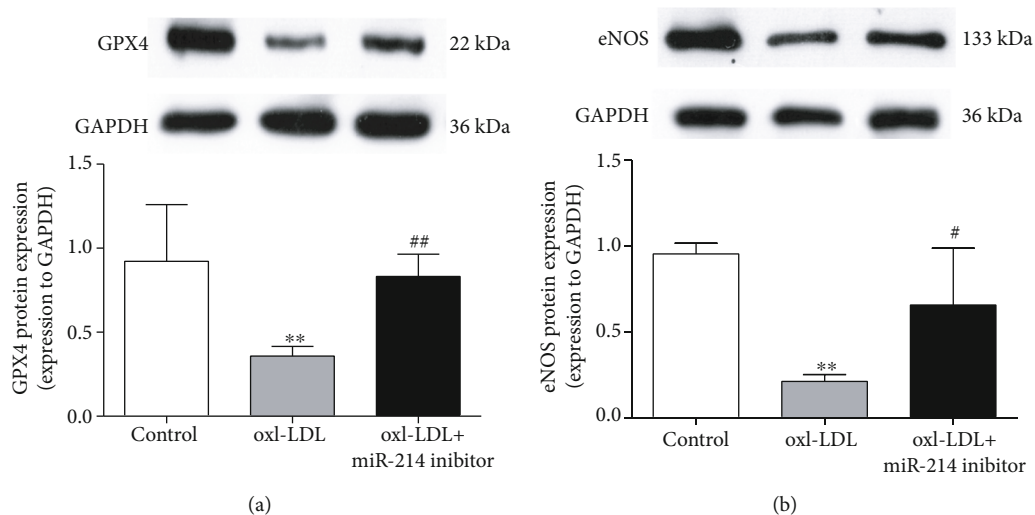


FIGURE 4: Inhibition of miR-214-3p reverses the decreased expression of GPX4 and eNOS upon ox-LDL treatment. (a) Representative Western blot and statistical analyses of VECs treated either with 100 mg/L ox-LDL or 100 mg/L ox-LDL+miR-214-3p inhibitor for GPX4; (b) representative Western blot and statistical analyses of eNOS in VECs treated either with 100 mg/L ox-LDL or 100 mg/L ox-LDL+miR-214-3p inhibitor. All values are expressed as the mean  $\pm$  SD,  $n = 3$ . \*\* $P < 0.01$ , compared with the control group; # $P < 0.05$  and ## $P < 0.01$ , compared with the ox-LDL treatment group.

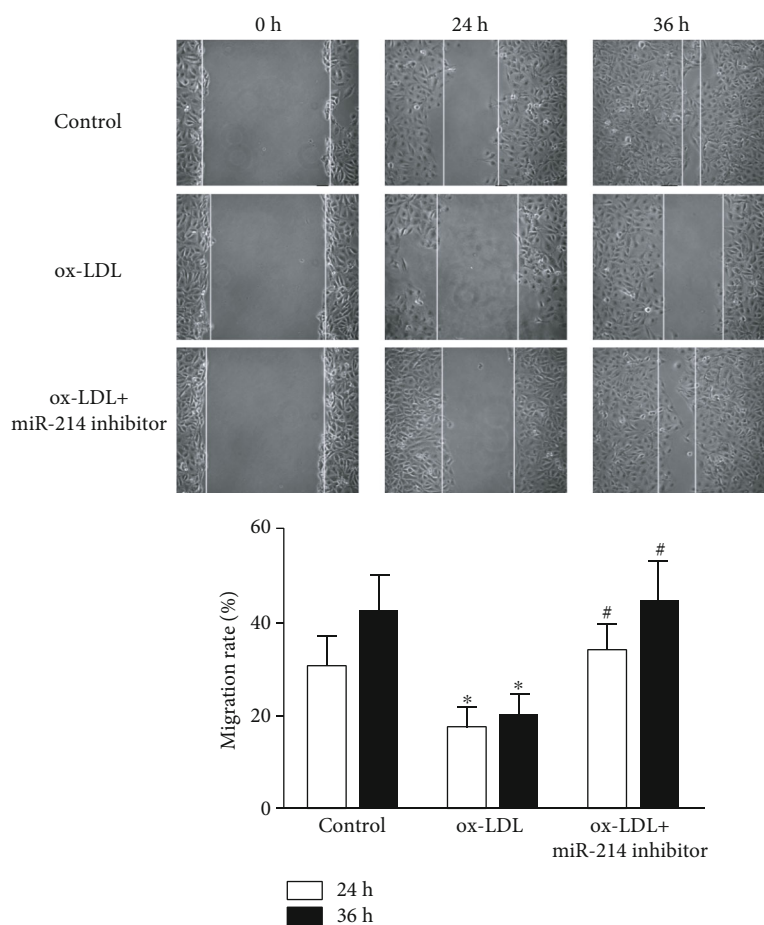


FIGURE 5: Depletion of miR-214-3p rescues ox-LDL-induced VEC migration impairments. Representative images of VECs treated either with 100 mg/L ox-LDL or 100 mg/L ox-LDL+miR-214-3p inhibitor for migration. All values are expressed as the mean  $\pm$  SD,  $n = 3$ . \* $P < 0.05$ , compared with the control group; # $P < 0.05$ , compared with the ox-LDL treatment group. Scale bar: 100  $\mu$ m.

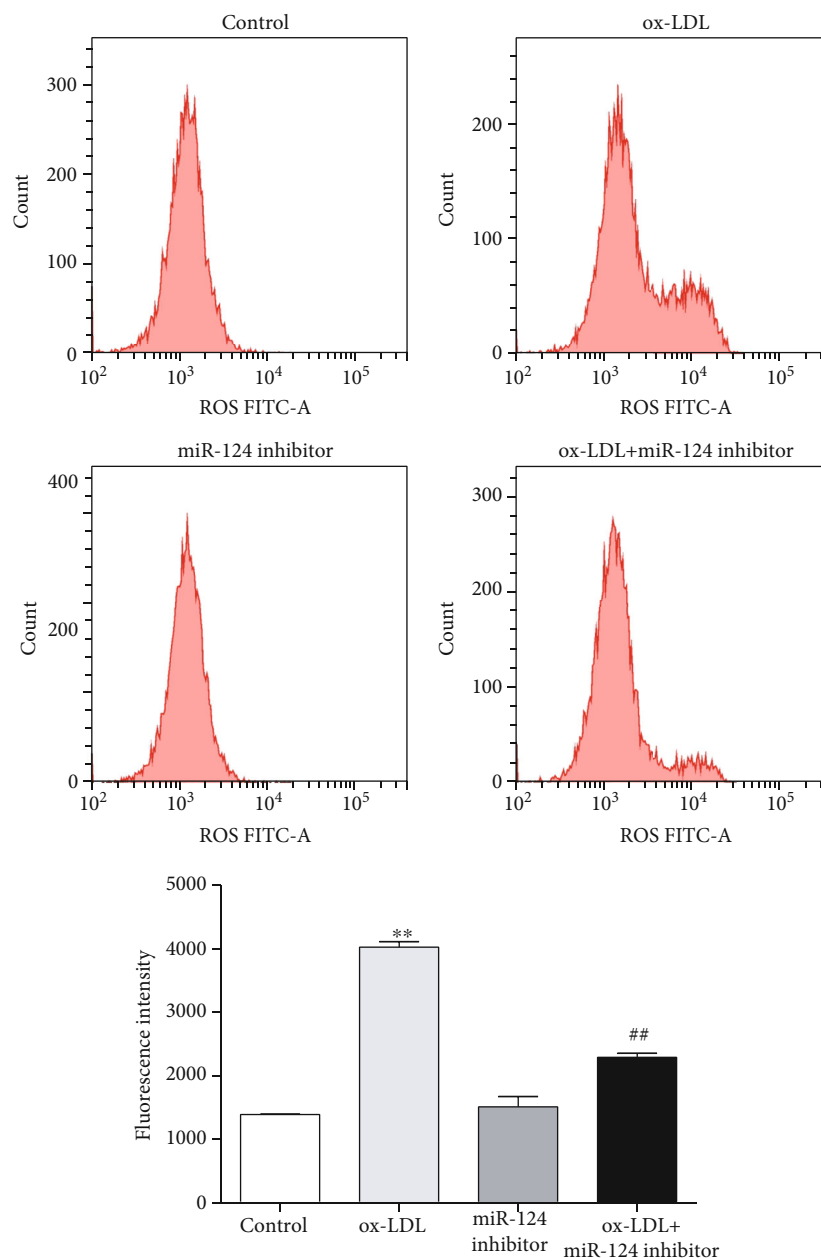


FIGURE 6: miR-214-3p upregulates the level of ROS in VECs upon ox-LDL treatment. Representative images of ROS levels in VECs treated with either 100 mg/L ox-LDL or 100 mg/L ox-LDL+miR-214-3p inhibitor. All values are expressed as the mean ± SD,  $n = 3$ . \*\* $P < 0.01$ , compared with the control group; ## $P < 0.01$ , compared with the ox-LDL treatment group. Scale bar: 100  $\mu$ m.

decreased viability, migration, and NO production of VECs [26–28]. Here, we observed that inhibition of miR-214-3p expression by a miR-214-3p inhibitor rescued the observed endothelial dysfunction, which showed that VEC viability and migration ability were improved under ox-LDL stimulation. NO produced by eNOS is the most important endothelium-derived relaxing factor to maintain normal vasodilation. Furthermore, ROS derived from eNOS uncoupling also show severe toxic effects on VECs during different disease states. Therefore, we investigated eNOS expression upon stimulation with ox-LDL and miR-214-3p inhibitor. Consistent with previously published data, 100 mg/L ox-LDL led to a significant decrease in eNOS expression, which

was partially reversed by pretreatment of VECs with the miR-214-3p inhibitor.

Our study reported that the expression of the vascular enriched miRNA miR-214-3p is stimulated by ox-LDL. Downregulating miR-214-3p expression under ox-LDL conditions can protect VECs from ROS-induced endothelial dysfunction, likely by reversing the miRNA-mediated inhibition of GPX4 expression. These results, together with previous findings showing the effects of miRNAs on the vasculature, suggest that miR-214-3p and other miRNAs represent novel therapeutic targets for cardiovascular diseases.

However, the current study also has some limitations. For example, GPX4 is an antioxidant enzyme whose expression

and activity both affect its ability to clear ROS. However, this study mainly focused on the expression change of GPX4 after ox-LDL administration. In addition, it has been recently reported that GPX4 is involved in the process of ferroptosis, a newly identified metabolic stress-induced programmed cell death that is different from apoptosis. Further research is also needed to investigate the possible association of miR-214-3p with ferroptosis in cardiovascular disease.

## Data Availability

The datasets used and/or analyzed during the current study are available from the corresponding author on reasonable request.

## Conflicts of Interest

The authors declare that they have no competing interests.

## Authors' Contributions

LC and RG conceived and designed the experiments. MX, HPH, and TW performed the experiments. MX and HPH analyzed the data. LC and TW contributed reagents/materials/analysis tools. RG wrote the paper. All authors read and approved the final manuscript.

## Acknowledgments

This project was supported by the Research Project of Hunan Provincial Health Commission (No. 20190967) and Natural Science Foundation of Hunan Province (No. 2019JJ80032).

## References

- [1] K. Li, F. A. White, T. Tipoe et al., "The current state of mobile phone apps for monitoring heart rate, heart rate variability, and atrial fibrillation: narrative review," *JMIR mHealth and uHealth*, vol. 7, no. 2, p. e11606, 2019.
- [2] V. F. Smolders, E. Zodda, P. Quax et al., "Metabolic alterations in cardiopulmonary vascular dysfunction," *Frontiers in Molecular Biosciences*, vol. 5, 2019.
- [3] M. B. Boffa and M. L. Koschinsky, "Oxidized phospholipids as a unifying theory for lipoprotein(a) and cardiovascular disease," *Nature Reviews Cardiology*, vol. 16, no. 5, pp. 305–318, 2019.
- [4] H. Haybar, S. Shahrabi, H. Rezaeeyan, R. Shirzad, and N. Saki, "Endothelial cells: from dysfunction mechanism to pharmacological effect in cardiovascular disease," *Cardiovascular Toxicology*, vol. 19, no. 1, pp. 13–22, 2019.
- [5] S. Li, Y. Sun, Z. Han, X. Bu, W. Yu, and J. Wang, "Retracted: cytoprotective effects of euxanthone against ox-LDL-induced endothelial cell injury is mediated via Nrf2," *Life Sciences*, vol. 223, pp. 174–184, 2019.
- [6] L. Chen, L. Qin, X. Liu, and X. Meng, "CTRP3 alleviates ox-LDL-induced inflammatory response and endothelial dysfunction in mouse aortic endothelial cells by activating the PI3K/Akt/eNOS pathway," *Inflammation*, vol. 42, no. 4, pp. 1350–1359, 2019.
- [7] Y. Zhu, M. Li, Y. Lu, J. Li, Y. Ke, and J. Yang, "Ilexgenin A inhibits mitochondrial fission and promote Drp1 degradation by Nrf2-induced PSMB5 in endothelial cells," *Drug Development Research*, vol. 80, no. 4, pp. 481–489, 2019.
- [8] M. Benhar, "Roles of mammalian glutathione peroxidase and thioredoxin reductase enzymes in the cellular response to nitrosative stress," *Free Radical Biology & Medicine*, vol. 127, pp. 160–164, 2018.
- [9] M. Conrad, V. E. Kagan, H. Bayir et al., "Regulation of lipid peroxidation and ferroptosis in diverse species," *Genes & Development*, vol. 32, no. 9–10, pp. 602–619, 2018.
- [10] Z. Guo, Q. Ran, L. N. Roberts et al., "Suppression of atherogenesis by overexpression of glutathione peroxidase-4 in apolipoprotein E-deficient mice," *Free Radical Biology & Medicine*, vol. 44, no. 3, pp. 343–352, 2008.
- [11] E. R. Dabkowski, C. L. Williamson, and J. M. Hollander, "Mitochondria-specific transgenic overexpression of phospholipid hydroperoxide glutathione peroxidase (*\_GPx4\_*) attenuates ischemia/reperfusion-associated cardiac dysfunction," *Free Radical Biology & Medicine*, vol. 45, no. 6, pp. 855–865, 2008.
- [12] Y. T. Bai, R. Chang, H. Wang, F. J. Xiao, R. L. Ge, and L. S. Wang, "ENPP2 protects cardiomyocytes from erastin-induced ferroptosis," *Biochemical and Biophysical Research Communications*, vol. 499, no. 1, pp. 44–51, 2018.
- [13] S. Kumar, D. Williams, S. Sur, J. Y. Wang, and H. Jo, "Role of flow-sensitive microRNAs and long noncoding RNAs in vascular dysfunction and atherosclerosis," *Vascular Pharmacology*, vol. 114, pp. 76–92, 2019.
- [14] G. Lo Russo, A. Tessari, M. Capece et al., "MicroRNAs for the diagnosis and Management of Malignant Pleural Mesothelioma: a literature review," *Frontiers in Oncology*, vol. 8, 2018.
- [15] L. Nigi, G. E. Grieco, G. Ventriglia et al., "MicroRNAs as regulators of insulin signaling: research updates and potential therapeutic perspectives in type 2 diabetes," *International Journal of Molecular Sciences*, vol. 19, no. 12, p. 3705, 2018.
- [16] L. Leggio, S. Vivarelli, F. L'Episcopo et al., "MicroRNAs in Parkinson's disease: from pathogenesis to novel diagnostic and therapeutic approaches," *International Journal of Molecular Sciences*, vol. 18, no. 12, p. 2698, 2017.
- [17] X. Guo, D. Li, M. Chen et al., "miRNA-145 inhibits VSMC proliferation by targeting CD40," *Scientific Reports*, vol. 6, no. 1, p. 35302, 2016.
- [18] X. Guo, L. Yu, M. Chen et al., "miR-145 mediated the role of aspirin in resisting VSMCs proliferation and anti-inflammation through CD40," *Journal of Translational Medicine*, vol. 14, no. 1, p. 211, 2016.
- [19] T. Wu, Y. Xiang, Y. Lv, D. Li, L. Yu, and R. Guo, "miR-590-3p mediates the protective effect of curcumin on injured endothelial cells induced by angiotensin II," *American Journal of Translational Research*, vol. 9, no. 2, pp. 289–300, 2017.
- [20] M. L. Lu, Y. Zhang, J. Li et al., "MicroRNA-124 inhibits colorectal cancer cell proliferation and suppresses tumor growth by interacting with PLCB1 and regulating Wnt/ $\beta$ -catenin signaling pathway," *European Review for Medical and Pharmacological Sciences*, vol. 23, no. 1, pp. 121–136, 2019.
- [21] L. Yao, Y. Ye, H. Mao et al., "MicroRNA-124 regulates the expression of MEKK3 in the inflammatory pathogenesis of Parkinson's disease," *Journal of Neuroinflammation*, vol. 15, no. 1, p. 13, 2018.
- [22] Y. Kinowaki, M. Kurata, S. Ishibashi et al., "Glutathione peroxidase 4 overexpression inhibits ROS-induced cell death in



- diffuse large B-cell lymphoma,” *Laboratory Investigation*, vol. 98, no. 5, pp. 609–619, 2018.
- [23] F. Basit, L. M. van Oppen, L. Schöckel et al., “Mitochondrial complex I inhibition triggers a mitophagy-dependent ROS increase leading to necroptosis and ferroptosis in melanoma cells,” *Cell Death & Disease*, vol. 8, no. 3, pp. e2716–e2716, 2017.
- [24] X. Sui, R. Zhang, S. Liu et al., “RSL3 drives ferroptosis through GPX4 inactivation and ROS production in colorectal cancer,” *Frontiers in Pharmacology*, vol. 9, p. 1371, 2018.
- [25] A. Holley, J. Pitman, J. Miller, S. Harding, and P. Larsen, “Glutathione peroxidase activity and expression levels are significantly increased in acute coronary syndromes,” *Journal of Investigative Medicine*, vol. 65, no. 5, pp. 919–925, 2017.
- [26] X. Shi, Y. Guan, S. Jiang, T. Li, B. Sun, and H. Cheng, “Renin-angiotensin system inhibitor attenuates oxidative stress induced human coronary artery endothelial cell dysfunction via the PI3K/AKT/mTOR pathway,” *Archives of Medical Science*, vol. 15, no. 1, pp. 152–164, 2019.
- [27] S. Zhao, Y. Wang, X. Zhang et al., “Melatonin protects against hypoxia/reoxygenation-induced dysfunction of human umbilical vein endothelial cells through inhibiting reactive oxygen species generation,” *Acta Cardiologica Sinica*, vol. 34, no. 5, pp. 424–431, 2018.
- [28] Z. Zhu, Z. Shi, C. Xie, W. Gong, Z. Hu, and Y. Peng, “A novel mechanism of gamma-aminobutyric acid (GABA) protecting human umbilical vein endothelial cells (HUVECs) against H<sub>2</sub>O<sub>2</sub>-induced oxidative injury,” *Comp Biochem Physiol C Toxicol Pharmacol*, vol. 217, pp. 68–75, 2019.

## Retraction

# Retracted: Antiangiogenic Effect of Platelet P2Y<sub>12</sub> Inhibitor in Ischemia-Induced Angiogenesis in Mice Hindlimb

### BioMed Research International

Received 12 March 2024; Accepted 12 March 2024; Published 20 March 2024

Copyright © 2024 BioMed Research International. This is an open access article distributed under the Creative Commons Attribution License, which permits unrestricted use, distribution, and reproduction in any medium, provided the original work is properly cited.

This article has been retracted by Hindawi following an investigation undertaken by the publisher [1]. This investigation has uncovered evidence of one or more of the following indicators of systematic manipulation of the publication process:

- (1) Discrepancies in scope
- (2) Discrepancies in the description of the research reported
- (3) Discrepancies between the availability of data and the research described
- (4) Inappropriate citations
- (5) Incoherent, meaningless and/or irrelevant content included in the article
- (6) Manipulated or compromised peer review

The presence of these indicators undermines our confidence in the integrity of the article's content and we cannot, therefore, vouch for its reliability. Please note that this notice is intended solely to alert readers that the content of this article is unreliable. We have not investigated whether authors were aware of or involved in the systematic manipulation of the publication process.

Wiley and Hindawi regrets that the usual quality checks did not identify these issues before publication and have since put additional measures in place to safeguard research integrity.

We wish to credit our own Research Integrity and Research Publishing teams and anonymous and named external researchers and research integrity experts for contributing to this investigation.

The corresponding author, as the representative of all authors, has been given the opportunity to register their agreement or disagreement to this retraction. We have kept a record of any response received.

### References

- [1] X. Wang, H. Zhao, N. Yang, Y. Jin, and J. Chen, "Antiangiogenic Effect of Platelet P2Y<sub>12</sub> Inhibitor in Ischemia-Induced Angiogenesis in Mice Hindlimb," *BioMed Research International*, vol. 2021, Article ID 5529431, 6 pages, 2021.

## Research Article

# Antiangiogenic Effect of Platelet P2Y<sub>12</sub> Inhibitor in Ischemia-Induced Angiogenesis in Mice Hindlimb

Xiaoli Wang,<sup>1,2</sup> Huan Zhao,<sup>3</sup> Naiquan Yang<sup>ID</sup>,<sup>4</sup> Yue Jin,<sup>2</sup> and Jianguo Chen<sup>ID</sup><sup>5</sup>

<sup>1</sup>School of Medicine, Jiangsu University, Zhenjiang 212013, China

<sup>2</sup>Clinical Laboratory, Huai'an Second People's Hospital Affiliated to Xuzhou Medical University, Huai'an 223002, China

<sup>3</sup>Department of Cardiology, The Affiliated Jiangning Hospital of Nanjing Medical University, Nanjing 211100, China

<sup>4</sup>Department of Cardiology, Huai'an Second People's Hospital Affiliated to Xuzhou Medical University, Huai'an 223002, China

<sup>5</sup>Clinical Laboratory, People's Hospital Affiliated to Jiangsu University, Zhenjiang 212002, China

Correspondence should be addressed to Naiquan Yang; [qnyang2005@163.com](mailto:qnyang2005@163.com) and Jianguo Chen; [cjg02@126.com](mailto:cjg02@126.com)

Received 5 February 2021; Revised 20 March 2021; Accepted 22 March 2021; Published 9 April 2021

Academic Editor: Dafeng Yang

Copyright © 2021 Xiaoli Wang et al. This is an open access article distributed under the Creative Commons Attribution License, which permits unrestricted use, distribution, and reproduction in any medium, provided the original work is properly cited.

**Purpose.** Postischemic inflammation induces angiogenesis, while platelet P2Y<sub>12</sub> inhibitors can alleviate this inflammation. Therefore, we studied the potential effects of P2Y<sub>12</sub> inhibitor, ticagrelor, on angiogenesis in a mouse model of hindlimb ischemia. **Methods.** Laser Doppler perfusion imaging and capillary density measurement were used for angiogenesis quantified. Immunofluorescence was used to detect the level of CD31. The mice muscle was harvested for enzyme-linked immunosorbent (ELISA) assay of interleukin- (IL) 10 activity and Western blot determination of vascular endothelial growth factor (VEGF) production. **Results.** Ischemic hindlimb angiogenesis was sharply decreased in IL-10<sup>+/+</sup> mice than IL-10<sup>-/-</sup> mice. Ticagrelor inhibited angiogenesis and blood reperfusion recovery significantly elevated the levels of IL-10 and decreased the expression of VEGF in the IL-10<sup>+/+</sup> mouse ischemic hindlimb, which were abolished in IL-10-deficient (IL-10<sup>-/-</sup>) C57BL/6J mice. **Conclusion.** The study underscores that the effect of ticagrelor antiangiogenic function is related with the higher IL-10 expression.

## 1. Introduction

Pathological angiogenesis is related with many circumstance such as ischemic diseases, diabetic retinopathy, and tumor growth [1–3]. Hence, understanding the mechanism of angiogenesis is very important for the treatment of pathological angiogenesis.

Ischemia-induced angiogenesis is controlled by the coordination between proangiogenic growth factors, for instance vascular endothelial growth factor (VEGF), and varieties of antiangiogenic endogenous factors. Previous study shows that VEGF is upregulated by growth factors [4], proinflammatory mediators, and tissue hypoxia [5]. Moreover, VEGF also participates in the activation of inflammatory pathways by inducing other proinflammatory cytokines [6, 7]. Therefore, angiogenesis and inflammation are interlinked.

Besides, it was reported that anti-inflammatory cytokines are also secreted and modulated the inflammatory process. IL-10, an endogenous angioinhibitor, has been identified as an important anti-inflammatory cytokine [8]. Furthermore, IL-10 has also decreased VEGF and matrix metalloproteinase-9 (MMP-9) synthesis to prevent angiogenesis [9].

A diverse group of reports suggested neovascularization contributes to the atherosclerotic lesions growth and is a major factor in plaque destabilization leading to rupture [1, 10, 11]. Ticagrelor, a P2Y<sub>12</sub> inhibitor, was shown to lead to a lower incidence of cardiovascular mortality, myocardial infarction, or stroke compared with clopidogrel [12]. In addition, P2Y<sub>12</sub> inhibitors significantly inhibited the aggregation of platelet-monocyte and reduced the expression of major proinflammatory cytokines, including tumor necrosis factor- (TNF-)  $\alpha$ , IL-6, and chemokine (C-C motif) ligand 2 and

conversely increased the expression of IL-10 [13]. These studies indicated that ticagrelor may regulate angiogenesis by inhibiting inflammation to play a plaque-stabilizing role. However, whether P2Y<sub>12</sub> inhibitors can inhibit angiogenesis by regulating inflammation is still unclear.

In our study, we aimed to determine the effects of ticagrelor on angiogenesis. We demonstrate that the ischemic hindlimb angiogenesis was sharply decreased in IL-10<sup>+/+</sup> mice than IL-10<sup>-/-</sup> mice. Notably, ticagrelor treatment inhibited angiogenesis and blood reperfusion recovery in IL-10<sup>+/+</sup> mice. Moreover, ticagrelor treatment also significantly increased the IL-10 protein level and decreased VEGF protein level in ischemic tissues. However, the ticagrelor anti-angiogenesis and anti-inflammation effects were abolished in IL-10-deficient mice, suggesting ticagrelor played a vital role in the ischemia-induced angiogenesis.

## 2. Materials and Methods

**2.1. Animal Model and Groups.** C57BL/6J male IL-10<sup>+/+</sup> and IL-10<sup>-/-</sup> mice were obtained from the Laboratory Animal Center of Nanjing Medical University. IL-10<sup>+/+</sup> mice were randomly divided into three groups: (1) IL-10<sup>+/+</sup> control group (IL-10<sup>+/+</sup> group), treatment with saline; (2) sham group, underwent open skin procedure but without femoral artery ligation, then treatment with saline; (3) IL-10<sup>+/+</sup>+ticagrelor group (IL-10<sup>+/+</sup>+tica), treatment with ticagrelor (150 mg•kg<sup>-1</sup>•d<sup>-1</sup>). C57BL/6J IL-10<sup>-/-</sup> mice were randomly divided into two groups: (1) IL-10<sup>-/-</sup> control group (IL-10<sup>-/-</sup>), treatment with saline; (2) IL-10<sup>-/-</sup>+ticagrelor group (IL-10<sup>-/-</sup>+tica), treatment with ticagrelor (150 mg•kg<sup>-1</sup>•d<sup>-1</sup>). Intragastric treatment of ticagrelor (AstraZeneca) was initiated 3 days before operationally induced unilateral limb ischemia and continued for 2 weeks postoperatively. Animal care and protocols for the experiments were complied with the Guidelines for the Care and Use of Laboratory Animals of Jiangsu University.

**2.2. Hindlimb Ischemia Model.** The mice were underwent unilateral hindlimb ischemia surgery as described previously [14]. Simply, mice were first intraperitoneally anesthetized with pentobarbital sodium (50 mg/kg), and then, the right femoral artery was dissected along its full length. Finally, all branches were ligated and resected, and the left hindlimb remained intact and was used as the nonischemic limb.

**2.3. Laser Doppler Perfusion Imaging.** Two weeks after surgery, laser Doppler perfusion imaging (Perimed, Sweden) was used to detect superficial blood flow in both feet. Then, the ratio of the ischemic (right) to normal (left) limb blood flow relative perfusion data was recorded.

**2.4. Immunofluorescence Staining.** Two weeks after surgery, the ischemic limb muscle tissue sections were fixed in 4% paraformaldehyde and permeabilized with xylene. After blocking (5% BSA in PBS), the sections were immunolabeled with primary antibody: CD31 (1:100; Abcam) and then incubated with Alexa Fluor<sup>®</sup>488 donkey anti-mouse secondary antibody (1:250; Invitrogen) after washing. The nuclei were counterstained using DAPI (Invitrogen),

and the cells were observed under a fluorescence microscope (Olympus, Japan).

**2.5. Detection of IL-10 by ELSIA.** Two weeks after surgery, the concentration of IL-10 (ab108870; Abcam) in the muscle was assessed using commercially available ELISA kits (USCN Business Co., Ltd.) according to the manufacturer's protocol.

**2.6. Western Blot.** At 2 weeks postsurgery, ischemic limb muscle tissue homogenate lysate was harvested for western blot analysis as described study [15]. The lysates were electrophoresed and separated on 10% SDS-PAGE and transblotted onto nitrocellulose membranes (Bio-Rad, Hercules, USA). After blocked with milk, the membranes were incubated against primary antibodies: VEGF (1:1000) and GAPDH (1:4000; Cell Signaling Technology) followed by secondary antibody for 30 min at room temperature.

**2.7. Statistical Analysis.** SPSS version 13.0 (IBM Corp.) was used to analyze all the data. Differences were statistically analyzed using a one-way ANOVA or two-tailed Students *t*-test. The Newman-Keuls test was used to show *post hoc* differences. *P* value of <0.05 shows the significant difference.

## 3. Results

**3.1. Ticagrelor Therapy Decreases Blood Perfusion in IL-10<sup>+/+</sup> Mice.** As depicted in Figures 1(a) and 1(b), compared in the IL-10<sup>+/+</sup> mice, the amount of ischemia (right leg) perfusion in mice treated with saline was significantly lower than that in the sham group (0.55 ± 0.08 vs. 1.01 ± 0.05, *P* < 0.01). After treatment with ticagrelor, the ischemic tissue blood flow restoration was decreased in the ticagrelor-treated IL-10<sup>+/+</sup> mice than the saline-treated controls (0.39 ± 0.12 vs. 0.55 ± 0.08, *P* < 0.05).

**3.2. Ticagrelor Therapy Decreases the Capillary Density in IL-10<sup>+/+</sup> Mice.** Measurement of capillary density corresponded to reduced ischemic hindlimb perfusion in mice. Indeed, the IL-10<sup>+/+</sup> mice showed the capillary number ratio was decreased in the ischemic leg in the saline-treated groups compared with the sham group (0.45 ± 0.06 vs. 0.91 ± 0.03, *P* < 0.01). After ticagrelor treatment, lower capillary density was seen in the ticagrelor-treated groups as comparison to the saline-treated groups (0.22 ± 0.08 vs. 0.45 ± 0.06, *P* < 0.05, Figures 2(a) and 2(b)).

**3.3. Determination the IL-10 and VEGF Level in IL-10<sup>+/+</sup> Mice.** As presented in Figure 3, the IL-10 expression was evidently elevated in the IL-10<sup>+/+</sup>+tica group than the IL-10<sup>+/+</sup> group (489.3 ± 170.9 vs. 305.9 ± 127.5 pg/100 mg protein, respectively, *P* < 0.05). We also checked whether treatment with ticagrelor changes the VEGF protein level of ischemic gastrocnemius muscle tissue. As expected, in Figures 4(a) and 4(b), the results showed that the VEGF protein expression was decreased in the IL-10<sup>+/+</sup>+tica group than the IL-10<sup>+/+</sup> group.

**3.4. Function of Ticagrelor in IL-10<sup>-/-</sup> Mice.** To verify that ticagrelor treatment of IL-10<sup>+/+</sup> mice with decreased ischemia-induced angiogenesis is associated with IL-10 pathway, ticagrelor treatment was tested in IL-10<sup>-/-</sup> mice. In the



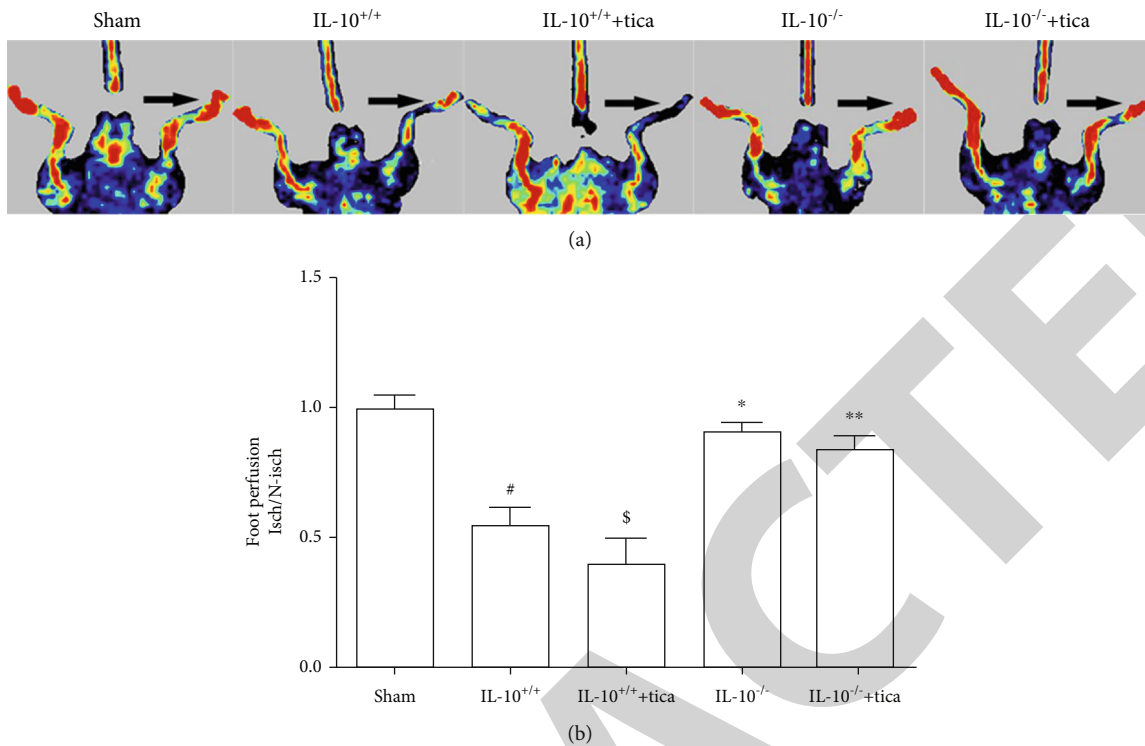


FIGURE 1: Effect of ticagrelor therapy on blood perfusion in IL-10<sup>+/+</sup> and IL-10<sup>-/-</sup> mice. (a) Representative figures of ischemic limb blood flow after the right femoral artery ligation for 14 days; arrows represent ischemic hindlimbs. (b) Quantitative analysis of superficial blood flow in ischemic and normal limbs ( $n = 6-10$ ). # $P < 0.01$  indicated compared with the sham group; \$ $P < 0.05$  indicated compared with the IL-10<sup>+/+</sup> group; \* $P < 0.01$  indicated compared with the IL-10<sup>+/+</sup> + tica group; \*\* $P < 0.01$  indicated compared with the IL-10<sup>+/+</sup> + tica group.

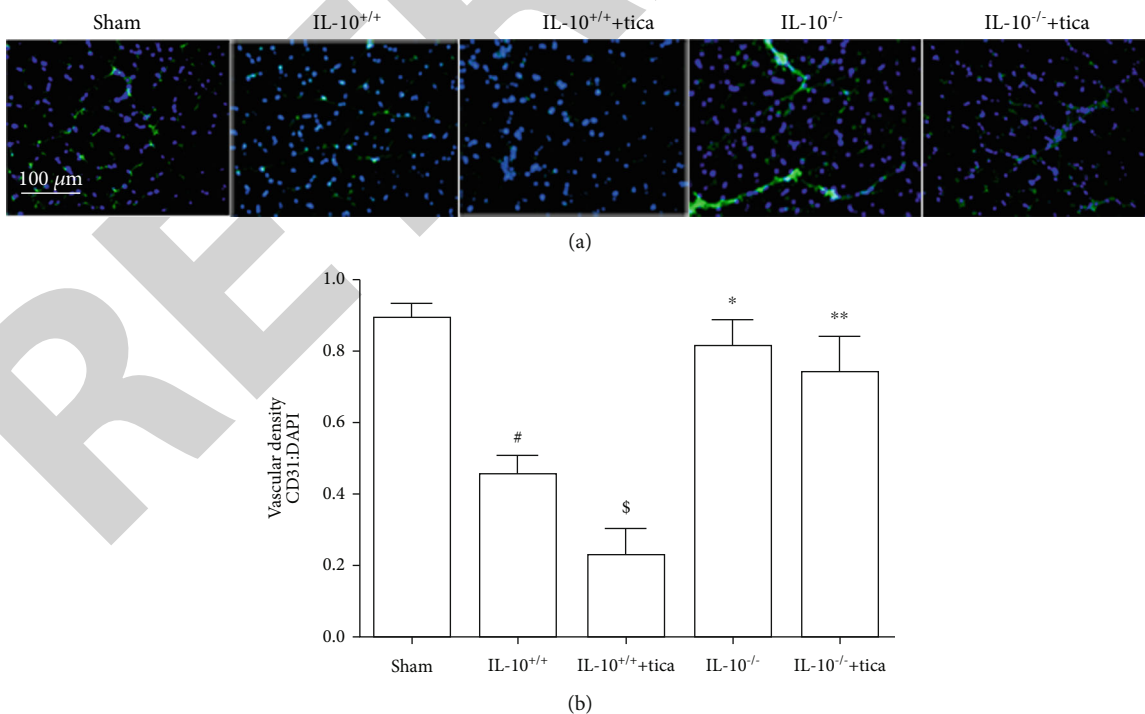


FIGURE 2: Effect of ticagrelor therapy on capillary density in IL-10<sup>+/+</sup> and IL-10<sup>-/-</sup> mice: (a) immunofluorescence staining of CD31; (b) quantification analysis of the CD31-stained vessel numbers in the sections of gastrocnemius muscle ( $n = 6-10$ ). # $P < 0.01$  indicated compared with the sham group; \$ $P < 0.05$  indicated compared with the IL-10<sup>+/+</sup> group; \* $P < 0.01$  indicated compared with the IL-10<sup>+/+</sup> + tica group; \*\* $P < 0.01$  indicated compared with the IL-10<sup>+/+</sup> + tica group.

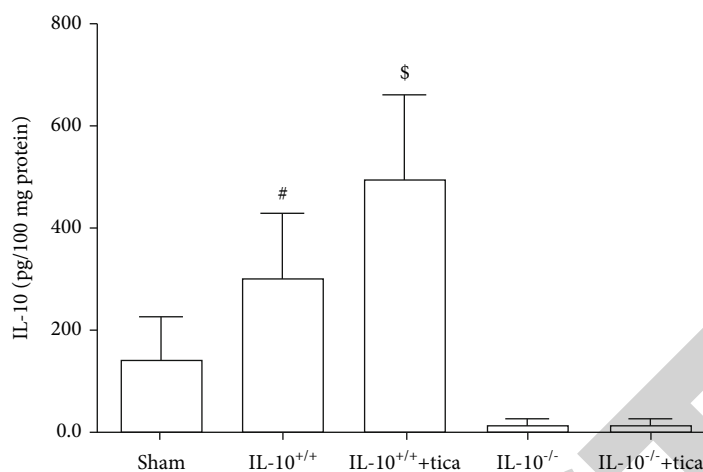


FIGURE 3: Ticagrelor therapy increases IL-10 protein levels in IL-10<sup>+/+</sup> mice. ELISA was conducted to detect the IL-10 expression in indicated groups ( $n = 6-10$ ). <sup>#</sup> $P < 0.01$  indicated compared with the sham group; <sup>\$</sup> $P < 0.05$  indicated compared with the IL-10<sup>+/+</sup> group.

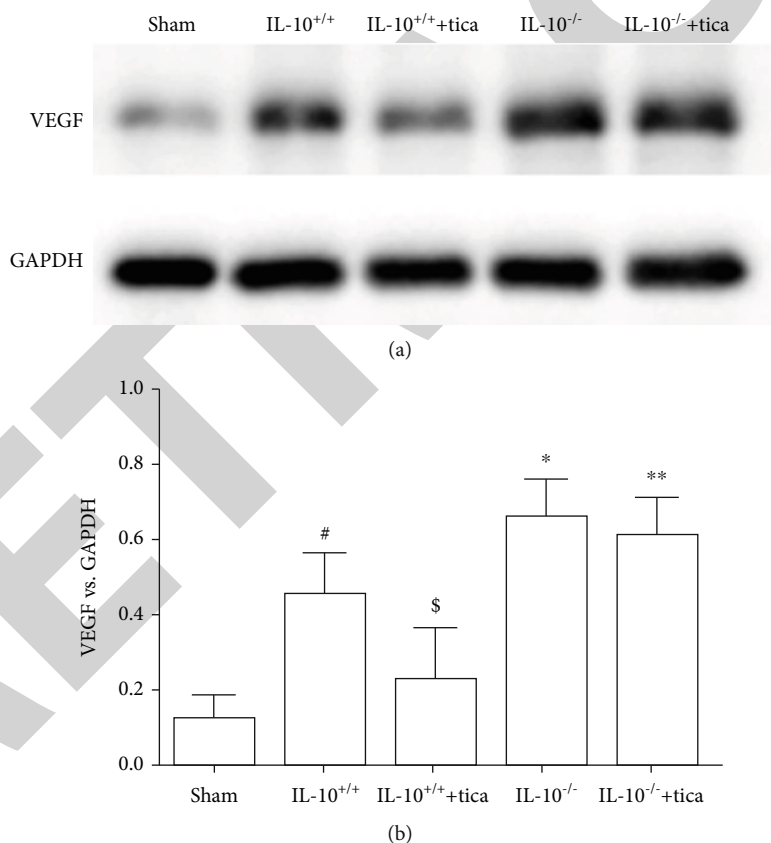


FIGURE 4: The detection of VEGF protein levels in the calf muscles of mice. (a) The VEGF protein levels in indicated groups were determined by western blot. (b) Densitometry of the VEGF expression normalized to GAPDH ( $n = 6-10$ ). <sup>#</sup> $P < 0.01$  indicated compared with the sham group; <sup>\$</sup> $P < 0.05$  indicated compared with the IL-10<sup>+/+</sup> group; <sup>\*</sup> $P < 0.01$  indicated compared with the IL-10<sup>+/+</sup> group; <sup>\*\*</sup> $P < 0.01$  indicated compared with the IL-10<sup>+/+</sup> + tica group.

two groups treated with ticagrelor, we found that the angiogenesis of ischemic hindlimbs in IL-10<sup>-/-</sup> mice is significantly higher than that in IL-10<sup>+/+</sup> mice (Figure 1(a) and 1(b) and Figures 2(a) and 2(b)). Besides, Figure 3 showed that the

anti-inflammation effects of ticagrelor were abolished in IL-10-deficient mice. Moreover, the IL-10<sup>-/-</sup> mice treated with ticagrelor showed no significant change in VEGF level (Figures 4(a) and 4(b)).

#### 4. Discussion

The major results of the study showed that IL-10 negatively adjusts angiogenesis induced by ischemia, and ticagrelor inhibits the angiogenesis and blood reperfusion recovery, significantly increases IL-10 level, and reduces the VEGF expression in the IL-10<sup>+/+</sup> mouse ischemic hindlimb, which were abolished in IL-10<sup>-/-</sup> mice.

Many experiments showed that the neovascularization contributes to the atherosclerotic lesions growth, and it plays a key role in plaque destabilization leading to rupture [1, 10, 11]. Wallentin et al. showed that the P2Y<sub>12</sub> inhibitor, ticagrelor, achieved better clinical outcomes in patients with ACS compared with clopidogrel treatment [12]. Besides, Thomas et al. demonstrated that P2Y<sub>12</sub> inhibitors remarkably decreased the expression of major proinflammatory cytokines and conversely increased the expression of anti-inflammatory cytokines such as IL-10 [13]. These studies indicated that ticagrelor may regulate angiogenesis by inhibiting inflammation to play a plaque-stabilizing role. Indeed, our study showed that ticagrelor inhibited angiogenesis and blood reperfusion recovery in IL-10<sup>+/+</sup> mice ischemic hindlimb. In addition, it also indicated that ticagrelor also significantly enhanced the IL-10 protein expression level in the IL-10<sup>+/+</sup> mice ischemic tissues.

Accumulating data have suggested that postischemic proinflammatory cytokines play an important role in inducing angiogenesis [16, 17]. The inflammatory action is simultaneously adjusted by anti-inflammatory cytokine production in major ischemic area. IL-10, as an anti-inflammatory cytokine produced by macrophages, has an antiangiogenic effect [18]. Consistent with these results, we verified that marked IL-10 was secreted in IL-10<sup>+/+</sup> mice ischemic tissue. Furthermore, we found that the ischemic hindlimb angiogenesis was sharply decreased in IL-10<sup>+/+</sup> mice than IL-10<sup>-/-</sup> mice.

VEGF protein has been shown to play a vital role in the development of hindlimb ischemia angiogenic. It is well known that tissue hypoxia and proinflammatory mediators induce high expression of VEGF [19]. In addition, VEGF can in turn activate the inflammatory pathways by inducing the expression of other proinflammatory cytokines [20]. In a previous study, IL-10 was proved to decrease the VEGF synthesis and prevent angiogenesis [18]. Similarly, the results in our study also showed that the expression of VEGF protein was evidently increased in the hindlimb ischemia IL-10<sup>-/-</sup> mice, accompanied with increased angiogenesis. We also demonstrated that the inhibitory effect of ticagrelor on angiogenesis and the VEGF expression in ischemic IL-10<sup>+/+</sup> mice was eliminated in IL-10<sup>-/-</sup> mice.

These studies, in addition to our data, suggested that the antiangiogenic effect of ticagrelor was associated with the elevated IL-10 expression.

#### 5. Conclusion

In summary, ticagrelor, a platelet P2Y<sub>12</sub> inhibitor has an antiangiogenic effect in hindlimb ischemia mouse. Furthermore, ticagrelor treatment significantly increased the IL-10 protein expression and inhibited the VEGF protein expression in

ischemic tissues of IL-10<sup>+/+</sup> mice. However, this antiangiogenic effect was not seen in IL-10<sup>-/-</sup> mice. The present work demonstrated that ticagrelor may regulate angiogenesis by inhibiting inflammation.

#### Data Availability

Data used to support this study finding have been included in the article and could be provided upon request from corresponding author Naiquan Yang (qnyang2005@163.com).

#### Conflicts of Interest

The authors declare that they have no conflicts of interest.

#### Authors' Contributions

Xiaoli Wang and Huan Zhao contribute equally to this work.

#### Acknowledgments

This work was supported by grants from the Huai'an talent support program (HAA201750).

#### References

- [1] D. E. Drachman and D. I. Simon, "Inflammation as a mechanism and therapeutic target for in-stent restenosis," *Current Atherosclerosis Reports*, vol. 7, no. 1, pp. 44–49, 2005.
- [2] S. Sajib, F. T. Zahra, M. S. Lionakis, N. A. German, and C. M. Mikelis, "Mechanisms of angiogenesis in microbe-regulated inflammatory and neoplastic conditions," *Angiogenesis*, vol. 21, no. 1, pp. 1–14, 2018.
- [3] M. Capitão and R. Soares, "Angiogenesis and inflammation crosstalk in diabetic retinopathy," *Journal of Cellular Biochemistry*, vol. 117, no. 11, pp. 2443–2453, 2016.
- [4] K. R. Alkharsah, "VEGF upregulation in viral infections and its possible therapeutic implications," *International Journal of Molecular Sciences*, vol. 19, no. 6, p. 1642, 2018.
- [5] J. Ye, K. Chen, L. Qi et al., "[Corrigendum] Metformin suppresses hypoxia-induced migration via the HIF-1 $\alpha$ /VEGF pathway in gallbladder cancer in vitro and in vivo," *oncology reports*, vol. 41, no. 6, p. 3587, 2019.
- [6] P. Carmeliet and R. K. Jain, "Molecular mechanisms and clinical applications of angiogenesis," *Nature*, vol. 473, no. 7347, pp. 298–307, 2011.
- [7] P. Nyberg, L. Xie, and R. Kalluri, "Endogenous inhibitors of angiogenesis," *Cancer Research*, vol. 65, no. 10, pp. 3967–3979, 2005.
- [8] W. Ouyang, S. Rutz, N. K. Crellin, P. A. Valdez, and S. G. Hymowitz, "Regulation and functions of the IL-10 family of cytokines in inflammation and disease," *Annual Review of Immunology*, vol. 29, no. 1, pp. 71–109, 2011.
- [9] K. M. M. Espíndola, R. G. Ferreira, L. E. M. Narvaez et al., "Chemical and pharmacological aspects of caffeic acid and its activity in hepatocarcinoma," *Frontiers in Oncology*, vol. 9, p. 541, 2019.
- [10] R. Khurana, M. Simons, J. F. Martin, and I. C. Zachary, "Role of angiogenesis in cardiovascular disease," *Circulation*, vol. 112, no. 12, pp. 1813–1824, 2005.